Hydration of cement mixtures containing contaminants

Design and application of the solidified product

Ronald J. van Eijk

Hydration of cement mixtures containing contaminants

Design and application of the solidified product

Hydratatie van cement mengsels met verontreinigingen

Ontwerp en toepassing van het verharde product

(met een samenvatting in het Nederlands)

HYDRATION OF CEMENT MIXTURES CONTAINING CONTAMINANTS

DESIGN AND APPLICATION OF THE SOLIDIFIED PRODUCT

PROEFSCHRIFT

ter verkrijging van

de graad van doctor aan de Universiteit Twente,

op gezag van de rector magnificus,

prof. dr. F.A. van Vught,

volgens besluit van het College voor Promoties,

in het openbaar te verdedigen

op vrijdag 22 juni 2001 te 15.00 uur.

door

Ronald Jozef van Eijk

geboren op 7 mei 1973

te 's-Gravenhage

Dit proefschrift is goedgekeurd door de promotoren:

prof. dr. ir. H.J. de Vriend
prof. mr. dr. H.M. de Jong

en door de assistent-promotor:

dr. ir. H.J.H. Brouwers

Voorwoord

Vroeger zei ik altijd dat ik "professor", uitvinder of schrijver wilde worden. In de vijfde klas van de lagere school kregen we op een dag een schematisch overzicht mee naar huis van het onderwijssysteem in Nederland. Helemaal bovenaan in dat schema stonden de magische letters W.O. (Wetenschappelijk Onderwijs) en ik dacht: Daar moet ik naar toe om uitvinder te worden. Zeven jaar later, in 1991, had ik inmiddels begrepen dat een "W.O. school" gewoon een universiteit was en ik begon aan mijn opleiding Scheikunde aan de Rijksuniversiteit Utrecht. Ik studeerde af in de biochemie, na maanden van microliters pipetteren, een techniek waar ik niet zo handig in was. Een promotieonderzoek op de Universiteit Twente, dat betrekking had bouwmaterialen, sprak me direct aan omdat het een combinatie was van chemie, modellering en praktijk. En omdat het beslist geen vakgebied van microliters was. In 1996 begon ik met de promotie als Assistent in Opleiding (A.I.O.), op de afdeling Civiele Technologie & Management (CT&M). Promoveren bleek niet gemakkelijk te zijn. Hoe meer ik me ingroef in het onderwerp (de microwereld van cement), hoe meer een gevoel van isolatie me bekroop. Gelukkig stond ik er niet alleen voor en heb ik van veel mensen steun gehad. Deze mensen wil ik hier bedanken.

Jos Brouwers heeft als assistent-promotor het belangrijkste deel van de begeleiding van het onderzoek op zich genomen. Hij nam zijn taak als "dagelijks begeleider" heel serieus, want dagelijks stormde hij mijn kamer binnen, omdat hij nieuwe literatuur voor me had, omdat hij wilde overleggen of omdat hij een afspraak had gemaakt met iemand uit het vakgebied of uit het bedrijfsleven. Deze afspraken waren voor mij het begin van nuttige contacten, die uiteindelijk veel hebben bijgedragen aan de toepasbaarheid en bekendheid van het onderzoek. Jos heeft mij ervan overtuigd dat drie dingen belangrijk zijn voor een wetenschapper: publiceren (conferentieartikelen), publiceren (in vaktijdschriften) en publiceren (in journals). Hij heeft mij geleerd hoe een goede paper in elkaar moet zitten en we hebben regelmatig samen gepubliceerd. Ook hebben we conferenties bezocht in Zweden, Engeland, Australië, Frankrijk en Italië, waar ikzelf altijd de presentaties deed en waar hij belangrijke contacten legde. Beste Jos, dankzij jouw professionele begeleiding en dankzij de hoge eisen die jij stelde aan mijn onderzoeksresultaten (met name aan mijn geschreven stukken) heb ik geleerd hoe wetenschap moet worden bedreven. Daar ben ik je zeer erkentelijk voor. Bedankt ook dat je me hebt laten zien wat er loos is in Maastricht en in Interlaken.

  Huib de Vriend wil ik bedanken voor zijn optreden als promotor, voor het vertrouwen dat hij stelde in mijn onderzoek en voor zijn kritische vragen over de modellen die ik gebruikte. Ik hoop dat ik heb aangetoond dat een cellulaire automaat de basis kan vormen van een informatief model en dat cementkorrels minstens zo interessant zijn als zandkorrels.

  Huib de Jong, mijn andere promotor, wil ik bedanken voor zijn aandeel in de beleidsmatige aspecten van het onderzoek. Ik weet nu dat er niet alleen een wereld is van C_3S en activiteitscoëfficiënten, maar ook een wereld van actoren en zelfregulering. De gesprekken met hem waren zeer prettig en opbouwend en hebben mij verheldering gebracht in de totaal structuur van mijn "boekje".

Gedurende mijn onderzoek heb ik veel baat gehad van de mensen in mijn gebruikersgroep. De mensen van ENCI, KEMA Sustainable, TNO MEP en de andere leden van deze groep wil ik bedanken voor hun technische inbreng, hun commentaar en hun interesse. Jan Blaakmeer van de ENCI wil ik in het bijzonder bedanken voor het laten uitvoeren van metingen ten behoeve van de calibratie van CEMHYD3D en voor zijn optreden als referent. Piet Bloem van de KEMA wil ik bedanken voor de prettige samenwerking in het kader van ons project over boraten. Naast al deze mensen wil ik ook Wim Albers van onze faculteit Toegepaste Wiskunde bedanken voor zijn hulp met het statistische plaatsingsmodel.

I would like to thank Dale Bentz from the National Instutute of Standards and Technolgy (NIST) in the U.S. for his help with the NIST CEMHYD3D model. It was a pleasure meeting you at the 10th ICCC, at NIST and at DTU in Denmark. Hopefully you will agree that I have proven the importance and possibilities of CEMHYD3D in this thesis.

De volgende CT&M collega's ben ik bijzonder dankbaar: Gerrit Snellink en René Buijsrogge (voor hun hulp met C compilers), Herman Menkehorst (voor zijn werk in het betonlab) en Anne-Marie (voor het vinden van subsidies, cursussen en de personen met de juiste informatie of bevoegdheden). Bert Maathuis en Jonas Kramer wil ik bedanken voor de bijdrage die hun afstudeerwerk aan het onderzoek heeft geleverd.

Dankzij de vele persoonlijke contacten met CT&M collega's heb ik een hele gezellige tijd gehad. Zij hebben mij laten rennen in de Batavierenrace en als ploegleider liet ik hen in 1997 de Veluweloop rennen. Beste mensen, de deuren van jullie kamers stonden vaak open. Bedankt dat ik dan naar binnen mocht lopen.

Mijn eigen kamer deelde ik lange tijd met Corina Schols. Beste Corina, het spijt me dat ik er altijd de nadruk op heb gelegd dat jij bij *mij* op de kamer zat. We zaten *samen* op de kamer en *samen* hebben we aangetoond dat een chemicus en een organisatie-deskundige dezelfde werkruimte kunnen delen en elk een positieve bijdrage kunnen leveren aan de werkzaamheden van de ander. Bedankt voor jouw bijdrage.

Geachte Musketiers, beste Chris, Jean-Luc en Andrew. Het was telkens een grote eer om met jullie aan mijn zijde Hengelo of de Bastille te bestormen. Chris, bedankt voor je diepere inzichten, de ontdekkingstochten door Zweden en mijn aanstelling als redacteur bij de Cociblabla. Nu onze proefschriften er liggen kunnen we ons allebei op onze roman richten.

De cellulaire automaat in mijn hoofd raakte wel eens overbelast en dan vertrok ik naar het Westen voor onderhoud. Daar heb ik met ene Alexander vele concerten bezocht, waaronder een indrukwekkende aftershow van Prince in Club Tivoli, Utrecht. We leefden ons vaak uit in Rotterdam en we hebben Londen en Barcelona onveilig gemaakt. Na dit soort uitstapjes had ik weer volop energie om in mijn onderzoek te duiken. Thanks Mate!

Brenda en Erwin wil ik zeggen dat hun grote broer op de universiteit nog veel kan leren van de lef van zijn zus en de wilskracht van zijn broer.

Pap, mam, zoals jullie kunnen zien ben ik schrijver en uitvinder tegelijk geworden, want ik heb een boek geschreven over mijn uitvindingen. Zonder jullie liefde, steun en vertrouwen was dit allemaal nooit gelukt. Geen enkel boek biedt genoeg ruimte om mijn dankbaarheid te beschrijven.

<div align="right">

Ronald van Eijk

Hengelo, 7 mei 2001

</div>

Contents

Chapter 1

Introduction

1.1 The waste problem

Humans require energy, living space and natural and artificial materials and these needs result in the production of all kinds of waste materials. The origin of waste materials are of a different kind. Some waste materials are released during energy production, e.g. the burning of coal or use of nuclear energy. Other waste materials are released as by-product in production processes, for example blast furnace slag, steel slag and phosphorous slag. In the construction industry large amounts of materials are used that have to be extracted from the environment. Examples are limestone, clay, sand, gravel and rocks. Alteration of landscape (digging and dredging) also produces large amounts of material that has to be dealt with. Finally, waste products are also released during the use, maintenance and removal of products. Examples are municipal waste, paint removal waste, demolition waste, contaminated soil and all types of sludge. The destination of all these materials may be reuse, disposal or incineration, which also results in new and other waste products, e.g. ashes.

In environment related literature, materials are classified as being *primary* or *secondary* materials. Primary materials are raw materials extracted from the earth and used for the first time in a production process. Secondary materials are materials that are released during industrial processes and used again in a new production process. In a sustainable environment all material life cycles are closed. Replacing primary materials with secondary materials that are released in other processes has two advantages: (1) it results in continuation of the life cycle of the secondary material and (2) it saves natural resources of materials.

In the period from 1960 till 1980 the production of waste materials increased dramatically in the Netherlands. A large part was dumped at waste disposal sites without adequate soil protection. Another part was used in embankments or other construction works, without proper treatment. In later years these actions were found to result in soil and surface water pollution. A small part was treated and re-used in a controlled way (Eikelboom, 1999).

Both governments, industry and public have concluded that using natural resources should be limited and handling of waste materials should be controlled as much as possible to promote a sustainable development. In a densely populated country such as The Netherlands, in which space is limited and precious, such considerations are of particular relevance. All activities that may have a negative impact on space and soil such as dumping and digging should be limited and controlled. Soil contamination has to be prevented, because the soil often will be required for new activities (agriculture, housing etc.) and if it has to be cleaned first, this will increase exploitation costs substantially. This can be accomplished by the meeting following objectives:

- Protecting the quality of soil and surface water
- Decreasing the use and exploration of primary materials
- Decreasing the amount of waste materials to be disposed
- Decreasing the diffusion of environmentally harmful compounds
- Stimulating the re-use of waste materials

A policy has been developed to achieve a substantial decrease in the amount of waste that has to be disposed, as well as preventing that the treatment, re-use or disposal of the waste has negative effects on the environment, especially on the soil. To promote re-use of materials and still protect soil and surface water, the Building Materials Decree (in Dutch "Bouwstoffenbesluit") was introduced in the Netherlands, in which composition and leaching of primary and secondary construction materials is regulated (Ministry of VROM, 1995 and 1998). Of all regulations, this specific decree had main implications for the handling of waste materials.

Both the Dutch government and Dutch industry stimulate the policy of sustainable development and execute technical research and pilot projects to find new treatment techniques and ways of using secondary materials (Eikelboom, 1999).

For the waste industry, following the policy of sustainable development, means in practice that it has to find the right treatment technique for a specific waste, resulting in a durable material that can be handled and applied more safely than the untreated material. When such a treatment is successful, the resulting material can be considered for use as building material. In that case, the supplier of such a material will have to operate on the construction market and deal with its parties and regulations.

1.2 Properties of waste

Waste materials differ strongly in chemical composition and physical appearance. The toxic components found in waste streams include both organic and inorganic compounds. Organic compounds include aromatic compounds, polycyclic aromatic compounds (PAC's) and chlorated compounds. Inorganic compounds include both metals (cadmium, lead, zinc) and non-metals (phosphates, chlorides).

Waste forms can be liquid, sludge or solid, depending on their water content. The physical appearances of a waste stream include solutions, powders, blocks and construction parts.

Based on the properties of the waste, a treatment method has to be chosen before the material can be disposed or re-used in an ecologically sound way.

1.3 Public administration

In the Netherlands, all legislation on environment and waste has been converted into the Environmental Management Act, which came into force in 1993. This act aims at an integrated approach to environmental problems. The present waste policy in the Netherlands (CUR, 1999) is based on a sequence of priorities for dealing with waste that has to be followed as much as financially and technically possible. This order is used by the administrative authorities during set-up of environmental policy. The waste industry has to comply with the regulations that follow from this policy based on priorities. The sequence of priorities is given below and referred to as "The ladder of Lansink." The list starts with the most desirable action:

- Prevention or reduction
- Re-use in same production process
- Re-use without treatment
- Re-use after upgrading
- Volume reduction, separation
- Incineration
- Disposal after upgrading
- Disposal without treatment

Many technical and political programs were set into working to encourage prevention and re-use, develop new types of secondary materials and new ways of usage, or for finding better ways of dumping if no other solutions remained. This was done by funding technical research and example projects and by regulating the use and disposal of waste products in a more consistent way. The main purpose of this policy was that 90 % of the waste would be re-used in the year 2000 (Eikelboom, 1999).

Handling, treatment and application of waste-related materials are mainly regulated by three decrees. First, disposal is regulated by a landfill ban decree, which is based on a list of waste materials that are not allowed to be disposed of. Secondly, disposal is regulated by a landfill decree in which different categories of disposal sites and correspondingly different categories of wastes are defined. Based on the toxicity of the waste category to be disposed, the category of disposal sites has to meet certain conditions. Thirdly, for building materials, including waste-related materials, the Building Materials Decree (BMD) was introduced in the Netherlands. In this decree, composition and leaching of construction materials is regulated. It gives norms and conditions that should be obeyed when soil or construction materials are applied in the outside environment. The decree prescribes the maximum allowed concentration of organic substances in or leaching of inorganic substances from construction materials. This decree gives both the producer of waste and the possible consumer a legal reference. It also prescribes how products should be certified and how their application should be controlled. This decree was formulated in narrow collaboration with research institutes and industry (CUR, 1999).

All materials have to meet functional criteria before they can be applied or disposed. Several test methods are available and used in the decrees to distinguish different types of waste or building materials (CUR, 1995). Purpose of these test methods is to give insight into the composition, toxicity, leachability, strength and durability of the material. The total set of

criteria that the material has to meet depends strongly on its intended application. When application as a building material is intended, this implies that more rules have to be complied with compared with the case where disposal is the intention. For instance, strength may be of more importance in case of application as a construction material and would be less important in case of disposal.

1.4 Waste management

The application scope of waste-related materials varies from non-applicable (the material has to be disposed) to applicable as building material. When the waste is highly toxic or even radioactive, re-use is not an option and disposal under strict conditions is the only possibility. When the amount of toxic components in a waste stream is expected not to be harmful for the environment, it can be re-used directly, i.e. without any treatment. Some good examples of this case are the use of fly ash and blastfurnace slag in the cement industry and the use of bottom ashes for road construction.

In many cases the material has to be treated before it can be re-used or disposed safely. Such methods can improve the quality and correspondingly the application scope and price of the resulting product. Finding the right treatment techniques is the task of the waste industry. The following types of treatment can be distinguished:

- Separation, sorting
- Washing
- Volume reduction, compaction
- Solidification/Stabilization (S/S)

It is preferable when the costs and energy consumption of the treatment process necessary for upgrading the waste material to a usable product is limited. Especially when use as construction material is intended, the product has to satisfy all kinds of commercial demands (e.g. low price).

It is difficult to choose a treatment technique for a specific waste stream, because of the variations in composition, toxicity, shape and costs of the waste and because of the costs and possibilities of the techniques itself. Furthermore, when the final product is applicable as building material, the market for such materials has to be dealt with. The task of the waste industry is to find out for every waste stream what treatment and application scenario would be best, taking into account material and market aspects.

14

1.5 Solidification/Stabilisation

1.5.1 Definition and techniques

In many cases it is necessary or advantageous to treat waste before re-use or disposal. The goal of such a treatment is making a product that is more manageable and that has higher quality and better application possibilities. The best method to prevent diffusion of contaminants and making a manageable product is a process known as Stabilization/Solidification or S/S. In the Netherlands the term *immobilisation* is used and defined as follows (CUR, 1995):

A technical treatment, in which the physical and chemical properties of a waste material are altered in such a way that the dispersion of environmentally dangerous substances by leaching or erosion is decreased significantly.

The resulting solid product of S/S treatment is called the *immobilisate*. There are several types of S/S techniques available or being developed. These types can be classified into the following groups (CUR, 1997):

Inorganic binders. Commonly, inorganic binders are mixtures of calcium compounds, for example cement, fly ash and $Ca(OH)_2$. The binders are added to the waste and the resulting mixture hardens into a solid product. The contaminants are enclosed in the solid matrix and bound both physically and chemically. Additives can be used for improved chemical binding. Clays are also used, because of their sorption properties.

Organic binders. Organic binders are mixtures of hydrocarbon compounds. Commonly, the waste is mixed with bitumen, a substance that and is known for its use in asphalt. The resulting solid product after mixing is dense and water-resistant. Other binders are polymers. Binding can be both physical (final structure is dense and non-porous) and chemical (hydrophobic properties).

Thermal methods. The waste is heated up to 1000 ^{o}C (sintering) or 1500 ^{o}C (melting) and cooled down resulting in glassy or crystalline solid products. Organic compounds are broken down and volatile compounds are removed. This method is difficult, consumes a lot of energy (fuel) and requires high investment costs.

Chemical fixation. Specific compounds are added to the waste stream to bind specific contaminants. Disadvantage is the reversibility of this process under outside conditions (change in pH or oxidation).

1.5.2 The use of cement-based binders

Of all treatment techniques mentioned in the former section, the use of cement as an inorganic binder is most common. Cement was first used for solidification of radioactive waste, the resulting immobilisate being dumped in the sea or stored (Conner, 1990). Later, cement was recognised as an advantageous binder for all kinds of both organic and inorganic wastes. The advantages are numerous (Macphee and Glasser, 1993). The raw materials are cheap and readily available. The technique is simple and based on simply mixing waste, binders and additives (see Fig. 1.1). The solidified product, also referred to as the *immobilisate* can be solid or granular.
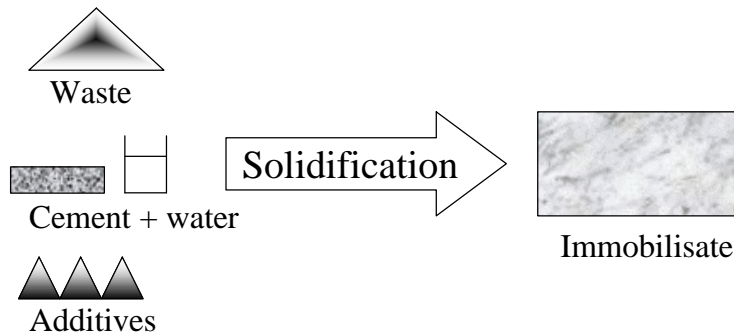
Figure 1.1. Principle of S/S using cement, yielding the immobilisate.

Application of cement to obtain solid products is a proven technology in the concrete industry from which equipment and standards are available (Macphee and Glasser, 1993). Cement can be combined with all kinds of additives that alter the products' final properties and make it a flexible technology. The product has good durability because of its strength and high alkalinity within its internal pore system. The solid product is relatively non-toxic and non-flammable. Cement can easily handle wet wastes because it needs water for its solidification itself. The energy consumption is low, investment costs are low and no new waste materials are released during the process. Disadvantages are the increase in mass and volume because of the addition of the binder, heat liberation and reaction with aluminium, causing gas evolution.

In this work the S/S process using cement as a binder will be studied because of its already successful application and its flexibility. When the waste industry decides to use cement as a binder, it has the choice between different types of cement to which different types of additives can be added. Thus, from these ingredients, a specific binder mixture can be designed for a specific waste.

1.5.3 Applications and problems in practice

From the former sections one can conclude that waste treatment has environmental advantages, that S/S treatment using cement as binder is expected to have the best result and that when S/S treatment is successful the product can be applied as construction material, implying additional environmental advantages. It is the task of the waste industry to do this. During the design of a waste/cement recipe the following two aspects have to be taken into account with respect to the material:

1. The final product must meet *functional* demands (e.g. strength) corresponding to its intended application.
2. The application of the final product must meet *institutional and commercial* demands, i.e. it must be applied within regulations and policies set and followed by authorities and industry in the market.

The simplest approach and order of actions with respect to waste treatment would be:
1. designing a cement/waste mixture based on experience with same types of waste streams,
2. mixing the waste with cement and water, 3. wait for strength development (solidification),
4. test the solidified product and 4. introduce the final product on the market (see Fig. 1.2).
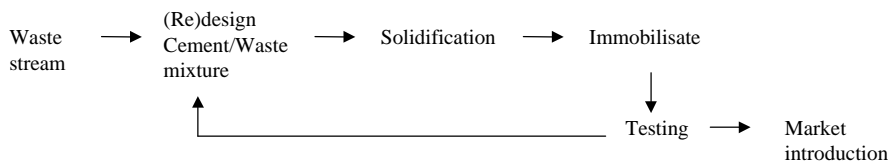
Figure 1.2. Empirical approach for waste treatment.

A more or less empirical approach as illustrated in Fig. 1.2 has been used in the past years in the field of waste treatment practice. One uses S/S techniques or materials that are known for their success in case of some waste material. When an immobilisate is obtained it is tested for leachability and exposed to extreme conditions in which contaminants are released. When these test results are not satisfactorily, the cement/waste recipe is changed with the purpose of obtaining an immobilisate that will meet the leach criteria. This empirical approach is based on adjusting the waste/cement recipe based on the test results of the obtained immobilisate. Although this approach works to a certain degree, there remain some problems. Some compounds found in most waste streams appeared difficult to bind by cement and are considered as critical with respect to strength development and leaching. A number of specific contaminants were found to have a negative influence on the solidification process. The presence of such a specific compound in a certain critical concentration has often lead to failure of the solidification process resulting in poor quality of the immobilisate (Conner, 1990, CUR, 1999). This problem can be summarised as follows:

17

When the initial design of a cement/waste mixture is mainly based on empirical knowledge about the waste stream and redesign of the mixture is based on test results for preliminary immobilisates, the final immobilisate may never obtain the desirable functional properties.

When S/S using cement has been applied on a waste successfully, an immobilisate is obtained that can be used as a construction material. However, even when the immobilisate satisfies all required functional properties, this has not always been sufficient for a successful market introduction as construction material. It is not accepted as an alternative for traditional materials or not accepted as a building material at all (CUR, 1999). This problem can be summarised as follows:

An immobilisate is not always accepted as a building material by the market, even when it has all required functional properties.

1.6 Improving the design and application of solidified products

1.6.1 The fundamental approach

To solve the problems with design and application mentioned in earlier sections, the mainly empirical approach is insufficient. First, there is a need for methods based on *fundamental* knowledge about the specific contaminants, the binder, the solidification process and the structure of the immobilisate, that can be used to find the right S/S recipe based on the properties of the waste and of the binder itself. Several technical developments and the availability of knowledge make such a more fundamental approach possible. All this fundamental knowledge about cement, waste and immobilisate can be used when designing cement/waste recipes. Contrary to the empirical approach, in which adjustments of the cement/waste recipe is mainly based on test results, in the fundamental approach such adjustments are based on knowledge about waste components, cement chemistry and structure of the immobilisate (see Fig. 1.3). Such an approach may reduce the amount of time and material necessary to develop a S/S recipe for a certain waste material or a specific problem contaminant.

Secondly, the characteristics of the market for building materials, i.e. its parties and regulations, should be taken into account with respect to immobilisates.

The fundamental approach and additional aspects to be taken into account during design and application are illustrated in Fig. 1.3. and will be explained in the next sections. This approach may give the waste industry better chances of obtaining an immobilisate that has the desired functional properties and can be introduced successfully as a building material.
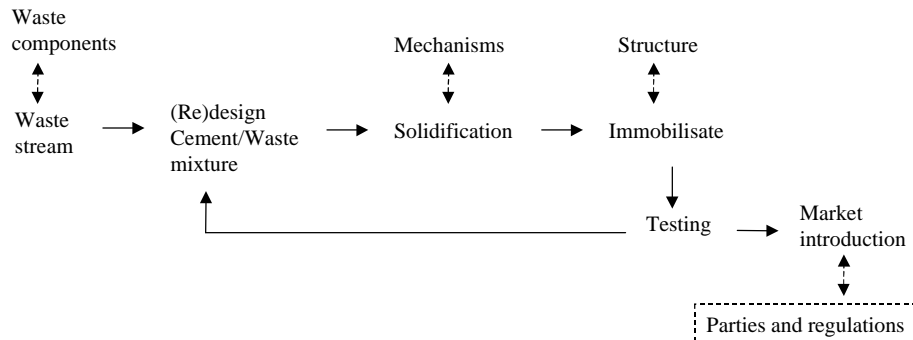
Figure 1.3. Fundamental approach for waste treatment

1.6.2 The solidification process. Cement hydration and the CEMHYD3D model.

The main mechanism taking place during solidification is cement hydration, i.e. the reactions between binder and water. Cement hydration has been studied in much detail using highly sophisticated analyzing techniques, for example SEM and XRD. As a result of this, the insight in the hydration reactions that take place and their effects on microstructural development has increased in the last decade. Hardening of a cement paste is the result of a complex set of hydration reactions and the formation of solid and stable compounds. This hydration process is characterised by chemical and physical changes in the microstructure of the hardening paste. The availability of increased computing power and random access memory (RAM) offered the possibility to represent a hydrating microstructure as a large collection of discrete volume elements and using cellular automaton rules and random walk algorithms to simulate the hydration process. A cellular-automaton is basically a computer algorithm that is discrete in space and time and operates on a lattice of sites. Such a method has been used by workers at the National Institute of Standards and Technology (NIST), who developed CEMHYD3D, a cement hydration computer model. This computer model has been successfully applied to describe and understand the microstructure development and the hardening process.

One can expect that such a computer model, which has a strong chemical and physical background, can also be used to understand why hardening of a cement/waste mixture is disturbed or fails. Therefore, all theories and mechanisms developed in this thesis will be implemented into this model.

1.6.3 Contaminants

With respect to S/S technology, fundamental knowledge about cement hydration has only been used since the last few years. Similar analyzing techniques as used in cement chemistry are being used to study the interaction between contaminants, unhydrated cement particles and hydration products. Several interfering mechanisms, recognised for different types of contaminants in waste streams, have been studied using these techniques.

1.6.4 Structure of the solidified product

Techniques that can be used to study solidified products have also been developed and applied. They have been used to study its strength, durability and leachability. This has resulted in new insights into the relation between the structure of a solidified product and its leaching properties. It makes it possible to determine the binding mechanisms involved in the cement-based S/S process. Furthermore, it gives opportunities to tailor the structure of the final product. The purpose of a cement hydration model, such as CEMHYD3D, is to predict composition and structure of the hardened sample. Such a predicted microstructure may be related to durability properties, e.g. leaching durability.

1.6.5 The construction market

The reason that introduction of immobilisates as building material has not always been successful is that in the market, financial and commercial aspects and additional demands play a significant role. More insight into this market could improve the chances for a successful introduction of immobilisates. Therefore the waste industry has to take into account all relevant market aspects, e.g. the parties of interest and the regulations and policies of interest. Knowledge about these aspects makes it possible to take them into account and using such knowledge at forehand will improve the chances of a successful introduction.

1.7 Outline of thesis

The two main goals of the study described in this thesis are the following:

1. **Using fundamental knowledge about cement, waste components, the solidification process and the final structure, to predict and improve the functional properties of the immobilisate.**

2. **Using knowledge about the market for building materials (i.e. its institutional and commercial parties and regulations) to improve acceptance of the immobilisate.**

To achieve these purposes, the following questions have to be answered in this thesis:

- What are the properties of the waste streams and what are the main components they contain?
- What effects do the waste components have on the solidification process?
- What effects do waste components have on the structure of the final immobilisate?
- How can these effects be modelled using CEMHYD3D?
- What is the relation between the structure of the immobilisate and its durability?
- How can waste industry use fundamental knowledge about binder, waste components and the solidification process when designing a binder/waste mixture?
- What institutional and commercial aspects of the market for building materials have to be taken into account when introducing an immobilisate?
- How should waste industry deal with regulations and policies set by the market to improve chances of a successful market introduction of immobilisate

In this thesis, the approach to be used to answer these questions will be strongly based on collecting relevant fundamental knowledge, modelling and comparing model results with the many experiments already presented in literature. Each chapter will start with a description of the latest knowledge, methods and models available, part of which will be used as a basis for improvements and extensions. Finally, the results are translated to recommendations and computation tools to be used by cement and waste industry during design and application of solidified products.

Waste producing industry has the task of finding, developing and choosing treatment techniques for their waste. This industry also has the task of introducing the final product. They may do this in collaboration with other industries, e.g. cement or waste treatment and handling industry. Therefore, the point of view of these types of industry will be used throughout this thesis.

The construction industry is considered as market because this industry is both the producer of waste materials and the consumer of waste products. It is strongly regulated by both private and public law. It is also a commercial market in which the customer must be convinced to use a product and the use of it should be financially advantageous.

Chapter 2 deals with cement hydration. In this chapter a sophisticated cement hydration computer model will be introduced. This model will be used for describing cement hydration, i.e. the solidification process and the corresponding structural development of cement-based materials.

Chapter 3 deals with pore water in hydrating cement mixtures. The pore water composition will be described and based on the chemical equilibria in pore water. The relevant equilibria will be implemented in the cement hydration model in such a way that pore water composition can be predicted as well.

Chapter 4 deals with hydration of cement/ fly ash mixtures. Fly ash is a major waste material and one of the main additives used in cement, and as binder in S/S as well. Its reaction is studied and described as a function of its composition and the composition of pore water.

Chapter 5 deals with the properties of waste materials of interest for solidification. Their effects on cement hydration will be described and the binding mechanisms will be dealt with. From this evaluation the main contaminants present in waste materials that should be studied in more detail are recognised. The main interference mechanism, coating of cement grains, will be defined and a model will be developed that describes this effect. This coating model will be implemented in the cement hydration model and modelling results will be compared with experiments.

Chapter 6 describes the link between material properties of the solidified product and it's leaching properties. The product properties that influence the leaching properties will be defined and ways of optimising the final structure will be presented.

Chapter 7 describes the problems that arise when the immobilisate is introduced as construction material. The parties and regulations of interest will be shown. Furthermore, it will be shown how the waste industry can deal with those parties and regulations when introducing new building materials. Application in the construction industry will be emphasized.

Chapter 8 summarises the conclusions of this thesis. Answers to the research questions will be presented, including strategies to be used by the industry during design and application of immobilisates.

Chapter 2

Hydration of cement: theory and modelling

2.1 Introduction

Cement paste, i.e. the mixture of cement and water, hardens as the result of hydration reactions and the formation of solid and stable hydration products. Hardened cement paste binds the aggregate (sand and gravel) in concrete (at construction site with ready mixed concrete) and concrete products (prefab). Hence, the development of properties of concrete is mainly determined by the cement paste. Production properties such as strength development, production rate, heat development and shrinkage result from the complex hardening process of the cement paste. Product properties as strength, elasticity, permeability (durability), crack growth etc. are governed by the properties of the hardened cement paste. Common additives used in concrete production are fly ash (FA) and silica fume (SF). These pozzolanic additives take part in the cement hydration reactions and contribute to the final product properties. Thus, understanding their reactions requires knowledge of the cement hydration.

Cement is the most common inorganic binder used for solidification and stabilisation (S/S) of waste in which many types of contaminants are present. To understand the effects of these contaminants on cement hardening and on the final properties of the immobilisate and to understand the mechanisms by which these contaminants are bound in the structure, a thorough knowledge of cement hydration is required.

In this chapter cement hydration and models that describe cement hydration and the properties of the hardened structure will be described. In section 2.2 some general definitions used in cement chemistry and some equations for mass and volume calculations are given. In section 2.3.1 the properties of cement are described, hydration of cement is described in section 2.3.2 in terms of mixture properties, reaction equations and time stages. In section 2.3.3 the structure of hydrated cement paste is described in terms of its main constituents and the changes of the corresponding volume fractions during hydration. Section 2.3.4 gives a relation between the volume fractions of constituents in hardened cement paste and its strength. In section 2.4 the cement hydration model CEMHYD3D is introduced. In section 2.4.1 its background is described and in section 2.4.2 its basic principles. In section 2.4.3 the output parameters produced by the model are described and in section 2.4.4 the model is calibrated for ENCI cements. In section 2.5 conclusions are drawn.

2.2 Definitions

The mass ratio of cement and water in the initial mixture is called the water/cement ratio, denoted w/c:

$$w/c = \frac{m_w^0}{m_c^0} = \frac{\rho_w \cdot V_w^0}{\rho_c \cdot V_c^0}$$

(2.1)

w/c = water/cement ratio
m_w^0 = initial water mass
m_c^0 = initial cement mass
ρ_w = density water
ρ_c = density cement
V_w^0 = initial water volume
V_c^0 = initial cement volume

In case of a mixture of binder components (e.g. cement, fly ash, silica fume) term water/solid ratio is used, denoted w/s:

$$w/s = \frac{m_w^0}{m_b^0} = \frac{\rho_w \cdot V_w^0}{\rho_b \cdot V_b^0}$$

(2.2)

w/s = water/solid ratio
m_b^0 = initial binder mass = $m_c^0 + m_{SF}^0 + m_{FA}^0$
ρ_b = binder density
V_b^0 = initial binder volume

Volume fractions in a microstructure or cement paste (including water and porosity) will be denoted as follows:

$$\varphi_i = \frac{V_i}{V_T}$$

(2.3)

φ_i = volume fraction component i in microstructure or (hydrated) cement paste
V_i = volume component i
V_T = total volume of all components in microstructure = $V_c + V_{hp} + V_p + \ldots$
V_c = volume of cement
V_{hp} = volume of hydration products
V_p = volume of (pore) water

24

In mixtures of solid binders, mass fractions of additions (e.g. silica fume or fly ash) are commonly given based on total mass of binder (no water). Such binder fractions will be denoted as follows:

$$\beta_i = \frac{m_i^0}{m_b^0} \tag{2.4}$$

β_i = mass fraction of addition i in binder
m_i^0 = initial mass of addition i

The total density of any material can be calculated from the densities of its components and its mass fractions or its volume fractions:

$$\rho_T = \frac{1}{\sum_i \frac{m_i}{m_T} \cdot \frac{1}{\rho_i}} \tag{2.5}$$

$$\rho_T = \sum_i \frac{V_i}{V_T} \cdot \rho_i \tag{2.6}$$

ρ_T = total density
i = component

Note that the total density of the material is inversely related to the mass fractions of its constituents. Eqs. (2.5-2.6) can be used to calculate the total density of a mixture from the fractions and densities of the mixture components (e.g. a mixture of cement and fly ash). The same equation can be used to calculate the density of one material from the fractions and densities of its components (e.g. cement clinker minerals).

Mass and volume fractions are related via the total density according to Eqs. (2.7-2.8). Note the use of inverse densities when calculating volume fractions from mass fractions.

$$\frac{m_x}{m_T} = \frac{\frac{V_x}{V_T} \cdot \rho_x}{\sum_i \frac{V_i}{V_T} \cdot \rho_i} = \frac{\rho_x}{\rho_T} \cdot \frac{V_x}{V_T} \tag{2.7}$$

$$\frac{V_x}{V_T} = \frac{\frac{m_x}{m_T} \cdot \frac{1}{\rho_x}}{\sum_i \frac{m_i}{m_T} \cdot \frac{1}{\rho_i}} = \frac{\rho_T}{\rho_x} \cdot \frac{m_x}{m_T} \tag{2.8}$$

2.3 Hydration of Portland cement

2.3.1. Production and properties

Cement is a hydraulic compound, i.e. it reacts with water, producing insoluble compounds and thus forming a solid product (Hewlett, 1998). Raw materials used for the production of cement include limestone, sand and clay, which are the main sources of CaO, SiO_2, Al_2O_3, Fe_2O_3 and many other oxides. Appendix 1 contains a complete overview of the conventional cement chemistry notation that will be used here. In this notation the formulae of common oxides are abbreviated to single letters, e.g. C = CaO, S = SiO_2, A = Al_2O_3, F = Fe_2O_3, $\bar{S}$ = SO_3 and H = H_2O.

Raw materials are heated in a kiln at temperatures up to 1450 ^{o}C. At this temperature the raw materials are converted into cement clinker. This clinker consists of clinker minerals, which are combinations of oxides. The main clinker minerals are given in Table 2.1, using cement chemistry notation. Names and composition of all cement minerals are presented in Appendix 2. The clinker is cooled and then mixed and grinded together with gypsum ($C\bar{S}H_2$) and anhydrite ($C\bar{S}$), which are materials that regulate setting of the paste. The final product is called Ordinary Portland Cement (OPC).

Table 2.1. Clinker minerals.

Compound	Name
C_3S	Alite
C_2S	Belite
C_3A	Aluminate
C_4AF	Ferrite

The chemical and mineralogical composition of cement strongly depends on the raw materials used and the heating and cooling process applied (Taylor, 1997). Characterisation of the distinctive mineral phases in cement clinker can be performed by combining BSE (Backscattered electrons) and XRD (X-Ray Diffraction) imaging techniques. In a BSE image, the phase having the highest average atomic number will show up the brightest and a distinction between mineral phases can be made. XRD is used for locating calcium, silicon and aluminium.

Mineralogical composition

The mineralogical composition can also be calculated quantitatively according to the modified Bogue method (Taylor, 1997). The Bogue method is a solution of a set of linear simultaneous equations, each giving the total fraction of one of the main oxides, namely CaO, SiO_2, Al_2O_3, Fe_2O_3 and SO_3, which can be measured in OPC. The total oxide contents in OPC come from the oxide contents of the main clinker and sulphate phases present, namely the oxides in C_3S, C_2S, C_3A, C_4AF and total sulphate phase. Each equation is a sum of contributions from each phase to the total oxide fraction.

26

When the oxide compositions of each phase are known, the following equation can be set up for each main oxide in OPC:

$$\sum_{ph} \frac{m_{ox}}{m_{ph}} \cdot \frac{m_{ph}}{m_c} = \frac{m_{ox}}{m_c} \qquad (2.9)$$

ph = phase (C_3S, C_2S, C_3A, C_4AF or sulphate (calcium and alkali sulphates))

ox = oxide (CaO, SiO_2, Al_2O_3, Fe_2O_3 or SO_3)

$\dfrac{m_{ox}}{m_{ph}}$ = mass fraction of oxide in mineral phase

$\dfrac{m_{ph}}{m_c}$ = mass fraction mineral phase in cement

$\dfrac{m_{ox}}{m_c}$ = mass fraction oxide in cement

In the standard Bogue equations the oxide fractions $\dfrac{m_{ox}}{m_{ph}}$ of the pure phases are used as parameters and all sulphates are assumed as being present as anhydrite ($C\bar{S}$) (see Table 2.2).

Table 2.2. Standard Bogue parameters $\dfrac{m_{ox}}{m_{ph}}$.

Mass fractions of oxides in pure phases (Taylor, 1997).

	CaO	SiO$_2$	Al$_2$O$_3$	Fe$_2$O$_3$	SO$_3$
C$_3$S	0.737	0.263	-	-	-
C$_2$S	0.651	0.349	-	-	-
C$_3$A	0.623	-	0.377	-	-
C$_4$AF	0.462	-	0.210	0.328	-
Sulphate	0.410	-	-	-	0.590

For example, when the total mass fraction of SiO_2 in OPC is 0.20, the unknown fractions of C_3S and C_2S appear in the following equation:

$$\frac{m_{SiO_2}}{m_c} = \frac{m_{SiO_2}}{m_{C_3S}} \cdot \frac{m_{C_3S}}{m_c} + \frac{m_{SiO_2}}{m_{C_2S}} \cdot \frac{m_{C_2S}}{m_c} = 0.20,$$

and using the parameters given in Table 2.2 gives:

$$0.263 \cdot \frac{m_{C_3S}}{m_c} + 0.349 \cdot \frac{m_{C_2S}}{m_c} = 0.20$$

Same equations are set up for all other known oxide mass fractions in OPC, giving the required number of equations to solve the unknown fractions of mineral phases.

The *modified* Bogue method uses the best available estimates of the oxide compositions of clinker phases as they are produced in the cement kiln. This gives more accurate results, because in real clinker phases small fractions of the main constituent oxides are substituted by other oxides. For instance silicate phases also contain small amounts of A and aluminate phases contain small amounts of S. The modified $\frac{m_{ox}}{m_{ph}}$ values are given in Table 2.3 and based on estimates of clinker and sulphate phase compositions, produced in modern cement kilns (Taylor, 1997).

Table 2.3. Modified Bogue parameters $\frac{m_{ox}}{m_{ph}}$.

Mass fractions of oxides in real OPC clinker and sulphate phases (Taylor,1997).

	CaO	SiO$_2$	Al$_2$O$_3$	Fe$_2$O$_3$	SO$_3$
C$_3$S	0.716	0.252	0.010	0.007	-
C$_2$S	0.635	0.315	0.021	0.009	0.010
C$_3$A	0.566	0.037	0.313	0.051	-
C$_4$AF	0.475	0.036	0.219	0.214	-
Sulphate	0.320	-	-	-	0.560

The total CaO mass fraction should be corrected for the amount of free CaO present in OPC. The set of five equations then can be solved for the unknown fractions of C$_3$S, C$_2$S, C$_3$A, C$_4$AF and total sulphates.

A typical cement clinker contains about 50 % (m/m) C$_3$S, 24 % C$_2$S, 11 % C$_3$A and 8 % C$_4$AF and a few % of alkali sulphates. Small differences in the oxide composition of the clinker have a significant effect on its corresponding mineral composition. For example a 2 % higher CaO content corresponds to a 20 % higher C$_3$S content at the expense of C$_2$S. Cements with special properties are sulphate-resistant cements (low in C$_3$A), white cements (low in C$_4$AF) and low alkali cements. To the cement clinker about 3-5 % (m/m) of calcium sulphates is added.

Particle size distribution (PSD)

OPC consists of particles that vary in size from about 1 to 100 μm. The particle size distribution (PSD) depends on the type and intensity of grinding that was applied. One of the methods that can be used to measure the PSD is laser granulometry. In this method light from a laser passes through a particle suspension either in air or in isopropyl alcohol and the PSD is calculated from the obtained diffraction pattern. A commonly used analytical expression that represents the PSD of cement is the Rosin-Rammler function (Taylor, 1997) that can be rewritten in the following form (Koenders, 1997):

$$G(d) = 1 - \exp(-b_{RR} \cdot d^{n_{RR}}) \qquad (2.10)$$

G(d) = cumulative mass fraction of the particles with diameter smaller than d
n_{RR} and b_{RR} are cement specific parameters describing its fineness.

When calculating the specific surface area (SSA) of a cement from its PSD, one must take into account the shape and sizes of the cement particles. Fair and Hatch (1933) discussed the geometry of particles of different shapes. The SSA of a sphere or a cube is 6/d, where d is diameter and length respectively. The value 6 was called shape factor and it was concluded that every shape has a constant shape factor which, when multiplied by 1/d (d is some characteristic size parameter, e.g. diameter or length), will give the SSA of that shape. This also holds for any irregular shape, despite the fact that its shape and size are difficult to define. Every shape should have a definite shape factor from which their definite SSA can be determined. This shape factor is minimal 6 in the case of spherical and cubic particles. Angular shaped particles have a shape factor of 7.7.

In (Taylor, 1997) an equation is proposed that can be used to calculate the SSA of a cement powder from the fractions of particles of equal mean diameter. Introducing the shape factor, denoted Sh, into this equation gives the following result:

$$\mathrm{SSA} = \mathrm{Sh} \cdot \rho_c \cdot 10^6 \cdot \sum_i \frac{f_i}{\overline{d_i}} \, , \qquad\qquad (2.11)$$

SSA = specific surface area in $[\mathrm{kg/m^3}]$
Sh = shape factor
ρ_c = cement density in $[\mathrm{kg/m^3}]$
f_i = fraction of particles with mean diameter $\overline{d_i}$
$\overline{d_i}$ = geometric mean particle diameter for fraction i [m]

where geometric mean diameter between diameter d_1 and d_2 is calculated as follows:

$$\overline{d} = \sqrt{d_1 \cdot d_2} \qquad\qquad (2.12)$$

The fractions of particles for each diameter are determined from the PSD curve by assuming that all particles in some diameter and corresponding fraction range have the same mean diameter. When all cement particles are assumed spherical and solid, Sh is 6. For a calculation starting from a PSD obtained using an X-ray sedigraph to give a specific surface area comparable to that obtained by an air permeability method (Blaine surface), Sh is typically about 6.8 (Taylor, 1997).

2.3.2. Cement hydration

The mixture of cement and water is called the cement paste (Hewlett, 1998). As soon as cement and water are mixed, cement hydration starts. Cement hydration is the totality of reactions taking place in the cement/water mixture resulting in setting and hardening of the paste. Setting is the loss of plasticity of the paste, making it a solid, but without measurable strength. Setting is immediately followed by hardening, meaning that the paste develops hardness and measurable strength. The properties of the final hardened product are strongly determined by (1) the composition of the initial cement/water mixture, (2) the progress of

hydration, i.e. the amount of cement that has reacted and is converted into solid hydration product and (3) the environmental conditions such as temperature and humidity.

The progress of hydration can be characterised by the fraction (m/m) or (V/V) of cement reacted and converted into hydration product at the corresponding moment. This fraction is called the *degree of hydration*, denoted α, where α is a function of time.

$$\alpha = \frac{m_c^r}{m_c^0} = \frac{V_c^r}{V_c^0} = 1 - \frac{V_c}{V_c^0} \qquad (2.13)$$

α = degree of hydration

m_c^0 = initial cement mass

m_c^r = reacted cement mass

V_c^0 = initial cement volume

V_c^r = reacted cement volume

V_c = current cement volume ($= V_c^0 - V_c^r$)

The degree of hydration of cement is not equal to the degrees of hydration of all separate clinker minerals because of their different reactivities. However, the overall degree of hydration is an important parameter for defining the current state of hydration. It correlates well with many different experimental parameters, e.g. the amount of water bound in hydration product or amount of released heat. The degree of hydration of C_3S, the main constituent of cement can be determined by X-Ray Diffraction (XRD).

When cement is mixed with water a large number of dissolution and precipitation processes is initiated. The water present in the original mixture will be strongly bound in the stable hydration products while remaining water is left in a fine network of water filled pores. Because the volume of hydration product is higher than the volume of the original binder it will replace the space that was first occupied by water. The formation of stable hydration products at the expense of water results in the fluid cement/water mixture being converted into a stony material.

Cement hydration is often described as the hydration of separate clinker phases. For an overview of symbols, compositions and names of compounds used in cement chemistry, see Appendices 1 and 2. The corresponding simplified reaction equations are as follows (Hewlett, 1998 and Taylor, 1997):

Silicates hydrate to calcium silicate hydrates (C-S-H) and calciumhydroxide ($Ca(OH)_2$ or CH). C-S-H is a nearly amorphous product of the general formula C_xSH_y where x is the C/S ratio and y is the H/S ratio, both varying over a wide range. C-S-H gel is also referred to as cementstone. It is the main contributor to strength in all cementitious systems. CH is a crystalline compound, also referred to as portlandite. C_2S will produce relatively less CH compared to C_3S.

$$2\ C_3S + 6\ H \rightarrow C_3S_2H_3 + 3\ CH \qquad (2.14)$$

$$2\ C_2S + 4\ H \rightarrow C_3S_2H_3 + CH \qquad (2.15)$$

30

Aluminate hydrates to hydrogarnet (C_3AH_6). This rapid reaction arises when there is no sulphate present and causes "flash set".

$$C_3A + 6\,H \rightarrow C_3AH_6 \qquad (2.16)$$

Aluminate and gypsum react to ettringite ($C_6A\bar{S}_3H_{32}$).

$$C_3A + 3\,C\bar{S}H_2 + 26\,H \rightarrow C_6A\bar{S}_3H_{32} \qquad (2.17)$$

Ettringite is a mineral that is structurally similar to the (Al_2O_3-Fe_2O_3-tri) mineral group and therefore is often referred to as the AFt phase.

Ettringite is converted into monosulphate ($C_4A\bar{S}H_{12}$) when the sulphate concentration becomes low.

$$2\,C_3A + C_6A\bar{S}_3H_{32} + 4\,H \rightarrow 3\,C_4A\bar{S}H_{12} \qquad (2.18)$$

Monosulphate is also referred to as the AFm phase because of the structural similarity with (Al_2O_3-Fe_2O_3-mono) minerals.

Hydration reactions of C_4AF are similar to C_3A, but aluminium in the reaction products may be replaced by iron and also an iron/aluminium-hydroxide is formed. The reactions are as follows ((A,F) means A *or* F):

$$C_4AF + 9\,H \rightarrow C4(A,F)H_6 + (A,F)H_3 \qquad (2.19)$$

$$3\,C_4AF + 12\,C\bar{S}H_2 + 110\,H \rightarrow 4\,C_6(A,F)\bar{S}_3H_{32} + 2\,(A,F)H_3 \qquad (2.20)$$

$$3\,C_4AF + 2\,C_6(A,F)\bar{S}_3H_{32} + 14\,H \rightarrow 6\,C_4(A,F)\bar{S}H_{12} + 2\,(A,F)H_3 \qquad (2.21)$$
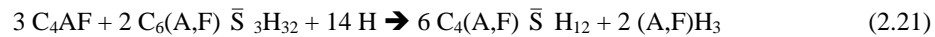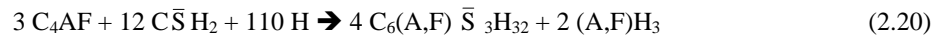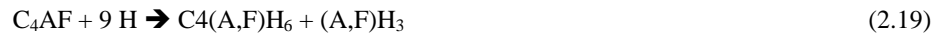
Reactive silica (S) (present in silica fume and fly ash) reacts with CH and produces pozzolanic C-S-H. Young and Hansen (1987) propose the following reaction equation:

$$S + 1.5\,CH + 2.3\,H \rightarrow C_{1.5}SH_{3.8} \qquad (2.22)$$

This so-called pozzolanic reaction lowers the CH content in the microstructure.

Cement hydration is the sum of the reactions given above and can be characterised by four different time stages (Hewlett, 1998):

Pre-induction period (first minutes after mixing). Alkali sulphates dissolve completely, producing K^+, Na^+ and SO_4^{2-} ions. Calcium sulphate dissolves until saturation, contributing Ca^{2+} and additional SO_4^{2-}. C_3A dissolves and reacts with Ca^{2+} and SO_4^{2-} ions present in the liquid phase, yielding ettringite, which is present in the form of rods on the aluminate surfaces.

31

Induction or dormant period (first few hours). After the initial period the overall hydration rate slows down significantly for a period of a few hours. Several explanations have been proposed for this phenomenon (Taylor, 1997):

1. The initial reactions form a protective layer on the cement particles; induction period ends when this layer becomes more permeable by structural changes.
2. The initial reactions form a semipermeable membrane around the cement particles which encloses an inner solution and is destroyed by osmotic bursting.
3. The induction period ends and hydration accelerates when C-S-H starts to nucleate and grow.
4. The induction period is caused by poisoning of CH nuclei by SiO_2 and ends when the level of supersaturation of CH is sufficient to overcome this effect.

According to (Taylor, 1997) a combination of hypotheses (1) and (3) is most likely.

Acceleration period (3-12 hours). Hydration accelerates again and is controlled by the nucleation and growth of the resultant hydration products. This is accompanied by strong heat evolution. The rate of C_3S hydration increases significantly and mainly C-S-H and CH are formed. The C-S-H layer grows to a thickness of about 1 μm around the cement particles and contact will be made with C-S-H layers on adjacent cement grains resulting in binding and strength development. CH is formed as massive crystals in the water and fills space between cement grains. Ettringite formation continues.

Post-acceleration period (12 hours and later). In this period the hydration slows down gradually, as the amount of still unreacted material declines and the rate of the hydration process becomes diffusion-controlled. The C-S-H phase continues to be formed due to the continuing hydration of both C_3S and C_2S. The contribution of C_2S increases with time and, as a consequence, the rate at which additional CH is formed declines. After the supply of calcium sulphate has become exhausted, the sulphate concentration in the liquid phase declines. As a consequence, the ettringite that has been formed in the earlier stages of hydration starts to react in a through-solution reaction with additional C_3A and C_4AF, yielding monosulphate.

2.3.3. Structure of hydrated cement paste

Powers and Brownyard (1948) developed a model that can be used to describe hardened cement paste (hcp) at different w/c ratios and degrees of hydration. This Powers-Brownyard model is largely based on non-evaporable and total water measurements and water vapour sorption isotherms. From these experiments they estimated densities for several components in hcp and were able to describe it from the *volumetric* point of view. The model can be summarised as follows (Taylor, 1997).

Hcp consists of (a) unreacted cement, (b) hydration product and (c) capillary pores. The water in the paste is categorised as evaporable and non-evaporable as defined earlier. Evaporable water includes water in the capillary pores and "gel water", defined as the water present in the gel pores of the hydration product. The hydration product was considered to

32

have fixed contents of non-evaporable water and gel water in gel pores. The hydration product occupies more space than the cement from which it is formed, so the total volume of solids (cement and hydration product) will increase as a result of cement hydration. In hydrating cement paste the volume of water thus decreases while the volume of hydration product (and thus gel pores and non-evaporable water) increases. The remaining water was assumed to be present in capillary pores (Fig. 2.1).

When water is converted into chemically bound water, its density decreases by 25 %. Therefore the volume of hydration product is lower than the sum of cement and water volume from which it was formed. This effect is known as chemical shrinkage and has a value of about 0.06 ml shrinkage per gram of reacted cement. This volume reduction is compensated by adsorbing water or air under water saturated or sealed conditions, respectively.
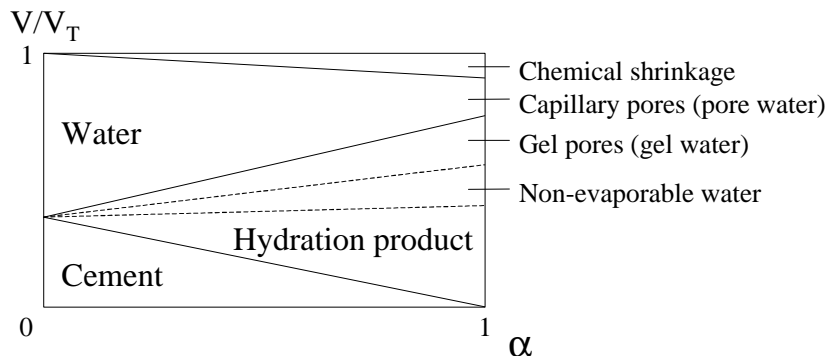
Figure 2.1. Changes in volume fractions during cement hydration.

From many experiments under water saturated conditions they found that complete hydration cannot occur if w/c is below 0.38. When such paste is fully hydrated, it consists entirely of hydration product, which in that case includes 0.227 kg of non-evaporable water and 0.211 kg of gel water per kg reacted cement.

From experiments under sealed conditions where no external water can be adsorbed, they concluded that when the w/c ratio is below 0.44, there will be insufficient water to fill gel pores and capillary pores completely. Hydration will become very slow or even stop, even though free space is still available for the formation of reaction products. This phenomenon is called *self-desiccation* and causes changes in pore structure and final strength.

The availability of analytical techniques e.g. XRD, NMR and electron microscopy has given more insight into the structure and properties of the hydration products. The most important products will be described here.

C-S-H. The main component in hydrated cement paste is C-S-H, also referred to as cementstone. The C/S ratio of C-S-H in mature pastes varies between 1.4 and 2.0, the value around about 1.7 being most probably correct (Taylor, 1997). There is controversy concerning the dependence of the C/S ratio on degree of hydration. Four morphological types of C-S-H can be distinguished with SEM techniques. At early ages Type I C-S-H is found, a fibrous material, with fibre lengths of about 2 μm long. Type II C-S-H is also an early hydration product, with a honeycomb or rectangular structure. Type I and II C-S-H are referred to as

"outer products" because they are formed on the surfaces of the original cement grains. In older pastes type III and type IV C-S-H are found, more massive and featureless materials. Type IV C-S-H is referred to as "inner product" because it is formed in the space that was originally occupied by cement minerals, i.e. within the original cement grains. Inner and outer C-S-H are considered as the main morphological varieties in hydrated OPC. C-S-H has a very high internal surface area because it contains a network of nanometer sized pores, called gel pores.

CH. Crystalline $Ca(OH)_2$ (CH), also referred to as portlandite, is the second most abundant product in hydrated Portland cement paste. It is present in the form of relatively large crystalline aggregates. CH is the main source of OH^- , which gives the internal pores in hardened cement paste its high pH.

Water. The water present in a water saturated hydrated cement paste may be divided into several categories (Taylor, 1997). It may be bound within the structure of C-S-H (chemically bound or crystal water), bound in the form of OH^- ions within the crystalline lattice of CH, physically bound in the gel pores of C-S-H or it may be present in the capillary pores. The definition of these types of water is not sharp, because of the blur distinction between gel pores and capillary pores and because results from water content measurements depend strongly on experimental conditions.

The most highly hydrated state of a cement paste is obtained when the system is water saturated and all pores are totally filled with water. For nearly saturated C_3S pastes, Young and Hansen (1997) concluded that the composition of C-S-H was approximately $C_{1.7}SH_4$, corresponding to a H/S ratio of 4. Determination of chemically bound water, (which includes the total H content in CH and the strongest bound H in C-S-H), is done by equilibrating a cement sample with an atmosphere of 11 % Relative Humidity (RH). Young and Hansen (1987) found the composition of C-S-H in such paste to be $C_{1.7}SH_{2.1}$. A more common experimental procedure is known as D-drying. In this method, the sample is equilibrated with ice at –79 ^oC. An equivalent procedure is heating to constant mass at 105 ^oC. These processes remove all pore water and physically bound water, but also part of chemically bound water. Water that is retained after such methods is known as non-evaporable water, which is less than the amount of chemically bound water. The results correspond with a H/S ratio of 1.3-1.5 in C-S-H. Finally, Powers and Brownyard (1948) called the water lost from C-S-H when going from the fully saturated to the D-dried condition evaporable water, which includes both pore water and water physically bound in C-S-H gel pores, which they called "gel water".

Young and Hansen (1987) proposed the following reaction equation for the hydration of C_3S under water saturated conditions:

$$1 \text{ } C_3S + 5.3 \text{ } H \rightarrow C_{1.7}SH_4 + 1.3 \text{ } CH \tag{2.23}$$

Based on the 5.3 moles of water used in this reaction, the different definitions for types of water in hydration products are summarised in Fig. 2.2.

Distribution of 5.3 moles of H

CH	C-S-H			Pore water	Method to remove:
1.3	1.4	0.7	1.9		
Non-evaporable	Gel		Evaporable		D-dry or 105 ºC ⟹
Chemically bound			Physically bound		11% RH ⟹

Figure 2.2. Definitions of different types of water (based on 5.3 moles of H) in hardened cement paste (Powers and Brownyard, 1948, Young and Hansen, 1987, Taylor, 1997).

Other constituents. The presence of AFt and AFm phases depend on the available amount of sulphate in the system and the maturity of the paste. During the hydration process, the amount of AFt reaches a maximum and then declines when it is converted to AFm. In mature pastes the AFt phase may be completely absent. Other minor constituents in the hydrated paste include hydrogarnet ($C_3(A,F)H_6$), iron or aluminium hydroxides (($A,F)H_3$), hydrotalcite ($Mg_3Al(OH)_8(CO_3)_{0.5}.2H_2O$) and brucite ($Mg(OH)_2$).

Porosity and pore water. Hardened cement paste includes a wide variety of pores ranging in diameter from nanometers (gel pores in C-S-H) and micrometers (capillary pores) up to millimetres (air voids). Capillary pores are generally filled with water, which is referred to as *pore water* or pore fluid. Under some conditions they can be empty (vacuum). During early hydration pore water concentrations change where in mature pastes it reaches an equilibrium with the solid hydration products in contact with it. In general the pore water contains high amounts of alkali ions (K^+ and Na^+) and hydroxyl ion (OH^-) giving it a pH of 12-13. Furthermore, it contains Ca^{2+} and SO_4^{2-} ions and low amounts of silicate and aluminate ions.

2.3.4. Calculation of strength

The strength of ordinary mortar and concrete is mainly determined by the strength of the hcp. Factors determining the compressive strength of cement paste include: (a) characteristics of the cement such as clinker composition, gypsum content and PSD, (b) the w/c ratio and contents of air and admixtures, (c) mixing and curing conditions, (d) age and (e) testing conditions. C-S-H contributes most to strength and therefore hydration of C_3S and C_2S are most characteristic for strength development. Because of their different reactivities C_3S contributes mainly to early strength and C_2S contributes mainly to long-term strength.

Powers (1962) found that the strength of mortar cubes is related to the gel-space ratio. This ratio is equal to the volume of hydration product divided by that of hydration product plus capillary porosity as defined in the Powers-Brownyard model. It can be calculated as follows:

$$\Phi = \frac{V_{hp}}{V_{hp} + V_p} = \frac{0.68 \cdot \alpha}{0.32 \cdot \alpha + w/c} \qquad (2.24)$$

Φ = gel/space ratio
V_{hp} = volume of hydration product
V_p = volume of porosity

Compressive strength of mortar cubes is then related to this gel-space ratio according to the relation:

$$F_{com} = F_{int} \cdot \Phi^n \qquad (2.25)$$

F_{com} = compressive strength in [N/mm^2]
F_{int} = intrinsic strength of the cement gel in [N/mm^2]
n = parameter

The intrinsic strength F_{int} depends on clinker composition and n takes on values between 2 and 3. This relation is empirical, but shows the importance of degree of hydration and w/c ratio.

2.4 CEMHYD3D

2.4.1. Background and history

An overview of the backgrounds and development of cement hydration models will be given and is based on Jennings et al. (1996) and an overview given by Bentz (1997).

One definition for a model is a "theoretical and mathematical representation that predicts experimental observations". Models can develop predictions within, or outside of, existing data sets. However, since a model incorporates several assumptions it should always be considered as a simplified representation of reality. It can be accepted as a theory when it consistently gives accurate predictions. Then, the model can be used to obtain information about a system without direct experimentation, which may be costly, time consuming, dangerous or even impossible.

Models may be divided into two categories: constitutive models and simulations. A constitutive model deals only with the observed patterns in properties and the underlying mechanisms are assumed but not directly used in such model. This is also referred to as a black-box approach. In a simulation model, such underlying mechanisms are used directly and implemented as a set of processes.

The basis of all models describing properties of cement-based materials is its microstructure. This microstructure can be seen directly using microscopic techniques or its properties are implied by other measurements, e.g. water evaporation or sorption experiments. Combination of these techniques gives information about volume fractions and distribution of hydration product and porosity. Model inputs include composition and PSD of cement grains, w/c ratio and curing conditions, and typical outputs include mass or volume fractions of

36

phases in a paste, content of non-evaporable water, cumulative heat evolution or physical properties such as strength, porosity or permeability, defined in various ways (Taylor, 1997).

Powers (1962) developed a model based on the assumptions mentioned earlier. From this model a set of equations was derived in which volume fractions of unhydrated cement, hydration product and capillary pores in a hydrating cement paste are related to degree of hydration and w/c ratio (Table 2.4).

Table 2.4. Volume fractions φ_i (see Eq. 2.3) in hydrating cement paste.

Powers (1962)	Young and Hansen (1987)	
Cement: $\dfrac{0.32(1-\alpha)}{w/c+0.32}$	C_3S: $\dfrac{0.31(1-\alpha)}{w/c+0.31}$	
Hydration product: $\dfrac{0.68\alpha}{w/c+0.32}$	C-S-H: $\dfrac{0.54\alpha}{w/c+0.32}$	
	CH: $\dfrac{0.19\boldsymbol{a}}{w/c+0.32}$	
Capillary pores: $\dfrac{w/c-0.36\alpha}{w/c+0.32}$	Capillary pores: $\dfrac{w/c-0.41\alpha}{w/c+0.31}$	

In the reaction equation for C_3S proposed by Young and Hansen (1987) (see Eq. 2.23) a distinction was made between C-S-H and CH in the hydration product. From this *molar* reaction equation and the product densities assumed by Young and Hansen (1987), equations can be derived for the corresponding *volume* fractions in hydrating cement paste also (Table 2.4).

The equations from Powers (based on cement) and the equations from Young and Hansen (based on C_3S) show a few differences. The values of 0.32 and 0.31 in the numerators arise from the reciprokes of the densities of cement (3.17 g/cm^3) and C_3S (3.21 g/cm^3) respectively. Young and Hansen predict more hydration product (C-S-H + CH) and less capillary pores. The reason for this is that they did not take into account chemical shrinkage and thus assigned relatively more water to hydration product. This results in a higher volume of hydration product to be formed per volume of cement (2.34 compared to 2.20). The models of Powers and Young and Hansen show the importance of degree of hydration and w/c ratio but do not relate the calculated volume fractions to real time.

Jennings and Johnson (1986) developed the first simulation model that attempted to simulate hydration and development of microstructure directly. They started with representing an initial cement/water paste by placing spherical C_3S particles with a prescribed PSD in a specified water volume. Then, a computer algorithm is started that cyclically reacts small volumes of C_3S and forms the appropriate volumes of C-S-H and CH. During the process the radii of C_3S spheres decrease and the particles are enveloped by shells of hydration product whose thickness increases. CH crystals were allowed to grow in remaining pore space. This

37

model is classified as being of the continuum type or vector type, because each particle can be described by its location and a set of radii corresponding to the unhydrated core and one or more shells of hydration product. A similar continuum approach was formulated by Van Breugel (1995). This approach also accounted for stereological aspects such as the embedded volumes of hydrating cement particles. The model can be classified as a kinetic model, because it incorporates the most important aspects of kinetics on the hydration rate and uses a sophisticated rate equation that includes temperature, reaction kinetics and diffusion rate. The cement PSD, C_3S/C_2S ratio and the w/c ratio are explicitly included in the rate equations and therefore influence hydration behaviour explicitly.

Thermodynamic models attempt to predict the equilibrium phase composition of a cement/water system based on phase equilibria. They assume that in a hydrated system all cement solid phases are in equilibrium with the pore water. Damidot and Glasser (1995) did pioneering work creating phase diagrams for cementitious solids and defining the corresponding equilibria constants. Using these equilibrium constants and methods for calculating activity coefficients in pore water, dissolution/precipitation programs are developed that calculate phase compositions and pore water concentrations in cementitious systems. The results depend strongly on the availability of equilibrium data and phase compositions assumed and only calculate the final equilibrium state, not the time to reach it.

The availability of increased computing power and random access memory (RAM) offered the possibility to represent a hydrating microstructure as a large collection of discrete volume elements and using cellular automaton rules and random walk algorithms to simulate the hydration process. Such models can be classified as being of the discrete type, because a particle is represented by discrete locations of its constituent elements. of A cellular automaton is basically a computer algorithm that is discrete in space and time and operates on a lattice of sites (Gutowitz, 1991). Starting from an initial configuration, at each iteration the state of each site is updated based on its current value and the current value of one or more neighbouring sites. Although often relatively simple in structure, the behaviour produced in these systems can be quite complex. Cellular automata have been applied successfully in materials science and biological systems. Bentz and Garboczi (1991) used this approach to develop cement hydration models. The microstructure was represented by a matrix of pixels, with a resolution of 1 μm, each representing a relevant phase (e.g. cement mineral phase, C-S-H or CH phase or water/porosity phase). Algorithms were developed for simulating dissolution, diffusion, reaction and nucleation of phases. A simulation consists of hydration cycles in which part of the cement particles are dissolved and converted into the appropriate reaction products similar to the continuum models of Jennings and Van Breugel. The model evolved from one based on a 2D representation and the hydration of C_3S only to one based on a 3D representation and based on all major cement phases, including aluminate and sulphate phases. This latest model is called CEMHYD3D.

CEMHYD3D, the model by Bentz and Garboczi is considered as the most advanced and evolved cement hydration model presently available, because it is a 3D model and because it includes all major cement mineral phases and reaction products. The input is straightforward and typically consists of the w/c ratio and both chemical composition and PSD of the cement. From this information the model predicts a number of properties including development of strength and heat. It is based on fundamental knowledge about hydration reactions and hydration products. Finally, the cellular automaton approach is very

38

flexible. New information can be implemented by simply adding new phases or rules. Because of these advantages, this model was chosen for use and extension in this study.

2.4.2 Basic principles

As said, CEMHYD3D is a 3D microstructural cement hydration model that has been developed by Bentz and Garboczi at the National Institute of Standards and Technology (NIST) and in which cement can be represented by its four main clinker phases (Bentz, 1997).

In the present model a hydrating cement paste is represented by a 3D box of $100 \cdot 100 \cdot 100$ pixels, each representing 1 μm^3. An initial microstructure is generated according to the water/solid ratio, the mass fractions of all mixture components, i.e. cement, fly ash, silica fume and inert filler and the corresponding PSD of each mixture component. The (mineralogical) composition of each mixture component can also be given as input parameters.

A digitised spherical particles consists of a group of pixels placed in the best spherical shape possible. A 1 μm particle is represented by 1 pixel. A 3 μm particle is based on a cube of $(3 \cdot 3 \cdot 3)$ pixels where on each corner 1 pixel is removed. This results in a 19 pixel particle (Fig. 2.3). Larger particles are based on larger cubes less some pixels on corners and along the sides.
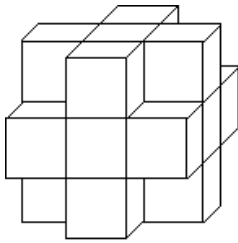
Figure. 2.3. Digitised 3 μm (19 pixels) particle.

In Appendix 3, for each particle diameter used in CEMHYD3D, the numbers of pixels from which such particle is build, is given. As can be seen from this list, the particles have discrete odd diameters in the range of 1 to 39 μm. The reason for this is that each digitised particle can be build from pixels grouped around one pixel in the centre (like in Fig. 2.3). In CEMHYD3D the particles can be placed in the initial box by giving the diameter and the number of particles of that diameter to be placed.

An initial microstructure is generated by placing digitised spherical particles in the 3D box at random locations from largest to smallest with periodic boundaries (see Fig. 2.4). The presence of aggregate, which size is an order of magnitude higher than the cement particle sizes, can be simulated by placing an inert plane in the box before the particles are placed. In this way, wall effects can be simulated.

Creating a diameter table from a PSD

Instead of giving numbers of particles it would be useful to have a list of diameters and corresponding normalised mass fractions of particles of that diameter. This list could then be

used to calculate numbers of particles from the total amount of material to be placed, e.g. from the w/c ratio and fractions of additives. A routine was developed to generate such a diameter lists from a PSD.

In The Netherlands, the ENCI company is the main producer of cements. Three ENCI Portland cement types CEM I 32,5 R, 42,5 R and 52,5 R (different in PSD only) were used. First, continuous Rosin–Rammler distributions were assumed for these three cement types using Eq. 2.10 and parameters given by Koenders (1997) and shown in Table 2.5.

Table 2.5. Rosin-Rammler PSD parameters from (Koenders, 1997).

	CEM I 32,5 R	CEM I 42,5 R	CEM I 52,5 R
n_{RR}	1.107	1.076	1.03
b_{RR}	0.023	0.041	0.067

To check these parameters calculated SSA were compared with measured SSA (Blaine surface) for the three cements. Using Eq. (2.11) and a shape factor $Sh = 6.8$ (Taylor, 1997) theoretical SSA were calculated numerically from the Rosin-Rammler curves with intervals between d_i and d_{i-1} of 1 µm.

$$SSA = Sh \cdot 10^6 \cdot \rho_c \cdot \sum_i \frac{G(d_i) - G(d_{i-1})}{\sqrt{d_i \cdot d_{i-1}}} \qquad (2.26)$$

The calculated SSA were found to be in good agreement with measured SSA for CEM 32,5 R and in reasonable agreement for CEM 42,5 R and 52,5 R (see Table 2.6). From these results it was concluded that Rosin-Rammler distributions based on the parameters given in Table 2.5 are a good representation of the PSDs of ENCI cements.

Then this generated continuous size distribution was converted to a list of discretised odd diameters ranging from 1 to 39 µm with for each diameter the normalised mass fraction of particles of that diameter. The 1 µm particles represented the mass fraction below 2 µm, the 3 µm particles corresponded with the 2 – 4 µm fraction and 39 µm particles represented all particles larger than 38 µm. The discretised PSDs determined for CEM 32,5 R, CEM 42,5 R and CEM 52,5 R are given in Appendix 3.

The initial volume fraction of cement to be placed in an initial microstructure that consists of cement and water only, can be calculated from the w/c ratio as follows:

$$\varphi_c^0 = \frac{V_c^0}{V_c^0 + V_w^0} = \frac{1}{(\rho_c \cdot w/c) + 1} \qquad (2.27)$$

From this φ_c^0 and the total number of pixels in the 3D box (10^6), the total amount of cement pixels to be placed can be determined. From this number and the mass fractions in the generated diameter tables, the numbers of particles of each diameter were calculated and placed in the 3D box.

The internal surface area of the digital water/cement mixture follows from the number of pixel sides (each 1 µm^2) adjacent to a water pixel. These pixel sides are exposed to water

and will be found at the surfaces of cement particles. The SSA of the digitised cement can be calculated in cm²/g using Eq. (2.28):

$$SSA = \frac{SA_c}{m_c^0} = \frac{n_{sides}^{exp}}{\varphi_c^0 \cdot \rho_c \cdot 10^6} \cdot 10^4 \qquad (2.28)$$

SA_c = internal surface area of cement in [μm^2]
n_{sides}^{exp} = number of cement pixel sides exposed to water in [μm^2]
10^4 = unity conversion factor [$\mu m^2/\mu m^3$] to [cm^2/cm^3]

The specific surface areas of the resulting digital samples were calculated using Eq. (2.28) and an overall density of 3.19 g/cm³ that was calculated using the mass fractions and densities of clinker minerals according to the equation used for calculating the overall density of a mixture of solids (see Eq. (2.5)). Table 2.6 contains the results of these calculations.

Table 2.6. Calculated and measured SSA (in [cm²/g]).

	CEM I 32,5R	CEM I 42,5 R	CEM I 52,5 R
Measured Blaine surface	2700	4200	5500
Calculated SSA (Rosin-Rammler PSD, Sh = 6.8)	2569	3711	4990
Calculated SSA (Rosin-Rammler PSD, Sh = 6)	2273	3284	4416
Calculated SSA (Digitised PSD)	2707	3666	4560

When explaining the observed differences between the digital surface areas and the surface areas calculated from the Rosin-Rammler distribution one should consider two things: the fact that the digitised structure represents a water/cement mixture in which particles are not dispersed and the surface to volume ratio of digitised spheres. A digitised particle has a shape factor of about 8.9, which is 1.5 times that of a spherical particle. An exception is formed by single pixel particles (1 μm^3 particles) which are exactly cubic and have the exact same shape factor as spheres. Therefore one should expect the digital surface to be higher than surfaces calculated from the Rosin-Rammler PSD using shape factor 6. The difference however, is not as high as one would expect, because the presence of the 1 μm digitised particles fraction is responsible for the main part of the total surface for both cement types and this results in a mean shape factor that is somewhere in between the values mentioned. Furthermore, in case of low w/c ratio, i.e. high cement fraction in the paste, a significant amount of the surface of this fraction is unavailable after the particle placement routine. The 1 μm pixels are placed after positioning of all larger particles in the 3D box, which results in a significant amount of 1 pixel particles that will be placed at positions directly adjacent to other particles. This will result in the reduction of two or more surface planes, because these planes are not exposed to water anymore. This means that a significant part of the 1 μm particles does not contribute to the SSA in a digitised microstructure.

The lists of diameters and mass fractions generated here for the three ENCI cements are presented in Appendix 3. These lists were used to calculate numbers of digitised spherical particles to be placed from the w/c ratio. The values and trends found for calculated SSA agreed well with measured SSA of real cements. The diameter tables give a good representation of the PSD of the cements. The routine described here can also be used to create diameter tables for other materials, e.g. gypsum and fly ash.

Phases

After placement of spheres in the 3D box each pixel is assigned to be a single phase. Table 2.7 gives an overview of all possible phases and their properties.

Table 2.7. Properties of the phases used in CEMHYD3D (Bentz, 1997).

Name	Density (g/cm^3)	Molar volume (cm^3/mole)	Molar mass (g/mole)	Heat of formation (kJ/mole)	Dissolution probability
C_3S	3.21	71.0	228	-2928	0.80
C_2S	3.28	52.0	171	-2312	0.15
C_3A	3.03	89.1	270	-3588	0.80
C_4AF	3.73	128.0	477	-5090	0.10
Gypsum	2.32	74.2	172	-2023	0.05
Hemihydrate	2.73	53.2	145	-1575	0.15
Anhydrite	2.61	52.2	136	-1425	0.04
$C_{1.7}SH_{4.0}$	2.12	108.0	229	-3283	
$C_{1.1}SH_{3.9}$ (pozzolanic)	1.69	101.8	172	-2299	
CH	2.24	33.1	74	-986	
Ettringite	1.70	735.0	1250	-17539	
AFm	1.99	313.0	623	-8778	
Hydrogarnet	2.52	150	378	-5548	
FH_3	3	69.8	209	-824	
S	2.20	27.0	59	-908	
H	1	18.0	18	-286	

Initially, only the phases C_3S, C_2S, C_3A, C_4AF, gypsum, anhydrite, hemihydrate, pozzolan, inert and water are present. Assigning phases to each pixel in all digitised particles can be performed in two ways. It can be done totally random resulting in a homogeneous phase distribution or it can be done using auto-correlation functions derived from 2D segmented SEM images (Bentz and Stutzman, 1994). This will result in clusters of pixels of equal phases. For both methods the result must match the measured phase volume fractions, given as input. Silica fume can be represented by pixels of 1 μm^3 each of S (vitreous, reactive S) and Inert (non-reactive) phase, corresponding to the reactive glass fraction in silica fume.

Reactions

Cement hydration is simulated by operating series of cellular automata-like rules on the original 3D box, continuously changing the phases of pixels. Rules are provided for the dissolution of solid material, diffusion of the generated diffusing pixels, and reactions of diffusing species with solid phases or each other. The cement model reactions, including the pozzolanic reaction, are given in Eqs. (2.29)-(2.37).

$$C_3S + 5.3\ H \rightarrow C_{1.7}SH_4 + 1.3\ CH \tag{2.29}$$

$$C_2S + 4.3\ H \rightarrow C_{1.7}SH_4 + 0.3\ CH \tag{2.30}$$

$$C_3A + 6\ H \rightarrow C_3AH_6 \tag{2.31}$$

$$C_4AF + 10\ H \rightarrow C_3AH_6 + CH + FH_3 \tag{2.32}$$

$$C_3A + 3\ C\bar{S}H_2 + 26\ H \rightarrow C_6A\bar{S}_3H_{32} \tag{2.33}$$

$$2\ C_3A + C_6A\bar{S}_3H_{32} + 4\ H \rightarrow 3\ C_4A\bar{S}H_{12} \tag{2.34}$$

$$C_4AF + 3\ C\bar{S}H_2 + 30\ H \rightarrow C_6A\bar{S}_3H_{32} + CH + FH_3 \tag{2.35}$$

$$2\ C_4AF + C_6A\bar{S}_3H_{32} + 12\ H \rightarrow 3\ C_4A\bar{S}H_{12} + 2\ CH + 2\ FH_3 \tag{2.36}$$

$$1.1\ CH + S + 2.8\ H \rightarrow C_{1.1}SH_{3.9} \tag{2.37}$$
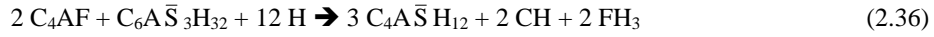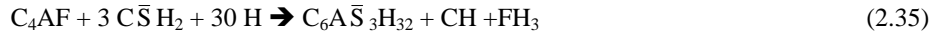
The corresponding volume reaction equations can be determined from the numbers of moles given in the reaction equations and the compound molar volumes. To obtain a reaction in terms of pixels these volumes have to be normalised using the volume of the main original compound in that reaction. For instance the reaction described in Eq. (2.29) means that 1 pixel volume of C_3S will produce 1.52 pixels of $C_{1.7}SH_4$ and 0.61 pixels of CH on average. In the model this implies that when a pixels of C_3S reacts there will be a probability that additional pixels of CH and C-S-H are formed. This probability is chosen in such a way that on average 100 pixels of C_3S will produce 152 pixels of C-S-H and 61 pixels of CH. This C-S-H comprises both chemically and physically bound water. The numbers of moles H in each reaction do not take part in the reaction step directly but are used to keep track of the number of moles H consumed in each reaction step.
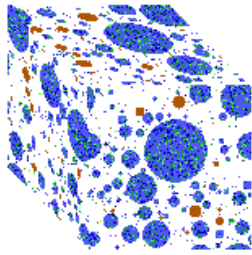
Figure 2.4. Initial microstructure in CEMHYD3D (w/c = 0.5, CEM 32,5R). Based on 100·100·100 pixels in 3D box. Blue = cement, brown = gypsum, white = water.
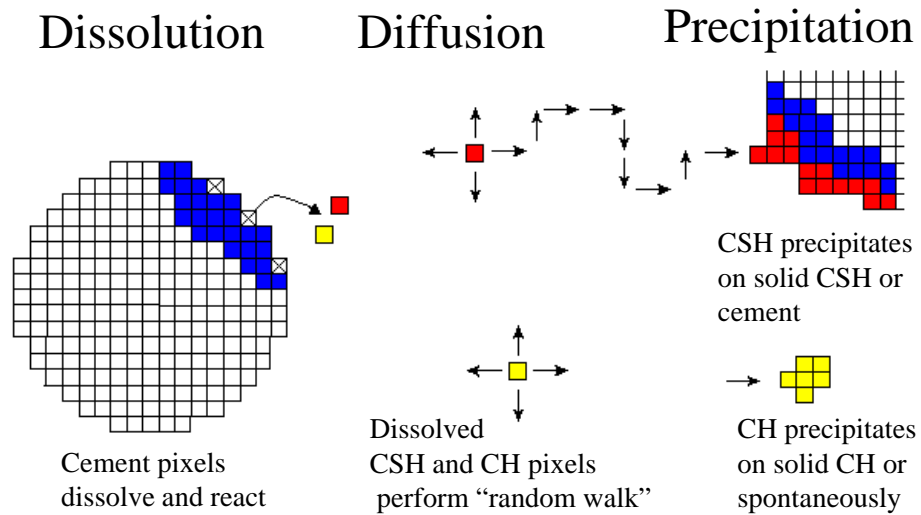

Figure 2.5. Illustration of dissolution, diffusion and reaction steps for C_3S reaction. Blue = C_3S, Red = C-S-H and yellow = CH.
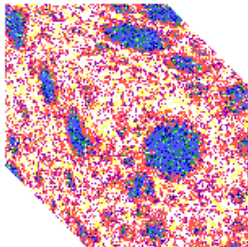

Figure 2.6. Hydrated microstructure after 500 cycles (w/c = 0.5, CEM 32,5R). Blue = cement, red = C-S-H, yellow = CH, white = porosity.

Rules are operated on the microstructure in a sequence of dissolution cycles, in which new part of the solid components dissolves and reacts. The phases C_3S, C_2S, C_3A, C_4AF, gypsum, anhydrite and hemihydrate were assigned different dissolution probabilities (see Table 2.7) so that they would dissolve and react at different rates. In this way reaction kinetics were taken into account. Each dissolution cycle starts with a scan through all pixels present in the box. All solid pixels in contact with pore space are marked for possible dissolution. In a second scan all marked pixels take a one-step random walk and if (a) this step is into porosity, (b) the phase of the pixel is currently soluble and (c) a randomly chosen number is higher than the dissolution probability of this phase, the dissolution is allowed. When dissolution is allowed the solid pixel is converted to one or more diffusing pixels, corresponding to the appropriate volume equations. The generated diffusing pixels execute one-step random walks in the available pore space until they react according to a set of reaction rules (see Fig. 2.5). The pozzolanic reaction is simulated by a reaction between diffusing CH and S, yielding pozzolanic C-S-H.

After a large number of diffusion and reaction steps, a new dissolution cycle is started, a new part of solids dissolves and new diffusing pixels are generated. In general, the solid hydration products occupy a larger volume than the solids from which they were formed. As a result, the original pore volume will be replaced by solid volume and the microstructure changes into a more solid product. After each dissolution cycle, the amount of solids reacting decreases as a result of decreasing amounts of unreacted material and pore water. Also the availability of the water still present decreases because C-S-H is deposited on the reacting cement spheres. Changes in microstructure will be smaller after each cycle and finally, an equilibrium structure will be approached (see Fig. 2.6).

2.4.3 Output parameters

After each dissolution cycle a new and changed microstructure is produced by the model. The composition of this simulated microstructure is known and microstructural properties can be determined from it. Because the model keeps track of all reactions that have taken place, hydration related properties can be calculated such as degree of hydration, heat development and chemical shrinkage.

In order to relate the time-dependent microstructure and the corresponding material properties to real time, the calculation cycles were related to time using a quadratic relation given by Bentz (1997) and based on parabolic hydration kinetics:

$$t(\text{hours}) = t_0 + B \cdot (\text{cycles})^2 \tag{2.38}$$

t = real time
t_0 = induction period
B = calibration parameter
cycles = number of executed calculation or model cycles

Using different experimental techniques to measure degrees of hydration in real hydrating systems and relating the results to the degree of hydration given by the model, it has been calibrated for U.S. CCRL and French Montalieu OPC. Then, the calibrated model was used to

45

predict strength and heat development of standard mortars using the empirical relations developed by Powers Eqs. (2.24) and (2.25) (Bentz 1997, Bentz et al. 1998).

The model has proven to be a useful tool in designing cement recipes because one can easily vary water/cement ratios, the amount of gypsum, fly ash or silica fume present and the PSD of cement and additives. Furthermore, the simulation can be performed assuming different environmental conditions, e.g. different temperatures and water saturated or sealed environment. These possibilities have been used to investigate temperature rise in silica fume pastes (Bentz et al.,1997) and the relation between cement PSD, water/cement ratio and achievable degree of hydration and strength (Bentz and Haecker,1999 and Bentz et al., 1999). Because the obtained digital microstructure gives a 3D representation of porosity and hydration products it is possible to study percolation and permeability aspects by looking at interconnectivity between one phase, e.g. porosity or C-S-H, throughout the structure. From this, one can predict relative diffusivities and leaching properties (Garboczi and Bentz, 1992).

2.4.4 Calibration ENCI cements

The cement hydration model will be validated for two ENCI (main producer of cements in The Netherlands) cements that possess the same oxide composition, but have different PSD: type CEM I 32,5 R and CEM I 52,5 R (Blaine surfaces of 286 m^2/kg and 489 m^2/kg, respectively). The oxide composition of the studied ENCI OPC is given in Table 2.8.

Table 2.8. Oxide composition of studied ENCI cements (Blaakmeer and De Loo, 1999).

Oxide	Mass fraction
CaO	64.40
SiO_2	20.36
Al_2O_3	4.96
Fe_2O_3	3.17
K_2O	0.64
Na_2O	0.14
SO_3	2.57
MgO	2.09
TiO_2	0.35
Mn_3O_4	0.14
P_2O_5	0.18
LOI	0.88

Two different techniques were used to measure degree of hydration as a function of time: calorimetry and chemical shrinkage. The mass fractions of the main clinker minerals in the cement were calculated from the oxide composition using the modified Bogue method described in paragraph 2.2.1. Using the oxide composition given in Table 2.8 and correcting total CaO content for 0.6 % free CaO present, the mineral composition was calculated including the fraction of total sulphate. The result was normalised based on the four clinker phases only. The calculated clinker composition is given in Table 2.9.

46

Table 2.9. Mineral composition of studied ENCI cement clinker calculated using modified Bogue method.

Mineral	% (m/m)
C_3S	66
C_2S	16
C_3A	7
C_4AF	11

From the hydration enthalpy for each mineral phase (Table 2.10) and the mineral composition (Table 2.9), a total heat release of 54 kJ per 100 gram of fully hydrated OPC paste was calculated.

Table 2.10. Enthalpy of complete hydration for main cement minerals (Bentz, 1997 and Taylor, 1997.

Mineral	Enthalpy (J/g)
C_3S	517
C_2S	262
C_3A	1144
C_4AF	725

Chemical shrinkage is defined as the volume reduction of a hydrating cement paste as a result of volume differences between starting materials and hydration products. In a water saturated system this volume reduction is compensated by absorbing extra water from the environment. This absorbed water volume can be measured. From the volume reaction equations of all relevant hydration reactions the chemical shrinkage for a fully hydrated paste was calculated as 6.9 ml per 100 g OPC.
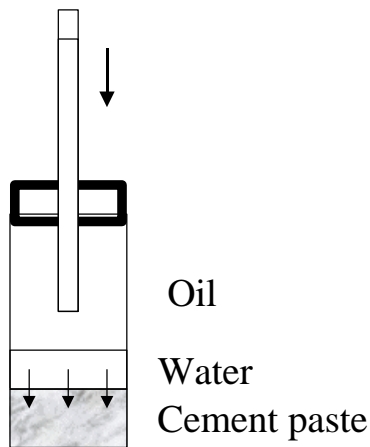

Figure. 2.7. Chemical shrinkage measurement.

Calorimetric measurements were performed on cement pastes having a w/c ratio of 0.4 (Blaakmeer and De Loo, 1999). Heat of hydration was measured under isotherm conditions at

a temperature of 20 °C during 7 days. Chemical shrinkage was measured following the method of Tazawa et al. (1995). Cement pastes (w/c = 0.4) were placed in a glass jar and 1 ml of extra water was placed on the paste surface. The jar was filled up with hydraulic oil and sealed with a rubber stop in which a pipette was placed. One control sample was prepared that only contained cement and oil to correct for temperature differences. All samples were placed in a 20 °C water bath during the whole experiment (see Fig. 2.7).

The volume of water taken up by the hydrating cement paste was measured by reading the oil level. Values were corrected using the control sample and calculated per gram of OPC present in each sample. Table 2.11 shows the degrees of hydration determined by both calorimetry and chemical shrinkage. Both methods appeared to produce similar results.

Table 2.11. Degrees of hydration measured by chemical shrinkage and calorimetry.

days	CEM I 32,5 R chemical shrinkage	calorimetry	CEM I 52,5 R chemical shrinkage	calorimetry
1	0.25	0.26	0.44	0.42
2	0.33	0.37	0.54	0.54
3	0.38	0.44	0.58	0.58
7	0.41	0.54	0.69	0.64

The chemical composition and particle size distributions of the cements were used to reconstruct a 3D representation of the cement at a w/c of 0.4. This system included 5 % (m/m) of gypsum. Because the constituent phases of a cement are not equally easy to grind and because gypsum and its dehydration products are weaker than cement clinker its particles will be present in the finer fractions of the total mixture (Taylor, 1997). Therefore a finer and separate PSD was used for gypsum than for cement clinker. The gypsum particles were assumed to have diameters ranging from 1-11 μm (see Appendix 3).

Simulations were conducted at a constant temperature of 20 °C under saturated conditions. After each dissolution cycle the current degree of hydration was determined. The best match between calculated and measured degrees of hydration was obtained when the values $t_0 = 6.7$ hours and $B = 0.0010$ were used in the cycle-to-real-time equation (Eq. 2.38). These values hold for both ENCI CEM I 32,5 R and CEM I 52,5 R, which differ in particle size distribution, only. Values of $t_0 = 6.7$ hours and $B = 0.0017$ (Bentz, 1997) and $t_0 = 7.5$ hours and $B = 0.0011$ (Bentz et al., 1998) were reported for American CCRL OPC and French Montalieu OPC, respectively.

Subsequently, the Powers formulas (Eqs. (2.24) and (2.25)) were used to relate compressive strength to degree of hydration and w/c ratio used in CEMHYD3D. Using the calibrated hydration model, the developments of degree of hydration were determined. Using Eqs. (2.24) and (2.25) the corresponding compressive strengths were calculated with parameters $n = 2.2$ en $F_{int} = 135$ N/mm^2 for both cements. The strength was measured according to the standard NEN-EN 196-1 (1995), see Table 2.12.

Table 2.12. Measured norm strengths (N/mm^2), (Blaakmeer and De Loo, 1999).

Days	CEM I 32,5R	CEM I 52,5R
1	11.3	28.9
2	23.8	40.9
3	27.8	47.0
5	34.5	49.9
7	40.0	53.7
28	54.3	62.9

Fig. 2.8 shows the calculated strength development compared to measured strengths From this figure it follows that strength development is described well by the model.
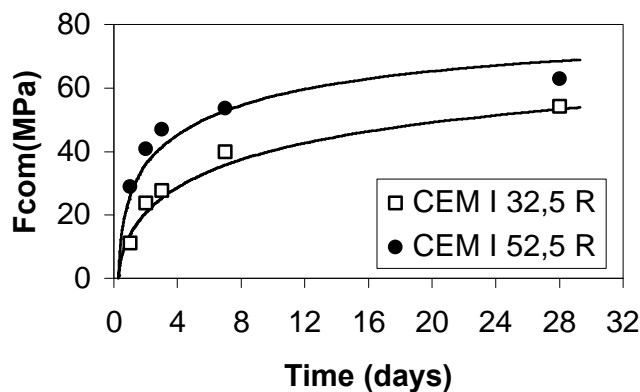
Figure 2.8. Measured and predicted strength of standard mortars (Blaakmeer and De Loo, 1999).

2.5 Conclusions

Cementitious binders are useful for binding several types of waste streams. In order to understand the properties of hardened products, e.g. concrete or immobilisate and to get insight into waste binding mechanisms and effects of additives it is important to look at cement hydration. Only then, the hardening process and related problems can be understood.

CEMHYD3D, a 3D cement hydration model developed at NIST has been presented. Its principles has been described and its possibilities has been explained. It has proven its use as a tool to describe cement hydration and to predict many properties of interest for both cement, concrete products and S/S technology. These properties include compressive strength, porosity and permeability. Hydration can be simulated starting with different recipes and under different environmental conditions. This is of great importance when designing waste/cement recipes. Additives commonly used in S/S technology can be handled by the model. The model predicts a microstructure from which the volume fractions of hydration

products and porosity and their 3D distribution can be derived. The hydration products are responsible for binding contaminants present in waste streams. The porosity distribution gives information about strength and leachability. Because the model is based on a fundamental chemical background, changes in the chemistry as a result of the presence of contaminants can be implemented into this model.

The CEMHYD3D model contains the pozzolanic reaction and can handle the presence of silica fume, consisting of a fraction of reactive silica (S) and non-reacting phase (inert). The presence of fly ash, however, is not treated well by this model or any other hydration model. Fly ash partially contains silica and its reaction is pH dependent, while pH is not included cement hydration models. Precipitation of contaminants also depends on concentrations in the pore water. This implies that for a complete understanding of cement hydration, pore water chemistry should be considered in detail.

Additional knowledge is required to combine with hydration models because otherwise, such models would be inadequate for use in S/S. Pore water concentrations have to be studied in more detail to implement fly ash properly and to be able to predict the solubility and precipitation of contaminants.

In general the conclusion can be drawn that when cement is used to solidify waste products, fundamental knowledge about cement hydration, can be used to understand and improve the solidification process. Furthermore, to simulate the solidification process and the final structure of the resulting immobilisate, a cement hydration model such as CEMHYD3D can be used.

Chapter 3

Pore water[*]

3.1 Introduction

3.1.1 Pore water composition

The hydration of OPC (i.e. the reactions of all its main clinker phases and added calcium sulphates) and the corresponding development of properties of the hardening paste, can be simulated by CEMHYD3D, as discussed in Chapter 2. CEMHYD3D describes the changing phase composition in a hardening cement paste as a function of time. One of these phases is the porosity phase, which is considered by the model as a volume containing free water (and in case of sealed hydration: air). The free water present in the pores in a real hydrating system is called the pore water and contains high amounts of dissolved ions. However, the composition of this pore water is not yet considered by CEMHYD3D. The reason for this is that the purpose of CEMHYD3D is to calculate *microstructural* development and for this purpose, the *volumes* of original materials and reaction products are the most important parameters and not the exact chemical compositions of the compounds or the chemical composition of the pore water. However, when additions or contaminants are present, it is important to know the pore water composition during hydration for several reasons. For instance, the hydroxyl concentration and related pH are important parameters that determine the reactivity of slags and fly ashes, which are common additions used in cement. For a good description of the hydration of such additives it is necessary to keep track of pore water composition. Furthermore, when cement hydration takes place in the presence of contaminants, the pore water composition will determine the solubility of many compounds, e.g. metals or calcium compounds and the occurrence of precipitates.

In order to measure pore water compositions pore fluids can be extracted by applying pressure on a hardened sample and collecting the pore fluid. This is done using a pore fluid expression apparatus first used by Longuet et al. (1973). Subsequently, the ion concentration in the extracted pore water can be determined using spectroscopic or titration techniques.

Data on the composition of the liquid phase of hydrating OPC paste can be summarised as follows (Hewlett, 1998). Immediately after mixing, the alkalis, which are present on the surface of cement grains in the form of very soluble alkali sulphates, enter the liquid phase instantaneously as K^+ and Na^+ ions, together with SO_4^{2-} ions. During further hydration, the alkalis that were bound in the clinker minerals are released into the pore water. The concentration of both K^+ and Na^+ attained in the liquid phase instantaneously may vary over a wide range, i.e. ~5-50 mM Na^+ and ~20-200 mM K^+, depending on the alkali content in the cement, the w/c (water/cement) ratio of the mix and the hydration time.

Ca^{2+} ions are released into the liquid phase as a result of the dissolution of free lime (CaO) and the hydration of C_3S and C_2S. The liquid phase is supersaturated with respect to CH ($Ca(OH)_2$) during the induction period. When the acceleration period starts, the Ca^{2+} concentration first declines due to CH precipitation and AFt (ettringite) formation and then declines further as a result of the increasing alkali and OH^- concentration.

The SO_4^{2-} ions in the liquid phase stem initially from the alkali sulphates present in cement and the initial SO_4^{2-} concentration depends on the amount of these water-soluble alkali sulphates and the water/cement ratio. During further hydration SO_4^{2-} ions are released as a result of the dissolution of calcium sulphates (e.g. gypsum) that were added to the OPC. This dissolution of calcium sulphates proceeds more slowly; it depends also on the form of calcium sulphate present (i.e. present as anhydrite, gypsum or hemihydrate). The form in which sulphates are present also has strong effects on setting of the paste and early age properties, but this is outside the scope of this thesis. As long as solid calcium sulphate is still present, the SO_4^{2-} concentration in the liquid phase changes only slightly, as the SO_4^{2-} consumed in the formation of AFt or adsorbed by the C-S-H phase is replenished by calcium sulphate dissolution. After that, the SO_4^{2-} concentration begins to decline and reaches values closer to zero within a few days.

The OH^- concentration stems from the dissolution of CH formed as a result of the hydration of C_3S and C_2S. Its concentration increases throughout the hydration and in a later stage it follows mainly from the released alkalis that were originally present in the clinker phases.

The concentration of silicate and aluminate ions in the liquid phase remains very low, i.e. below 0.1 mM, throughout the course of hydration.

3.1.2 Pore water modelling

The main ions found in pore water are alkalis (comprising Na^+ and K^+), OH^-, Ca^{2+}, SO_4^{2-} and silicate and aluminate ions. All ions except the alkalis are in equilibrium with low solubility cementitious compounds, e.g. CH, C-S-H and ettringite. Therefore their concentrations are determined by the equilibria of the corresponding solid compounds containing these ions. Such equilibrium is described by a concentration product, which has a certain value at equilibrium and thus relates the concentrations of the constituent ions of the compound. On the other hand, alkali concentrations are not determined by such equilibria, because alkali compounds are very soluble and, except in the case of high alkali cements, no solid alkali compounds are found to be in equilibrium with the pore water. In other words, the pore water is saturated with respect to all ions except for the alkali ions. This means that two different approaches have to be taken to compute pore water concentrations: a non-equilibrium approach for the alkalis and an equilibrium approach for the non-alkalis.

A non-equilibrium approach for alkali ions has been developed by Taylor (1987). In this work an empirical model was developed describing the release of alkali ions by cement and the sorption of these ions by hydration products. From this information and from an estimate of the amount of free water it was possible to compute alkali concentrations. In systems hydrated for more than one day the OH^- concentration could also be estimated from the charge balance.

An equilibrium approach is based on defining a set of solid compounds that are in equilibrium with water and solving the set of corresponding equilibria (concentration products) and mass and charge balances mathematically.

Diamond (1975) and Moragues et al. (1987) executed pore water computations taking into account the $Ca(OH)_2$ equilibrium and the $Ca(OH)_2$ and $CaSO_4$ equilibrium respectively. The problem in these studies was defining the proper values for the concentration products at the high concentrations found in cement pore water.

Reardon (1990, 1992) used the ion interaction approach developed by Pitzer (1979) for describing concentration products of cementitious compounds at high concentrations. Using this ion interaction approach, Warren and Reardon (1994), Duchesne and Reardon (1995) and Reardon (1992) determined the solubility of $Ca(OH)_2$, ettringite and C-S-H respectively at high concentrations.

In the field of groundwater and geochemistry different computer programs have been developed to solve large sets of equilibria. These programs contain a database of solid compounds, their corresponding ions in solution and their equilibrium properties, i.e. thermodynamic equilibrium constants. The program then uses iterative mathematical techniques to solve these sets of equilibria simultaneously.

One of these programs is MINTEQA2 (Allison et al., 1991). Batchelor and Wu (1993) extended the database of this model with cementitious compounds, e.g. C-S-H, and improved computation of concentration products at high concentrations. This resulted in the SOLTEQ model (Batchelor and Wu, 1993, Park and Batchelor, 1999a, 1999b).

In the approach by Park and Batchelor (1999a), two distinctive steps are taken for the computation of pore water concentrations. First, the amounts of hydrated clinker phases C_3S, C_2S, C_3A and C_4AF at one point in time are computed using empirical equations also used by Taylor (1987) and then converted to amounts of solid hydration products using simplified hydration stoichiometries. These solids are chosen from the SOLTEQ database. The amount of free water (containing all ions) is also computed using an empirical equation used by Taylor (1987). Taylor's empirical model (Taylor, 1987) was used to compute alkali concentrations in the pore water. Secondly, for each solid assumed present, a corresponding equation is set up and iterative computations are performed to solve all equations and find all concentrations of interest. Computations were done for cement systems that were hydrated more than 1 day and therefore, sulphate phases, e.g. gypsum or anhydrite were not considered.

SOLTEQ was able to predict pore water composition in pure binder systems such as OPC and OPC + fly ash at different w/c ratios and hydration times (Park and Batchelor, 1999a). The good predictions are mainly owed to the good numeric values for equation constants in the SOLTEQ database.

To simulate changes in both microstructure and pore water concentrations during cement hydration, CEMHYD3D could be used to compute a microstructure and a simulation could be followed by a separate SOLTEQ computation for pore water concentrations. But except for practical problems to be expected when using two computer programs that process input and output in a completely different manner, this approach has some other disadvantages, which will be explained below.

First, hydration of fly ash and slags strongly depend on the current pore water composition and the presence of fly ash influences pore water composition itself. Furthermore, cement hydration in the presence of contaminants is strongly influenced by precipitation processes. Because pore water concentration affects hydration and hydration

affects pore water composition, both processes and corresponding properties have to be computed dynamically, i.e. at the same time.

Secondly, Taylor (1987) and Park and Batchelor (1999a) considered hydrated pastes at only one point in time and always after 1 day of hydration and therefore defined a set of solids correspondingly, i.e. after calcium sulphates were consumed. To consider precipitation processes taking place instantaneously and in order to describe OH$^-$ composition earlier than one day, it is necessary to consider the hydration before 1 day also. This implies the presence of other solids than during later ages. So, to consider the proper solids at each point in time, the phase composition of a microstructure must be known at each point in time. Then, the equilibria to be considered can be changed during the hydration, when required.

Finally, because many solids are available in the SOLTEQ database, instead of making a selection of solids at forehand, one may choose a large set of solids and solve the obtained system, even when solids are not found to be in equilibrium at the end. This may give problems because the system to be solved is then over determined (more equations than variables) and because of the iterative solving process, the possibility exists that the routine does not converge to the right solution.

Because of the problems mentioned it is not useful to create a microstructure using CEMHYD3D first and then compute pore water computations separately using a model such as SOLTEQ. These computations have to be integrated, in a way that pore water composition can be computed quickly after each hydration cycle in CEMHYD3D.

3.1.3 CEMHYD3D and pore water

CEMHYD3D provides the following information that can be used for the computation of pore water composition: (1) Degree of hydration of cement and additives. As a result of hydration, solids and ions are produced. (2) Which solids are (still) present in the microstructure. Solids can be in equilibrium with the pore water and determine the concentrations of its constituent ions. (3) Volume fraction of porosity and amount of unreacted water. These parameters determine the amount of water that is free and thus available for containing all ions.

All information related to cement hydration can be provided by CEMHYD3D for different hydration behaviours, i.e. different types of cements hydrating under different conditions. CEMHYD3D takes into account the main cement properties (PSD, phase composition), mixture properties (e.g. w/c ratio) and hydration conditions (e.g. temperature, water saturated or sealed conditions). This has been shown in Chapter 2. In that respect, the use of CEMHYD3D makes the use of empirical hydration equations used for example by Taylor (1987), Reardon (1992) and Park and Batchelor (1999a) superfluous when computing pore water composition.

It is important to note that the hydration equations used in CEMHYD3D are *not* based on equilibria. The hydration reactions of C_3S etc. are assumed being one-directional, producing hydration products that are stable end products. The mutual reaction rates of clinkers therefore do not depend on ion concentrations but were based on fixed mutual reactivities of the specific minerals. These rates are *kinetically* determined, i.e. they are determined by availability and contact with water. On the other hand, the hydration products itself are in equilibrium with the surrounding pore water and all ions within. Such

54

concentrations are *thermodynamically* determined, i.e. based on concentrations and equilibrium constants.

To predict pore water concentrations using CEMHYD3D, two methods are required:

1. A non-equilibrium model that describes release and sorption of alkalis.
2. An equilibrium-based method to set up and solve a simplified system of equilibria of cementitious solids. Such a method requires:
   - Information about the solubility properties of cement hydrates
   - A method to compute concentration products at high concentrations
   - Selection of solid compounds to be considered

In this chapter these methods will be discussed and routines will be developed that enable the computation of pore water composition during the hydration of cement. The routines will be implemented in the cement hydration model CEMHYD3D.

     In section 3.2 some general concepts about solubility and the computation of concentration products at high concentrations will be explained using the concept of activity. In section 3.3 a non-equilibrium approach is described for computation of alkali concentrations ($[Na^+]$ and $[K^+]$) and a comparison with experimental results is made. In section 3.4 the equilibria approach is described. Solubility properties of cementitious solids and a method to compute concentration products at high concentrations will be presented, and small sets of equilibria to be considered are determined. Routines to compute pore water concentrations during hydration are developed and coupled to CEMHYD3D. Computed pore water concentrations ($[OH^-]$, $[Ca^{2+}]$ and $[SO_4^{2-}]$) are compared with experimental results. Finally, in section 3.5 conclusions are presented.

3.2 Theoretical background

3.2.1 Concentration product and activity product

When 1 mole of a compound C_cA_a dissolves it produces c moles of C cations and a moles of A anions. When this compound is in equilibrium with the solution, an equilibrium constant, denoted K can be defined as the product of concentrations of each of its constituent ions (Butler, 1998):

$$K_{CcAa} = [C]^c \cdot [A]^a \tag{3.1}$$

At low concentrations (<0.01 M), e.g. in the case of slightly soluble salts, this equilibrium constant has a fixed value, which is often referred to as "solubility product". In this work the term *concentration product* will be used. At higher concentrations the concentration product of a salt is not constant, but depends on the concentration itself. The formal way to account for this deviation is to include activity coefficients in the product.

The activity of an ion is defined as the product of its concentration and its activity coefficient:

$$\{i\} = [i] \cdot \gamma_i \tag{3.2}$$

$\{i\}$ = activity of ion i
$[i]$ = concentration ion i
γ_i = activity coefficient of ion i

So, actually the concentration product is not a constant in non-dilute solution, but changes with total concentration. By definition, the concentration product K is related to the thermodynamic activity product K^0 by the activity coefficients.

$$K_{CcAa} = [C]^c \cdot [A]^a = \frac{K^0_{CcAa}}{g^c_+ \cdot g^a_-} \tag{3.3}$$

Activity products are thermodynamic properties and can be found in handbooks and literature (Butler, 1998, Lide, 1995, Reardon, 1992). When the activity coefficient of each ion is known in a specific solution (see section 3.2.5 for computation of activity coefficients), the concentration product of a solid in this solution can be computed from its activity product according to Eq. (3.3).

Replacing concentrations in Eq. (3.1) by activities yields a product that has a real constant value. This product will be referred to as the *activity product* in this work. The activity product is a function of temperature only. It is denoted as K^0, and defined as follows (Butler, 1998):

$$K^0_{C_cA_a} = \{C\}^c \cdot \{A\}^a = ([C]\cdot\gamma_+)^c \cdot ([A]\cdot\gamma_-)^a \tag{3.4}$$

$\{C\}$ = activity of cation C
$\{A\}$ = activity of anion A
γ_+ = activity coefficient of cation
γ_- = activity coefficient of anion
$[C]$ = concentration of cation C
$[A]$ = concentration of anion A

In very dilute solutions activity coefficients are approximately unity and activity almost equals concentration. The activity of a solid is defined as unity and the activity of H_2O is proportional to the mole fraction of water in the solution and thus will be very close to unity in most cases as well (Butler, 1998).

3.2.2 Molar solubility

If excess of a solid phase is present in a solution and it is in equilibrium with the solution, the total number of moles of that compound dissolved in one liter solution is called the molar

solubility, denoted by S (Butler, 1998). For example when S moles of AgCl dissolve in pure water to form one liter of saturated solution, the mass balance gives:

$$[Ag^+] = [Cl^-] = S \tag{3.5}$$

and S can be computed from the concentration product:

$$K_{AgCl} = [Ag^+][Cl^-] = S^2 \tag{3.6}$$

or

$$S = \sqrt{K_{AgCl}} \tag{3.7}$$

The general equation giving the molar solubility S of a salt C_cA_a can be derived as follows:

$$K_{CcAa} = [C]^c \cdot [A]^a = (cS)^c \cdot (aS)^a = c^c \cdot S^c \cdot a^a \cdot S^a = S^{c+a} \cdot c^c \cdot a^a \tag{3.8}$$

yielding

$$S = \left(\frac{K_{CcAa}}{c^c a^a} \right)^{1/(c+a)} \tag{3.9}$$

These equations only hold in a saturated solution in which only one salt is dissolved.

In case of a multi-component solution, i.e. when a solution is in equilibrium with a number of different solids, the solubility of one specific solid and the concentration of one of its constituent ions, may be strongly influenced by the presence of the other solids and ions. In such case the molar solubility of that specific solid is always based on the constituent ion which is present in the *lowest* concentration in such a solution (Butler, 1998). That ion is referred to as the solubility determining ion of that compound. For example, when a solution is saturated with respect to AgCl, and $[Cl^-]$ is high because of the presence of other solids, this implies that $[Ag^+]$ is the solubility determining ion for AgCl and S_{AgCl} is equal to $[Ag^+]$ and thus also low.

3.2.3 Solving a set of equilibria

When a number of solids is in equilibrium with a solution at the same time, the concentrations of all ions can be found by considering them as variables in a set of equations given by the concentration product of each solid in equilibrium. Furthermore, for every neutral solution a charge balance can be made up by counting negative and positive charges, giving an additional equation that should be obeyed:

$$\sum_i [i] \cdot z_i = 0 \tag{3.10}$$

$[i]$ = concentration of ion i
z_i = charge of ion i

For example, when a solution is in equilibrium with two solids CA and BA, where C and B are two different cations and A is an anion, the following system of equations has to be solved:

$$K_{CA} = [C] \cdot [A]$$
$$K_{BA} = [B] \cdot [A]$$ \hfill (3.11)
$$[C] + [B] - [A] = 0$$

When the numeric values of both concentration products K_{CA} and K_{BA} are known, this system has three equations and three unknowns ([C], [B] and [A]) and can be solved.

The anion A in the above system is called a *common ion*. In a cement system, addition of another, more soluble salt containing one common ion, will increase the concentration of that common ion and as a result will decrease the solubility of the less soluble salt. This is known as the "common-ion effect" (Butler, 1998). For example addition of NaOH to a saturated $Ca(OH)_2$ solution will increase the OH^- concentration and consequently Ca^{2+} concentration will be decreased according to the concentration product of $Ca(OH)_2$. This will result in the precipitation of $Ca(OH)_2$ thus lowering its molar solubility S, for the solubility of $Ca(OH)_2$ is then determined by the remaining and lowered $[Ca^{2+}]$. In that case, the molar solubility of $Ca(OH)_2$ is lower compared to the case of a saturated $Ca(OH)_2$ solution without NaOH.

3.2.4 Activity

Activity coefficients are determined by the total composition of the solution. In Appendix 4 two methods are presented to compute activity coefficients: Davies equation and Pitzer's method. These methods can be summarised as follows:

Davies equation. First**,** the ionic strength of a solution according to the Debye-Hückel theory is calculated according to Eq. (1) given in Appendix 4 and from this, activity coefficient for single ions are computed using the Davies equation (Butler, 1998) (Eq. (2) in Appendix 4). This equation only requires the ionic strength of the solution and the charge of the ion of interest. Computed example values and the temperature dependence of this equation are given in Appendix 4.

Pitzer's method. Pitzer (1979) developed a method for the computation of activity coefficients at very high concentrations, using an ion interaction approach. In this approach, parameters are defined that describe interactions between specific combinations of ions. This approach has been very successful in predicting the composition of multi-component systems at high concentrations, e.g. sea water. Appendix 4 gives an explanation of Pitzer's ion interaction approach, including some example computations of activity coefficients and a comparison with activity coefficients computed using the Davies equation.

As Pitzer's equations are more robust and applicable at high concentrations, this theory will be used henceforth.

58

3.3 Alkalis

3.3.1 Relevance of alkali concentrations

During cement hydration substantial amounts of alkalis (sodium and potassium) are released. This is a result of the dissolution of alkali sulphates and the reaction of cement clinker phases. Furthermore, it is assumed that the solution is always saturated with regard to $Ca(OH)_2$ and corresponding concentration product always applies. While the concentration products of KOH, NaOH and the corresponding alkali sulphates are significantly higher compared to that of $Ca(OH)_2$, the presence of alkalis will increase $[OH^-]$ according to the common-ion effect. This means that $[Ca^{2+}]$ will be decreased according to the concentration product of $Ca(OH)_2$. From this effect it is obvious that alkali concentration is important because it effects the important $Ca(OH)_2$ equilibrium and will effect other related equilibria consequently. The concentrations of alkalis itself are not determined by equilibria.

Taylor (1987) developed a method to describe the alkali concentrations in cement pore water. It is based on the total alkali content in cement, the w/c ratio used and empirical equations describing the degrees of hydration of clinker minerals and the amount of free water. Taylor's approach will be used for the development of equations that can be implemented into the CEMHYD3D model.

3.3.2 Porosity and pore water

According to Taylor (1987) all water present in reaction products should not be considered as the pore water in which all ions are dissolved. Therefore, in the pore water modelling studies by Reardon (1992) water mass balance expressions were used to distribute the total mass of water between hydration products and pore water available for the dissolution of ions. CEMHYD3D is based on a number of hydration products with fixed stoichiometries and fixed water contents. Thus, during a simulation, the amount of unreacted water can be directly determined from initial (total) amount of water and the amount of water that is part of one of the formed hydration products. Furthermore, hydration under water saturated conditions is always assumed (vacuum (self-desiccation) and air voids do not occur), so all porosity is assumed completely filled with water. Hence, the porosity volume fraction computed by CEMHYD3D equals the pore water fraction available for the dissolution of ions. When the porosity fraction is known, the concentrations of Na^+ and K^+ can be computed straightforwardly from the number of moles.

3.3.3 Release

The total numbers of moles of Na^+ and K^+ present per gram of cement can be computed from the corresponding mass fractions and molar masses. For Na the computation is as follows:

$$Na_T = \frac{\dfrac{m_{Na_2O}}{m_c} \cdot 2}{M_{Na_2O}}$$ (3.12)

Na_T = total molar Na content in cement [mole/g OPC]

$\dfrac{m_{Na_2O}}{m_c}$ = Na$_2$O mass fraction in cement [g/g]

M_{Na2O} = molar mass of Na$_2$O [g/mole]

Alkalis in cement are partly present as readily soluble sulphates at the surface of cement grains and partly bound in the clinker minerals (Taylor, 1997). The fraction of alkalis present as sulphate will be released into the solution instantaneously, so before any part of the clinker minerals have been hydrated. The remaining alkalis, bound in the clinker minerals are released during hydration of these clinker minerals. Pollit and Brown (1969) studied the distribution of alkalis and SO$_3$ in many clinkers with different amounts of alkalis and sulphates. From their data overview and an estimation of the SO$_3$ content of pure clinker used for the production of ENCI cements, it was assumed that in the ENCI cements 35% and 70% of Na and K, respectively, are present as readily soluble sulphates. Table 3.1 summarises these values.

Table 3.1. Fractions of Na and K present in sulphates or clinker minerals in ENCI cements.

Source	Release	Na$^+$	K$^+$
Alkali Sulphates	instantaneously	0.35	0.70
Clinker Minerals	during hydration	0.65	0.30

The amount of Na$^+$ released instantaneously (in mole per litre of pore water) is computed as follows:

$$[Na^+]_{sulphate} = \frac{f_{Na,sulphate} \cdot Na_T \cdot m_c}{\dfrac{\varphi_p}{\varphi_p^0} \cdot \dfrac{m_w}{\rho_w}} = \frac{f_{Na,sulphate} \cdot Na_T}{\dfrac{\varphi_p}{\varphi_p^0} \cdot w/c} \cdot \rho_w$$ (3.13)

$[Na^+]_{sulphate}$ = Na$^+$ released from sulphates in [mole/l]

$f_{Na,sulphate}$ = fraction of Na present as sulphate

$\dfrac{\varphi_p}{\varphi_p^0}$ = concentration factor

ρ_w = water density = 1000 [g/dm^3]

The concentration factor used in Eqs. (3.13) and (3.14) is defined as the ratio of the porosity fraction to the initial porosity fraction. The concentration factor is introduced to account for the decrease in porosity (= free water) during hydration and is therefore α dependent. As a

result of this decrease in porosity all ions present in the pore solution are concentrated correspondingly.

It is assumed that the alkalis bound in the clinker mineral, will be released into the pore water as soon as the clinker reacts and dissolves. The amount of Na^+ released from the clinker is thus linear proportional with the degree of hydration:

$$[Na^+]_{clin\,ker} = \frac{(1-f_{Na,sulphate}) \cdot Na_T \cdot \alpha \cdot m_c}{\frac{\varphi_p}{\varphi_p^0} \cdot \frac{m_w}{\rho_w}} = \frac{(1-f_{Na,sulphate}) \cdot Na_T \cdot \alpha}{\frac{\varphi_p}{\varphi_p^0} \cdot w/c} \cdot \rho_w \tag{3.14}$$

$[Na^+]_{clinker} = Na^+$ released from clinker in [mole/l]

The total amount of Na released as a result of hydration of cement, per litre of pore water is the sum of Na released from sulphates and from clinker minerals. This sum (all amounts in mole per litre of pore water) reads

$$[Na^+]_{released} = [Na^+]_{sulphate} + [Na^+]_{clinker} \tag{3.15}$$

3.3.4 Sorption

From many pore water measurements, Taylor (1987) concluded that a large part of released alkalis is not found in the pore water and apparently part of it is taken up by the hydration products in some way. The exact nature of this uptake of is not known yet. Gougar et al. (1996) reviewed the possibilities of C-S-H and ettringite as host for waste ions. They concluded that the mechanisms for C-S-H include sorption, phase mixing as well as substitution. Taylor (1987) mentions that substitution for Ca^{2+} is unlikely, because of the alkali/Ca^{2+} ratio found in C-S-H. Accordingly, it is believed that alkali ions are sorbed by the interlayers of C-S-H and not substituted.

Taylor (1987) proposed that the amount of each alkali cation taken up by the hydration products, C-S-H and AFm is proportional to the concentration present in the solution and the quantity of these hydration products formed. Taylor introduced two empirical constants, called binding factors, which are numerically equal to the amount of alkali in mmole that can be taken up from a 1 M alkali solution by the total quantity of hydration products formed from 100 g OPC. From his data Taylor assumed binding factors of 0.31 and 0.20 mmole alkali sorbed per g of hydrated OPC and per mole/l of total alkali released into the pore water for Na^+ and K^+, respectively. This is based on the assumption that 1 g of OPC produces a fixed amount of hydration product that is able to sorb ions. The linear relation between amount of alkali present in solution and amount sorbed by hydration product has been confirmed by Hong and Glasser (2000) who used synthetic C-S-H for their experiments. However, in these experiments, no significant differences were found in the binding capacities for Na^+ and K^+.

In the present study binding factors of 0.30 and 0.28 were assumed for Na^+ and K^+, respectively. These values produced best agreement between computed alkali concentrations and the measured concentrations presented by Reardon (1992) for different cements with

different alkali contents. Therefore it is assumed that these average values can be used for most types of cements. Hence, the amount of Na^+ consumed, in mole/l, is:

$$[Na^+]_{consumed} = \frac{bf_{Na} \cdot \alpha \cdot m_c \cdot [Na^+]_{released}}{m_w} = \frac{bf_{Na} \cdot \alpha}{w/c} \cdot [Na^+]_{released} = \frac{bf_{Na} \cdot Na_T \cdot \rho_w \cdot \alpha^2}{\frac{\varphi_p}{\varphi_p^0} \cdot (w/c)^2} \quad (3.16)$$

bf_{Na} = Na binding factor = 0.30 [ml/g]
bf_K = K binding factor = 0.28 [ml/g]

Computations for $[K^+]$ are done using the same equations and the corresponding values for K^+. The difference between the amounts of alkali released and consumed gives the actual alkali concentration in cement pore water.

$$[Na^+ + K^+] = [Na^+]_{released} - [Na^+]_{consumed} + [K^+]_{released} - [K^+]_{consumed} \quad (3.17)$$

3.3.5 Comparison between model and experiments

Larbi et al. (1990) determined pore water concentrations in pastes prepared with ENCI OPC having a PSD corresponding to CEM 32,5R cement. The composition of this cement is given in Table 3.2. A w/c ratio of 0.45 was used. Curing took place at a temperature of 20 ^{o}C. Pore water was obtained at different points in time using a pore fluid expression apparatus similar to that used by Longuet et al. (1973). Then, $[Na^+]$ and $[K^+]$ in the extracted pore water were determined using flame emission spectroscopy.

Table 3.2. Oxide composition of cement used for pore water determination (Larbi et al., 1990).

Oxide	Mass fraction
CaO	61.90
SiO_2	19.94
Al_2O_3	5.57
Fe_2O_3	2.91
K_2O	0.82
Na_2O	0.21
SO_3	3.10
MgO	1.50

CEMHYD3D simulations were executed using the discretised PSD of CEM 32,5 R (as presented in section 2.3.2), water saturated conditions, and w/c ratio and temperature corresponding to experimental conditions. The alkali fractions shown in Table 3.2, the alkali distribution given in Table 3.1 and binding factors of 0.30 and 0.28 for Na^+ and K^+, respectively were used for the computations. Table 3.3 gives the result for computations of

alkali concentrations using CEMHYD3D and the equations developed in sections 3.3.2 and 3.3.3. Because the model has been calibrated for CEM 32,5R (see section 2.3.4), cycles could be related to real time. The amounts released, amounts consumed by hydration products and the actual concentration are presented. For both Na^+ and K^+, the percentages of alkalis consumed (related to the amounts released) are also given. Table 3.4 gives the results of the pore water measurements by Larbi et al. (1990). Results are given at different points in time.

Table 3.3. Computed alkali concentrations released and consumed (cons.).

Time (days)	α	$\dfrac{\varphi_p}{\varphi_p^0}$	$[Na^+]$ released	$[Na^+]$ cons.	Na^+ cons. (%)	$[K^+]$ released	$[K^+]$ cons.	K^+ cons. (%)
0.25	0	1.00	0.05	0	0	0.27	0	0
0.50	0.21	0.80	0.09	0.01	15	0.36	0.05	14
1	0.30	0.72	0.11	0.02	21	0.41	0.08	19
2	0.38	0.66	0.13	0.03	26	0.45	0.11	24
3	0.43	0.63	0.14	0.04	29	0.48	0.13	27
7	0.53	0.56	0.17	0.06	36	0.55	0.18	34
14	0.61	0.51	0.20	0.08	41	0.61	0.24	39
28	0.68	0.46	0.24	0.11	47	0.68	0.30	44

Table 3.4. Computed and measured alkali concentrations Larbi et al. (1990).

Time (days)	$[Na^+]$ meas.	$[Na^+]$ calc.	$[K^+]$ meas.	$[K^+]$ calc.
0.25	0.05	0.05	0.21	0.27
0.50	0.05	0.08	0.23	0.31
1	0.05	0.09	0.24	0.33
2	0.06	0.10	0.26	0.34
3	0.07	0.10	0.26	0.35
7	0.11	0.11	0.33	0.36
14	0.13	0.12	0.36	0.38
28	0.14	0.13	0.37	0.39

The agreement between computed (Table 3.3) and measured (Table 3.4) $[Na^+]$ and $[K^+]$ is reasonable for hydration times up to 7 days and very well after 7 days. The trends are predicted well. This means that Taylor's model, although empirical, still gives a good method to describe release and sorption of alkalis. CEMHYD3D can be used to give the degree of hydration and the amount of free water as a function of time. For each of the two alkali ions only two parameters have to be estimated: the fraction present as alkali sulphate and the binding factor.

Larbi et al. (1990) also presented results for mixtures in which 20 % (m/m) of cement was replaced by silica fume. For these mixtures, also $[Na^+]$ and $[K^+]$ were determined at different times and found to be significant lower compared with OPC mixtures. CEMHYD3D computations were executed, using a 20 % (m/m) replacement of cement by silica fume, represented as S particles of 1 pixel (1 μm^3), i.e. 100 % reactive. As a result of the pozzolanic reaction, converting CH into pozzolanic C-S-H, this resulted in microstructures having

different C-S-H/CH ratios compared with OPC and a significant fraction of pozzolanic C-S-H, with a different C/S ratio compared with ordinary C-S-H. Hong and Glasser (2000) found that the binding capacity was a strong function of the C/S ratio of C-S-H. When C/S ratio decreased from 1.8 to 1.2, binding capacity of C-S-H increased by a factor of 2 (Hong and Glasser, 2000). These C/S ratios agree with the ratios of 1.7 and 1.1 assumed for ordinary C-S-H and pozzolanic C-S-H respectively. Therefore, for pozzolanic C-S-H, binding factors of 0.7 (two times as high compared with ordinary C-S-H) for both Na and K were chosen, yielding very good results. In fact, using the lower binding factors (used for the OPC simulation) for all C-S-H did not result in the strong decrease in Na^+ and K^+ as had been found by Larbi et al. (1990).

Tables 3.5 and 3.6 show computed and measured alkali concentrations of the 20 % (m/m) silica fume mixtures. It should be noted that computed porosity fractions for the silica fume mixtures were almost identical compared with mixtures without silica fume. The pozzolanic reaction produced additional solid volume of pozzolanic C-S-H, but on the other hand, because 20 % (m/m) of cement has been replaced, less ordinary C-S-H is produced, leaving extra porosity. These effects cancelled each other out in the simulations, giving almost equal porosity fractions in both systems.

Table 3.5. Computed alkali concentrations released and consumed (cons.) in SF mixtures.

Time (days)	α	$\dfrac{\varphi_p}{\varphi_p^0}$	$[Na^+]$ released	$[Na^+]$ cons.	Na^+ cons. (%)	$[K^+]$ released	$[K^+]$ cons.	K^+ cons. (%)
0.25	0	1.00	0.04	0.00	0	0.22	0.00	0
0.50	0.19	0.80	0.07	0.01	19	0.29	0.05	18
1	0.28	0.72	0.09	0.03	29	0.34	0.09	28
2	0.35	0.66	0.11	0.04	38	0.38	0.14	37
3	0.40	0.63	0.12	0.05	44	0.40	0.17	43
7	0.50	0.56	0.15	0.09	59	0.47	0.27	57
14	0.58	0.50	0.17	0.13	74	0.54	0.38	71
28	0.66	0.45	0.21	0.19	91	0.62	0.55	88

Table 3.6. Computed and measured alkali concentrations 20 % (m/m) silica fume mixtures Larbi et al. (1990).

Time (days)	$[Na^+]$ meas.	$[Na^+]$ calc.	$[K^+]$ meas.	$[K^+]$ calc.
0.25	0.06	0.04	0.19	0.22
0.50	0.06	0.06	0.19	0.24
1	0.1	0.06	0.23	0.24
2	0.09	0.07	0.21	0.24
3	0.08	0.07	0.19	0.23
7	0.05	0.06	0.09	0.20
14	0.04	0.05	0.07	0.15
28	0.03	0.02	0.05	0.07

From Table 3.6 it can be seen that computed alkali concentrations agree well with experimental results, proving that the binding factors chosen for pozzolanic C-S-H are

64

reasonable and that the computations can be used for OPC mixtures and silica fume mixtures as well. Note, that the agreement is particularly well, considering the *sum* of ($[Na^+] + [K^+]$) and that in the subsequent sections this *sum* of alkali concentration will be used. This means that this method will produce results that are accurate enough for further computations.

The computations of $[Na^+]$ and $[K^+]$ and their sum can be executed after each computation cycle, corresponding to some point in hydration time. Then, these values can be used as input for equilibrium computations, which will be described in the next section.

3.4 Non alkalis

3.4.1 Solving a set of pore water equilibria

To find the concentrations of all ions determined by equilibria in the pore water, the following information is required:

- The solubility properties of cementitious compounds, i.e. which ions are formed when the solid dissolves
- Activity products of the solids
- The activity of the ions at high concentrations
- The solids considered in equilibrium with pore water during a specific hydration period.

When the solids in equilibrium are known and all activity coefficients are known, for each solid an equation can be set up corresponding to its concentration product. Because neutrality always prevails, the charge balance (see Eq. (3.10)) should always apply, giving an additional equation. When the number of equations equals the number of unknown ion concentrations, the system of equations can be solved, giving the concentrations that satisfy all equilibria products and the charge balance.

3.4.2 Solubility properties of hydration products

The thermodynamic database used in SOLTEQ (Park and Batchelor, 1999a, 1999b) contains all relevant cement hydrates. For each relevant cement hydrate, the composition in terms of constituent ions and its activity product is given (see Table 3.7). Table 3.8 gives the activity products used in SOLTEQ and used in the work of Reardon (1992). Properties of hemihydrate are not mentioned in both studies.

Table 3.7. Cement hydrates equilibria (Park and Batchelor, 1999a).

Compound	Equilibrium
Portlandite	$Ca(OH)_2 \Leftrightarrow Ca^{2+} + 2OH^-$
Anhydrite	$CaSO_4 \Leftrightarrow Ca^{2+} + SO_4^{2-}$
Gypsum	$CaSO_4.2H_2O \Leftrightarrow Ca^{2+} + SO_4^{2-} + 2H_2O$
Ettringite	$Ca_6Al_2O_6(SO_4)_3.32H_2O \Leftrightarrow 6Ca^{2+} + 2Al(OH)_4^- + 3SO_4^{2-} + 4OH^- + 6H_2O$
Monosulphate	$Ca_4Al_2O_6SO_4.12H_2O \Leftrightarrow 4Ca^{2+} + 2Al(OH)_4^- + SO_4^{2-} + 4OH^- + 6H_2O$
C_4AH_{13}	$4CaO.Al_2O_3.13H_2O \Leftrightarrow 4Ca^{2+} + 2Al(OH)_4^- + 6OH^- + 6H_2O$
Hydrogarnet	$3CaO.Al_2O_3.6H_2O \Leftrightarrow 3Ca^{2+} + 2Al(OH)_4^- + 4OH^-$

Table 3.8. Thermodynamic activity products used in SOLTEQ (Park and Batchelor, 1999) and used by Reardon (1992).

	$Log(K^0)$ (SOLTEQ)	$Log(K^0)$ (Reardon)
Portlandite	-5.32	-5.19
Anhydrite	-4.64	-
Gypsum	-4.85	-4.58
Ettringite	-43.13	-43.94
AFm	-27.62	-29.25
C_4AH_{13}	-27.49	-
Hydrogarnet	-	-23.13

The situation for C-S-H is complicated because of its amorphous nature and various compositions (such as C/S ratio). The solubility of C-S-H cannot simply be described by a fixed activity product. Many models are proposed for describing the structure at different scales and for describing the solubility of C-S-H at different pH (Reardon (1990)). One way of presenting the C-S-H equilibrium is as follows:

$$(C/S)CaO.SiO_2.(C/S)H_2O + H_2O \rightarrow (C/S)\ Ca^{2+} + H_3SiO_4^- + (2(C/S)-1)\ OH^- \quad (3.18)$$
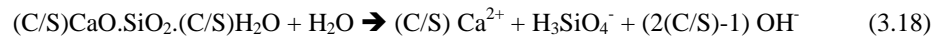
For this equilibrium the activity product is (Reardon, 1992):

$$K^0_{CSH} = 9.044 - 0.568 \cdot R + 0.193 \cdot R^2 \quad (3.19)$$

with

$$R = \frac{Ln(C/S - 0.88) - Ln(0.03)}{0.513} \quad (3.20)$$

$C/S = CaO/SiO_2$ molar ratio.

This gives the practical values as presented in Table 3.9.

Table 3.9. Solubility C-S-H.

C/S	R	$log(K^0)$
1	2.70	-8.92
1.1	3.88	-9.75
1.4	5.56	-11.85
1.7	6.45	-13.41

3.4.3 Activity coefficients

The ionic strength of pore water is very high because it contains high concentrations of alkalis. Ionic strength values ranging from 0.5 to more than 1 in mature pastes have been reported (Reardon, 1992). At those values, using the Davies equation and other equations based on ion-specific parameters are not sufficient and will produce large errors in activity coefficients. This results in large errors in concentration products of the cementitious compounds. This is especially the case when the solid constitutes several ions and its concentration product is of high order. For example, ettringite is of the 15th order according to its composition (see also Table 3.7) and therefore its concentration product is very sensitive to errors in the activity coefficients.

In Appendix 4 all equations and interaction parameters can be found which were used to compute activity coefficients according to the method by Pitzer (1979). Some interactions were neglected because they were assumed being insignificant. Example computations show that in a 0.5 M solution, activity coefficients have a value of around 0.7 for monovalent ions, e.g. Na^+, and around 0.15 for divalent ions, e.g. Ca^{2+}, according to Pitzer's ion interaction approach.

Because Pitzer equations are used in this study, the K^0 values to be used should also be based on the Pitzer approach. Therefore, in all computations K^0 values reported by Reardon (1992) will be used consequently, because these values were determined from solubility measurements in which the ion interaction approach was taken into account (Reardon, 1995).

3.4.4 Reducing number of equilibria

After each hydration cycle in CEMHYD3D, concentrations will have to be computed by solving a set of equilibrium equations. To develop a reliable computation method that always converges to the right solution, it is required to use as little iterations as possible and therefore, the number of solids and corresponding equations to be solved should be reduced to a minimum. This makes the computations more straightforward and also would give a clearer and better understanding of the equilibrium system and the relations between specific equilibria and specific concentrations.

The number of equations can be reduced by considering some common properties of the pore water solution known at forehand and by preliminary computations and mathematical considerations of the different equilibria available.

It is known that $[OH^-]$ in all common system is high and because of the common ion effect, this means that the OH^- dependent solubility of ettringite, the AFm phase or C-S-H will be lower than their solubility as a single compound (which can be computed from Eq. (3.9)). This means that their contributions to total concentrations are expected to be very low. Indeed, Park and Batchelor (1999) concluded from their SOLTEQ computations that changes in the K^0 value of ettringite or AFm only affected SO_4^{2-} predictions and had little effect on Ca^{2+}, $H_3SiO_4^-$ and $Al(OH)_4^-$. The K^0 value for C-S-H only affected $H_3SiO_4^-$ predictions. They concluded that the CH equilibrium, i.e. changes in its K^0 value, affected all solutions the most and particularly determined Ca^{2+} and OH^- predictions.

Before sets of equations will be set up in this section, first note that the total alkali concentration $[Na^+ + K^+]$ and the activity coefficients will always be computed at forehand, i.e. before the set of equations will be solved. $[Na^+ + K^+]$ will be computed at forehand using the non-equilibrium approach. Activity coefficients will be determined at forehand using estimations or using the concentrations found in the previous time cycle. When these coefficients are known, concentration products can be derived from the activity products using Eq. (3.3) and hence, concentrations can be used in the equations to be solved.

Already during the first hours of hydration, the pore water is saturated with respect to $Ca(OH)_2$ and this will also be the case in mature pastes. Thus, the corresponding equilibrium equation should always be fulfilled. This equation reads:

$$K_{CH} = [Ca^{2+}] \cdot [OH^-]^2 \qquad (3.21)$$

Now let us consider the early hydration period (first few days) during which gypsum or some other calcium sulphate phase is still present. Only one of the corresponding equilibria is then sufficient to determine $[SO_4^{2-}]$. The gypsum equilibrium will be used in this study, because it is the most stable calcium sulphate compound. Taking the activity of H_2O as unity, this gives:

$$K_{gypsum} = [Ca^{2+}] \cdot [SO_4^{2-}] \qquad (3.22)$$

Finally, the charge balance needs to be applied. This gives the following equation:

$$2 \cdot [Ca^{2+}] + [Na^+ + K^+] - [OH^-] - 2 \cdot [SO_4^{2-}] = 0 \qquad (3.23)$$

Now we have three equations (Eqs. (3.21)–(3.23)) and assuming that the total alkali concentration is known and the numeric values for the concentration products are known, we also have three unknowns: $[OH^-]$, $[Ca^{2+}]$ and $[SO_4^{2-}]$. This means we have a closed system of equations that can be solved.

Adding a second sulphate containing solid, e.g. an aluminium sulphate such as ettringite gives one extra equilibrium, but also one extra unknown, namely $[Al(OH)_4^-]$, yielding again a closed system. However, this extension of the system is not expected to have a significant influence on predicted $[SO_4^{2-}]$, because $[OH^-]$ is high from the beginning of hydration and all aluminium sulphates will be very slightly soluble. Therefore, these sulphates will not contribute to total concentrations in general and especially not to $[SO_4^{2-}]$ because of the more soluble gypsum assumed present. Such additional equations would only be useful when Al concentration $(Al(OH)_4^-)$ is of interest. The same accounts for adding the C-S-H equilibrium, which will only be relevant when computing Si concentration $(H_3SiO_4^-)$.

In conclusion, to find $[OH^-]$, $[Ca^{2+}]$ and $[SO_4^{2-}]$ and as long as gypsum is still present, the equilibria for $Ca(OH)_2$ and $C\overline{S}H_2$ and the charge balance have to be solved simultaneously. Table 3.10 gives an overview of the equations.

Table 3.10. Equations to be solved in the presence of calcium sulphates.

	Equation
Portlandite	$K_{CH} = [Ca^{2+}] \cdot [OH^-]^2$
Gypsum	$K_{C\overline{S}H_2} = [Ca^{2+}] \cdot [SO_4^{2-}]$
Charge	$2 \cdot [Ca^{2+}] + [Na^+ + K^+] - [OH^-] - 2 \cdot [SO_4^{2-}] = 0$

When gypsum is fully consumed a new situation in the pore water is encountered. Now the gypsum equilibrium (Eq. (3.22)) does not apply anymore, and other sulphate containing solids have to be taken into account, e.g. ettringite and monosulphate. Because these solids form $Al(OH)_4^-$ ions, their presence implies a new variable in the system of equations: $[Al(OH)_4^-]$, now yielding four unknowns: $[OH^-]$, $[Ca^{2+}]$, $[SO_4^{2-}]$ and $[Al(OH)_4^-]$. This means that four equations are required, from which two are known already: the CH equilibrium (Eq. 3.21) and the charge balance, including $Al(OH)_4^-$:

$$2 \cdot [Ca^{2+}] + [Na^+ + K^+] - [OH^-] - 2 \cdot [SO_4^{2-}] - [Al(OH)_4^-] = 0 \tag{3.24}$$

Two additional equilibria are required to obtain a closed system of equations and have to be selected from ettringite, monosulphate, C_4AH_{13} and hydrogarnet (C_3AH_6). To find the mathematical relations between those four equilibria we consider their *activity* products, which read as follows (invoking $\{H_2O\} = 1$):

$$K^0_{C_6A\bar{S}_3H_{32}} = \{Ca^{2+}\}^6 \cdot \{Al(OH)_4^-\}^2 \cdot \{SO_4^{2-}\}^3 \cdot \{OH^-\}^4 \tag{3.25}$$

$$K^0_{C_4A\bar{S}H_{12}} = \{Ca^{2+}\}^4 \cdot \{Al(OH)_4^-\}^2 \cdot \{SO_4^{2-}\} \cdot \{OH^-\}^4 \tag{3.26}$$

$$K^0_{C_3AH_6} = \{Ca^{2+}\}^3 \cdot \{Al(OH)_4^-\}^2 \cdot \{OH^-\}^4 \tag{3.27}$$

$$K^0_{C_4AH_{13}} = \{Ca^{2+}\}^4 \cdot \{Al(OH)_4^-\}^2 \cdot \{OH^-\}^6 \tag{3.28}$$

First, note that combining Eqs. (3.27) and (3.28) gives

$$K^0_{C_4AH_{13}} / K^0_{C_3AH_6} =$$

$$\{Ca^{2+}\}^4 \cdot \{Al(OH)_4^-\}^2 \cdot \{OH^-\}^6 / \{Ca^{2+}\}^3 \cdot \{Al(OH)_4^-\}^2 \cdot \{OH^-\}^4 = \tag{3.29}$$

$$\{Ca^{2+}\} \cdot \{OH^-\}^2$$

so a combination of the equilibria of C_4AH_{13} and C_3AH_6 is conflicting with the CH equilibrium. For this reason C_4AH_{13} will not be used and three solids remain to be considered: ettringite, monosulphate and hydrogarnet, from which only two are required to solve the system. Combining Eqs. (3.25)- (3.27) yields

$$(K^0_{C_4A\bar{S}H_{12}})^3 = (K^0_{C_3AH_6})^2 \cdot K^0_{C_6A\bar{S}_3H_{32}} \tag{3.30}$$

However, substituting the corresponding numeric values given by Reardon (1992) (see the second column of Table 3.8) into Eq. (3.30) yields an inequality:

$$(10^{-29.25})^3 \neq (10^{-23.13})^2 \cdot (10^{-43.94})$$

69

This implies that the equations for ettringite, monosulphate and hydrogarnet (Eqs. (3.25)–(3.27)) can never be true at the same time. In other words, the three equations are not independent, because the corresponding numeric values are in contradiction.

When two out of the three solids are chosen, and assumed present, this would always imply some numeric value for the activity product of the third solid. The combinations monosulphate/hydrogarnet and monosulphate/ettringite would imply a numeric value for the activity product of the third remaining solid which is higher than the equilibrium value of this third solid, which would mean a supersaturation and thus the actual presence of this third solid, which is not allowed. This can be shown as follows:

Monosulphate and hydrogarnet assumed present:

$$(K^0_{C_4A\bar{S}H_{12}})^3 / (K^0_{C_3AH_6})^2 > K^0_{C_6A\bar{S}_3H_{32}} \tag{3.31}$$

Monosulphate and ettringite assumed present:

$$(K^0_{C_4A\bar{S}H_{12}})^3 / K^0_{C_6A\bar{S}_3H_{32}} > (K^0_{C_3AH_6})^2 \tag{3.32}$$

The combination ettringite/hydrogarnet implies a numeric value for the activity product of the third solid, monosulphate, that is lower than its equilibrium value which is allowed, because it means monosulphate is not assumed present as a solid:

Ettringite and hydrogarnet assumed present:

$$K^0_{C_6A\bar{S}_3H_{32}} \cdot (K^0_{C_3AH_6})^2 < (K^0_{C_4A\bar{S}H_{12}})^3 \tag{3.33}$$

From these considerations it is concluded that the solids ettringite and hydrogarnet should be taken into account to obtain a system of equilibria which represents the system in pore water after gypsum or any other calcium sulphate is consumed. This follows from thermodynamics of the pure aluminium minerals. The reason that in real cement/water systems monosulphate appears to be more stable than ettringite is not clear, but may be a result of substituted ions (Reardon, 1992).

In conclusion, to find $[OH^-]$, $[Ca^{2+}]$, $[SO_4^{2-}]$ and $[Al(OH)_4^-]$ after gypsum is consumed, the equilibria for $Ca(OH)_2$, ettringite and hydrogarnet and the charge balance have to be solved simultaneously. Table 3.11 gives an overview of the equations to be solved.

Table 3.11. Equations to be solved in the absence of calcium sulphates.

	Equation
Portlandite	$K_{CH} = [Ca^{2+}] \cdot [OH^-]^2$
Ettringite	$K_{C_6A\bar{S}_3H_{32}} = [Ca^{2+}]^6 \cdot [Al(OH)_4^-]^2 \cdot [SO_4^{2-}]^3 \cdot [OH^-]^4$
Hydrogarnet	$K_{C_3AH_6} = [Ca^{2+}]^3 \cdot [Al(OH)_4^-]^2 \cdot [OH^-]^4$
Charge	$2 \cdot [Ca^{2+}] + [Na^+ + K^+] - [OH^-] - 2 \cdot [SO_4^{2-}] - [Al(OH)_4^-] = 0$

Summarising, in further computations it will be assumed that, with regards to the solids assumed to be in equilibrium with the pore water, during cement hydration two periods should be distinguished; one during which gypsum is present and one during which gypsum has been consumed.

In the first period, pore water concentrations can be computed taking into account the portlandite and gypsum equilibria. This period ends when gypsum is consumed. The moment at which this will occur depends on the amount and types of calcium sulphates added to the OPC. CEMHYD3D computes the distinctive degrees of hydration of gypsum, anhydrite and hemihydrate and will predict when all these phases are consumed. This depends on their solubility probabilities and the availability of C_3A during the simulation.

When gypsum is consumed, its equilibrium equation does not apply anymore. From that point, pore water concentrations have to be computed taking into account the portlandite, ettringite and hydrogarnet equilibria.

3.4.5 Implementing equilibrium computations in CEMHYD3D

CEMHYD3D provides degree of hydration of the cement and of the calcium sulphate phases and the pore volume fraction, all as function of time. This information is sufficient for the computation of alkali concentrations, $[Na^+]$ and $[K^+]$ according to the method described in section 3.3. Therefore, the first step in each computation cycle is computation of alkali concentrations without taking into account any equilibria.

In the equilibrium computations only K^0 values reported by Reardon (1992) will be used consequently, because they were determined taking into account Pitzer's method of calculating activity coefficients (see second column in Table 3.8).

To use concentrations when solving the system of equilibrium equations and charge balance, numeric values for concentrations are required firstly. To compute a concentration product K from a thermodynamic activity product K^0 (see Eq. (3.3)), activity coefficients are required. At the start of the simulation, when concentrations are not known yet, activity coefficients have to be estimated, for example by estimating the initial ionic strength and then using the Davies equation (Eq. (2) in Appendix 4). In the following cycles, the concentrations of the previous cycle can be used to compute activity coefficients according to Pitzer's ion interaction approach (see Appendix 4).

During a simulation of cement hydration the pore water is assumed to be in equilibrium with portlandite and gypsum or with portlandite, ettringite and hydrogarnet. This assumption is *not* related to the phases present in the simulated microstructure. For example, in CEMHYD3D, up to three types of calcium sulphate phases (gypsum, anhydrite or hemihydrate) may be present, ettringite may be present from the start of hydration and later ettringite and monosulphate are both present. This means that CEMHYD3D computations and the solving of equilibria are *independent* procedures in that respect.

Then, from the concentration products and the known total alkali concentration, a system of equilibrium equations and the charge balance can be solved. Here, the system was always solved for $[OH^-]$ first and all other concentrations could then be computed from $[OH^-]$ and the numeric values of concentration products. For example, during early hydration, when $[OH^-]$ was found, $[Ca^{2+}]$ was computed from the CH equilibrium:

$$[Ca^{2+}] = K_{CH}/[OH^-]^2 \tag{3.34}$$

and $[SO_4^{2-}]$ from the CH and $C\overline{S}H_2$ equilibria:

$$[SO_4^{2-}] = (K_{C\overline{S}H_2}/K_{CH})[OH^-]^2 \tag{3.35}$$

The computed concentrations can then be used to compute more accurate activity coefficients using the Pitzer equations. Then new concentration products can be computed and the system can be solved again. In general only one or two iterations are required.

For each hydration cycle, the procedure is equal. When CEMHYD3D predicts the consumption of gypsum (e.g. after one day of hydration) the new corresponding set of equilibria has to be solved from that point.

Summarising, the following steps were executed after each hydration cycle during a CEMHYD3D simulation:

- Computation microstructural parameters (degree of hydration, phase composition, porosity and calcium sulphate fraction)
- Computation of $[Na^+ + K^+]$
- Computation or estimation of activity coefficients
- Computing concentration products from K^0 values and activity coefficients
- Solving $[OH^-]$ from system of equations (Table 3.10 or Table 3.11)
- Computing $[Ca^{2+}]$, $[SO_4^{2-}]$ and $[Al(OH)_4^-]$ from concentration products

3.4.6 Comparison with experimental results

Larbi et al. (1990) not only measured $[Na^+]$ and $[K^+]$ (see section 3.3) but also $[Ca^{2+}]$ and $[OH^-]$ in the pore water of hydrating OPC. Measurement of $[OH^-]$ was done by titration against HNO_3 and using phenolphthalein as an indicator. CEMHYD3D simulations were executed using the PSD of CEM 32,5R, water saturated conditions, and w/c ratio and temperature corresponding to experimental conditions. The $[OH^-]$ and $[Ca^{2+}]$ computed using CEMHYD3D and the equilibrium model are compared with their results. Tables 3.12 and 3.13 and Fig. 3.1 show computed and measured pore water concentrations.

Table 3.12. Computed pore water concentrations.

Time (days)	α	$[Na^+ + K^+]$	$[OH^-]$	$10^3 \cdot [Ca^{2+}]$	$10^5 \cdot [Al(OH)_4^-]$	$10^3 \cdot [SO_4^{2-}]$
0.25	0	0.32	0.10	15.0	-	124
0.50	0.22	0.39	0.11	12.0	-	158
1	0.31	0.42	0.11	11.0	-	168
2	0.39	0.44	0.43	1.0	8.1	11
3	0.44	0.45	0.44	1.0	8.3	12
7	0.54	0.47	0.45	0.9	8.5	12
14	0.62	0.49	0.47	0.8	8.8	13
28	0.70	0.51	0.48	0.8	9.2	14

72

Table 3.13. Measured pore water concentrations.

Time (days)	[OH⁻]	$10^3 \cdot [Ca^{2+}]$
0.25	0.12	
0.50	0.13	
1	0.14	14.0
2	0.21	
3	0.27	6.0
7	0.41	
14	0.45	
28	0.47	0.8
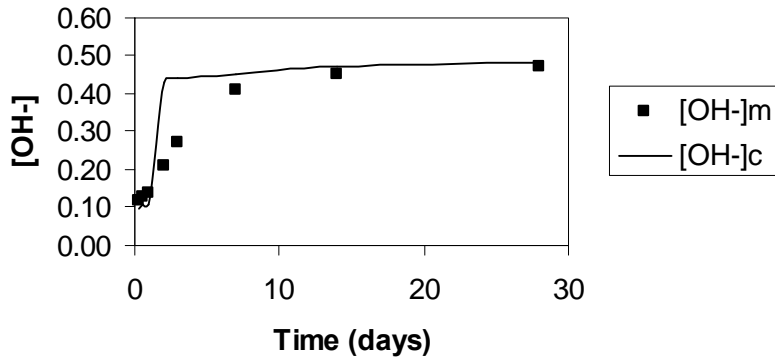
Figure 3.1. Pore water pH development.
[OH-]m = measured [OH⁻]. [OH-]c = computed [OH⁻].

Comparing computed [OH⁻] (Table 3.12) and measured [OH⁻] (Table 3.13) gives a good agreement. More particularly, the agreement during the first day of hydration and after 7 days of hydration is good. This implies that for both early and late hydration stages, the proper equilibria have been selected, i.e. no important equilibria have been ignored. The computations show an extreme rise for [OH⁻] after 1 day (from 0.11 to 0.43 M). This is a result from ignoring the gypsum equilibrium from that point in time. Before that point in time, $[SO_4^{2-}]$ was mainly determined by the gypsum equilibrium, giving a SO_4^{2-} concentration of 0.12 M. This concentration does not change significantly during the first day. When gypsum is consumed, $[SO_4^{2-}]$ is mainly determined by the ettringite equilibrium, which has a much lower solubility compared to gypsum and this results in a drop in $[SO_4^{2-}]$ to 0.012 M. Because alkali concentrations are not influenced by changes in equilibria they will remain unchanged. Therefore, the drop in $[SO_4^{2-}]$ will be compensated by an increase in [OH⁻] because of charge balance.

However, when considering the pore water measurements, the increase in OH⁻ is not as extreme as in the computations. [OH⁻] rises strongly between 1 and 7 days (see also Fig. 3.1). This different behavior can be explained as follows. In a hydrating microstructure, all solids are located randomly throughout the structure. The phase composition is not the same

everywhere and because of this, different equilibria may exist at the same time but at different locations. So, the measured pore water concentrations may be considered as an average of local equilibria values. As a result, the transition from the calcium sulphate equilibrium to the aluminum sulphate equilibrium occurs more smoothly in practice.

The computed $[Ca^{2+}]$ agrees well with results from measurements, again showing that no relevant equilibria were ignored.

Larbi et al. (1990) did not measure $[SO_4^{2-}]$ as a function of time. Reardon (1992) reported a few $[SO_4^{2-}]$ measurements in matured hydrated pastes (ranging from 3 to 27 mM) and one measurement for a high alkali cement paste at an early age (212 mM). The computed $[SO_4^{2-}]$ listed in Table 3.12 (14 to 124 mM) agree qualitatively with these experimental results.

3.5 Conclusions

In this chapter routines were developed for the computation of pore water concentrations and prediction of $[Na^+]$, $[K^+]$, $[OH^-]$, $[Ca^{2+}]$ and $[SO_4^{2-}]$. Computed pore water concentrations agreed well with experimental results reported in literature, for OPC as well as mixtures containing silica fume, taking into account stronger binding of alkalis by pozzolanic C-S-H. Concentrations during the first day of hydration as well as concentrations in mature hydrated pastes were predicted well.

All information required for the computations, e.g. the activity products and ion interaction parameters required for computation of activity coefficients, was available in the literature. Except for the empirical binding parameters describing binding of alkalis by hydration products, no other empirical parameters were required. This gives the routines a solid fundamental background. When more or more detailed information about the binding of alkalis comes available, or when better activity products are published, this can be easily implemented in the equations developed here.

Cement parameters required by the routines are also commonly known, e.g. alkali contents, SO_3 content of the clinker and type of calcium sulphate (gypsum, anhydrite or hemihydrate) added. If they are not known exactly, they can be estimated well. Also, the effects of these parameters on pore water concentrations can be studied using the extended model.

The extensions of CEMHYD3D, especially the $[OH^-]$ development can be used for the simulation of the hydration of fly ash and slags. Their reactions start at a threshold pore water pH, which can now be predicted by CEMHYD3D for different types of cement (different PSD or alkali content).

Because the equilibria mainly determining $[Ca^{2+}]$ and $[SO_4^{2-}]$ have been determined, the solubility of calcium and sulphate containing solids can now be treated. Such compounds are often formed as a result of the presence of contaminants in the pore water of cement/waste mixtures.

Chapter 4

Reactivity of fly ash

4.1 Introduction

In the use and production of cement and concrete nowadays more and more secondary materials are employed such as pulverised coal fly ash, granulated blast furnace slag and silica fume. These products exhibit hydraulic and pozzolanic behaviour, i.e. they are able to react with water and water-dissolved calcium hydroxide (CH), respectively, to form pozzolanic C-S-H, a cement hydration product.

It is understood that the ability of secondary materials to react strongly depends on the alkali content and temperature of the water (Fraay et al. (1989), Xu and Sarkar (1994), Taylor (1997), Hewlett (1998), Song and Jennings (1999), Song et al. (2000)). To investigate this, Pietersen (1990, 1993) performed pulverised coal fly ash dissolution experiments. During these experiments several pulverised fly ashes were dissolved in sodium hydroxide solutions of pH 13, 13.4 and 13.7, at various temperatures. As expected, dissolution rates (and related reaction rates as well) increased significantly with increasing pH and temperature.

As said, several authors have mentioned the relation between reaction rate at one hand and pH and temperature on the other hand. However, to the authors' knowledge, no analytical relation has been derived between reaction rate and pH and temperature. As this is of major importance to understand the hydration of cements blended with said secondary raw materials, in this paper such a relation is derived and applied.

In sections 4.2 dissolution experiments (Pietersen, 1990, 1993) are presented. In section 4.3 a comprehensive model is presented of the dissolution of a sphere, using a shrinking core model approach as first proposed by Yagi and Kunii (1955). Here, the sphere is allowed to be hollow (to account for cenospheres) and to consist of two (concentric) regions (to account for different composition and reactivity). Subsequently, in section 4.4 the resulting equations are applied to the experiments of Pietersen (1990, 1993). Based on this application, in section 4.5 a reaction equation for fly ash is put forward that contains the silica, aluminium, alkali and alkaline earth contents. From this application and proposed reaction mechanism the solubility of the fly ashes as a function of pH is obtained. In section 4.6 the reaction mechanism and experiments of Pietersen (1990, 1993) are furthermore used to analyse the composition of the fly ash, in particular, the difference between the outer region (outer hull) and inner region. Finally, in section 4.7 thermodynamic properties (such as the equilibrium constant and free energy of reaction) are determined of the considered fly ashes. In section 4.8 conclusions are presented.

4.2 Experiments

Pietersen (1990, 1993) reported dissolution experiments with two different class F fly ashes ("EFA" and "LM") at pH = 13, 13.4 and 13.7. The dissolution experiments were executed at temperatures of 20 ^{o}C, 30 ^{o}C and 40 ^{o}C. Sodium hydroxide (NaOH) was chosen as reaction medium and each time 100 mg of fly ash was reacted with 100 ml of solution in sealed plastic bottles. Actually, the OH^- concentration (thus pOH) has been imposed, and the pH been determined via pH + pOH = 14 (Pietersen (2000)). However, this relation is applicable only in case the temperature is 20 ^{o}C and hence, here the pOH is used henceforth.

The two investigated fly ashes originate from two different power plants and have broad and mutually different particle size distributions. One power plant is a "wet-bottom" type plant that operates at 1800 ^{o}C (EFA); the other fly ash originates from a low NO_x furnace plant (LM).

All experiments were executed with a sieved part of the fly ashes, the diameter lying between 38 μm and 50 μm. The fly ashes were also ultrasonically vibrated to prevent agglomeration of small particles to large ones. Moreover, for the experiments the particles were separated into a fraction of low density ("cenospheres") with a density smaller than 1400 kg/m^3 and in a fraction of high density ("solid spheres") with a density of 2300-2600 kg/m^3. SEM images of polished sections of these fractions revealed that the cenospheres were hollow thin-walled spheres.

In Table 4.1 the most important properties of both fly ashes are summarised. In this table also the crystalline SiO_2 and Al_2O_3 that are part of the mullite are specified, using the molar masses of both substances (M_A = 102 g/mole, M_S = 60 g/mole) and considering that mullite contains (by mass) 306/426 Al_2O_3 and 120/426 silica.

The dissolution experiments were also executed with the hollow cenospheres and the solid spheres, which differ in density about a factor of two (Pietersen 1990, 1993). The experiments revealed that for these two fly ashes Si, Al and K all dissolve congruently, implying bulk dissolution. Accordingly, the dissolution of the major component, Si, represents an adequate measure for the dissolution of the entire glass mass. This principle was used for the experiments, which are used here.

In Figs. 4.1 and 4.2 the mass fraction of silica in glass dissolved, α_S ($= m_S^r / m_S^0$), at 40 ^{o}C, is depicted against time for EFA and LM solid spheres, respectively, for three pOH levels. One can readily see that all experiments show a similar path in time, and that at lower pOH (larger OH^- concentration) the removal is largest. Images of leached particles revealed the creation of a hollow structure originating from the leached glass phase with remains of needle shape inert (crystalline) material. This finding is in agreement with etching experiments (Hulett and Weinberger (1980), Hemmings and Berry (1988)).

In Figs. 4.3 and 4.4 the mass dissolved from cenospheres and solid spheres for EFA and LM, respectively, are depicted at pOH = 0.3 and 40 ^{o}C. In Figs. 4.5 and 4.6 the dissolution of solid spheres for EFA and LM, respectively, are set out for 20 ^{o}C, 30 ^{o}C and 40 ^{o}C and at pOH = 0.3. One can see that cenospheres dissolve faster, and that higher temperature enhance the dissolution rate.

In the subsequent section a model is derived which adequately describes the dissolution experiments. The observation of a removed glass phase and an inert crystalline phase suggests the application of a shrinking core model (Yagi and Kunii (1955), Levenspiel (1999)). Furthermore, the trend of the dissolved mass versus time suggests a control by diffusion through the dissolved shell.

Table 4.1. Composition (in m/m %) of investigated fly ashes (Pietersen (1993)), specification of crystalline SiO_2 and Al_2O_3 in mullite (all percentages based on total fly ash mass).

Overall Composition	EFA		LM	
	solid	ceno	solid	ceno
SiO_2	55.56%	51.55%	57.39%	52.21%
Al_2O_3	27.39%	31.96%	31.18%	39.54%
Fe_2O_3	4.65%	2.96%	3.50%	2.02%
TiO_2	1.20%	0.91%	1.90%	1.43%
MgO	1.82%	1.41%	0.28%	0.24%
CaO	2.83%	0.80%	2.75%	1.15%
Na_2O	1.84%	1.94%	0.37%	0.38%
K_2O	4.40%	5.68%	1.00%	1.02%
P_2O_5	n.d.	n.d.	0.54%	n.d.
H_2O	0.3%	0.4%	1.1%	1.4%
LOI (carbon)	0.0%	2.4%	0.0%	0.6%
Of which				
Mullite ($3Al_2O_3.2SiO_2$)	2.1%	5.4%	20.5%	36.2%
Quartz (SiO_2)	3.0%	3.0%	12.8%	1.6%
	--------	--------	--------	--------
Total crystalline	5.1%	8.4%	33.3%	37.8%
Total non-crystalline	94.9%	91.6%	66.7%	62.2%
Hence				
SiO_2 in mullite	0.6%	1.5%	5.8%	10.2%
Al_2O_3 in mullite	1.5%	3.9%	14.7%	26.0%

Figure 4.1. Fraction of mass dissolved α_S (α) versus time (Pietersen (1993)) and fit (Eqs. (4.31) (line) and (4.32) (dotted line)) for EFA solid spheres (b = 1) at pOH = 0.3, 0.6 and 1 (T = 40 ^{0}C).

Figure 4.2. Fraction of mass dissolved α_S (α) versus time (Pietersen (1993)) and fit (Eqs. (4.31) (line) and (4.32) (dotted line)) for LM solid spheres (b = 1) at pOH = 0.3, 0.6 and 1 (T = 40 ^{0}C).

Figure 4.3. Fraction of mass dissolved α_S (α) versus time (Pietersen (1993)) and fit (Eqs. (4.31) (line) and (4.32) (dotted line)) for EFA cenospheres (b = 0.5) and solid spheres (pOH = 0.3, T = 40 ^{0}C).
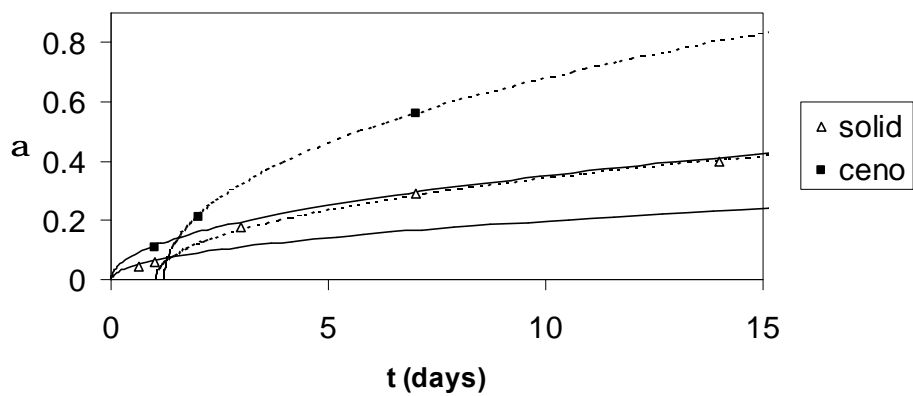
Figure 4.4. Fraction of mass dissolved α_S (α) versus time (Pietersen (1993)) and fit (Eqs. (4.31) (line) and (4.32) (dotted line)) for LM cenospheres (b = 0.5) and solid spheres (pOH = 0.3, T = 40 ^{0}C).
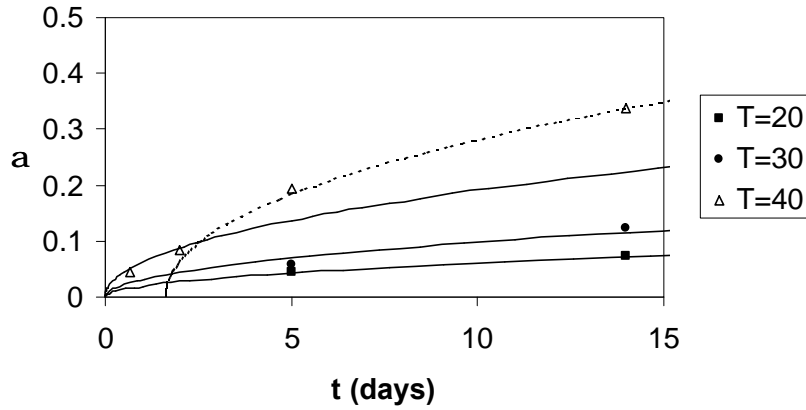
Figure 4.5. Fraction of mass dissolved α_S (α) versus time (Pietersen (1993)) and fit (Eqs. (4.31) (line) and (4.32) (dotted line)) for EFA solid spheres at T = 20 ^{0}C, 30 ^{0}C and 40 ^{0}C (pOH = 0.3).
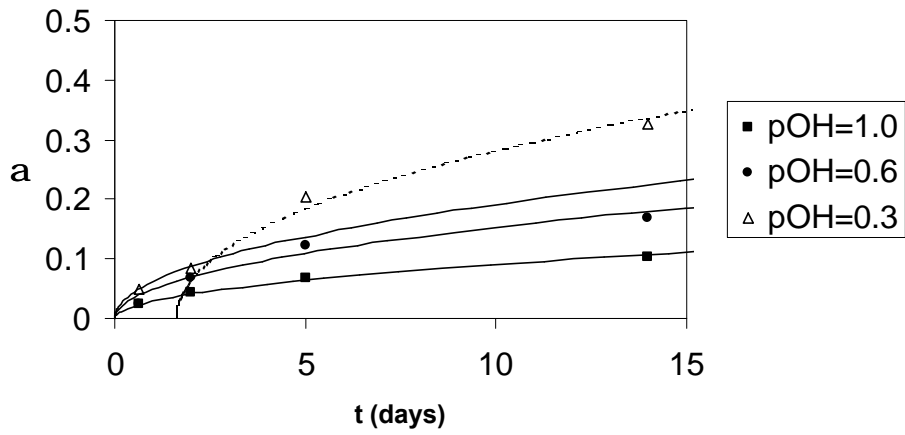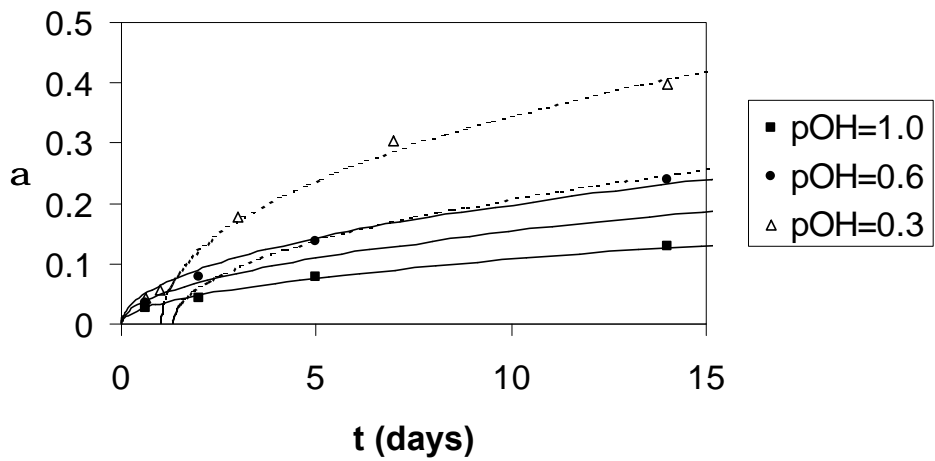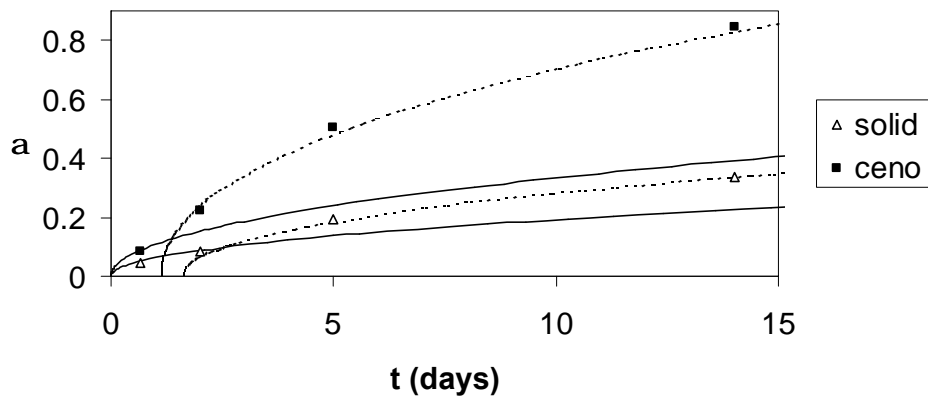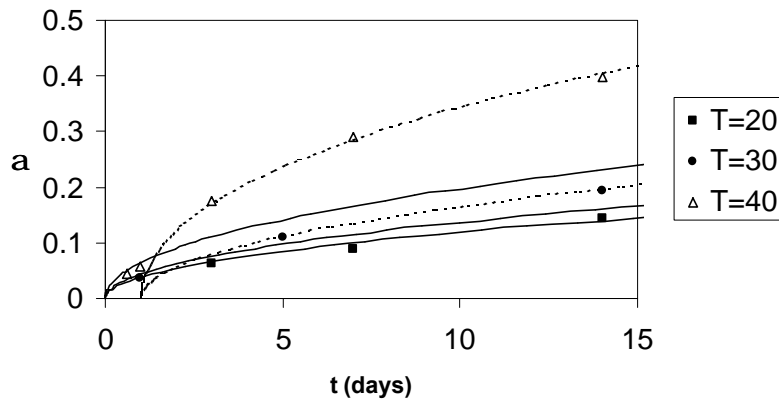

Figure 4.6. Faction of mass dissolved α_S (α) versus time (Pietersen (1993)) and fit (Eqs. (4.31) (line) and (4.32) (dotted line)) for LM solid spheres at T = 20 ^{0}C, 30 ^{0}C and 40 ^{0}C (pOH = 0.3).

4.3 Dissolution model

In this section the dissolution of a spherical particle in an infinite reservoir of liquid is modelled. This particle is considered to have a phase that dissolves and leaves porosity, and an inert part that is unaffected. In fly ash and slag the dissolving part corresponds to the glass phase, whereas the inert part can be thought of as crystalline. The unreacted core shrinks, and the dissolved glass diffuses through the porous shell of inert material towards the solvent. Therefore, the part of the volume that is dissolving is named porosity ϕ and hence the inert part 1 - ϕ. This shrinking unreacted core model was first presented by Yagi and Kunii (1955) and an extensive treatment can be found in Levenspiel (1999). Here, this model will be

applied to the leaching of glass from fly ash assuming control by diffusion through the dissolved shell, following the treatment of Levenspiel (1999). The model presented here differs in two aspects from the conventional model:

1. Here we permit the sphere to be hollow, as is the case in cenospheres. From analyses by among others Pietersen (1990, 1993), Hemmings and Berry (1988) it follows that some fly ash particles have a hollow core, which results in a lower mean density of these cenospheres.
2. From Figs. 4.1-4.6 it follows that for glass removal rates up to about 20% the experiments follow a path which can be explained with a diffusion rate limited shrinking core model. For higher removal rates (appearing at higher OH^- concentrations and/or higher temperature), however, it seems that glass removal accelerates. Accordingly, here the sphere is considered to consist of two regions, the interior glass and the exterior glass, a concept, which is also mentioned by Hemmings and Berry (1988).

Hence, consider a hollow spherical particle with a hollow radius r_h, an inner radius r_{in} and an outer radius r_{out}, an external surface area A, and glass volume V.. The particle possesses an outer and an inner region, the boundary between both regions designated as r_{in} and the reacting surface designated as r_r (Fig. 4.7).
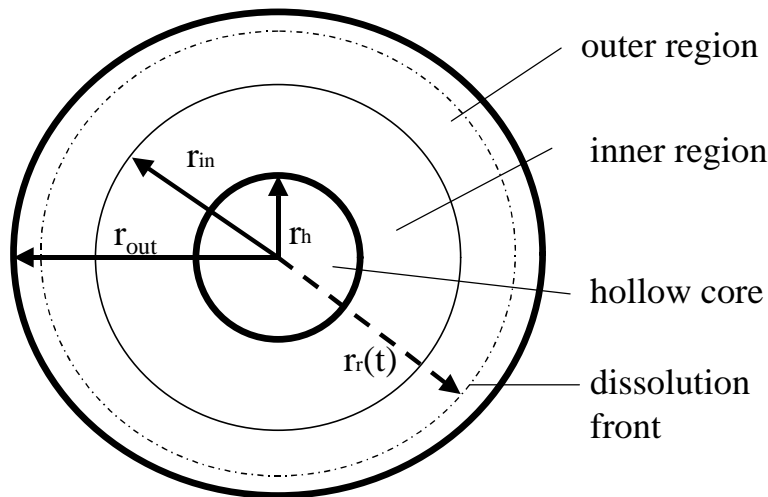
Figure 4.7. Schematic representation of dissolving hollow sphere containing two regions.

In an alkali environment, OH^- ions are diffusing towards the reacting surface, whereas released glass ions (SiO_3^{2-} and others such as AlO_2^-) are diffusing from glass core to the surrounding liquid. Both SiO_2 and Al_2O_3 are the major constituents of the glass (Table 4.1)) and are hydrated to aforesaid ions for pH larger than about 12 (Paul (1977, 1990)). As the silica release has been measured by Pietersen (1990, 1993), here the release of this constituent is focused on. For all other constituents a similar analysis can be performed.

Moreover, in section 4.7 it will be reasoned that the dissolution process is governed indeed by the diffusion of the SiO_3^{2-} ion.

The steady-state diffusion equation for SiO_3^{2-} ion diffusing through the leached shell now reads:

$$\frac{d(r^2 D_{eS} \frac{dC_S}{dr})}{dr} = 0 \tag{4.1}$$

$C_S = [SiO_3^{2-}]$
r = radius
D_e = effective diffusion coefficient

The effective diffusion coefficient depends on the ion concentrations (Helfferich (1995)) and on the porosity of the leached shell (Dullien (1979)). When the concentration of one ion is smaller than the other, the effective diffusion coefficient takes the value of that ion present in smaller concentration (Helfferich (1995)). Here it is assumed a priori that the concentration of the SiO_3^{2-} ion is much smaller than the OH^- concentration, so that D_e is constant. This assumption will be verified a posteriori. The effective diffusion coefficient in the porous shell is related to the bulk diffusion coefficient via Archie's law (Dullien (1980)):

$$D_{eS} = \phi^n D_S \tag{4.2}$$

The parameter n varies between 1.5 and 2.5, here a value of 2 is imposed, which is also recommended by Wakao and Smith (1962). The boundary conditions of Eq. (4.1) read:

$$C_S(r = r_{out}) = 0 \tag{4.3}$$

$$C_S(r = r_r) = C_{Sr} \tag{4.4}$$

The first condition reflects the negligible small SiO_3^{2-} concentration in the surrounding liquid, whereas the second boundary condition states the SiO_3^{2-} concentration at the glass core. Solving Eqs. (4.1), (4.3) and (4.4) yields

$$C_S(r) = \left[\frac{C_{Sr} r_r}{r_{out} - r_r} \right] \left[\frac{r_{out}}{r} - 1 \right] \tag{4.5}$$

The SiO_3^{2-} molar flux from the glass surface now reads

$$\overset{\bullet}{m}_S = -D_{eS} \frac{dC_S}{dr} \bigg|_{r_r} = \frac{D_{eS} C_{Sr} r_{out}}{(r_{out} - r_r) r_r} \tag{4.6}$$

The silica decrease of the particle by dissolution now reads

$$\phi x_S \rho_g \frac{4\pi}{3} \frac{dr_r^3}{dt} = -A_c \dot{m}_S \tag{4.7}$$

x = mole fraction

in which ρ_g is the molar density of the glass and x_S its mole fraction of silica and whereby $\dot{m}_S$ follows from Eq. (4.6). Inserting

$$A_r = 4\pi r_r^2 \tag{4.8}$$

and introducing

$$r^* = \frac{r}{r_{out}} \tag{4.9}$$

$$\tau = \frac{x_S \rho_g r_{out}^2}{6\phi D_S C_{Sr}} \tag{4.10}$$

in which Eq. (4.2) has been substituted, yields the following first order ordinary differential equation for the dimensionless radius:

$$\frac{dr_r^*}{dt}(r_r^* - 1)r_r^* = \frac{1}{6\tau} \tag{4.11}$$

With as initial condition

$$r_r^*(t = 0) = 1 \tag{4.12}$$

in case the outer region is considered, and

$$r_r^*(t = t_{in}) = r_{in}^* \tag{4.13}$$

when the dissolution of the inner region is considered. Note that τ is different for the inner and outer regions, which are therefore denoted by τ_{in} and τ_{out}, respectively. Integrating Eq. (4.11) and application of Eqs. (4.12) and (4.13) yields, respectively:

$$t = (1 - 3r_r^{*2} + 2r_r^{*3})\tau_{out} \tag{4.14}$$

$$t = (3r_{in}^{*2} - 2r_{in}^{*3} - 3r_r^{*2} + 2r_r^{*3})\tau_{in} + t_{in} \tag{4.15}$$

which are both implicit relations of r^* as a function of time.

Note that r_{in}^* and t_{in}, using Eq. (4.14), are related by:

$$t_{in} = (1 - 3r_{in}^{*2} + 2r_{in}^{*3})\tau_{out} \tag{4.16}$$

Substituting this equation into Eq. (4.15) produces:

$$t = (1 - 3r_r^{*2} + 2r_r^{*3})\tau_{in} + t_{in}(1 - \frac{\tau_{in}}{\tau_{out}}) \tag{4.17}$$

for the inner region.

Here distinction has been made between an outer and inner region that may have among others different porosity (glass fraction), glass molar density and glass silica content. Often, also by Pietersen (1990, 1993), average values are given, such as the conversion factor. Hence, the expressions derived here will be related to average particle quantities.

The mean glass density of the particle is related to the properties of inner and outer region via

$$\overline{\phi\rho_g}\,(r_{out}^3 - r_h^3) = \phi_{out}\rho_{gout}(r_{out}^3 - r_{in}^3) + \phi_{in}\rho_{gin}(r_{in}^3 - r_h^3) \tag{4.18}$$

Similarly, the average glass silica content is related to the contents in outer and inner region via:

$$\overline{x_S\phi\rho_g}\,(r_{out}^3 - r_h^3) = x_{Sout}\phi_{out}\rho_{gout}(r_{out}^3 - r_{in}^3) + x_{Sin}\phi_{in}\rho_{gin}(r_{in}^3 - r_h^3) \tag{4.19}$$

The glass mass removed (or, conversion factor) for the outer region reads:

$$\alpha_g = 1 - \frac{\phi_{out}\rho_{gout}(r_r^3 - r_{in}^3) + \phi_{in}\rho_{gin}(r_{in}^3 - r_h^3)}{\overline{\phi\rho_g}(r_{out}^3 - r_h^3)} \tag{4.20}$$

$\alpha_g =$ glass mass fraction removed $= m_g^r / m_g^0$

Analogously, the fraction of glass silica dissolved (or, silica conversion factor) for the outer region follows from

$$\alpha_S = 1 - \frac{x_{Sout}\phi_{out}\rho_{gout}(r_r^3 - r_{in}^3) + x_{Sin}\phi_{in}\rho_{gin}(r_{in}^3 - r_h^3)}{\overline{x_S\phi\rho_g}(r_{out}^3 - r_h^3)} \tag{4.21}$$

$\alpha_S =$ silica (in glass) mass fraction removed $= m_S^r / m_S^0$

Combining Eqs. (4.18) and (4.20) and Eqs. (4.19) and (4.21) reveals

$$\alpha_S = \alpha_g \frac{x_{Sout}}{\overline{x_S}} \tag{4.22}$$

The glass conversion rate of the inner region reads

$$\alpha_g = 1 - \frac{\phi_{in}\rho_{gin}(r_r^3 - r_h^3)}{\overline{\phi\rho_g}(r_{out}^3 - r_h^3)}$$

(4.23)

and the silica conversion rate for the inner region is

$$\alpha_S = 1 - \frac{x_{Sin}\phi_{in}\rho_{gin}(r_r^3 - r_h^3)}{x_S\overline{\phi\rho_g}(r_{out}^3 - r_h^3)}$$

(4.24)

Combining Eqs. (4.23) and (4.24) reveals that for the inner region holds:

$$1 - \alpha_S = (1 - \alpha_g)\frac{x_{Sin}}{\overline{x_S}}$$

(4.25)

Note that Eq. (4.20) coincides with Eq. (4.23) and Eq. (4.22) with Eq. (4.24) for $r_r = r_{in}$ (i.e. on the transition of inner and outer region), as would be expected.

In order to express r_r in to α_g and α_S, Eq. (4.21) is rewritten by inserting Eq. (4.19) in the nominator and introducing b (which can be seen as is the ratio between apparent mean density of the hollow sphere and the mean glass density):

$$b = \frac{\rho_{ap}}{\rho_g} = 1 - \frac{r_h^3}{r_{out}^3} = 1 - r_h^{*3}$$

(4.26)

yielding for the outer region:

$$r_r^{*3} = 1 - \alpha_S b \frac{\overline{x_S\phi\rho_g}}{x_{Sout}\phi_{out}\rho_{gout}} = 1 - \alpha_g b \frac{\overline{\phi\rho_g}}{\phi_{out}\rho_{gout}}$$

(4.27)

see Eqs. (4.9) and (4.22). Substituting Eqs. (4.19) and (4.26) into Eq. (4.23) yields for the inner region

$$r_r^{*3} = 1 - b + (1 - \alpha_S)b\frac{\overline{x_S\phi\rho_g}}{x_{Sin}\phi_{in}\rho_{gin}} = 1 - b + (1 - \alpha_g)b\frac{\overline{\phi\rho_g}}{\phi_i\rho_{gin}}$$

(4.28)

see Eqs. (4.9) and (4.25).

Eqs. (4.27) and (4.28) can be combined with Eqs. (4.14) and (4.17), respectively, yielding

$$t = (1 - 3(1 - \alpha_S b\frac{\overline{x_S\phi\rho_g}}{x_{Sout}\phi_{out}\rho_{gout}})^{\frac{2}{3}} + 2(1 - \alpha_S b\frac{\overline{x_S\phi\rho_g}}{x_{Sout}\phi_{out}\rho_{gout}}))\tau_{out}$$

(4.29)

$$t = (1 - 3(1 - b + (1 - \alpha_S)b \frac{\overline{x_S \phi \rho_g}}{x_{Sin} \phi_{in} \rho_{gin}})^{\frac{2}{3}} + 2(1 - b + (1 - \alpha_S)b \frac{\overline{x_S \phi \rho_g}}{x_{Sin} \phi_{in} \rho_{gin}}))\tau_{in} + t_{in}(1 - \frac{\tau_{in}}{\tau_{out}})$$

$$(4.30)$$

Note that Eqs. (4.27) and (4.28) become identical when the spheres are homogeneous, i.e. when $\overline{x_S \phi \rho_g} = x_{Sout} \phi_{out} \rho_{gout} = x_{Sin} \phi_{in} \rho_{gin}$, and that Eqs. (4.29) and (4.30) than reduce to

$$t = (1 - 3(1 - \alpha_g b)^{\frac{2}{3}} + 2(1 - \alpha_g b))\tau_{out} \tag{4.31}$$

$$t = (1 - 3(1 - \alpha_g b)^{\frac{2}{3}} + 2(1 - \alpha_g b))\tau_{in} + t_{in}(1 - \frac{\tau_{in}}{\tau_{out}}) \tag{4.32}$$

Furthermore, note that for $\tau_{in} = \tau_{out}$ (see Eq. (4.10)), Eqs. (4.31) and (4.32) are identical, in case of solid spheres (b = 1) they then reduce to the common shrinking core model expressions.

In Fig. 4.8a α_g is depicted against t for b = 1 (massive spheres) using Eqs. (4.31) and (4.32). As example, τ_{out} has been set equal to 30 s., τ_{in} to 10 s. and t_{in} $(1-\tau_{in}/\tau_{out})$ to 3 s., i.e. a case whereby the inner region is more reactive than the outer region.

One can readily see that for $\tau_{in} < \tau_{out}$ the glass removal line crosses the horizontal axis at t > 0 and climbs steeper in time. This behaviour was also seen in Figs. 4.1-4.6, implying two regions with two different τ. In the following section Eqs. (4.31) and (4.32) are applied to the experimental data depicted in said figures. In Fig. 4.8b, a case whereby the inner region is less reactive than the outer region is depicted, τ_{out} has been set equal to 30 s., τ_{in} to 80 s. and t_{in} $(1-\tau_{in}/\tau_{out})$ to - 3 s. One can see that when the inner region is attained, removal proceeds slower.

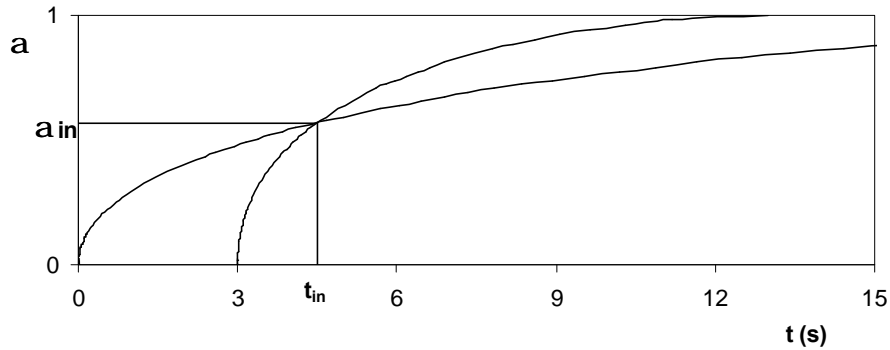**Figure 4.8a.** Mass removal versus time for a solid sphere (b = 1) using Eqs. (4.31) and (4.32), $\tau_{out} = 30$ s., $\tau_{in} = 10$ s. and t_{in} $(1-\tau_{in}/\tau_{out}) = 3$ s.
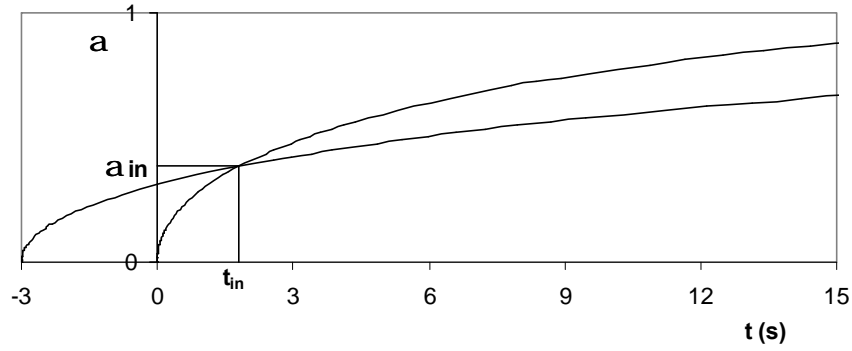
Figure 4.8b. Mass removal (α) versus time for a solid sphere (b = 1) using Eqs. (4.31) and (4.32), τ_{out} = 30 s., τ_{in} = 80 s. and t_{in} (1-τ_{in}/τ_{out}) = -3 s.

4.4 Model application

In Figs. 4.1-4.6 Eq. (4.31) has been fitted to the experimental data by adapting τ_{out}. For the solid spheres b has been set equal to unity, whereas for the cenospheres b equals 0.5 (Pietersen (1990, 1993)). Furthermore, it has been assumed a priori that the silica is homogeneously distributed, i.e. $\overline{x_S \phi \rho_g}$ = $x_{Sout} \phi_{out} \rho_{gout}$ = $x_{Sin} \phi_{in} \rho_{gin}$ and hence, $\alpha_g = \alpha_S$ (the fraction of removed glass is identical to fraction of removed silica, this latter quantity was measured by Pietersen (1990, 1993)). When the inner region has been reached, i.e. when Eq. (4.31) is not able to match the measured removal rates anymore (at larger t), Eq. (4.32) was fitted to these data by adapting τ_{in}.

From Figs. 4.1-4.6 it follows that for the solid spheres the inner region is attained when about 7% (LM) to 9% (EFA) of the silica/glass has been dissolved (= $\alpha g_{in} = \alpha_{Sin}$). Said values imply that the boundary between both regions is located at about 96-97% of the external radius of the sphere. These values are identical for all experiments, regardless the pOH and temperature of the experiment. At higher pH and higher temperature the lines intersect after 1-2 days (= t_{in}), whereas for low temperatures even after 15 days the – more reactive- inner region has not been attained yet. For the cenospheres, Figs. 4.3 and 4.4 learn that the outer region comprises 12% (EFA) to 13% (LM) of sphere mass. As b = 0.5 (and hence r_h^{*3} = 0.80, see Eq. (4.26)), the inner core mass of cenospheres is effectively reduced by about 50% in comparison to solid spheres, it can be concluded that the thickness of the outer layer of hollow spheres is the same (for LM) or a little thinner (EFA) than for their solid counterparts, and amounts about 2 μm as d = 38–50 μm. Note that this outer hull comprises about half of the thickness of the cenosphere wall: 0.2 x (38–50 μm)/2 = 3.8–5 μm.

For each set of experimental data the best τ has been chosen at first sight. In Tables 4.2-4.7 the assessed values of τ have been listed for all experiments.

Table 4.2. Reaction time τ for various pOH and [OH⁻] for EFA solid spheres (T = 40 ^{0}C) assuming $\overline{x}_S/x_{Sin} = 1$ and $\overline{x}_S/x_{Sout} = 1$.

pOH (mole/l)	[OH⁻] (mole/l)	τ_{out} (days)	τ_{in} (days)	$t_{in}(1-\tau_{in}/\tau_{out})$ (days)
1.0	0.100	3500		
0.6	0.251	1200		
0.3	0.501	750	275	1.6

Table 4.3. Reaction time τ for various pOH and [OH⁻] for LM solid spheres (T = 40 ^{0}C) assuming $\overline{x}_S/x_{Sin} = 1$ and $\overline{x}_S/x_{Sout} = 1$.

pOH (mole/l)	[OH⁻] (mole/l)	τ_{out} (days)	τ_{in} (days)	$t_{in}(1-\tau_{in}/\tau_{out})$ (days)
1.0	0.100	2500		
0.6	0.251	1200	550	1.3
0.3	0.501	700	190	1.0

Table 4.4. Reaction time τ for EFA cenospheres and solid spheres (pOH = 0.3, T = 40 ^{0}C) assuming $\overline{x}_S/x_{Sin} = 1$ and $\overline{x}_S/x_{Sout} = 1$.

Sphere	τ_{out} (days)	τ_{in} (days)	$t_{in}(1-\tau_{in}/\tau_{out})$ (days)
ceno	1000	180	1.1
solid	750	275	1.6

Table 4.5. Reaction time τ for LM cenospheres and solid spheres (pOH = 0.3, T = 40 ^{0}C) assuming $\overline{x}_S/x_{Sin} = 1$ and $\overline{x}_S/x_{Sout} = 1$.

Sphere	τ_{out} (days)	τ_{in} (days)	$t_{in}(1-\tau_{in}/\tau_{out})$ (days)
ceno	900	190	1.2
solid	700	190	1.0

Table 4.6. Reaction time τ for EFA solid spheres for various temperatures (pOH = 0.3) assuming $\overline{x}_S/x_{Sin} = 1$ and $\overline{x}_S/x_{Sout} = 1$.

T (K)	τ_{out} (days)	τ_{in} (days)	$t_{in}(1-\tau_{in}/\tau_{out})$ (days)	K_{out} (l/mole)	ΔG_{out} (J/mole)
293	8000			4.46 10^{-17}	9.1717 10^4
303	3000			2.84 10^{-16}	9.0179 10^4
313	750	275	1.6	4.02 10^{-15}	8.6264 10^4
ΔH (J/mole)					1.80 10^5
ΔS (J/moleK)					- 298

Table 4.7. Reaction time τ for LM solid spheres for various temperatures (pOH = 0.3) assuming $\overline{x}_S / x_{S_{in}} = 1$ and $\overline{x}_S / x_{S_{out}} = 1$.

T (K)	τ_{out} (days)	τ_{in} (days)	$t_{in}(1-\tau_{in}/\tau_{out})$ (days)	K_{out} (l/mole)	ΔG_{out} (J/mole)	K_{in} (l/mole)	ΔG_{in} (J/mole)
293	2000			$8.99\ 10^{-14}$	$7.3181\ 10^4$		
303	1500	900	1.0	$1.40\ 10^{-13}$	$7.4563\ 10^4$	$3.41\ 10^{-13}$	$7.2322\ 10^4$
313	700	190	1.0	$4.99\ 10^{-13}$	$7.3716\ 10^4$	$4.84\ 10^{-12}$	$6.7805\ 10^4$
ΔH (J/mole)					$8.00\ 10^4$		$1.90\ 10^5$
ΔS (J/moleK)					- 19		-390

One can see that the reaction time τ decreases, i.e. increasing reactivity, with increasing hydroxide concentration and temperature (Tables 4.2 4.3, 4.6 and 4.7). Moreover, the inner region appears to be more reactive that the outer region ($\tau_{in} < \tau_{out}$). Both for the ceno and solid spheres of both LM and EFA fly ash and for all temperatures and pOH, the reactivity of the inner region is about 2-5 times the reactivity of the outer region (Tables 4.4 and 4.5). Moreover, it seems that for the LM fly ash the inner region of both ceno and solid spheres have the same reactivity. For both EFA and LM fly ash the outer region of cenospheres is less reactive than the outer region of solid spheres.

In order to investigate the dependence of τ against the hydroxide content, in Tables 4.2 and 4.3 also [OH⁻] has been included, which directly follows from the pOH. Subsequently, in Figs. 4.9 and 4.10, τ^{-1} has been set out against [OH⁻] pertaining to the outer region of EFA and LM, respectively. For LM (Fig. 4.10) also τ^{-1} has been set out for the inner region, as two values are listed in Table 4.3.

From both figures one might conclude that, τ for the outer region depends linearly on [OH⁻], or is a power of [OH⁻]. Accordingly, the following function has been fitted in through the inner and out region τ^{-1} (Figs. 4.9 and 4.10):

$$\tau^{-1} = c\ [OH^-]^a \tag{4.33}$$

with c = 0.0026 (mole/l)$^{-a}$s^{-1} and a = 0.9 (EFA outer region), c = 0.0030 (mole/l)$^{-a}$s^{-1} and a = 1 (LM outer region) and c = 0.0140 (mole/l)$^{-a}$s^{-1} and a = 1.4 (LM inner region).

The dissolution process seems to have a direct and positive relation with [OH⁻]. Song and Jennings (1999) found a similar dependence for dissolution of slags: their measured dissolution was proportional to $10^{a\ pH}$ (with a ranging from 0.97 to 1.60), which corresponds to Eq. (4.33). Slags contain the same glass components as fly ashes, but usually in different quantities (slags are usually richer in CaO). In the next section a brief chemical explanation is presented which will support the experimental findings of this section.
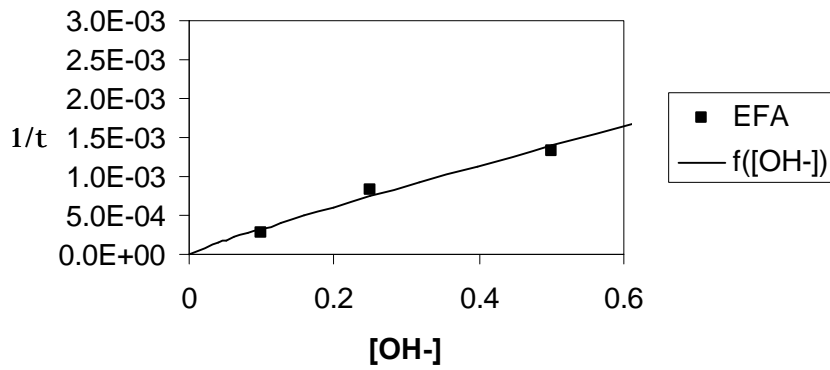
Figure 4.9. Reaction time τ against [OH⁻] for EFA solid spheres (T = 40 ^{0}C). f([OH⁻]) = 0.026 [OH⁻]$^{0.9}$
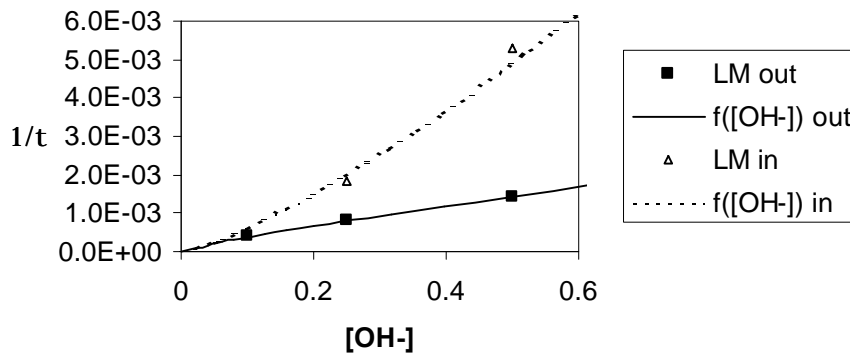
Figure 4.10. Reaction time τ against [OH⁻] for LM solid spheres (T = 40 ^{0}C). f([OH⁻]) out = 0.0030 [OH⁻] and f([OH⁻]) in = 0.0140 [OH⁻]$^{1.4}$.

4.5 Chemical analysis

From the composition of the fly ashes as presented in Table 4.1 it is clear that the glass phases of both fly ashes consist of SiO_2, as well as the network formers Al_2O_3, Fe_2O_3, TiO_2 and P_2O_5, and the network modifiers CaO, MgO, Na_2O and K_2O (Hemmings and Berry (1988)).

In Pourbaix (1966) the prevailing equilibria of the various substances can be found at for pH > 12 and an electric potential ranging from –0.3 to 0.2 V, values that are found in ordinary Portland and slag cement systems (MacPhee and Glasser, (1993)). Paul (1977, 1990) also presented hydration reactions for SiO_2, Al_2O_3, Na_2O and K_2O. Accordingly, from this literature it follows that for pH > 12 vitreous silica is hydrated as

90

$$SiO_2 + 2OH^- \Leftrightarrow SiO_3^{2-} + H_2O \tag{4.34}$$

and that Al_2O_3 is hydrated according to

$$Al_2O_3 + 2OH^- \Leftrightarrow 2AlO_2^- + H_2O \tag{4.35}$$

that CaO reacts as follows

$$CaO + H_2O \Leftrightarrow Ca^{2+} + 2OH^- \tag{4.36}$$

that Na_2O reacts as follows

$$Na_2O + H_2O \Leftrightarrow 2Na^+ + 2OH^- \tag{4.37}$$

that Fe_2O_3 is reacts as follows

$$Fe_2O_3 + 3H_2O \Leftrightarrow 2Fe^{3+} + 6OH^- \tag{4.38}$$

and that TiO_2 hydrates as follows

$$TiO_2 + OH^- \Leftrightarrow HTiO_3^- \tag{4.39}$$

Accordingly, the following reaction of the fly ash glass is proposed as

$$SiO_2.\zeta\,Al_2O_3.\eta CaO.\kappa\,Na_2O.\lambda Fe_2O_3.\theta TiO_2 + (\eta+\kappa+3\lambda)\,H_2O + (2+2\zeta+\theta)\,OH^- \Leftrightarrow$$

$$SiO_3^{2-} + 2\zeta AlO_2^- + \eta Ca^{2+} + 2\kappa Na^+ + 2\lambda Fe^{3+} + \theta HTiO_3^- + (1+\zeta)\,H_2O + 2(\eta+\kappa+3\lambda)\,OH^-$$

$$\tag{4.40}$$
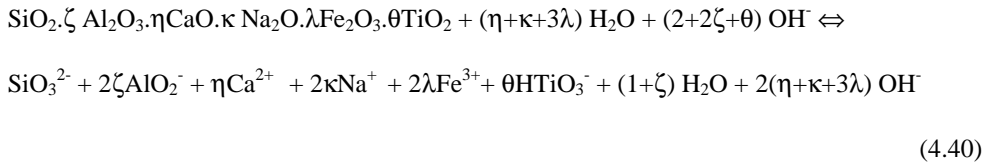
(see Table 4.8b for definitions of mole ratios ζ, η, κ, λ and θ).

Note that silica, aluminium oxide and titanium oxide consume hydroxides, whereas the earth alkalis (CaO, MgO), alkalis (Na_2O, K_2O) and iron oxide produce them. As slag contain the same components as fly ashes, it is believed that the model might be applicable to the dissolution of these materials as well. In case a fly ash or a slag also contains MnO and SO_3, the former reacts as CaO/MgO (to Mn^{2+}), and the latter likewise SiO_2 (to SO_4^{2-}).
As the activity of pure liquids and solids are unity, the reaction product is defined as

$$K = \frac{[AlO_2^-]^{2\zeta}[Ca^{2+}]^{\eta}[Na^+]^{2\kappa}[Fe^{3+}]^{2\lambda}[HTiO_3^-]^{\theta}[SiO_3^{2-}]}{[OH^-]^{2+2\zeta-2\eta-2\kappa-6\lambda+\theta}} \tag{4.41}$$

Invoking $[AlO_2^-] = 2\zeta\,[SiO_3^{2-}]$, $[Ca^{2+}] = \eta\,[SiO_3^{2-}]$, $[Na^+] = 2\kappa\,[SiO_3^{2-}]$, $[Fe^{3+}] = 2\lambda\,[SiO_3^{2-}]$ and $[HTiO_3^-] = \theta\,[SiO_3^{2-}]$ yields

$$[SiO_3^{2-}] = \left(\frac{K}{(2\zeta)^{2\zeta}\,\eta^\eta(2\kappa)^{2\kappa}(2\lambda)^{2\lambda}\,\theta^\theta}\right)^{\frac{1}{1+2\zeta+\eta+2\kappa+2\lambda+\theta}}[OH^-]^a \tag{4.42}$$

with

$$a = \frac{2+2\zeta-2\eta-2\kappa-6\lambda+\theta}{1+2\zeta+\eta+2\kappa+2\lambda+\theta} \tag{4.43}$$

a = power ($[OH^-]^a$ in fly ash reaction)

Note that the powers appearing in the denominator of the first product of Eq. (4.42), $(2\zeta)^{2\zeta}$ etc., are of order unity. The function x^x namely attains a value of 1 at x = 0 and x = 1, and has a minimum of $(1/e)^{(1/e)}$ (≈ 0.69) at $x = e^{-1}$. From Table 4.8a it can be seen that the values of ζ etc. are such that 2ζ etc. all fall in the range 0 to 1, so that $(2\zeta)^{2\zeta}$ etc. all have a value between 0.69 and 1. Furthermore, it will be demonstrated that K is (much) smaller than unity.

Table 4.8a. Mass fraction in glass and crystalline phase and mole fraction ($\bar{x}$) in glass phase of LM and EFA spheres.

	EFA solid		ceno	LM solid		ceno	M (g/mole)
Crystalline							
$SiO_2 + Al_2O_3$	5.1%		8.4%	33.3%		37.8%	
Glass		($\bar{x}$)			($\bar{x}$)		
SiO_2 (S)	51.96%	0.648	47.05%	38.79%	0.695	40.41%	60
Al_2O_3 (A)	25.89%	0.190	28.06%	16.48%	0.174	13.54%	102
Fe_2O_3 (F)	4.65%	0.022	2.96%	3.50%	0.024	2.02%	160
P_2O_5 (P)	n.d.		n.d.	0.54%	0.004	n.d.	142
TiO_2 (T)	1.20%	0.011	0.91%	1.90%	0.026	1.43%	80
CaO (C)	2.83%	0.038	0.80%	2.75%	0.053	1.15%	56
MgO (M)	1.82%	0.034	1.41%	0.28%	0.008	0.24%	40
Na_2O (N)	1.84%	0.022	1.94%	0.37%	0.006	0.38%	62
K_2O (K)	4.40%	0.035	5.68%	1.00%	0.011	1.02%	94

Table 4.8b. Molar ratios. Definitions and values.

	EFA	LM
$\zeta\ (=\bar{x}_A/\bar{x}_S)$	0.293	0.250
$\eta\ (=(\bar{x}_C+\bar{x}_M)/\bar{x}_S)$	0.111	0.087
$\kappa\ (=(\bar{x}_N+\bar{x}_K)/\bar{x}_S)$	0.088	0.026
$\lambda\ (=\bar{x}_F/\bar{x}_S)$	0.034	0.034
$\theta\ (=\bar{x}_T/\bar{x}_S)$	0.017	0.037
$\bar{a}$ (Eq. (4.43))	1.022	1.208
$\bar{M}$	71	72

So, with increasing ζ etc. (i.e. less silica) the power of the first factor decreases, and hence, the factor increase. Accordingly, when the silica content diminishes, the solubility is enhanced. This trend is also supported by the second factor on the right-hand side of Eq.

(4.42). The power a decreases with increasing ζ, η etc., see Eq. (4.43). For η, κ and λ this effect is obvious. But this trend also holds for ζ and θ: the function $(2+x)/(1+x)$ attains a value of 2 at $x = 0$, and monotonically decreases towards the asymptotic value of 1 for large x. Considering that [OH⁻] is usually smaller than 1 mole/l, increasing ζ, η etc. imply a smaller a and also a larger second factor in Eq. (4.42).

Considering the equilibrium products it follows that the hydration of pure silica is quadratically dependent on [OH⁻] ($\zeta = \eta = \kappa = \lambda = \theta = 0$). In case of a pure aluminosilicate glass ($\eta = \kappa = \lambda = \theta = 0$), the power a is located between unity and 2, but depending weakly on changes in ζ. E.g., for ζ ranging from ¼ to 1, this power ranges from 1.66 to 1.33 (it equals 1.5 for $\zeta = 0.5$). For a alkali silicate glasses ($\zeta = \eta = \lambda = \theta = 0$), it follows from Eq. (4.43) that the power a is smaller than unity when $\kappa > 0.25$.

In Table 4.8a the mass fraction of all glass phases in the studied fly ashes are listed, based on the data of Table 4.1. For vitreous SiO_2 and Al_2O_3 they follow from the total mass fraction of each substance minus the crystalline SiO_2 (in quartz and in mullite) and crystalline Al_2O_3 (in mullite only), see Table 4.1, respectively. Using these mass fractions, the mean mole fraction of all components in the glass can be computed using the molecular mass of each component, which are included in Table 4.8a for the EFA and LM solid spheres only (between the brackets). With these mole fractions subsequently the mean ζ, η, κ, λ and θ and a can be computed for solid EFA and LM, which are included in Table 4.8b. For this calculation it is assumed MgO to react as CaO and K_2O as Na_2O. P_2O_5 can be neglected, as its presence is minor (Tables 4.1 and 4.8a).

One can readily see that the power a takes a value of 1.022 (EFA) and 1.208 (LM), which is not in line with the fitted power of the previous section (1.4 in LM inner region, 0.9 and 1 in EFA and LM outer region, respectively). This deviation can probably be attributed to the inhomogeneity of the fly ash, as will be reasoned in more detail in the following section.

4.6 Effect of inhomogeneity

Pietersen (1990,1993) has measured that the release of SiO_2, Al_2O_3, and K_2O is virtually congruent. The release of CaO and MgO was, however, not measured. Moreover, experiments by Dudas and Warren (1987) reveal that the glass components K_2O, Na_2O, CaO, MgO, and Fe_2O_3 are concentrated in the exterior (outer) hull. Smith (1980) found a similar enrichment in the outer layer, and explained this inhomogeneity by the fact that the boiling point of silica and aluminiumoxide are practically the same (2950 $^{\circ}$C and 2980 $^{\circ}$C), and higher than the boiling points of all other components. This will result in a concentration of more volatile components (i.e. the other oxides) in the outer layer.

In section 4.4 it was found that for the solid LM spheres the power a is higher in outer region (0.9) than in inner region (1.4), also implying higher values of η, κ etc. in outer region. To explore the effect of a inhomogeneous composition, the silica, aluminiumoxide, alkalis, earth alkalis etc. are redistributed: the outer region is enriched with the (minor) constituents K_2O, Na_2O, CaO, MgO, Fe_2O_3 and TiO_2. The molar ratio of the major components aluminiumoxide and silica is not altered: $\zeta_{in} = \zeta_{out} = \bar{\zeta}$. However, the redistribution of the other components has to obey the mass balance of each component.

Assuming the spheres to have a constant glass molar density ($\overline{\phi\rho_g} = \phi_{out}\rho_{gout} = \phi_{in}\rho_{gin}$) and applying Eq. (4.19) to $x_C + x_M (= \eta x_S)$ and inserting $r_h = 0$ (solid sphere) yields:

$$\overline{\eta} = \eta_{out}(1 - r_{in}^{*3})\frac{x_{Sout}}{x_S} + \eta_{in}r_{in}^{*3}\frac{x_{Sin}}{x_S} = \eta_{out}\alpha_{Sin} + \eta_{in}(1 - \alpha_{Sin}) \tag{4.44}$$

see Eqs. (4.27) and (4.28), whereby $\alpha_{Sin} = 7\%$ (volume fraction outer region, see section 4.). Similar equations hold for κ, λ and θ. As example values for η_{in}, η_{out}, κ_{in} κ_{out} etc. are given in Table 4.9 that obey Eq. (4.44).

Table 4.9. Mean composition of LM solid spheres and redistribution of phases in inner and outer region.

	mean value	inner region	outer region
ζ	0.250	0.250	0.250
η	0.087	0.080	0.174
κ	0.026	0.024	0.052
λ	0.034	0.031	0.068
θ	0.037	0.034	0.074
a (Eq. 4.43)	1.208	1.238	0.862

As can been seen from this table, as example, the values in outer region are enriched by a factor of about 2 in comparison with the mean values. In Table 4.9 also the pertaining a of inner and outer region (a_{in} and a_{out}) have been included. The values of a_{in} and a_{out} that follow from the redistribution of the minor constituents indeed approach the values of a_{in} and a_{out} that have been found in the previous section.

Following the redistribution, the silica (and aluminiumoxide) is concentrated in the inner region. Consequently, Eqs. (4.29) and (4.30) need to be fit again through the experiments, but now taking into account that $\overline{x_S}/x_{Sin}$ and $\overline{x_S}/x_{Sout}$ are not equal to unity. By definition, the mole fraction of silica is related to ζ, η, κ, λ, and θ via

$$(\zeta + \eta + \kappa + \lambda + \theta + 1)x_S = 1 \tag{4.45}$$

and therefore

$$\frac{\overline{x_S}}{x_{Sout}} = \frac{\zeta + \eta_{out} + \kappa_{out} + \lambda_{out} + \theta_{out} + 1}{\zeta + \overline{\eta} + \overline{\kappa} + \overline{\lambda} + \overline{\theta} + 1} \tag{4.46}$$

$$\frac{\overline{x_S}}{x_{Sin}} = \frac{\zeta + \eta_{in} + \kappa_{in} + \lambda_{in} + \theta_{in} + 1}{\zeta + \overline{\eta} + \overline{\kappa} + \overline{\lambda} + \overline{\theta} + 1} \tag{4.47}$$

yielding $\overline{x_S}/x_{Sout} = 1.128$ and $\overline{x_S}/x_{Sin} = 0.990$, i.e. $x_{Sin}/\overline{x_S} = 1.010$ and $x_{Sout}/\overline{x_S} = 0.886$. So, by the redistribution the silica concentration is reduced by 11% in the outer hull, whereas it is enlarged by about 1% in the inner region (relative to the average mole fraction). With

94

said values Eqs. (4.29) and (4.30) yielding new values of τ_{out} and τ_{in}, which are included in Tables 4.10 and 4.11.

Table 4.10. Reaction time τ for various pOH and [OH⁻] for LM solid spheres (T = 40 ^{0}C) based on $\overline{x_S}/x_{Sin} = 0.990$ and $\overline{x_S}/x_{Sout} = 1.128$.

pOH (mole/l)	[OH⁻] (mole/l)	τ_{out} (days)	τ_{in} (days)	$t_{in}(1-\tau_{in}/\tau_{out})$ (days)
1.0	0.100	2100		
0.6	0.251	1000	550	1.3
0.3	0.501	600	190	1.0

Table 4.11. Reaction time τ for LM solid spheres for various temperatures (pOH = 0.3) based on $\overline{x_S}/x_{Sin} = 0.990$ and $\overline{x_S}/x_{Sout} = 1.128$.

T (K)	τ_{out} (days)	τ_{in} (days)	$t_{in}(1-\tau_{in}/\tau_{out})$ (days)	K_{out} (l/mole)	ΔG_{out} (J/mole)	K_{in} (l/mole)	ΔG_{in} (J/mole)
293	1800			$3.46\ 10^{-16}$	$8.6724\ 10^4$		
303	1300	900	1.0	$6.19\ 10^{-16}$	$8.8222\ 10^4$	$2.97\ 10^{-13}$	$7.2670\ 10^4$
313	650	190	1.0	$2.30\ 10^{-15}$	$8.7715\ 10^4$	$4.10\ 10^{-12}$	$6.8235\ 10^4$
ΔH (J/mole)					$9.20\ 10^4$		$1.81\ 10^5$
ΔS (J/moleK)					- 15		-359

Comparing the newly determined τ_{out} and τ_{in} in Tables 4.10 and 4.11 with the values in Tables 4.3 and 4.7, respectively, reveal that the τ_{in} are the same. This is no surprise as $\overline{x_S}/x_{Sin}$ is close to unity so that the fitted lines have the same form. On the other hand, for the outer region all newly fitted τ_{out} are about 15% smaller than the fit with $x_{Sout} = \overline{x_S}$. Note that x_S appears in τ (Eq. (4.10)), and that for the first fit it corresponds to $\overline{x_S}$, and the second fit to x_{Sout} (which is about 15% smaller than $\overline{x_S}$ due to the concentration of earth alkalines in outer region). Consequently, fitting based on mean particle composition ($\overline{x_S}/x_{Sout} = 1$, resulting in Tables 4.3 and 4.7) and based on different inner an outer composition ($\overline{x_S}/x_{Sout} = 1.128$, resulting in Tables 4.9 and 4.10), yields the same C_{Sr} (as r_{out}, ϕ, ρ_g and D_S are constant).

4.7 Thermodynamic analysis

On the basis of the experimental data and the proposed reaction mechanism in the previous section, thermodynamic data for the fly ash can be determined. The first step in this analysis is the determination of K that appears in Eqs. (4.41) and (4.42).

It is expected that the dissolution process to be governed by the ion that diffuses the slowest. Here, only the diffusion coefficients of [AlO$_2$⁻] and [SiO$_3$²⁻] are compared, which are not both directly available. Accordingly, D_A^0 was estimated using the diffusion coefficients

of the similar ions NO_2^- (1.912 10^{-9} m^2/s) and ClO_2^- (1.385 10^{-9} m^2/s), yielding $D_A^0 = 1.7 \ 10^{-9}$ m^2/s at T = 298 K (Lide (1995)). Similarly, D_S^0 was estimated using the diffusion coefficients of CO_3^{2-} (0.912 10^{-9} m^2/s) and SO_3^{2-} (1.064 10^{-9} m^2/s), yielding $D_S^0 = 1.0 \ 10^{-9}$ m^2/s at T = 298 K (Lide (1995)). Note that the molecular mass of aluminium lies between the molecular masses of nitrogen and chloride, and silicon between carbon and sulphur, so that the estimation is expected to a yield reasonable result. As D_A is larger than D_S, it is believed henceforth that the process is governed by the diffusion of SiO_3^{2-} and hence, $D_S C_{Sr}$ appearing in Eq. (4.10) to correspond to $D_S [SiO_3^{2-}]$. For deviating temperatures, D_S is determined via

$$D_S = \frac{T}{298K} D_S^0 \tag{4.48}$$

Combining Eqs. (4.10), (4.42) and (4.48) yields

$$K = (2\zeta)^\zeta (\eta)^\eta (2\kappa)^{2\kappa} (2\lambda)^{2\lambda} (\theta)^\theta \left[\frac{x_S \rho_g r_{out}^2}{6\phi D_S^0 \tau} \frac{298K}{T} \right]^{1+2\zeta+\eta+2\kappa+2\lambda+\theta} [OH^-]^{-2-2\zeta+2\eta+2\kappa+6\lambda-\theta} \tag{4.49}$$

The physical properties that appear in this equation are known: r_{out} (22 μm), ϕ (Table 4.1), while ρ_g follows from the density (about 2450 kg/m^3) divided by the mean molar mass. The mean molar mass follows from the sum of the molar fraction of each constituent times its molar mass ($\overline{M} = \sum x_k M_k$), which are included in Table 4.8b as well. The τ at various temperature have been determined in the previous sections and are listed in Tables 4.6, 4.7 and 4.11, as well as [OH$^-$] and the temperature.

Using the data of Tables 4.6 and 4.7, the K of EFA and LM solid spheres, respectively, are computed using Eq. (4.49) and the result is included in both tables as well. For inner and outer region K is denoted by K_{in} and K_{out}, respectively. For these computations the mean values η and x_S have been used. Using the data of Table 4.11, K of LM solid spheres are computed using Eq. (4.49) and the result is included in this table as well. For these computations the prevailing values of outer (η_{out}, κ_{out}, λ_{out}, θ_{out} and x_{Sout}) and inner region (η_{in}, κ_{in}, λ_{in}, θ_{in} and x_{Sin}) have been used.

The three tables indicate that K increases with temperature, implying improved dissolution/reaction with increasing temperature. With these K one can determine the standard free energy of reaction ΔG by

$$K = e^{\frac{-\Delta G}{RT}} \tag{4.50}$$

ΔG is the sum of free energies of formation of the products in their standard states minus the free energies of formation of the reactants in their standard states (Paul (1977, 1990), Babushkin et al. (1985)). In Tables 4.6, 4.7 and 4.11 the resulting ΔG are included using R = 8.31439 J/moleK.
The connection of ΔG with enthalpy and entropy of reaction is

$$\Delta G = \Delta H - T\Delta S \tag{4.51}$$

96

in which ΔH and ΔS are the sum of standard heats of formation and the standard entropies, respectively, where each sum is constituted by the sum of the products minus the sum of the reactants. In order to specify ΔH and ΔS, $-R \ Ln \ (K)$ has been set out against $1/T$ for LM and EFA in Fig. 4.11, taking the values of Tables 4.6 and 4.7 and Fig. 4.12, taking the values of Table 4.10. A straight line has been fitted through the experimental values, whereby

$$- R \ Ln \ (K) = \Delta H \ T^{-1} - \Delta S \qquad\qquad (4.52)$$

see Eqs. (4.50) and (4.51). The fitted values of ΔH and ΔS have been included in Tables 4.6, 4.7 and 4.11.

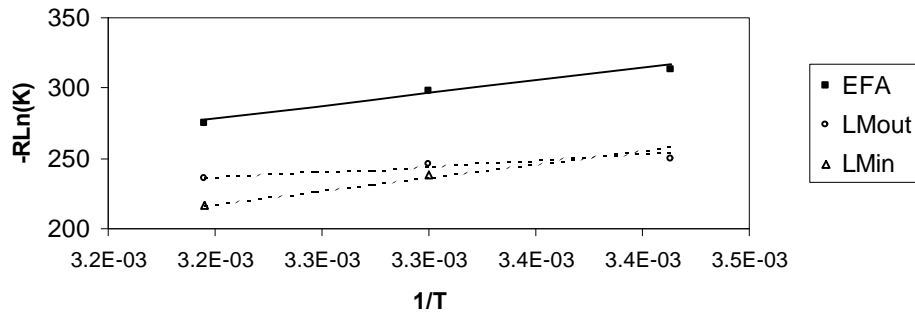**Figure 4.11.** $-R \ Ln \ K$ versus $1/T$ for LM (inner and outer region) and EFA (outer region only) solid fly ash, based on $\overline{x}_S / x_{S_{in}} = 1$ and $\overline{x}_S / x_{S_{out}} = 1$.
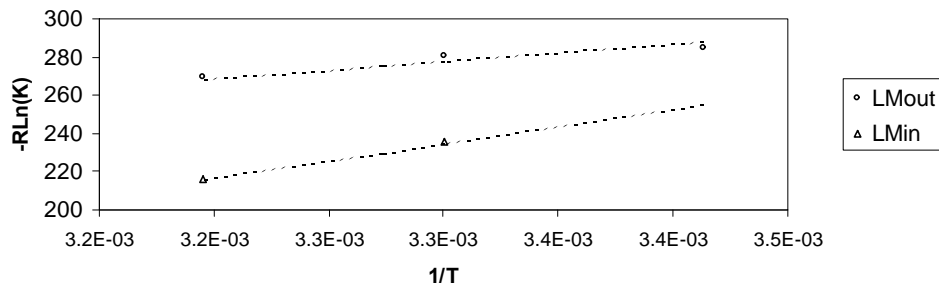

Figure 4.12. $-R \ Ln \ K$ versus $1/T$ for LM (inner and outer region) solid fly ash, based on $\overline{x}_S / x_{S_{in}} = 0.990$ and $\overline{x}_S / x_{S_{out}} = 1.128$.

4.8 Conclusions

Pietersen (1990, 1993) has carefully executed and reported dissolution experiments of several types of pulverised powder coal (class F) fly ashes. To this end, the silica release in time was measured for various pOH and temperatures. In order to understand the dissolution and reaction behaviour of these fly ashes, in particular the EFA and LM fly ash, a theoretical study has been executed and the results applied to said experiments.

From the present analysis one can confirm that the available amount of reactive fly ash is proportional to the glass (non-crystalline) part of the fly ash. Moreover, as the crystalline part forms a connected network, dissolution rates are also proportional to the glass content, especially while the effective diffusion coefficient is proportional to the square of the glass content (Eq. (4.2)).

The derivation of an extended shrinking core model yields analytical equations that reckon with a hollow core, as well as the possibility of two regions with different composition and reactivity. In Fig. 4.8 the shrinking behaviour in case of a more and less reactive outer region has been depicted. Application of the derived equations to the experiments of Pietersen (1990, 1993) provides values of the reactivity time τ (Eq. (4.10)) for inner and outer region (τ_{in} and τ_{out}). Assuming a homogeneous silica distribution over the fly ash particle, the application reveals that the inner region is more reactive, and that about 7% and 9% of the silica is found in the outer region of LM and EFA solid spheres, respectively. From the fitting it also follows that the outer region of solid spheres and cenospheres have nearly the same thickness (about 2 μm). After dissolution of this layer, which needs less time in case of higher pH and/or temperature, the dissolution of the inner region at a higher rate starts.

Furthermore, a reaction mechanism for fly ash glass is put forward that accounts for its silica, aluminium oxide, iron oxide, titanium oxide, alkali and earth alkali content (and which also be useful for slags). The resulting reaction product and the experimental application indicate a dissolution rate proportional to $[OH^-]^{0.9-1}$ for the outer region (EFA and LM), and to $[OH^-]^{1.4}$ in inner region (information available about LM only). This result suggests that the outer layer of solid LM is poorer in silica and aluminiumoxide, which is in line with findings in previous publications. Combining the reaction product and the experimental data at various temperatures, also the free energy, enthalpy and entropy of reaction are computed.

As most information is obtained for solid LM, for this fly ash the silica and aluminiumoxide is concentrated in the inner region, and the model again applied. This application yields new reaction times, reaction products and free energy, enthalpy and entropy of reaction. However, the same trends as for the previous application are found (e.g. a more reactive inner region).

Chapter 5

Contaminants[*]

5.1 Introduction

When cement is used for Solidification/Stabilisation (S/S) it is mixed with waste containing many types of contaminants. Purpose of cement addition is binding of these contaminants to obtain a product that can be applied or stored more safely compared with the original untreated waste product. First the waste is mixed with cement, water and additives and the mixture is cured for setting (binding) and hardening. When the hardening process is successful, a solidified product is obtained and called the immobilisate, which can be granular (e.g. soil or ash) or shaped (e.g. bricks) (see Fig. 1.1 and Chapter 1).

Traditionally, design of cement/waste recipes is mainly based on a specific waste stream (see also Chapter 1). One type of waste stream contains many different contaminants that may have different effects on cement hydration and thus on hardening of the mixture. These effects may strongly depend on content of specific contaminants. At some content hardening may take place, while at a higher content hardening and thus S/S may fail. For many contaminants it is known that they always give problems, i.e. they are not bound well or they disturb hardening, no matter in what kind of waste stream they occur. Therefore, in this chapter, specific *contaminants* will be studied instead of specific waste streams. The following questions will be dealt with:

- How are contaminants bound in the hardened cement paste?
- How can contaminants affect cement hydration?
- How can knowledge of cement chemistry in the presence of contaminants be used for the design of cement/waste recipes?

In section 5.2 an overview of binding mechanisms will be given. In section 5.3 the effects of contaminants on cement hydration will be shown, both in general and for specific metals and anions found in waste streams. In section 5.4 the main effect contaminants have on cement hydration, coating of cement particles, will be treated in detail. The theory of coating will be outlined. Hydration of surface coated cement mixtures will be modelled. The coating by calcium borates will be modelled, introducing the principle of coating layers and redissolution of coated material. Results will be compared with experiments. In section 5.5 ways on how to deal with contaminants will be presented. In section 5.6 conclusions will be given, including practical solutions for the design of cement/waste recipes.

5.2 Binding mechanisms

The chemistry of cement-solidified wastes has been described in a number of articles published in Spence (1993) and has been reviewed thoroughly by Glasser in a number of articles (Glasser, 1993, 1996, 1997). The immobilisation potential of cement can be summarised by three mechanisms (Glasser, 1993):

1. Precipitation as insoluble hydroxides, silicates or calcium salts
2. Chemical incorporation into hydration products, e.g. C-S-H.
3. Absorption of ions into, and adsorption on, surface area of hydration products

Precipitation. Cement-solidified waste contains a water filled pore system. This pore water is in contact with the hydration products, e.g. $Ca(OH)_2$, which act as a source of OH^-. In the presence of high amounts of alkalis, this will result in a high pH (see Chapter 3) of 12 - 14. At such pore water pH most metals will precipitate as hydroxides and thus will be slightly soluble. On the other hand, some metals are *amphoteric*. This means that a metal will form negatively charged hydroxides, e.g. $Zn(OH)_4^{2-}$, at high pH, and thus remains soluble.

The hydration products are also a source of calcium and silicate ions that will form insoluble complexes with anions, e.g. with sulphates, phosphates and borates and with metal hydroxyl anions, e.g. $Zn(OH)_4^{2-}$.

Incorporation. Both crystalline and amorphous hydration products are characterised by their open structure consisting of micropores or having a sheet or channel like morphology. Because of this open structure the ions that make up the framework are readily available for exchange with ions present in the surrounding pore water until equilibrium is reached.
Table 5.1 shows which substitutions are possible.

Table 5.1. Examples of ion substitution (Glasser,1993) and (Gougar et al., 1996).

Ions present in Hydration product	Substituted ions reported
Ca^{2+}	Sr^{2+}, Ba^{2+}, Pb^{2+}, Cd^{2+}, Ni^{2+}, Zn^{2+}
OH^-	F^-, Cl^-, Br^-, I^-
$SO4^{2-}$	IO_3^-, CO_3^{2-} etc.
	CrO_4^{2-}, SeO_4^{2-} etc
	$B(OH)_4^-$, MoO_4^- etc.
Al, Fe	Cr^{3+}, Mn^{3+}, Ti^{3+}

The amount of ions incorporated into hydration product depends on the amount of product present and the concentration of the ion. However, often these amounts are not significant and the final outcome is difficult to predict. When concentrations in pore water change or when other products are formed during the progress of hydration or because of external causes, ions bound by this mechanism will easily redissolve.

Absorption. C-S-H has a high specific surface area in the order of 10 to 100 m^2/g. The silicon groups at the surface give it a surface charge. Ca-rich C-S-H give it a positive surface charge and tends to sorb anions. When the C/S ratio of C-S-H decreases, the surface charge decreases, passing through zero at C/S = 1.2 and becoming negative at lower ratios.

The binding efficiency of a waste containing sample can be measured using leaching experiments (as described in the next chapter). In general precipitated compounds are available for leaching, while substituted ions are strongly bound. The location of foreign ions in the hardened cement paste can be measured by XPS.

5.3 Effects of contaminants on cement hydration

5.3.1 Overview of effects

Many salts precipitate additional phases when added to cement pastes. If the hydroxide of an added cation is less soluble than CH, either (1) the hydroxide or (2) a basic or complex salt is precipitated. Examples of hydroxide precipitates are $Zn(OH)_2$, $Mg(OH)_2$ and $Cd(OH)_2$ and examples of complex salts are AFm phases, $CaZn_2(OH)_6.2H_2O$ and basic lead nitrate or sulphate. Precipitation will leave in solution all or part of the added anion and an equivalent amount of Ca^{2+}. The calcium salt of an added anion, if of sufficiently low solubility, is similarly precipitated; examples are provided by SO_4^{2-}, CO_3^{2-}, PO_4^{3-}, F^-, silicate, aluminate and borate. In this case, the added cation remains in solution with an equivalent amount of OH^-. The salts in these categories have widely varying effects on setting and hardening. Some, such as lead or zinc salts, phosphates or borates, are strong retarders. Others, such as magnesium salts, behave as setting and hardening accelerators in much the same way as ones not precipitating additional phases. Yet others, such as carbonates, have effects ranging from flash setting to retardation of setting depending on the concentrations in which they are added (Taylor, 1997).

The effects contaminants can have on cement hydration can be categorised as follows:

- Disturbing nucleation/precipitation of hydration product (setting)
- Disturbing dissolution of clinker minerals (hardening)
- Increased ettringite formation
- Formation of new compounds (hydroxides, calcium salts, silicates, sulphates, H_2 forma

Disturbing of hardening is caused by precipitation of hydroxides and other salts on the unhydrated cement particle. This prevents dissolution and reaction of the clinker minerals and retards cement hydration. Such retardation leads to a lower degree of hydration and this leads to higher porosity and lower amounts of C-S-H. This will result in poor strength development and high leachability of the solid product or there may even be no solid product at all.

To get an overview of possible effects of contaminants on cement hydration, an extensive literature study was done. Two types of research could be distinguished. (1) Fundamental research, in which microscopic, surface and analytical techniques (SEM, Si-NMR, XRD,

XPS) were used to obtain information about location and nature of contaminants and interaction between contaminant, cement and hydration products. (2) More practical research in which properties such as setting times, compressive strength and leaching are measured. The fundamental studies are mainly based on one contaminant to simplify the system and exclude combinational effects. Literature reviews describing effects of specific contaminants on cement hydration are given by (Mattus and Mattus, 1996, Macphee and Glasser, 1993, Trussel and Spence, 1994). Macphee and Glasser (1993) presented a periodic table in which elements were divided based on their solubility properties in cementitious systems.

In the next sections, an integral overview of effects of several contaminants on cement hydration will be presented. This information can then be used to decide which effects are most important. Furthermore, when effects are known, they can be modelled and finally it will be possible to design cement/based recipes on specific contaminants.

5.3.2 Cations

Aluminium

Aluminium particles are vulnerable to corrosion in highly alkaline environments, because of the dissolution of the thin Al_2O_3 film taking place as follows (Matsuo et al.,1995):

$$Al_2O_3 + 2\ OH^- \rightarrow 2\ Al(OH)_4^- \hspace{3cm} (5.1)$$

The next step is oxidation of the now exposed Al surface with generation of hydrogen gas as follows:

$$Al + 3\ H_2O \rightarrow Al(OH)_3 + {}^3/_2\ H_2 \hspace{1cm} \uparrow \hspace{2.5cm} (5.2)$$

The release of hydrogen gas will reduce the strength of the waste product. $LiNO_3$ can be added to prevent corrosion by formation of an impermeable Li-Al salt layer (Matsuo et al., 1995). In practice aluminium compounds are used to introduce air voids in concrete.

Arsenic

As(III) is well retained in cement, especially slag cements (Macphee and Glasser, 1993). Arsenic chemistry is very complex and involves a variety of valence states, anionic and cationic species, and both inorganic and organic species. As fixation is strongly pH and E_h dependent (Conner, 1990). According to Akhter and Cartledge (1991) arsenic incorporation influences the depolymerization of the silicates and changes the aluminium co-ordination in aluminate hydration products (MacPhee and Glasser, 1993).

Barium

Precipitates on clinker grains as carbonate or sulphate. $BaSO_4$ is very stable over a wide pH range (Macphee and Glasser, 1993). Barium has similar effects as lead and cadmium (McWhinney et al., 1990).

102

Cadmium

Mollah et al. (1992) studied Cd in Portland cement and found that the presence of cadmium resulted in the formation of calcium hydroxycadmiates on the surfaces of cement grains. They suggested that this may be the cause of retardation of cement setting and hydration. A few other authors found an accelerated setting of cement in the presence of Cd because $Cd(OH)_2$ that is formed provides nucleation sites for CH and C-S-H precipitation. McWhinney and Cocke (1993) studied the surface of Cd doped cement using XPS. Cd was added as nitrate as 10 % (m/m) and 20 % (m/m). Carbonation of the samples was induced in both cases according to the following equation:

$$Cd(OH)_2 + CO_2 \rightarrow CdCO_3 + H_2O \qquad\qquad (5.3)$$

At the higher doping level (20 % (m/m)), the formation of $CdCO_3$ is suppressed as CdO is formed because of the drastic decrease in buffering activity of the cement.

Cartledge et al. (1990) investigated the behaviour of Cd and Pb salts toward cement-based solidification using TCLP leaching tests, conduction calorimetry, and solid-state NMR as a function of time. Cd was added to both OPC and white (low iron) cements as hydroxide or nitrate and the hydration was followed by measuring the development of both C-S-H and CH and aluminate phases. Both cadmium hydroxide and nitrate have the effect of shortening the dormant period by up to an hour. The acceleration phase that follows is associated with rapid growth of CH and C-S-H, and the early start for the acceleration phase may be the result of the presence of the solid $Cd(OH)_2$, which provides nucleation sites for the precipitation of $Ca(OH)_2$. This $Cd(OH)_2$ may be formed before cement is added in the case of a sludge or immediately afterwards in the case of a soluble Cd salt. Despite these effects, minor differences, like an increase in the proportion of C-S-H, were found in the cement matrix after 28 days.

Diez et al. (1997) immobilised Cd waste using OPC. Very high concentrations (50000 mg/l Cd) were added and found to be well retained without any negative influence on physical properties of the solid product. The influence of Cd on the hydration process could be deduced from heat curves. The heat evolution was enhanced during the first hour and the induction period was extended. The initial precipitation of $Cd(OH)_2$ induces a stiffening of the paste leading to a shortening of the initial setting time. The data presented showed that setting started 35 minutes earlier and finished 10 minutes earlier. The pore solution was analysed for several ions during curing. While the mixing water contained spiking concentrations of Cd varying between 5000 and 50000 mg/l, a concentration below 0.1 mg/l was always found in the resulting pore water, suggesting a solubility-limiting mechanism taking place.

Chromium

Chromium occurs in aqueous solutions in two oxidation states, trivalent Cr(III) and hexavalent Cr(VI). The latter is more toxic and more difficult to fix into solids. It is however easily reduced to trivalent chromium by metals (e.g. Zn) or by ferrous salts. Cr(III) reacts with OH- to form $Cr(OH)_3.3H_2O$ which solubility has a typical value of $10^{-3.5}$ mole/l at pH = 12 (Kindness et al., 1994). Low levels of Cr(III) can accelerate cement setting. Ivey et al. (1993) used different electron microscope techniques for the characterisation of Cr-doped OPC

103

samples. They found that Cr(III) inhibited ettringite formation and was incorporated in both CH and C-S-H and in a Ca-Cr rich polycrystalline phase. Cr(III) replaces Al in the calcium aluminate hydrate phase (Kindness et al., 1994) and can substitute for Si in C-S-H (Cocke and Mollah, 1993; Macphee and Glasser, 1993; Heimann et al., 1992).

Kindness et al. (1994) found that Cr(VI) is not readily incorporated in these phases and did not find Cr absorption of C-S-H. They also found that several calcium aluminate phases are formed and that these phases contain chromium that partially replaces Al(III). The presence of a gel in many of the sample preparations suggested that these samples have not yet fully reacted. The Cr/Al ratio in these phases varies greatly and does not appear to be a function of the Cr/Al ratio of the starting materials, also suggesting incomplete reaction. The authors summarize their findings as follows: The intrinsic solubility of Cr(III) in OPC pore water is shown to be about 1 mg/l. This plateau is obtained over a wide limit of total Cr and arises because Cr(III) reacts with OH^- to form $Cr(OH)_3.3H_2O$ as well as Cr(III) substituted calcium aluminate hydrates. The most important of these are based on $Ca_2Al_2O_5.6\text{-}8\ H_2O$, $Ca_2Al(OH)_7.3H_2O$ and $3CaO.Al_2O_3.6H_2O$; other, less well characterised phases also occur. Cr(VI) is very much more soluble than Cr(III). Although ettringite type chromates are reported they do not appear to develop in cement. Conditions favourable for retaining Cr in cement are therefore characterised by (1) available aluminate ions to form calcium aluminate hosts and (2) chemically reducing conditions to stabilise Cr(III) and reduce Cr(VI) to the less soluble Cr(III) species.

Chromium has parallels with cadmium and also nucleates the precipitation of hydrates. All these effects result in low Cr levels in the pore fluid of the final sample and strong containment in the cement matrix (Trussel and Batchelor, 1996). The presence of chromium strongly influences the porosity structure. It causes a loss of the largest pores formed by air voids, and an increase in the amount of the smaller capillary and gel pores (Cocke and Mollah, 1993). Cr containing waste is best immobilised by slag containing cements because all Cr(VI) is reduced (Kindness et al., 1994).

According to Glasser (1997) the solubility of Cr lies well below the value based on simple hydroxide solubility. The explanation for this observation lies in the fact that cement hydration products contain octahedrally co-ordinated Al, which is readily replaced by Cr(III). Thus while Cr(III) is amphoteric (see section 5.2), it remains insoluble in the cement environment. According to Glasser this reaction may not be rapid; initially, Cr may partly precipitate as $Cr(OH)_3$, and the true solubility-limiting phase may require weeks or months to form, during which the pore fluid Cr solubility decreases to a steady state value in the range of 0.1-1.0 ppm.

Omotoso et al. (1996) studied the hydration of C_3S in the presence of different Cr(III) concentrations. Two types of Ca-Cr complexes were identified. The early complex generally starts to form within a few hours, increasing in concentration until most of the Cr has been consumed. No CH was found until that point was reached. When the paste was cured in the presence of water vapour, this early complex decomposed within a few days to form CH and a late Ca-Cr complex. Otherwise the early complex was retained. No chromium hydroxide was found. Cr(III) was found to accelerate the C_3S reaction. The accelerating effect increased with increasing Cr(III) concentration.

Copper

CuO forms a heterogeneous solution with C_3A and is physically entrapped by C_3A hydration products (Lin et al., 1994). Lin and Lin (1994) studied hydration of a C_2S/CuO system and concluded that Cu was bound in the reaction products around the C_2S particles. The precipitation of copper hydroxide is strongly pH dependent (Conner, 1990). According to Conner (1990), precipitation as sulphide is the most effective way to bind Cu specifically, because the solubility of coppersulphide is 10^{11} times lower compared with the hydroxide.

Lead

Lead is amphoteric (see section 5.2) and its mobility in the high-pH cement environment is mainly caused by the formation of $Pb(OH)_3^-$. During solidification lead forms insoluble lead sulphates, carbonates and mixed salts that precipitate onto the surface of the reacting cement grains (Cocke et al., 1989; Thomas et al. 1981). This results in an impermeable coating that acts as a barrier to the diffusion of water and strongly retards cement setting (Trussel and Spence, 1994). A 5 % (m/m) addition of Pb can cause a tenfold increase in binding time and a weakened paste.

Thomas et al. (1981) used solution analysis, calorimetry and electron microscopy to study the retardation effect of $Pb(NO_3)_2$ admixtures on the early stages of hydration of Portland cement. The obtained results confirmed the idea that the retardation of the hydration of cement by a lead salt admixture is the result of a very rapid precipitation of protective lead hydroxide coatings around the cement grains. This precipitate is probably a rather variable mixture of lead hydroxide incorporating SO_4^{2-} and NO_3^- and possibly also silicate and aluminate. The fact that hydration is not completely stopped implies that diffusion processes through the coating are still active, bringing water into contact with the reacting cement at a reduced rate. Retardation was quantified by determining degree of hydration by measuring the areas under heat curves measured. 20 % retardation was found when 0.15 % (m/m) Pb was added while an additional 10 % retardation was found when the amount of Pb was increased to 4 % (m/m). Potentiometric titrations of lead nitrate solutions were carried out against $Ca(OH)_2$ and against $Ca(OH)_2$ and $CaSO_4$, representing the situation during early cement hydration. The results of the titrations indicate the formation of mixed salts of lead, containing all three ions: hydroxide, nitrate and sulphate. In the titrations against $Ca(OH)_2$ and $CaSO_4$, a quite ill-defined end point was observed, with pH fluctuating between 8.5 and 10. This was explained in terms of dissolution of the first-formed solids into secondary precipitates through reprecipitation.

Cartledge et al. (1990) performed the same measurements on lead samples as they did on Cd samples. They suggested that, as pH in the cement pore waters undergoes fluctuations during the progress of hydration, the Pb salts undergo solubilization and reprecipitation. The result is the presence of Pb salts on the surfaces of cement minerals even in mature cement pastes. Because of its presence at the surfaces of cement grains Pb compounds stay in contact with the pore water and are available for leaching. This explains the observation that Portland cement does not retain lead very well. Even though the complex lead salts are not highly water soluble, they are sufficiently soluble to result in undesirable high Pb levels in the leachates. They also found that the most dramatic effect of the lead salts (10 % (m/m)) is an extreme retardation of the hydration reactions, and NMR measurements indicate that both the

hydration of aluminate and silicate phases are retarded. After a delay of up to 3 days due to the presence of the Pb salts, normal hydration reactions occur and continue, but there are significant differences in the mature cement structure. NMR measurements of the Pb samples indicate that at 28 days there is a higher proportion of free and unreacted water and a lower proportion of both C-S-H and calcium hydroxide, compared to cement alone. Some differences between the hydroxide and nitrate Pb salts were also found. Retardation of setting did occur when the nitrate salt was added but was not so dramatic as when the hydroxide salt was added.

Based on leach results, pore water analyses and surface area calculations, Trussel and Batchelor (1996) suggest both precipitation and incorporation of lead during solidification.

Wang and Vipulanandan (1996) studied the potential of partly replacing cement with class C fly ash to immobilise lead. Lead nitrate up to a concentration of 10 % (m/m) was solidified with binders among which was OPC. Concentrations of calcium, silicon and lead were measured by pore fluid analysis and initial and final setting times of the samples were measured. The presence of 10 % (m/m) lead nitrate caused the final setting time of cement to 260 hours compared to 9.5 hours for the control sample (w/c = 0.5).

Mercury

Mercury does not form hydroxides but will be present as highly dispersed HgO precipitates in the pores after hydration (McWhinney et al., 1990, 1993). There was no chemical evidence found from XPS study to support any theory of complexation of mercury with other compounds. There is evidence for physical association of simple mercuric compounds (oxides and carbonates) with matrix components in localized areas. Sorption at the surface of cement grains was also suggested (Trussel and Batchelor, 1996). A part of Hg may be dissolved in the pore solution. According to Trussel and Spence (1994), no studies link mercury to the extending of cement setting, but mercury has been associated with increased calcium carbonate formation via conversion of calcium hydroxide to calcium carbonate upon exposure to atmospheric carbon dioxide. The increased calcium carbonate may weaken the cement structure. The calcium-rich formations near mercury in cured cement appear to contain less silicate. Mercury oxide is fairly soluble at 10^{-3}-10^{-4} M, and it is either sorbed on the surface of the cement matrix or dissolved in the pore solution.

Molybdenum

Kindness et al. (1994) studied the immobilisation of molybdenum using both model cement systems (mixtures of C_3S, C_2S, C_3A and gypsum) and real cement systems (OPC and GBFS). After hardening of these systems in the presence of 2000 ppm molybdenum, the larger part was bound, while the rest stayed in solution as molybdate MoO_4^{2-}. Concentrations in the pore water varied between 50-80 ppm, independent of initial concentration of Mo or cement system used. Mo appeared to be bound in two structures: $CaMoO_4$, having a powellite structure and Mo-AFm. The ettringite phase did not contain Mo and therefore was not involved in fixation.

Nickel

Akhter et al. (1993) and Zamorani et al. (1989) studied the effect of additions of various amounts of $NiCl_2$. At low concentrations it works as an accelerator by precipitating as hydroxide and thus releasing chloride ions. This mechanism can be compared with calcium chloride. At high concentrations of $NiCl_2$, hydration is retarded, probably by $Ni(OH)_2$ gel coating cement grains.

Akhter et al. (1993) studied cement samples containing amounts of $CaCl_2$ and $NiCl_2$ ranging from approximately 1 to 20 % (m/m) using NMR and XRD. They found that both salts accelerate both aluminate and silicate hydration and the effects appear to be almost entirely due to chloride. Minor variations in hydration rates at high Ni concentrations may be the result of nickel salt precipitation. With both salts chloride is apparently incorporated into the hydrated aluminate phase as well as causing alterations to the silicate phase.

Zamorani et al. (1989) studied the solidification of nickel chloride in cement prepared at a water-to-cement ratio, w/c = 0.65 and observed an accelerating effect on the physical characteristics of the matrix. The leaching results on nickel present an extremely low constant concentration in leachate media of pH = 12.5, revealing a good retention capacity of cement matrix. Chloride on the other hand appears to have adverse affects on matrix durability through enhanced leachability of calcium contents.
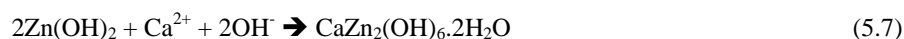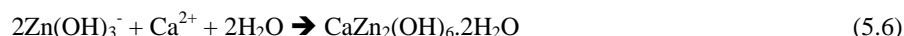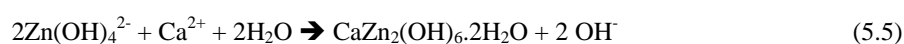
Selenium and sulphur

Selenium and sulphur form many very low-soluble compounds with heavy metals (Adaska et al., 1991). Sulphur can be used specifically for this purpose (see Section 5.5).

Zinc

Cocke and Mollah (1993) discuss the chemistry of zinc compounds. Zinc, just like Pb is amphoteric (see section 5.2) and forms both hydroxides and sulphides. $Zn(OH)_2$ may function both as an acid and a base according to the following equilibria:

$$Zn^{2+} + 2OH^- \Leftrightarrow Zn(OH)_2 \Leftrightarrow ZnO_2^{2-} + 2H^+ \tag{5.4}$$

In strongly basic solutions, as found in the cement environment, Zn is present in the form of hydroxy-complexes like $Zn(OH)_3^-$ or $Zn(OH)_4^{2-}$. The coating substance is most likely $CaZn_2(OH)_6.2H_2O$ (Arliguie et al., 1990). This compound may be formed in the following ways:

$$2Zn(OH)_4^{2-} + Ca^{2+} + 2H_2O \rightarrow CaZn_2(OH)_6.2H_2O + 2\ OH^- \tag{5.5}$$

$$2Zn(OH)_3^- + Ca^{2+} + 2H_2O \rightarrow CaZn_2(OH)_6.2H_2O \tag{5.6}$$

$$2Zn(OH)_2 + Ca^{2+} + 2OH^- \rightarrow CaZn_2(OH)_6.2H_2O \tag{5.7}$$

$CaZn_2(OH)_6.2H_2O$ acts as amorphous surface coating preventing water and ion transport necessary for hydration of the cement clinker. This results in effective retardation or, when 20

% (m/m) is added, even prevention of cement hardening. The precise coating mechanism is not known in detail, but according to Cocke and Mollah (1993) cations like $Zn(OH)_3^-$ and $Zn(OH)_4^{2-}$ will be rejected by the negatively coated hydrating cement clinker and therefore compounds like $CaZn(OH)_3^+$ and $CaZn(OH)_4$ are more likely to be involved. The presence of Ca^{2+} near the surface provides such a pathway. Zinc-doped Portland cement samples (unleached and leached) have been investigated by XPS, AES, EDS and SEM techniques. The results indicate that Zn is mainly on the outer surface and is effectively removed during acid leaching.

Ortego et al. (1989) found that the FTIR spectra of zinc-cement samples (more than 20 % (m/m) was added) resembled the spectra of dry cement clinker. When added in these amounts zinc effectively prevents cement hydration.

Gawlicki and Czamarska (1992) studied the influence of ZnO on OPC hydration. 0.5 and 1.0 % (m/m) ZnO was added as percentage by mass of cement and heat evolution was measured during hydration. ZnO was also added to C_3S, C_3A and combined systems (w/s = 0.5) where the formation of the normal hydration products (CH and aluminate hydrates) and a new phase ($CaZn_2(OH)_6.2H_2O$) was followed. From their results they concluded that the presence of ZnO strongly decelerates OPC hydration by prolonging the dormant period and that the presence of zinc clearly disturbs CH formation. The C_3A reaction was not influenced by zinc, which could be explained by the high growth rate of calcium aluminate crystals.

Poon et al. (1986) found that zinc increased the permeability of cement, probably by promoting ettringite formation. This increased permeability did not lead to a corresponding increase in zinc concentration in leachates, suggesting that zinc is retained in the matrix by a primarily chemical mechanism.

According to McWhinney and Cocke (1993), Zn compounds induce carbonation in the same way as cadmium.

5.3.3 Anions

Borates

In Taylor (1997) borates are mentioned very briefly as being compounds that generally retard cement hydration, possibly by a precipitation mechanism. In Conner (1990) borates are listed as short-term setting retarders that disrupt the cement matrix. In both standard works nothing is mentioned about the mechanisms taking place during hardening.

Zhou and Colombo (1984) used masonry cement, consisting of 50 % (m/m) Portland type I cement and slaked lime ($Ca(OH)_2$). Using this type of cement they were able to immobilize up to 15 % (m/m) dry boric acid (based on total mass of binder, water and dry waste). When 5 to 15 % (m/m) boric acid was added, compressive strength was found to be 18 to 50 % compared to plain masonry cement. The authors mention that as little as 5 % (m/m) would inhibit the curing of a Portland type I cement waste form.

Jeffrey et al. (1991) found that it was difficult to stabilise any liquid boric acid waste having a concentration of dissolved boron of more than 12 % (m/m) using cement and extra lime for pH control. Using a patented pre-treatment method that partially neutralised the boric acid waste they were able to process liquid wastes containing up to 30 % dissolved boron. The neutralising agent was not mentioned in this article.

108

Csetenyi and Glasser (1993) investigated the extent to which borate can be insolubilised by inclusion into ettringite where it replaces the sulphates. They synthesised a wide range of borate substituted ettringites with different ratios of borates to sulphates and obtained products that were stable across a broad range of physicochemical conditions and had very low solubility. Therefore they concluded that ettringite may function as a borate trap in cementitious systems.

Csetenyi and Glasser (1995) investigated the effects of borate in a Na_2O-CaO-B_2O_3-H_2O system. Twenty-one closely related compositions were prepared and reacted in sealed containers. Solid phases were characterised and the aqueous phase was analysed chemically for Ca, Na and B. Extensive thermodynamic modelling of solubility relations was also undertaken. Combining these two methods they were able to determine the equilibrium features of the system. In the CaO-B_2O_3 system at 25 ^oC the solubility of $Ca(OH)_2$ is initially increased by addition of boric oxide. However at a certain point maximum solubility is reached. Thereafter, with addition of more boric oxide, calcium borate hydrates precipitate with the result that boron solubility decreases to 0.005-0.01 M. They concluded that the presence of soluble borate in cement-water mixes initially enhances the solubility of calcium. Eventually precipitation of calcium borate hydrate occurs. This tends to precipitate much of the soluble Ca, initially in relatively amorphous form, directly onto the cement clinker grains, thereby forming a barrier layer. Under these conditions the amorphous barrier layer causes particles to coagulate, giving rise to false setting. From their results they also found an explanation for the known effect that addition of NaOH may overcome extended setting. They found that the presence of NaOH increases the solubility of the borates and therefore suppresses the initial precipitation of hydrated calcium borates. As a result the aqueous phase remains saturated in $Ca(OH)_2$ and cement hydration can proceed at a normal rate.

Casabonne-Masonnave (1993) studied the immobilisation of borates and phosphate anions with saturated lime solutions. The aim of this study was to characterise the precipitated phases obtained when adding borate and phosphate anions to alkaline lime-saturated solutions simulating the interstitial phase of cement pastes. From his experiments and thermodynamic calculations the author concluded that in basic solutions of borax at 20 ^oC, boron is mainly contained in the form of tetrahydroxyborate ions $[B(OH)_4]^-$. The precipitated phase was determined as being $Ca[B(OH)_4]_2.2H_2O$ (or CBH_6 where $B = B_2O_3$). The solubility of this compound was determined: $1.62 \cdot 10^{-6}$ [mole/l]^3.

Phosphate and ammonium anions

Phosphate compounds are known for their retarding effects and are used in practice for that purpose.

Barret et al. (1992) studied the effects of many radioactive elements including borax ($Na_2B_4O_7.10H_2O$), $CaHPO_4$ and NH_4NO_3 on the hydration of tricalcium silicate (C_3S). C_3S was used, because its hydration is easier to follow than hydration of the more complex cement. Objective of this study was a better understanding of the particular physico-chemical processes involved in cement hydration in the presence of these elements. These and many other ions were added separately (1 % (mole/mole) quantities) to a stirred aqueous C_3S suspension and hydration was followed by measuring the conductivity during a certain period. In a pure C_3S suspension it can be assumed that the electrical conductivity is nearly all due to the lime in solution that is formed when C_3S hydrates. By measuring this conductivity, C_3S

hydration can be followed. During pure and undisturbed C_3S hydration the obtained curve shows a maximum after 6 hours. The position of this maximum allows the accelerating or slowing down effect of the additive to be seen. When borax was added a strong decelerating effect was evident. During the first hour of hydration, the conductivity did not increase at all and the measurements showed a plateau. It was also shown that at a given L/S (liquid to solid) ratio the length of this plateau increased with increasing molar percent of borax. For a given borax concentration it increases with decreasing L/S. This plateau can be interpreted as a stationary state due to the precipitation of Ca ions as calcium borate hydrates. Among the numeral borate compounds that may exist, only $Ca[B(OH)_4)].2H_2O$ would be stable at room temperature. This compound can coat the cement grains inhibiting or even preventing further hydration (Casabonne-Masonnave, 1987).

Using the same measuring methods, Barret et al. (1992) found a slight influence for $CaHPO_4$ and an accelerating effect for NH_4NO_3. When they used thermal flux microcalorimetry on samples having a L/S = 0.5 to measure the dormant period the slowing down effect of borax was confirmed. The possible causes of these effects are not given. The prolongations of the dormant period varied between 42.5 hours (0.25 % (mole/mole)) to 7 days (1 % (mole/mole)) compared to 3 hours for the reference sample. The addition of 5 % (m/m) $CaHPO_4$ and NH_4NO_3 resulted in dormant periods of 3.5 and 1.5 hours respectively. This was in agreement with the data obtained by the electrical conductivity method. An explanation for these observed effects is not given but probably these ions increase the solubility of $Ca(OH)_2$, thus increasing the hydration rate of silicates. It is mentioned that next to the accelerating effect of NH_4NO_3 the presence of this compound may cause liberation of ammonia gas when a strong base like $Ca(OH)_2$ is present according to the following reaction:

$$NH_4^+(aq) + OH^- (aq) \rightarrow NH_3 (g) \uparrow + H_2O(l) \qquad (5.8)$$
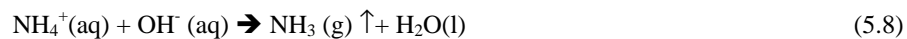
Finally the authors state that the only possibility for fixation of HPO_4^{2-} is the maintenance of a pH > 13. At this pH, PO_4^{3-} will be the prevailing species according to the equilibrium

$$HPO_4^{2-} + OH^- \Leftrightarrow PO_4^{3-} + H_2O \qquad (5.9)$$

and will then be fixed by the formation of the very insoluble $Ca_3(PO_4)_2$.

Casabonne-Masonnave (1993) studied the immobilisation of phosphate anions with saturated lime solutions. It was also found that all phosphate ions were immobilised as long as pH remained above 13. The solubility product of $Ca_3(PO_4)_2$ was determined: $2.0 \cdot 10^{-29}$ $[mole/l]^5$.

Chlorides and sulphates

Both chlorides and sulphates are known to have an accelerating effect on cement hydration (Ramachandran, 1984). $CaCl_2$ has been used in the past as an accelerator. This compound decreases the dormant period and increases the hydration rate of C_3S. In a $C_3S{:}C_2S$ mixture containing 0, 1 and 2 % (m/m) $CaCl_2$ the setting times have been found to occur at 790, 525 and 105 minutes respectively. The exact mechanism is not clear. One of the explanations is the diffusion of chloride ions through the initially formed hydrates on the silicates into the zone of active reaction, which would increase the rate at which OH^- ions would diffuse

outwards. Thus the precipitation of Ca(OH)$_2$ would occur more rapidly, resulting in an accelerated decomposition of the calcium silicates in the inner reaction zone. Acceleration can also be explained in terms of pH. CaCl$_2$ decreases the pH of the liquid phase during cement hydration and consequently increases the dissolution rate of lime. This corresponds with an increase of reaction rate of C$_3$S and C$_2$S.

The presence of high amounts of sulphates, e.g. gypsum, in a waste steam will strongly increase ettringite formation, which results in a large increase in volume of solids (see volume stoichiometry of ettringite reaction in Chapter 2). When this increase in volume occurs in a solidified paste, this may result in expansion and cracks.

5.3.4 Organics

Hills et al. (1995) studied the effects of organic compounds on the heat of hydration, setting, strength development and microstructure of OPC. Seven different compounds were used, representing seven different functional groups (-NH$_2$, -NO$_2$, -Cl / C=C, -CHO, -CO$_2$-, -OH, and -Cl / -OH). They found that most organics influenced early hydration by retardation or acceleration but mature samples displayed a similar phase composition to the OPC control. Effects on setting times and strength were small for the additions used (0.1 to 5 % (m/m)). Strength was nearly always negatively influenced. The reason that organics are not fixed very well is a result of several factors: (1) Many organics are relatively stable compounds that do not combine with the components of a hydrating cement. (2) If they are found to produce salts, complexes or precipitates then they may still compromise cement hydration and still remain unfixed. (3) The resulting low-strength and high permeability products have a negative effect on physical retention.

Banfill (1986) reports results that confirm the suggestion that organic retarding admixtures may adsorb on to calcium hydroxide nuclei and prevent their growth. Organic compounds were dissolved in a saturated calcium hydroxide solution and a precipitation index was assigned according to the time of appearance of precipitate and the amount of precipitate. Then a retardation index was assigned based on results from heat curves and conduction calorimetry found in literature. It was shown that there is a negative exponential correlation between retarding index and precipitation index. The observation that organic compounds that retard the hydration of cement also delay the precipitation of calcium hydroxide from aqueous solution is evidence for a mechanism of retardation based on the poisoning by the organic compound of the growth of calcium hydroxide nuclei in hydrating cement.

Banfill and Saunders (1986) studied the sorption of several organic compounds on to cement and related materials. They found that there was a poor correlation between retardation and the sorption of organic compounds on to unhydrated cement. The retardation correlated well with the sorption on to both hydrated cement and calcium hydroxide. This confirmed the theory of retardation based on both the hindered nucleation and growth of CH and the reduced permeability of the C-S-H around cement particles.

According to Trussel and Spence (1994) organic compounds retard or interfere with cement setting by the same mechanisms as described earlier. The most important difference however is that in most cases they do not form strong chemical bonds like most inorganic compounds do. Therefore their retention is strongly dependent on physical entrapment.

Active carbon can be added to the cement matrix to bind organic contaminants (Conner, 1990). However its presence during hydration causes extra porosity in the cement as it removes the water needed for the cement reactions. The carbon is able to bind water several times its weight (Capelle and de Vooys, 1983). This effect has been simulated using CEMHYD3D and using 10 μm carbon particles, able to bind 5 times its volume in water. This bound water was not available for reaction anymore. The simulations revealed that the presence of such a water absorbing phase (5 to 10 % (m/m)) will result in a strong decrease in degree of hydration and higher porosities (Van Eijk and Brouwers, 1997).

5.3.5 Comparison between different ions

Hills et al. (1994) studied the changes in heat evolution and phase development during early hydration of OPC in the presence of several anions, cations and organics, added separately and in combination. Heat curves were recorded for all additions and Q_{max} values (maximum total heat evolved) were plotted vs. $1/t$ Q_{max} (the reciprocal of time to Q_{max} in seconds) to illustrate retardation and acceleration effects. Of all the cationic additions, Cu and Zn were found to significantly retard Q_{max}, and in comparison to the other metals and to the control, the total heat evolved was much reduced, being approximately 74 % (1 % Zn based on total mass of mix) and 33 % (0.4 % Cu). Phases present after hydration were measured using XRD but did not differ significantly from the control sample for the additions used in these experiments. Although small changes in heat curves and phase intensities were observed, poisoning of hydration was only found when metal ions were added as mixtures.

Tashiro et al. (1977) studied the hardening and leaching behaviour and solubility of cement mortar containing several heavy metal compounds. Strengths were measured after 3 and 28 days of curing and compared with undoped samples. 0.5 % (m/m) additions hardly had any effect. At 5 % (m/m) addition, Cu, Zn and Pb compounds retarded early hydration. As_2O_3 had a slightly negative influence on strength development.

Bobrowski et al. (1997) studied the setting of cement doped with 1 % (m/m) cadmium, lead, zinc and chromium respectively. They found that cadmium and chromium had little effect on setting, while zinc caused flash setting, meaning that mortars set immediately, but regained plasticity after stirring. Lead prolonged setting times by several hours and reduced strength of the final sample by 30 %.

Uchikawa et al. (1997) measured the rate of hydration, morphology of hydrates, effects on pore structure and distribution of metals in cement pastes doped separately with small amounts (0.1-0.5 % (m/m)) of several heavy metals. The rate of hydration was determined by measuring the amount of bound water based on ignition loss at 1000 °C. The elements F, P and Ti decreased hydration most. Cl, Cr, Sr and Sb accelerated hydration compared to plain cement. Most elements were mainly found in the C-S-H phase or AFm phase and hardly in the $Ca(OH)_2$ phase after hydration, except for P and Sr; those elements were mainly found in the AFm phase and $Ca(OH)_2$ phase.

Nocun-Wczelik and Malolepszy. (1997) investigated the effects of Zn, Pb, Cd en Cr salts on phase composition, microstructure and leaching behaviour of calcium silicate hydrates formed from. They found that Zn, Pb and Cd were immobilised in C-S-H and changed its structure. The C-S-H formed at room temperature in the presence of heavy metal

compounds was poorly crystallised. The presence of heavy metals also increased $Ca(OH)_2$ consumption and increased the amount of bound water in the hydrated sample.

Rossetti and Medici (1995) studied the effect of Cd, Cr, Pb and Zn chlorides on the hydration process of white cement. Variations in the physical-mechanical properties of the cement mixes, the development of the heat over time and the development of phases formed during hydration were observed by XRD.

Cd and Cr were found to accelerate setting and the development of the main hydration peak, where Pb retarded setting and delayed further hydration. Zn accelerated setting, but retarded hydration. Furthermore, the XRD analyses performed at 1 and 3 days hydration of the Zn-doped sample showed the formation of a crystalline phase, namely calcium hydroxyzincate.

5.3.6 Conclusions from literature

From literature one can conclude that several mechanisms take place when contaminants are present in a hydrating cement mixture. These mechanism are based on solubility of the ions or compounds and the compounds they will form in the high pH pore water. The pH is a strongly regulating parameter. Generally, metal hydroxides show a minimal solubility at pH values between 9 and 12 (Conner, 1990). After mixing of cement and water the pH will rise immediately to a value of 12.5 or higher and this will result in direct precipitation of metal salts. Because such salts will precipitate on cement grains, this results in coating, which inhibits transport of water to the cement grain and will therefore inhibit hydration. In most cases, the coating compounds are known and in the case of zinc, a model is developed that describes the coating mechanism. In the case of borates, coating by calcium borate hydrate is responsible for the observed retardation effects. Coating effects are also described for cadmium and lead. Solubilities of the coating compounds involved in these processes are known in most cases. The effects on hydration can be visualised using heat or conduction curves.

The coating mechanism is better described and analysed in literature compared to the other mechanisms, e.g. nucleation. Coating can have significant effects from retardation to cement hydration not taking place at all. Therefore the mechanism of precipitation, resulting in *coating* of cement particles will be studied in more detail in the next section. The pore water and especially pH calculations presented in Chapter 3 can be useful to determine solubility of new compounds.

5.4 Coating

5.4.1 Mechanism

After mixing of water or the waste suspension with cement the pH will rise immediately to some pH value around 12 - 13 (see Chapter 3) and instantaneous precipitation of metal salts on the cement grains occurs. Experiments with cadmium and lead showed that coating took place in the first minutes after mixing (Diez et al. 1997 and Thomas et al., 1981). The coating inhibits transport of water to the cement grain and will therefore inhibit further hydration.

The most detailed proposal for a coating mechanism was done by Yousuf et al. (1995) and Cocke et al. (1995). In their work the interfacial chemistry of metal ions in cementitious systems was studied. They concluded that the phenomena at the mineral-water interface are of fundamental importance in understanding the mechanisms of s/s processes in cement-based systems. They describe a so-called "Charge Dispersal Model" that successfully describes the pH dependent surface coating and retardation of cement setting by Zn and Cd. This model can be described as follows: The main phase in hydrated Portland cement is colloidal C-S-H gel. The hydrated cement paste is highly alkaline (pH = 13.0 ± 0.5) and in this environment the cement surface or the premature C-S-H phase (Type II) that will be formed immediately when cement comes into contact with water, will possess a negative charge. The most abundant counter ions in cement solution are Ca^{2+} cations extruded from inside the hydrating cement clinker through the semi-permeable C-S-H gel membrane, which acts as a diffusion barrier after the initial period of hydration reaction. These oppositely charged Ca^{2+} counter ions will immediately surround the negatively charged C-S-H surface and preferentially adsorb, due to their higher charge density, to form a layer of positive charge. The negative surface and the layer of positive charge combine together to constitute an "Electrical Double Layer". The ions forming the electrical double layer are expected to be tightly bound.
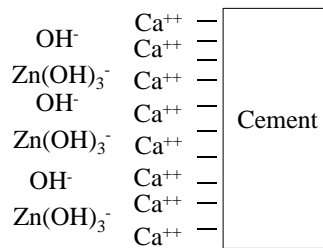

Figure. 5.1. Schematic overview of the Charge-Dispersal Model by Yousuf et al. (1995).

Between pH 12 and 13, the $Zn(OH)_3^-$ and $Zn(OH)_4^{2-}$ anions are dominant species constituting 40 % and 60 % respectively. These ions will be dispersed by the presence of OH^- ions. The negatively charged zinc hydroxyl ions would not be expected to adsorb on the negative C-S-H surface. However, the negative surface is charge-compensated by Ca^{2+} ions. The next zone in the solution will consist mainly of a diffuse layer of ions constituting of what is known as "A Tri-layer of Diffuse Ions". This latter layer is composed of mainly $Zn(OH)_3^-$ and $Zn(OH)_4^{2-}$ anions. An overview of the zones present is given in Fig. 5.1. This uniform dispersion of zinc anions over the entire C-S-H surface may lead to reactions Eq. (5.5) and Eq. (5.6). The reaction given by Eq. (5.7) is considered less likely in a high-alkaline environment for thermodynamic reasons. In the presence of sufficient Ca^{2+} ions in solution the zinc hydroxyl anions are transformed in $CaZn_2(OH)_6 \cdot 2H_2O$ which completely covers the cement grains and thus inhibits further hydration reactions. Cd^{2+} will inhibit hydration in the same way. The aqueous chemistry of Ba^{2+}, Ag^+, Hg^{2+} and Cr^{3+} suggests that these ionic species do not form negative charges in highly alkaline environments and the behaviour of these ions will be different.

5.4.2 Implementing coating routines in CEMHYD3D

In order to use CEMHYD3D to simulate the hydration of a cement mixture in which cement particles are coated, adjustments have to be made in the dissolution routine of the program, because coating effects this dissolution process. Before adjustments in the model can be made, some assumptions and simplifications have to be made about the coating mechanism. Table 5.2 gives an overview of the assumptions and the consequences for adjustments to be made in the model.

Table 5.2. Coating in CEMHYD3D.

Assumption	Implication for model
Instantaneous precipitation	Coating before start of simulation
Precipitation on surface of cement particle	Only part of particle exposed to water available for coating
No mineral preference	C_3S, C_2S, C_3A, C_4AF and sulphate pixels coated with equal probabilities
No particle size preference	All particles coated with equal probabilities
Precipitated compound impermeable	Coated part of particle not available for dissolution

Coating of cement particles was observed taking place already in the first minutes after mixing of the aqueous waste and cement (Diez et al., 1997 and Thomas et al., 1981). This observation and the fact that in the model used here hydration is simulated after an induction period of 7 hours, cement particles should be coated directly at the beginning of a simulation run. Because precipitation is assumed to take place on the surface of a particle (where Ca^{2+} and OH^- are released), in the model, only that part of a particle exposed to water, will be available for coating. All main clinker minerals C_3S, C_2S, C_3A and C_4AF and sulphates are considered to be coated with equal probabilities. Furthermore, because precipitation is a very rapid process it is assumed that there is no particle size preference for a coating compound. This means that both small and large particles will be coated with equal probabilities. Finally, the precipitated compound is crystalline in most cases and impermeable to water. Therefore, the coated part of a cement particle is not in contact with water and not available for dissolution anymore.

To prepare CEMHYD3D for taking into account coating, its dissolution mechanism had to be changed and three possibilities were considered to do this:

Change dissolution probabilities

The dissolution probabilities (see Table 2.7) of all minerals and sulphates initially present could be changed. However, these probabilities are empirical and were only introduced to create mutual differences in reaction rates. It is difficult to make assumptions on how these mutual differences are changed by coating and decreasing all rates will only result in a slower execution of the complete hydration process.

Rendering pixels on surface inert

Pixels present on the surface of cement particles could be made inert (i.e. converted to the inert phase) in an initial scan before hydration starts. In this way they would be treated as a non-cement phase and prevented to go into solution during the complete hydration process. A disadvantage of this method is that the amount of pixels in contact with water is a relatively high percentage in terms of volume due to the scale of the simulation program. A 3 μm particle for example consists of one inner pixel surrounded by 18 outer pixels. A coating percentage of 50 % would imply that 9 pixels are made inert, which is almost 50 % of its volume. As a result of this more than 33 % and 49 % of all solid pixels are present at the surface of a particle and exposed to water for CEM 32,5 R and 52,5 R respectively. Another more practical disadvantage is the requirement of some more adjustments in the program because diffusing C-S-H is only allowed to precipitate on solid C-S-H, C_3S or C_2S and not on the inert phase.

Both methods were not used for the reasons explained. Instead two more advanced methods were developed, which were based on blocking directions to be chosen for dissolution. Directions that pixels on the surface of a particle may choose when they perform a random step for dissolution can be blocked. So instead off complete *pixels* only the *directions* it can choose to dissolve are considered in this case as if some of the pixels *planes* are coated. This should be done for all pixels present at the surface of cement particles at the beginning of hydration. In this way 1 pixel particles, having 6 sides can be partly coated. And pixels coated initially may dissolve later when a neighbour pixel is removed and the plane in between is exposed to water. Furthermore, using this option, all pixels will keep their phase identity and in case of silicates they will still be available for precipitation of C-S-H.

The following 2 methods were developed and used:

1. Coating fraction method

The presence of a layer of coating compound on the cement surface was be obtained by first scanning all pixels located at the surface of cement particles and counting the number of planes for each pixel that is exposed to water. When the fraction of the total cement surface to be coated, is known, this *coating fraction* can then be used as a probability that a plane will be blocked during the hydration. This will be illustrated by the following example. A single pixel particle, for example, has six surface planes and assuming that all six of them are exposed to water and 50 % of the cement surface is coated, on average three of these planes will be chosen randomly and blocked irreversible. This results in 3 out of 6 directions that are not allowed for steps into water (Fig. 5.2).
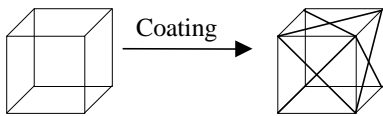

Figure 5.2. The principle of coating 50 % of the surface of a digitised 1 μm particle. After the coating scan, 3 planes are covered (indicated by a cross) and each coated plane blocks a direction the pixel may choose during dissolution.

116

2. Coating packages method

According to the chemical equilibria an amount of precipitated product will be formed and this amount of volume will coat the unhydrated cement surface. Furthermore it is assumed that the precipitated volume is made up of layers of coating units of thickness d_{layer} and volume $d_{layer} \cdot 1 \, \mu m \cdot 1 \, \mu m$ (see Fig. 5.3).
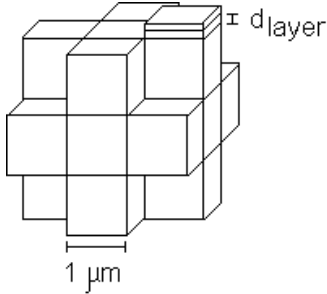

Figure 5.3. Digitised 3 μm particle (19 pixels). One water exposed cement pixel plane is covered with two coating units and thus coated. All other water exposed planes are uncoated and thus free for dissolution/reaction.

The total number of coating layers present on the initial surface of the cement particles is dependent on the initial amount of precipitate and can be computed according to Eq. (5.10):

$$n_{layers} = \frac{m_{prp}^{layer} / m_c}{d_{layer} \cdot SSA \cdot \rho_{prp}} \tag{5.10}$$

n_{layers} = average number of coating layers
m_{prp}^{layer} / m_c = mass fraction precipitate present in coating layer [g/g of cement]
d_{layer} = coating layer thickness [cm]
SSA = specific surface area of cement [cm^2/g]
ρ_{prp} = precipitate density

During cement hydration the total mass of precipitate should always comprise the amount in solution plus the amount present in coating layers. This implies that the following mass balance should be obeyed, in which all fractions are in [g/g] unreacted cement:

$$m_{Tprp} = m_{prp}^{sol} + m_{prp}^{layer} \tag{5.11}$$

m_{Tprp} = total initial mass precipitate [g]
m_{prp}^{sol} = mass precipitate in solution [g]
m_{prp}^{layer} = mass precipitate in coating layer [g]

Mass fraction precipitate based on cement can be computed from pore water concentration of precipitate using Eq. (5.12).

$$\frac{m_{prp}^{layer}}{m_c} = \frac{[prp]^{layer} \cdot w/c \cdot \dfrac{\varphi_p}{\varphi_p^0} \cdot M_{prp}}{\rho_w} \tag{5.12}$$

m_{prp}^{layer} = mass precipitated product [g]

m_c = mass cement [g]

$[prp]^{layer}$ = amount of precipitate present in coating layer [mole/dm^3]

$\dfrac{\varphi_p}{\varphi_p^0}$ = concentration factor (ratio actual porosity to initial porosity)

M_{prp} = molar mass of precipitate [g/mole]

The total mass fraction of precipitate m_{Tprp}/m_c can be also be computed from Eq. (5.12), assuming that all added contaminant will precipitate, (note possible molar differences that may follow from different composition of added product and precipitate), and taking concentration factor = 1 (see section 3.3.2 for meaning of concentration factor). m_{prp}^{sol}/m_c can be computed from Eq. (5.12) using the equilibrium concentration of precipitate, which can be computed after each hydration cycle.

When the total volume of precipitate is known, it has to be placed at the water exposed surface of the unhydrated cement particles. In the hydration model, the smallest size unit is 1 µm^3 and the water exposed cement particle surface consists of m_s surface planes of 1 µm^2. Then the total volume of precipitate consists of n units of volume d_{layer} times 1 µm^2 that have to be placed randomly on the cement particle surface (see Fig. 5.3).

Subsequently, from statistics (Feller, 1950) one can compute the surface fraction p(x) that is coated by x units after placing the total of n units. The probability p that one unit is placed on one specific water exposed pixel side is inversely proportional to the number of pixel sides n_{sides}^{exp} it can choose from, so $p(1) = 1/n_{sides}^{exp}$ when n = 1. The probability of a surface plane being uncoated after randomly placing n units on n_{sides}^{exp} possible pixel sides, can be computed as follows:

$$p(0) = (1-1/n_{sides}^{exp})^n \tag{5.13}$$

Note that a surface of 100 planes (n_{sides}^{exp} = 100 and the number of units n to be placed randomly should be 100·n_{layers}) is sufficiently representative to produce an accurate probability distribution. From Eq. (5.13) it follows that when the cement surface could be coated by more than 5 coating layers on average, and using the probabilistic placement procedure proposed here, the percentage of uncoated surface decreases to less than 1 %. From preliminary simulations it followed that reasonable hydration still take place when 5 % of the surface is uncoated, corresponding with a probabilistic distribution of 3 coating layers in average.

118

To incorporate both coating methods, the following program routines were implemented into the CEMHYD3D model.

Coating. The coating routine consists of one scan over all pixels, determining which planes are exposed to water. When the coating fraction method was used, a given coating fraction is used as a probability that this plane will be coated. When the coating packages method was used, the volume of precipitate to be placed on particle planes is computed and the number of packages determined. The scan and coating routine is always executed before simulation of the hydration starts.

Checking dissolution. When hydration starts, in every dissolution cycle, an extra check is performed to see if the step of a soluble pixel into water is in an allowed direction. If this is not the case, i.e. if the chosen direction corresponds with a coated surface, or contains more than one coating package, the pixel will not be dissolved during that specific hydration cycle.

Checking diffusion of sulphates. When a diffusing sulphate pixel hits a pixel of an aluminate phase (C_3A or C_4AF), this aluminate pixel is also checked for coating. When this is the case, (and the coated plane corresponds with the direction the diffusing sulphate pixel was coming from), the aluminate and sulphate pixels will not be converted to ettringite.

Checking for redissolution. When coating packages are used, the pore water composition is computed and the amount of precipitate is adjusted according to the result. When precipitate has to dissolve, coating packages will be removed randomly.

5.5. Application of two coating methods in CEMHYD3D

5.5.1 Coating fraction method

In order to study the relation between coating fraction and degrees of hydration, simulations were executed in which different fractions of the initial cement surface were coated using the mechanism described earlier. Two particle size distributions (PSD), corresponding to cement types CEM 32,5 R and CEM 52,5 R (given in Appendix 3), were used to study PSD effects. For both cement types 0, 25, 50, 75, 95 % and 100 % coatings were performed by determining the total amount of surface planes (equivalent with the inner surface of the structure) and blocking these directions permanently for dissolution using the coating percentage as a coating probability. An equal coating percentage for both cement types would correspond with different quantities of precipitated product, because of the difference between the specific surface areas (SSA). These areas differ by a factor of about 2 (see Chapter 2). To compare the effects of equal quantities of a precipitated compound for both cement types used, hydration of CEM 52,5 R was also simulated with coating percentages of 12.5, 37.5 and 47.5 %, which correspond with the difference in SSA. In this way the absolute quantities of surface coated were kept equal. All simulations were run and the hydration process was followed during an equal time of 28 days and in saturated conditions at 25 ^{o}C.

In Tables 5.3 and 5.4 the results of the hydration simulations are presented. Degrees of hydration after 28 days of hardening are given in absolute values and the percentages

reduction of degree of hydration compared to uncoated or blank cement samples are given in brackets.

Table 5.3. Degrees of hydration after 28 days of hardening at equal coating percentages.

% of surface coated	CEM 32,5 R	CEM 52,5 R
0	0.57	0.73
25	0.54 (-5 %)	0.71 (-3 %)
50	0.50 (-12 %)	0.67 (-8%)
75	0.41 (-28 %)	0.60 (-18%)
95	0.24 (-58 %)	0.36 (-51 %)
100	0.00 (-100 %)	0.00 (-100%)

Table 5.4. Degrees of hydration after 28 days of hardening at equal quantities of coating compound.

% of surface coated (32,5 R/52,5 R)	CEM 32,5 R	CEM 52,5 R
0 / 0	0.57	0.73
25 / 12.5	0.54 (-5 %)	0.72 (- 1 %)
50 / 25	0.50 (-12 %)	0.71 (- 3 %)
75 / 37.5	0.41 (-28 %)	0.69 (- 5 %)
95 / 47.5	0.24 (-58%)	0.68 (-7 %)
100 / 50	0.00 (-100 %)	0.67 (- 8 %)

In Figs. 5.4, 5.5 and 5.6 the degrees of hydration are given as a function of hydration time for each simulation. In Figs. 5.8 and 5.9 degree of hydration as a function of coating percentage is presented for both cement types.

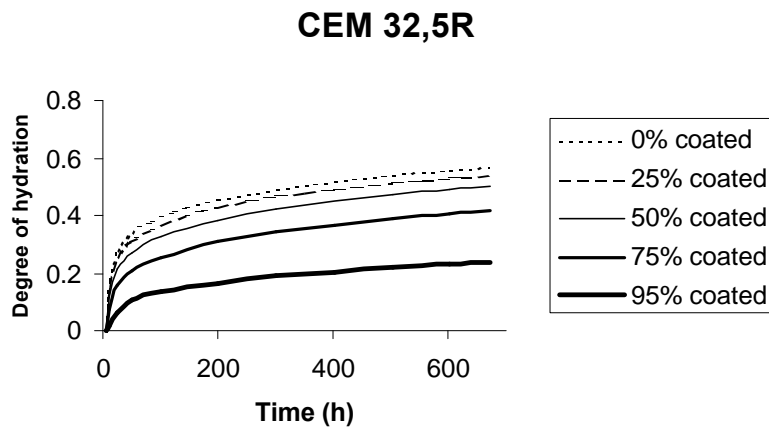**Figure 5.4.** Degree of hydration versus time at different coating percentages (CEM 32,5R).

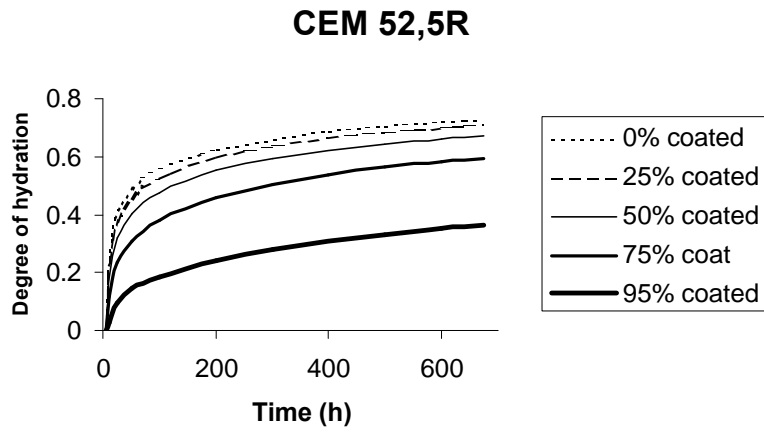**CEM 52,5R**

Figure 5.5. Degree of hydration versus time at different coating percentages (CEM 52,5R).
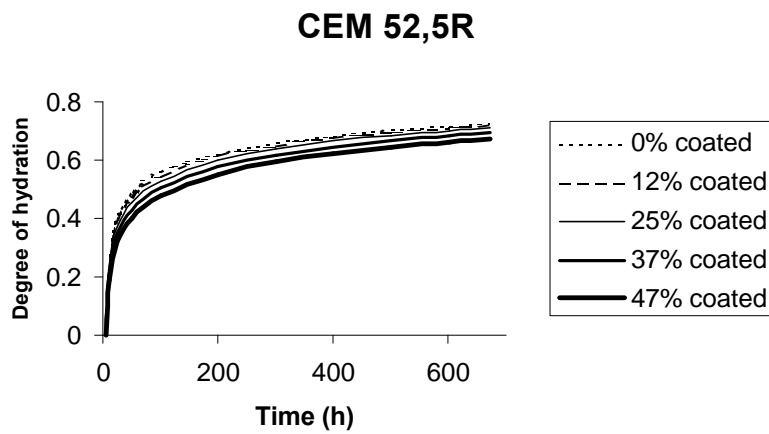
CEM 52,5R

Figure 5.6. Degree of hydration versus time at different coating percentages (CEM 52,5R). Half percentages (accordingly equal concentrations) compared with CEM 32,5R in Fig. 5.4.
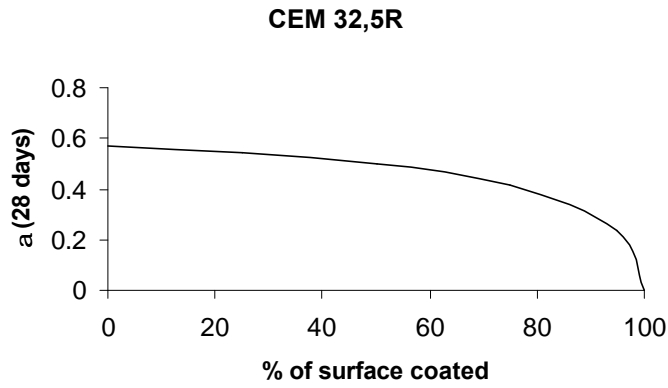
CEM 32,5R

Figure 5.7. Degree of hydration (α) after 28 days as a function of surface coating percentage (CEM 32,5R).
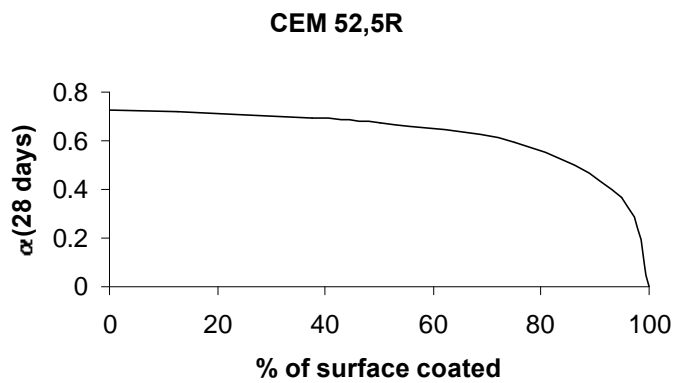
CEM 52,5R

Figure 5.8. Degree of hydration (α) after 28 days as a function of surface coating percentage (CEM 52,5R).

During undisturbed hydration (0 % coating) the finer CEM 52,5R cement reaches a higher degree of hydration at equal time compared to the coarser CEM 32,5R cement, which would be expected. This is a result from the higher number of surface sides present in the initial cement structure resulting in more contact sides between cement and water and higher probabilities for pixels to perform a step into solution. From Figs. 5.4-5.8 it can be seen that significant poisoning and reduction in degree of hydration occurs at relatively high coating percentages. This is due to the fact that a cement pixel that was not allowed to dissolve during a hydration cycle may still dissolve in one of the subsequent cycles. Then this pixel may perform a random step in an allowed direction or into the direction where an adjacent cement pixel has gone in solution and is replaced by water. Then a new possible direction for dissolution is created. When coating percentages are higher than 90 % the retardation effects become significant and hydration is strongly reduced. When the complete surface is coated

122

hydration is blocked completely because from the start all contact sides between cement and water are blocked and no dissolution and reaction is possible at all.

It can also be seen from the results that the reduction of degree of hydration of CEM 52,5 R is lower than the reduction of CEM 32,5 R hydration, both if the coating percentage is increased (see Table 5.3) or when the quantities of precipitated compounds are increased (see Table 5.4). This is a result from the higher specific surface of CEM 52,5 R, then exposing relatively more cement to the surrounding water phase during the complete hydration process. This increases both the total dissolution probability in general and the probability that adjacent pixels will create a new plane exposed to water as described earlier. Based on the model results one may conclude that the specific surface of cement is an important parameter.

5.5.2 Coating packages method (applied to calcium borates)

The coating packages method will be presented using the well-known retarding effects of borates. Calcium diborate $Ca[B(OH)_4]_2.2H_2O$ (CBH_6 in cement chemistry notation) is formed instantaneously after mixing cement and borate containing water, as a result of the high pH and high calcium concentration in the pore water. When boric acid (H_3BO_3) is dissolved in the pore water, it forms $[B(OH)_4^-]$ ions and in the presence of Ca^{2+}, the equilibrium of interest is the following (Casabonne-Masonnave, 1993):

$$Ca[B(OH)_4]_2 \text{ (s)} \Leftrightarrow Ca^{2+} + 2 [B(OH)_4^-] \tag{5.14}$$

$$K_{CBH_6} = [Ca^{2+}][B(OH)_4^-]^2 = 1.62 \cdot 10^{-6} \text{ [mol}^3/\text{dm}^3] \tag{5.15}$$

Note that 2 moles of added product are required to form 1 mole of precipitate (CBH_6 in which B = B_2O_3, see Appendix 1). When $[B(OH)_4^-]$ is determined, $[Ca^{2+}]$ can be computed according to the ion product K_{CBH_6} and $[OH^-]$ can be computed using the ion product of $Ca(OH)_2$, K_{CH}.

In Fig. 5.9, the development of pore water concentrations during undisturbed hydration is plotted against time. When hydration starts, $[Ca^{2+}]$ is high and $[B(OH)_4^-]$ must be low because of its ion product and CBH_6 precipitates. Then alkalis are released as a result of cement hydration and $[Na^+]$ and correspondingly $[OH^-]$ in the pore water increase. This results in a decrease in $[Ca^{2+}]$ because of the CH ion product. As a result of this CBH_6 can redissolve, the surface coating percentage decreases, hydration rate will increase and more alkali will be released. This is a self-accelerating process. From these trends it is also clear that when coating percentages approach 100 %, the hydration rate is too slow to release sufficient alkalis for redissolution of the coating compound. In that case hydration is completely stopped.
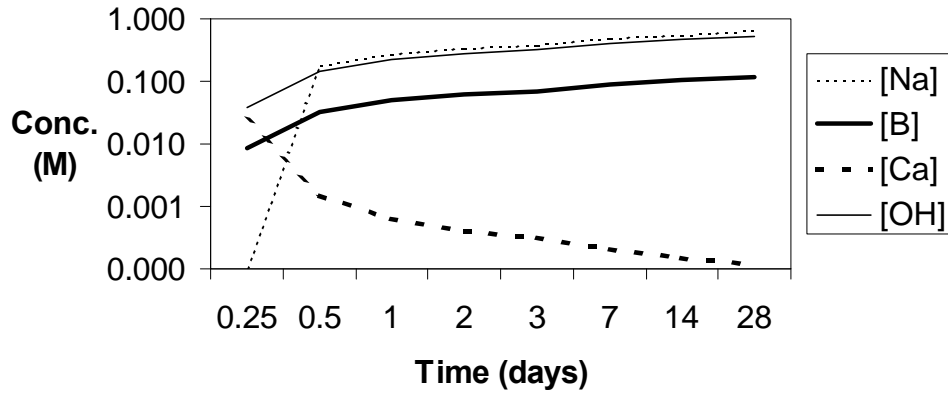
Figure 5.9. Pore water concentrations during hydration: ([Na$^+$] ([Na]), [B(OH)$_4^-$] ([B]), [Ca^{2+}] ([Ca]) and [OH$^-$] ([OH]).

Based on the assumption that the thickness of a coating layer has the order of magnitude of a monolayer, is impermeable for water transport and is evenly distributed over the cement surface concentrations were computed at which complete coverage would take place resulting in a stop of hydration. When the cement surface is coated with a multilayer instead of the assumed monolayer, a smaller part of the total initial cement surface is coated. This is confirmed by experiments in which concentrations of boric acid were added that would correspond to the presence of a multilayer and hydration still continued.

5.5.3 Comparison with experiments

From experiments by Lieber and Richartz (1972) it is known that hydration can finally proceed, even when pollutant additions up to 1 % (mass of pollutant over mass of binder) are used. Assuming that the crystal layer thickness $d_{crystal}$ is equal to the unit cell size of the CBH$_6$ crystal (about $6 \cdot 10^{-10}$ m according to the database at "l'Ecole des mines de Paris"), this addition would correspond with 39 coating layers. According to Eq. (5.13), this corresponds with a completely coated surface and hydration would be stopped completely. From this observation it is assumed that the minimum precipitation layer thickness d_{layer} is build up from a number of crystal layers ($n_{crystal}$) with the size of one crystal unit of CBH$_6$ ($n_{crystal}$), so

$$d_{layer} = n_{crystal} \cdot d_{crystal} \tag{5.16}$$

The equilibria and coating mechanism described above were implemented in the cement hydration model. When concentrations are computed during cement hydration it is assumed there is an equilibrium at the end of every hydration cycle. All parameters were chosen according to the experimental conditions used by Lieber and Richartz (1972), who examined the effect of boric acid on setting properties and strength development of Portland cement. They used OPC with a SSA of 4080 [cm^2/g], a Na content of 0.92 in the cement clinker, a w/c ratio of 0.5 and borate concentrations of up to 1 % (g H$_3$BO$_3$ per g OPC). Preliminary

124

computations revealed that hydration could only proceed when the total number of coating layers was about 3. Therefore, $n_{crystal}$ was estimated as 13, so that the 1 % addition corresponded with 3 coating layers in average.

Before cement hydration starts, the total initial $[B(OH)_4^-]$ and m_{prp}^{layer} at $[Na^+] = 0$ is computed. A digital initial cement microstructure is generated and the cement particle surface is coated according to the probabilistic placement procedure. After performing this procedure, only the uncoated surface planes are initially available for dissolution and reaction.

After each hydration cycle, the α and actual porosity of the cement paste is given by the cement hydration computer model and all parameters of interest can be computed in the order, $[Na^+]$, $[B(OH)_4^-]$, m_{prp}^{sol} and m_{prp}^{layer}. According to this recomputed precipitated mass m_{prp}^{layer}, a corresponding removal of coating units from the cement particle surface is performed. This is done by randomly decreasing the number of coating units from surface planes that are coated by 1 or more coating units. This adjustment results in an increase in uncoated surface planes, making them available for dissolution in the following hydration cycles. H_3BO_3 additions of 1.0, 0.5, 0.2 and 0.1 % were used in the simulations and hydration was allowed to proceed to an equivalent hydration time of 28 days. Degrees of hydration were computed by CEMHYD3D and Powers' relation was used to compute the corresponding strength.
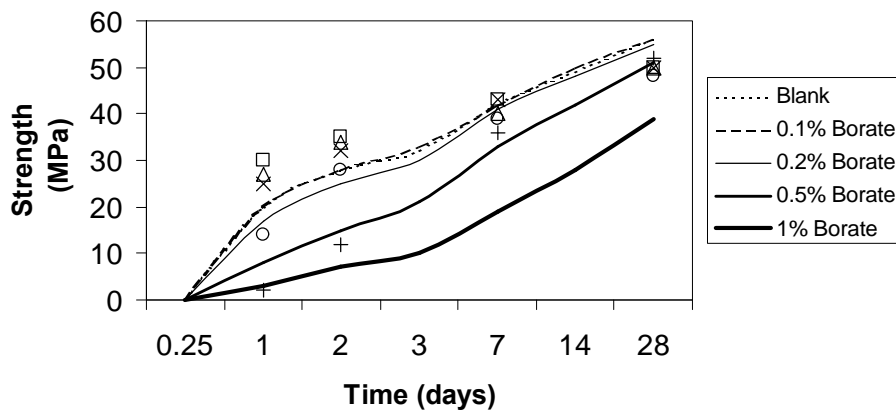
Figure 5.10. Strength development according to numerical simulations (lines) and experimental results (symbols) by Lieber and Richartz (1972).
($^{[]}$ = blank, Δ = 0.1%, x = 0.2%, o = 0.5% and + = 1% (m/m) borate added).

Fig. 5.10 shows the computed strengths (lines) and measured strengths (symbols) (Lieber and Richartz, 1972) of hardened OPC pastes with different H_3BO_3 additions. For the computed strength developments one can see a clear difference between the lower 0.1 and 0.2 % and the two higher 0.5 and 1.0 % pollutant additions. For the higher 1 and 0.5 % additions, initially degrees of hydration are significantly lower compared to the blank sample. After two or three days their hydration rates increase (as a result of redissolution of precipitate), while hydration rate of the blank sample is decreasing. At 28 days there was still precipitate and thus coated surface present in both cases. It can be expected that, while hydration continues, all remaining

precipitate will redissolve and final degree of hydration will be comparable to the blank sample. For the two lower additions 0.2 and 0.1 %, the initial coating percentages were less than 50 %, which results in a much quicker initial hydration rate and redissolution of precipitate compared to the other polluted samples. This results in strengths that are comparable to the blank sample.

The trends found in the simulations agree qualitatively with the experimental strengths measured by Lieber and Richartz (1972). For the 0.5 % (m/m) and 1.0 % (m/m) H_3BO_3 additions, both measured strengths are decreased at ages less than 3 days, but approach blank values after 28 days. The 0.1 and 0.2 % additions showed equal strength development compared to the blank sample. Thus, computed strength development agrees qualitatively with experimental results.

5.6 Practical solutions in waste treatment

Conner (1990) describes many solutions for treating all sorts of waste streams and specific contaminants are presented. Methods can be categorised in physical containment and chemical containment. The use of cement gives both physical containment (hardened cement paste is a solid, dense material in which diffusion is minimised) and chemical containment (the pore water composition, e.g. its high internal pH and the presence of dissolved silicates and calcium, results in binding of contaminants).

Physical containment by a hardened cement paste is obtained when high hydration rate is reached and porosity is low. A dense microstructure can be obtained by using silica fume. Optimising the structure of immobilisate will be treated in the next chapter (see Chapter 6).

In case of metals, pH regulation is the most straightforward method for binding. Conner (1990) gives solubility curves as a function of pH for several metals. Most metals are slightly soluble in cement systems, while others (like chromium and copper) show amphoteric behaviour, which means that their solubility is high at both low and high pH. At high pH such compounds will form soluble hydroxide anions.

In Chapter 3 it was shown that pH strongly depends on alkali content of cement and additions such as fly ash. This implies that varying alkali content in cement or the use of fly ash containing alkalis may offer possibilities of adjusting pH in pore water.

The negative effects of precipitation can be overcome by using high PSD cement. A higher cement surface implies less dense coating layers.

A second parameter is redox potential of the pore water. The solubility of compounds, especially metals, also varies with redox potential. In potential-pH equilibrium diagrams, presented in (Pourbaix, 1966), the presence of solids and ions of one metal is given as a function of both pH and redox potential (E(V)). Glasser (1993) presents the location of cementitious environments in such diagrams for cement and BFS cement. The pH is 12.5-13.0 in an OPC system and the potential is about 0 to 0.3 V, so light oxidising. In case of a BFS cement pH is between 11.5-12.5.and the potential is reducing: -0.3 to –0.4 V. This different environment may improve binding of specific contaminants.

To promote precipitation of specific contaminants, many additions are proposed (Conner, 1990). One of these additions is sulphur (S^{2-}), because metal sulphides generally have a solubility that is orders of magnitude lower compared with the hydroxide. In practice, a solution of Na_2S is added to the waste, before binders are added.

126

In general cement is a good binder for waste streams containing metals and less results are presented for waste containing high amounts of salts (e.g. sulphates and chlorides, which will form high amounts of ettringite and Friedel's salt respectively) or organics (e.g. oil). Salts are washed out before binders are added (Mulder, 1996). Organics are better bound by clays or zeolites and activated carbon (Conner, 1990).

Another addition commonly used in combination with cement is waterglas (Conner, 1990). Waterglas is a 35-40 % m/m solution of polymeric and colloidal sodium silicates. In commercial products the type number (e.g. type 3.3) refers to the mass ratio SiO_2/Na_2O in the solution. Originally it was used as fixation medium in combination with OPC to quickly thicken waste streams containing more than 80 % (m/m) water. From this practice it was found that waterglas was able to overcome the negative effects heavy metals and fine particle or oily contaminants had on hardening. The dissolved silicates are able to bind metal ions before they can precipitate and they keep oil and organics in suspension.

The dissolved silicates form a gel by a quick reaction with metal and calcium ions in solution (Conner, 1990). A 3D cross-linked gel structure is formed in which high amounts of water are bound. The formation of this gel is critical. When concentrations of metal ions are too high, a solid precipitate will form instead of a gel. When concentrations are too low, no gel will form at all. The gel formation and suspension processes must have finished in a few minutes after which cement hydration can start. Calcium ions released by cement will initially be consumed by the silicates from waterglas and have preference over formation of C-S-H and CH. When all soluble silicates are consumed, these hydration products will start to form. When the amount of waterglas is too high, cement hydration may never start.

5.7 Conclusions

Precipitation of compounds onto unhydrated cement particles has been studied and modelled. Two methods are presented to do so. The coating fraction method is based on covering a fraction of cement surface. The coating packages method was based on covering cement particle surface by volume packages of precipitate. Both methods were implemented in the NIST cement hydration model CEMHYD3D and the model made it possible to study coating effects on hardening. Preliminary computations show that it is possible to simulate the initial presence of a coating compound by making part of digital surface unavailable for dissolution before starting simulation of hydration. More than 90 % of the surface had to be coated before any significant decrease in hydration could be observed.

From the modelling results it was clear that the finer cement (higher PSD) requires higher contaminant concentrations and higher coating fractions for an equal reduction in degree of hydration. Its higher specific surface area resulted in less interference from the simulated presence of precipitated compounds on the initial cement particle surface compared to the coarser cement. This difference was found both when equal percentages of surface were coated and when equal contaminant concentrations were compared. There are two factors that can explain these results. First the amount of source compound required to coat some percentage of the cement surface is directly proportional to the specific surface area. Secondly, a higher SSA results in a quick and early removal of cement parts creating new and free dissolution possibilities for coated pixels.

Based on chemical equilibria of calcium borates in the presence of alkalis, quantities of precipitates were computed. It is shown that depending on the degree of hydration and related alkali release, calcium salts will precipitate and redissolve. In order to model this using CEMHYD3D an advanced coating routine was developed based on precipitation of packages of precipitated compound, which randomly precipitate on the initial surface and which may redissolve when pore water concentrations change during hydration. Modelling results were compared with experimental data of calcium borates. This yielded good qualitative agreement. In other words, using CEMHYD3D it was possible to predict when a concentration of a contaminant would lead to significant retardation.

An important unknown in the computations is the number of crystal layers per coating layer. This value was assumed to be equal to 13 in case of calcium borates, but this should be validated experimentally using surface analysis techniques. This number is an important parameter that is required for relating used contaminant concentrations and layer thicknesses initially present on the cement surface. The approach presented here can also be used to describe the retarding effects of other contaminants, e.g. Cd and Zn.

Chapter 6

Leaching[*]

6.1 Introduction

Portland cement can be combined with wastes to prevent leaching of species such as heavy metals into the environment. This technique is referred to as immobilisation or stabilisation/solidification (S/S). The ability of cement with respect to fixing hazardous components and prevention of leaching lies in both the physical and chemical properties of the hydrated cement paste (hcp). In leaching tests, cement specimens are subjected to acidified water for prescribed time periods after which metal concentrations in the leachant are measured. In the U.S. the TCLP (1985) and ANS/ANSI 16.1 (1986) prescribe the execution of such tests, whereas in The Netherlands NEN 7343 (1995) and NEN 7345 (1995) have been introduced as regulatory tests (see Chapter 7). The results of these tests determine whether the building material (e.g. an immobilisate), represented by the test sample, is applicable. If the material is applicable, the leaching results also determine the isolation measures to be taken in that case. This implies that the leaching results strongly determine the application scope of the material including that of cement solidified waste materials. To obtain an application scope as wide as possible, a cement/waste mixture has to be designed to minimise leaching of contaminants. In order to make such an optimisation possible, a model is required that relates the composition of hydrated cement paste to leaching properties. Such a model can be used to predict leaching properties of solidified waste materials and minimise this at forehand taking into account the design of the cement/waste mixture. This will result in an effective containment of hazardous contaminants. For such a type of model the following is required:

- A model that describes the leaching process in a hcp.
- The relation between composition of the hcp and its leaching properties.

In the past efforts has been made to model the leaching from immobilisates and predicting leaching test results. Godbee and Joy (1974) used a semi-infinite medium bulk diffusion model and obtained an expression for the leaching from monoliths. Based on the same bulk diffusion model, Brouwers (1997) derived an expression for the leaching from granular materials. Bulk diffusion model however do not account for the leachant pH nor the observed decomposition of the hcp during exposure to an acidic environment (Fattuhi and Hudges, 1988, Cheng, 1991). During this process the portlandite present in the hcp dissolves. This results in the presence of an unaltered shrinking core and a moving leached shell in which the CH is removed (Cheng et al., 1991, 1992). Cheng and Bishop (1992) found that in the leached

---

[*] The main part of this chapter has been published in:
R.J. van Eijk and H.J.H. Brouwers (1998), Study of the relation between hydrated portland cement composition and leaching resistance, Cement and Concrete Research, Vol. 28 , p. 815 – 828.

shell stabilised metals were removed while metal concentrations in the core were still unchanged. Hinsenveld and Bishop (1994) presented a shrinking core model that describes the transport of species by diffusion through this leached shell.

The presence of CH in the hcp is of major importance for the leaching. First, this component acts as acid buffer for the acidified water that enters the hcp and releases the contaminants. On the other hand, after dissolution the removed CH generates extra porosity facilitating transport of species by diffusion through the leached shell and resulting in an increasing progress of the dissolution front in the hcp.

The composition of hardened cement paste can be described in terms of volume fractions in the microstructure, e.g. the volume fractions of water (porosity), CH and C-S-H). These fractions are given by CEMHYD3D. On the other hand these volume fractions can be computed directly using simplified hydration equations. In that case w/c ratio and degree of hydration are required and have to be known or estimated at forehand. Such equations will be used in this chapter to obtain the relevant volume fractions.

In this chapter the hcp phase composition computed using simplified hydration equations will be coupled to a leaching model to predict leaching rates as a function of hcp composition. In section 6.2 the relation between composition of hcp and leaching will be discussed and described by equations. In section 6.3 these equations will be used to determine which hydration conditions will result in minimal leaching. In section 6.4 theoretical predictions will be compared with experimental leaching results. In section 6.5 the effect of the addition of pozzolanic additions on leaching will be discussed. Finally, in section 6.6 conclusions will be given.

6.2 The relation between hcp composition and leaching

Following the shrinking core model the cumulative amount leached per unit exposed surface area can be computed as follows (Hinsenveld and Bishop, 19994, Baker and Bishop, 1997):

$$CAL(t) = \sqrt{\frac{2 \cdot D_e \cdot [Me]_0^2 \cdot f_{mob}^2 \cdot [H^+]}{ANC}} \cdot \sqrt{t} \; , \qquad (6.1)$$

$CAL(t)$ = cumulative amount leached contaminant per unit exposed surface area $[mole/m^2]$,
D_e = effective diffusion coefficient $[m^2/s]$,
$[Me]_o$ = initial metal concentration in sample $[mole/m^3]$,
f_{mob} = mobile fraction of metal,
$[H^+]$ = H^+ concentration in leachant $[mole/m^3]$,
ANC = acid neutralisation (or buffering) capacity $[mole/m^3]$,
t = time $[s]$.

As can be seen from Eq. (6.1) the release rate depends both on the effective diffusion coefficient of the contaminant species in the leached shell and the acid buffering capacity of the cement specimen.

Earlier versions of the cement hydration model (Bentz and Garboczi, 1991) were based on the hydration of C_3S only and the corresponding volume stoichiometries of this reaction as determined by Young and Hansen (1987). Many studies revealed this hydration to be representative for the hydration of OPC (Ordinary Portland Cement). Therefore, in this chapter, cement will be represented by C_3S only.

In the present analysis it is assumed that the acid buffering capacity of cement is directly related to the amount of free calcium present in cement. This calcium originates from both the CH and cement hydrate (C-S-H). In a leached shell CH is considered completely dissolved and contributes directly to the ANC, where each mole of CH directly contributes 1 mole of Ca^{2+}.

C-S-H also contributes to the ANC, but diffusion of calcium from C-S-H is less complete and much slower than dissolution of CH (Revertegate et al., 1992, Carde et al., 1996, Faucon et al., 1996. Buil et al., 1992). Revertegate et al. (1992) performed experiments in which OPC cement samples (w/c ratio 0.37) were immersed in water at different pH values. After certain periods the samples were analysed: the total calcium content was determined by XRF, while CH was analysed by thermogravimetry. In this way they were able to separate the leaching of calcium from CH and C-S-H phases. At pH 4.6, all CH dissolved and 68 % of the C-S-H calcium was dissolved. This agrees fairly well with results of Carde et al. (1996) who measured calcium profiles of cement samples with and without CH after chemical attack by ammonium nitrate. They observed that the C-S-H phase had a linear decalcification profile from the surface of the sample to the end of the degraded zone, while decalcification of the CH phase in this zone was complete. For the samples without CH they found a 50 % decalcification of the C-S-H in the degraded zone. Considering these experiments an average decalcification value of 0.6 for the C-S-H will be used in this analysis.

The composition of C-S-H in a saturated cement paste was found to be $C_{1.7}SH_4$ (Young and Hansen, 1987). This means that 1 mole of C-S-H can release 1.7 mole Ca^{2+}. Using the given molar volumes of $33.1 \cdot 10^{-3}$ l/mole and $108 \cdot 10^{-3}$ l/mole for CH and C-S-H, respectively (Bentz, 1997), and the fact that every Ca^{2+} ion is capable of consuming two H^+ ions, the equation for the ANC finally takes the following form:

$$ANC = 2 \cdot \frac{\varphi_{CH}}{33.1 \cdot 10^{-3} \left[\frac{l}{mole}\right]} + 2 \cdot 0.6 \cdot 1.7 \cdot \frac{\varphi_{CSH}}{108 \cdot 10^{-3} \left[\frac{l}{mole}\right]} =$$

$$\left(60.4 \cdot \varphi_{CH} + 18.9 \cdot \varphi_{CSH}\right)\left[\frac{mole}{l}\right]$$

(6.2)

φ_{CH} = CH volume fraction in hcp
φ_{CSH} = C-S-H volume fraction in hcp

Next, the effective diffusion coefficient of H^+ appearing in Eq. (6.1) is related to the porosity of the leached shell. Garboczi and Bentz (1992) derived an equation in which the relative diffusion coefficient of a species in a hcp is related to the porosity in the hcp microstructure as follows:

$$\frac{D_e}{D_{H+}} = 0.001 + 0.07\varphi_p^2 + H(\varphi_p - 0.18) \cdot 1.8 \cdot (\varphi_p - 0.18)^2, \tag{6.3}$$

where

φ_p = porosity volume fraction in hcp
$H(x) = 0$ when $x \leq 0$,
$H(x) = 1$ when $x > 0$,
D_{H+} = molecular diffusion coefficient H^+ ion

The reciprocal of the left-hand side of Eq. (6.3) is also referred to as MacMullin number (Kyi and Batchelor, 1994) which depends on the structure of the cement matrix only, whereas $H(x)$ is the Heaviside function. The value of 0.18 is called the percolation threshold (Bentz and Garboczi, 1992). It is the volume fraction at which porosity is connected throughout the microstructure. When porosity is connected, pathways are available for diffusion and leaching is increased. On the contrary, when porosity is not percolated, but consists of isolated fractions throughout the microstructure, such continuous pathways do not occur, because they are blocked by the presence of other phases.

Eq. (6.3) holds for a standard unleached hcp. During leaching, however, CH in the sample is dissolved, resulting in extra porosity. The total porosity in a leached sample, denoted φ_t, therefore exists of both initial (water) porosity φ_p, and a porosity fraction originating from the CH fraction φ_{CH} that was present before leaching:

$$\varphi_{pal} = \varphi_p + \varphi_{CH}, \tag{6.4}$$

where

φ_{pal} = "porosity after leaching" volume fraction in hcp

Unfortunately, Eq. (6.3) does not hold because the increase in diffusivity as a result of increasing porosity during leaching is stronger than the decrease in diffusivity as a result of decreasing porosity during hydration (Bentz and Garboczi, 1992, Snyder and Clifton, 1995). This means that for a certain porosity fraction the diffusivity in a leached sample is higher than it would be for the same porosity fraction in the unleached form. Thus, diffusivity during leaching cannot be simply computed by substituting φ_{pal} into Eq. (6.3). Snyder and Clifton (1995) developed equations that take this effect into account. They defined the following functions ϑ_p and ϑ_{pal} as the results of substituting φ_p and φ_{pal} respectively into Eq. (6.3):

$$\vartheta_p = 0.001 + 0.07\varphi_p^2 + H(\varphi_p - 0.18) \cdot 1.8 \cdot (\varphi_p - 0.18)^2 \tag{6.5}$$

$$\vartheta_{pal} = 0.001 + 0.07\varphi_{pal}^2 + H(\varphi_{pal} - 0.16) \cdot 1.8 \cdot (\varphi_{pal} - 0.16)^2 \tag{6.6}$$

132

Using these expressions the relative diffusion coefficient in a leached sample was computed as follows:

$$\frac{D_e}{D_{H+}} = 2\vartheta_{pal} - \vartheta_p \tag{6.7}$$

As indicated by Eq. (6.6), during leaching a percolation threshold of 0.16 is used instead of 0.18 (Bentz and Garboczi, 1992). Therefore this value should be used for computing ϑ_{pal} for a leached sample while 0.18 is appropriate for computing ϑ_p of the original sample. Using these two different percolation thresholds the relative diffusion coefficient can now be computed according to Eq. (6.7). The first term of the final equation however should be a cut-off value in case both φ_p and φ_{pal} tend to zero. A value of 0.001 is considered an appropriate mean value for samples that still contain a certain amount of CH. However, in a leached shell that consists purely of C-S-H and does not contain CH anymore, a cut-off value of 0.0025 should be used, which is the relative diffusion coefficient for the C-S-H phase. Combining all equations now yields:

$$\frac{D_e}{D_{H+}} = 0.0025 - 0.07\varphi_p^2 - H(\varphi_p - 0.18) \cdot 1.8 \cdot (\varphi_p - 0.18)^2$$
$$+ 0.14\varphi_{pal}^2 + H(\varphi_{pal} - 0.16) \cdot 3.6 \cdot (\varphi_{pal} - 0.16)^2 \tag{6.8}$$

As can be concluded from the previous analysis, the φ_{CH} fraction has two opposite effects on the metal release rate during acid attack, namely:

1. A positive effect by increasing acid buffering capacity.
2. A negative effect by increasing porosity in the leached shell, thereby increasing the effective diffusion coefficient.

This means that the cement composition can be optimised by varying this variable to obtain an optimal resistance against acid attack. To this end, using Eq. (6.2) and (6.8), Eq. (6.1) is rewritten as:

$$\frac{CAL(t)}{\sqrt{2 \cdot [Me]_0^2 \cdot f_{mob}^2 \cdot [H^+] \cdot D_{H+}}} = f(\varphi_{CH}, \varphi_p, \varphi_{CSH}) =$$

$$\sqrt{\frac{0.0025 - 0.07\varphi_p^2 - H(\varphi_p - 0.18) \cdot 1.8 \cdot (\varphi_p - 0.18)^2 + 0.14\varphi_{pal}^2 + H(\varphi_{pal} - 0.16) \cdot 3.6 \cdot (\varphi_{pal} - 0.16)^2}{60.4 \cdot \varphi_{CH} + 18.9 \cdot \varphi_{CSH}}} \tag{6.9}$$

Note that the right-hand side solely depends on the cement composition, while the left-hand side contains all contaminant properties.

(Bentz, 1997) included saturated curing and chemical shrinkage into the CEMHYD3D model and the following stoichiometries were found to give the best model results:

Molar:

$$C_3S + 5.3\ H \rightarrow C_{1.7}SH_4 + 1.3\ CH \tag{6.10}$$

Volume (solids only):

$$C_3S \rightarrow 1.52\ C\text{-}S\text{-}H + 0.61\ CH \tag{6.11}$$

Assuming that the hydration reaction given by Eq. (6.10) is representative for the hydration of OPC and assuming that no silica is present the volume fractions of C-S-H and CH in the hcp are directly related to each other as follows:

$$\varphi_{CSH} = 2.5 \cdot \varphi_{CH} \tag{6.12}$$

and Eq. (6.2) then becomes:

$$ANC = 107.6 \varphi_{CH} \left[\frac{mole}{l} \right] \tag{6.13}$$

Inserting Eq. (6.12) into Eq. (6.9), one obtains a "leaching resistance" function $f(\varphi_{CH}, \varphi_p)$ that describes leaching rate as a function of material properties:

$$\frac{CAL(t)}{\sqrt{2 \cdot [Me]_0^2 \cdot f_{mob}^2 \cdot [H^+] \cdot D_{H+}}} = f(\varphi_{CH}, \varphi_p) = \tag{6.14}$$

$$\sqrt{\frac{0.0025 - 0.07\varphi_p^2 - H(\varphi_p - 0.18) \cdot 1.8 \cdot (\varphi_p - 0.18)^2 + 0.14\varphi_{pal}^2 + H(\varphi_{pal} - 0.16) \cdot 3.6 \cdot (\varphi_{pal} - 0.16)^2}{107.6 \cdot \varphi_{CH}}}$$

In Fig. 6.1 this "leaching resistance" function $f(\varphi_{CH}, \varphi_p)$ is drawn versus φ_{CH} for various values of φ_p. One can see from Fig. 6.1 that for each φ_p, a φ_{CH} exists for which $f(\varphi_{CH}, \varphi_p)$ is minimal. Fig. 6.1 also shows that the positive dependency on φ_{CH} of the leaching rate f is more pronounced at low water porosity, and the negative dependency on φ_{CH} is more pronounced at high water porosity. As expected, for every φ_{CH}, f is lowest when φ_p is lowest.
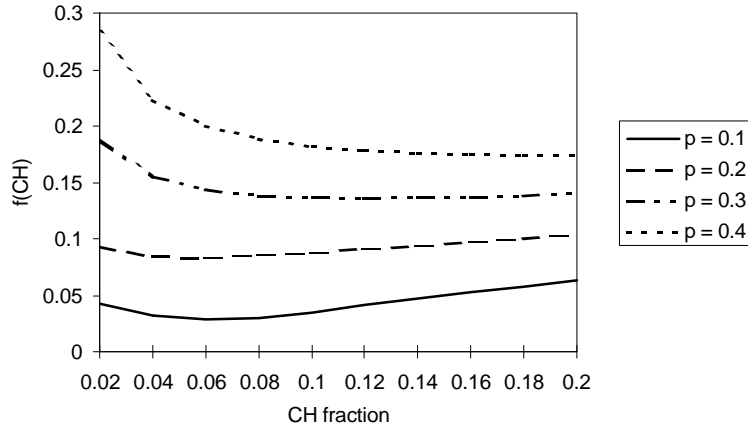
Figure 6.1. Leaching resistance function f(φ_{CH}) (f(CH)) plotted against φ_{CH} (CH fraction) for various φ_p (p = 0.1, 0.2, 0.3 and 0.4) .

The φ_{CH} for which f(φ_{CH}, φ_p) is minimal, denoted as $\varphi_{CH\,min}$, follows from differentiating the right-hand side of Eq. (6.14) with respect to φ_{CH} :

$$\frac{df(\varphi_{CH},\varphi_p)}{d\varphi_{CH}} = \frac{1}{2f} \cdot \frac{0.14\varphi_{CH}^2 + H(\varphi_p - 0.18) \cdot 1.8 \cdot (\varphi_p - 0.18)^2 - 0.0025 - 0.07\varphi_p^2}{\varphi_{CH}^2}$$
$$+ \frac{1}{2f} \cdot \frac{H(\varphi_{pal} - 0.16) \cdot 3.6 \cdot (\varphi_{CH}^2 - \varphi_p^2 + 0.32\varphi_p - (0.16)^2)}{\varphi_{CH}^2} \qquad (6.15)$$

Setting the right-hand side equal to zero yields:

$$\varphi_{CH} = \sqrt{0.5\varphi_p^2 + 0.0178} \qquad\qquad \text{for } \varphi_p < 0.16,\ \varphi_{pal} < 0.16. \qquad (6.16)$$

$$\varphi_{CH} = \sqrt{0.98\varphi_p^2 - 0.308\varphi_p + 0.025} \qquad \text{for } \varphi_p < 0.18,\ \varphi_{pal} > 0.16 \qquad (6.17)$$

$$\varphi_{CH} = \sqrt{0.5\varphi_p^2 - 0.135\varphi_p + 0.0097} \qquad \text{for } \varphi_p > 0.18,\ \varphi_{pal} > 0.18 \qquad (6.18)$$

In Fig. 6.2 this $\varphi_{CH\,min}$ is plotted for different values of φ_p . In Fig. 6.3 the corresponding f(φ_{pal}) minima, denoted as f()$_{min}$ are plotted versus φ_p.

The shape of Fig. 6.2 again shows the dual effect of φ_{CH}. At high water porosity, when water porosity increases, φ_{CH} must also increase to keep f() minimal. At low water porosity however, φ_{CH} must decrease as in that case φ_{CH} also has an increasing effect on f(). From Fig. 6.3 the major effect of φ_p on f()$_{min}$ is illustrated. From Figs. 6.2 and 6.3 one can conclude that f(φ_{CH},φ_p) is lowest if φ_p equals zero and φ_{CH} is about 0.13.
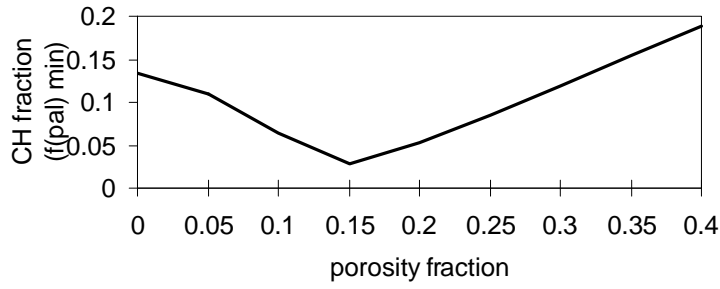
Figure 6.2. φ_{CH} for which leaching resistance function $f(\varphi_{pal})$ is minimal (CH fraction (f(pal) min)) plotted for various values of φ_p (porosity fraction).
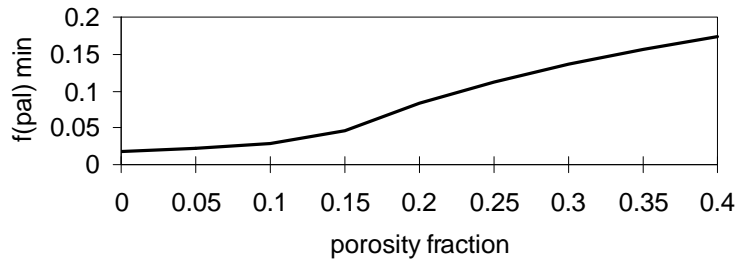
Figure 6.3. Minimum leaching resistance function $f(\varphi_{pal})$ (f(pal) min) plotted against φ_p (porosity fraction).

6.3 Mixture composition and leaching

In the previous section φ_{CH} and φ_p have been treated as independent properties. These properties can, however, be related using the equation for C$_3$S hydration used by Bentz (1997), which was given in Eq. (6.11). Using a typical specific gravity of 3.2 kg/dm^3 for cement and assuming that all cement consists of C$_3$S only, the volume fraction of reacted C$_3$S in the hcp, denoted $\varphi_{C_3S}^r$ is computed as follows:

$$\varphi_{C_3S}^r = \frac{0.313\alpha}{w/c + 0.313} \tag{6.19}$$

$\varphi_{C_3S}^r$ = volume fraction of reacted C$_3$S = $\varphi_{C_3S}^0 - \varphi_{C_3S}$

136

Using Eq. (6.19), and the volume stoichiometry (see Eq. (6.11)), all other relevant volume fractions in the hcp can be computed from the amount of reacted C_3S as follows:

$$\varphi_{CH} = 0.61 \cdot \varphi^r_{C_3S} = \frac{0.191\alpha}{w/c + 0.313},$$

(6.20)

$$\varphi_p = 1 - \varphi_{C_3S} - \varphi_{CSH} - \varphi_{CH} = \frac{w/c - 0.410\alpha}{w/c + 0.313},$$

(6.21)

and hence,

$$\varphi_{lp} = \varphi_p + \varphi_{CH} = \frac{w/c - 0.219\alpha}{w/c + 0.313},$$

(6.22)

Both fractions φ_{CH} and φ_p can be substituted into Eq. (6.14), yielding f() as a function of w/c and α. In Fig. 6.4 f(w/c) is depicted for various α, namely α = 0.30, 0.60, 0.90 and 1. Considering that $\alpha \leq$ w/c ratio/ 0.41, for every w/c < 0.41 hydration cannot be attained completely (α = 1). Hence, in this case there is a maximum achievable α, depicted as α_{max}. For w/c > 0.41, hydration can proceed until α_{max} = 1. The function f(α_{max}) is also drawn in Fig. 6.4.
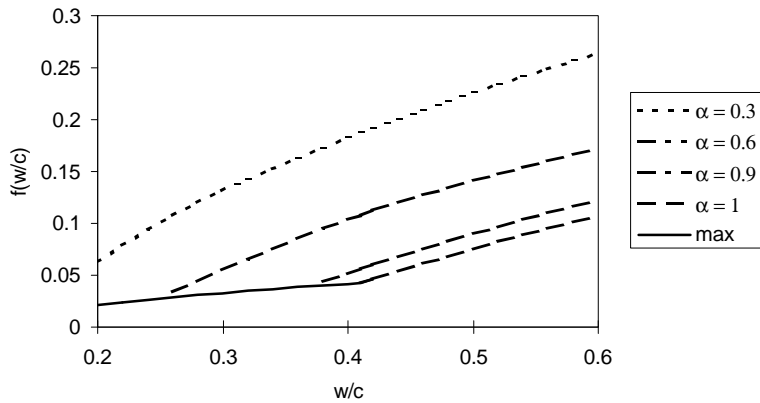
Figure 6.4. Leaching resistance function f(w/c) plotted against w/c for various α and for maximal achievable α at specific w/c ratio (max).

As both time and hydration proceed, for each w/c ratio the function f decreases till the lines corresponding to α_{max} or α = 1 are attained. One can readily see that for practical purposes w/c ratio should be as low as possible. At low w/c ratio however, the differences in lowest achievable f() values are very small with f ranging from about 0.025 to 0.05 for w/c ratio ranging from 0.2 to 0.41, respectively. Therefore, using a w/c ratio < 0.41 will be of no use in practice as it does not result in a substantial decrease in f anymore. Moreover, unhydrated cement will then remain, being unused for binding and immobilisation.

137
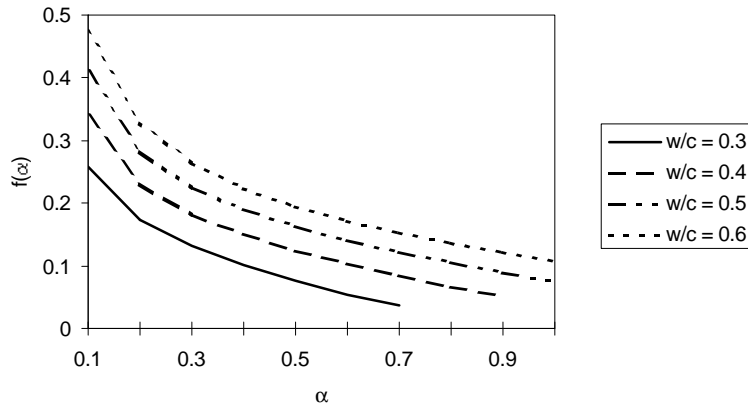
Figure 6.5. Leaching resistance function f(α) plotted against α for various w/c.

In Fig. 6.5 f(α) is depicted for various w/c ratio, namely w/c = 0.3, 0.4, 0.5 and 0.6 for α = 0 till α = α_{max}. From this figure it is clear that f(α) decreases during hydration. One may also conclude from Fig. 6.5 that using a higher w/c ratio can only result in a lower leaching rate f() when degree of hydration is significantly higher. At complete hydration, a higher w/c ratio will always result in a higher leaching rate.

6.4 Comparison with experiments

In the previous section a theoretical model has been presented for the leaching from hydrated cement pastes. In this section the theoretical predictions are compared with some experimental data obtained from the literature.

Zamorani and Serrini (1992) performed leaching experiments on Cs^+ -ions immobilised in cement samples at different w/c values. Ordinary Portland cement was used and all samples were cured at 60 ^{o}C, 98% R.H. for 11 days. The samples were leached in water at a surface-to-liquid volume of 0.1/cm. It was found that the cumulative fraction leached (CFR) depends on both $\sqrt{t}$, which is in qualitative agreement with Eq. (6.1) and the w/c ratio. $[Me]_0$, f_{mob}, $[H^+]$ and D_{H^+} can be assumed constant for each of their experiments and were calibrated using their results for w/c = 0.4. The CFR can now be related to f() via:

$$\frac{CFR}{CFR_{w/c=0.4}} = \frac{f(w/c)}{f(w/c=0.4)}$$

(6.23)

Densities and total pore volumes of all samples are given by the reference in [g/cm^3] and [cm^3/g], respectively. To obtain the water porosity fractions φ_p for each sample the given total pore volumes in [cm^3/g] were multiplied with the measured and reported sample densities. These resulting water porosity fractions were then used to estimate the degree of hydration α of every sample using the relation between these two as given in Eq. (6.19). Using this estimated degree of hydration α, f() was computed for each w/c ratio used in the experiments.

Table 6.1. Computed leaching resistance f() ratios compared to CFR ratios (Zamorano and Serrini, 1992).

w/c	Estimated α	CFR/CFR$_{w/c = 0.4}$	f()/f(w/c = 0.4)
0.35	0.49	0.89	0.89
0.4	0.53	1.00	1.00
0.45	0.52	1.24	1.19
0.5	0.65	1.36	1.25

In Table 6.1 the computed f() ratios are compared with CFR ratios for various w/c ratio. One can readily conclude that the agreement between experiments and the here presented model predictions are good, especially when one considers the simplifications invoked in the present analysis. This implies that the combination of leaching model and cement composition, resulting in the leaching function f(), adequately describes the leaching process as a function of hcp composition.

6.5 Effects of pozzolanic additions on leaching

Silica fume (SF) is a fine powder (diameter < 1 μm) that mainly consists of amorphous SiO_2 (S). Because of its high internal surface area and composition it is very reactivity and can be used as a pozzolanic addition in binder mixtures. Silica fume, i.e. S, reacts with the CH released during hydration and forms C-S-H. A typical density of 2.2 kg/dm^3 for amorphous S will be used. In accordance with the work of Bentz and Garboczi (1992), the following stoichiometries will be used to describe the pozzolanic reaction, although this stoichiometry was changed in later work (Bentz et al., 1998).

Molar:
$$S + 1.7\ CH + 2.3\ H \rightarrow C_{1.7}SH_{4.0} \tag{6.24}$$

Volume (solids only):
$$S + 2.08\ CH \rightarrow 4\ C\text{-}S\text{-}H \tag{6.25}$$

Note that as a result of this reaction, water is consumed and the volume of solids increases (from 3.08 to 4). Therefore the presence of silica fume will lower the maximum achievable degree of hydration of the cement.

To compute volume fractions in the hcp as a function of degree of hydration, the initial volume fractions of the binders (here only C_3S and S) have to be computed first. The total initial binder volume fraction in the hcp is defined as follows:

$$\varphi_b^0 = \varphi_{C_3S}^0 + \varphi_S^0 \tag{6.26}$$

φ_b^0 = initial volume fraction of binders (cement and silica fume) in hcp

$\varphi_{C_3S}^0$ = initial volume fraction of C_3S in hcp

φ_S^0 = initial volume fraction of S in hcp

The initial volumes of binder phases (C₃S and S only) are simply related as follows:

$$V_b^0 = V_{C_3S}^0 + V_S^0$$
(6.27)

The initial volume fractions of C₃S and S in the total paste are related to the initial volume fraction of binder φ_b^0 by the initial volume fraction of silica fume in the *binder* as follows:

$$\varphi_{C_3S}^0 = (1 - \frac{V_{SF}^0}{V_b^0}) \cdot \varphi_b^0$$
(6.28)

$$\varphi_S^0 = \frac{V_{SF}^0}{V_b^0} \cdot \varphi_b^0$$
(6.29)

$\varphi_{C_3S}^0$ = initial volume fraction of C₃S in paste

φ_S^0 = initial volume fraction of S in paste

φ_b^0 = initial volume fraction of binders (C₃S + S) in paste

$\dfrac{V_{SF}^0}{V_b^0}$ = volume fraction of silica fume in binder

From the definition of the w/s ratio, it follows that:

$$\frac{w}{s} = \frac{m_w^0}{m_b^0} = \frac{m_w^0}{m_c^0 + m_{SF}^0} = \frac{1 \cdot (1 - \varphi_b^0)}{3.2 \cdot (1 - \frac{V_{SF}^0}{V_b^0}) \cdot \varphi_b^0 + 2.2 \cdot \frac{V_{SF}^0}{V_b^0} \cdot \varphi_b^0}$$
(6.30)

Rewriting Eq. (6.30) yields:

$$\varphi_b^0 = \frac{1}{(3.2 - \frac{V_{SF}^0}{V_b^0}) \cdot w/s + 1}$$
(6.31)

In common practice, the *mass* fraction of silica fume in the binder is used instead of the volume fraction. This binder mass fraction will be denoted as follows (see definition 2.4):

$$\beta_{SF} = \frac{m_{SF}^0}{m_b^0}$$
(6.32)

$$\beta_c = \frac{m_c^0}{m_b^0}$$
(6.33)

140

Using the relation

$$\beta_c = 1 - \beta_{SF} \tag{6.34}$$

mass and volume fractions of cement and silica fume can be related, using their densities (see also Eq. 2.8) as follows:

$$\frac{V_{SF}^0}{V_b^0} = \frac{V_{SF}^0}{V_c^0 + V_{SF}^0} = \frac{\beta_{SF}/\rho_{SF}}{\beta_c/\rho_c + \beta_{SF}/\rho_{SF}} \cdot \left(\frac{\rho_{SF} \cdot \rho_c}{\rho_{SF} \cdot \rho_c}\right) = \frac{\beta_{SF} \cdot \rho_c}{\beta_c \cdot \rho_{SF} + \beta_{SF} \cdot \rho_c}$$
$$= \frac{\beta_{SF} \cdot \rho_c}{(1 - \beta_{SF}) \cdot \rho_{SF} + \beta_{SF} \cdot \rho_c} \tag{6.35}$$

Filling in the densities yields the equation required to compute the volume fraction SF from the mass fraction SF as given in practice:

$$\frac{V_{SF}^0}{V_b^0} = \frac{3.2 \cdot \beta_{SF}}{2.2(1 - \beta_{SF}) + 3.2 \cdot \beta_{SF}}, \tag{6.36}$$

where 3.2 and 2.2 are typical densities in kg/dm^3 for cement and SF respectively. Substituting $\frac{V_{SF}^0}{V_b^0}$ and φ_b^0 in Eqs. (6.28) and (6.29) with Eqs. (6.31) and (6.35) yields equations for the initial volume fractions of the phases C$_3$S and S in the hcp as a function of binder composition (w/s and β_{SF}):

$$\varphi_{C_3S}^0 = \frac{1 - \beta_{SF}}{3.2 \cdot (w/s + 0.14\beta_{SF}) + 1} \tag{6.37}$$

$$\varphi_S^0 = \frac{1.45 \cdot \beta_{SF}}{3.2 \cdot (w/s + 0.14\beta_{SF}) + 1} \tag{6.38}$$

These equations for initial fractions are required for the computation of all other relevant volume fractions as a function of degree of hydration and the amount of reacted C$_3$S as defined in Eq. (6.39):

$$\varphi_{C_3S}^r = \alpha\varphi_{C_3S}^0 \tag{6.39}$$

During hydration of a cement/silica fume/water mixture, two situations should be considered (Bentz and Garboczi, 1992):

1. All CH produced is consumed by silica fume ($\varphi_{CH} = 0$)

All CH produced during hydration of the cement is consumed by silica fume, forming C-S-H. This implies that all reacted C_3S is converted into C-S-H only, no CH is left ($\varphi_{CH} = 0$) and some unreacted silica remains in the hcp.

From Eq. (6.11) follows that for every volume reacted unit of C_3S, 1.52 volume units of C-S-H and 0.61 volume units of CH are produced. Per volume of C_3S, 0.61 volumes of CH reacts with $2.08/0.61 = 0.293$ volumes of S. In that case $4 \cdot 0.293 = 1.173$ volumes of C-S-H are produced additional to the 1.52 volumes produced in the C_3S reaction, making the total 2.693 volumes of C-S-H produced per volume of reacted C_3S. Taking these numbers into account, all relevant volume fractions can now be computed as follows:

$$\varphi_{CSH} = 2.693 \cdot \varphi_{C_3S}^r = \frac{2.693 \cdot \alpha \cdot (1 - \beta_{SF})}{3.2 \cdot (w/s + 0.14 \cdot \beta_{SF}) + 1}, \tag{6.40}$$

$$\varphi_S = \varphi_S^0 - 0.293 \cdot \varphi_{C_3S}^r = \frac{1.45 \cdot \beta_{SF} - 0.293 \cdot \alpha \cdot (1 - \beta_{SF})}{3.2 \cdot (w/s + 0.14 \cdot \beta_{SF}) + 1} \tag{6.41}$$

and

$$\varphi_p = 1 - \varphi_{C_3S} - \varphi_{CSH} - \varphi_S = 1 - \frac{(1 + 1.755\alpha)(1 - \beta_{SF}) + 1.45\beta_{SF}}{3.2 \cdot (w/s + 0.14\beta_{SF}) + 1} \tag{6.42}$$

φ_S = S volume fraction in hcp

2. All silica fume has reacted with CH ($\mu_S = 0$)

More CH is produced during hydration than can be consumed by the initial amount of S. This situation occurs when the amount of CH produced is higher than the amount of CH consumed, in other words, when:

$$0.61(1 - \frac{V_{SF}^0}{V_b^0})\alpha > 2.08 \cdot \frac{V_{SF}^0}{V_b^0} \tag{6.43}$$

or

$$\beta_{SF} \le \frac{\alpha}{\alpha + 4.96} \tag{6.44}$$

where 0.61 is the amount of CH produced by one volume element of C_3S and 2.08 is the amount of CH consumed by one volume element of S (this value is referred to as the pozzolanic reactivity factor).

When the silica fume fraction fulfils condition given by Eq. (6.44), all initial silica fume has reacted with CH and produced C-S-H. For every volume of initial S, 4 volumes of C-S-H are produced and 2.08 volumes of CH are consumed.

142

Taking these values into account, all volume fractions of interest can be computed as follows:

$$\varphi_{CSH} = 1.52 \cdot \varphi_{C_3S}^r + 4 \cdot \varphi_S^0 = \frac{1.52\alpha(1-\beta_{SF}) + 6.67\beta_{SF}}{3.2 \cdot (w/s + 0.14\beta_{SF}) + 1} \qquad (6.45)$$

$$\varphi_{CH} = 0.61 \cdot \varphi_{C_3S}^r - 2.08 \cdot \varphi_S^0 = \frac{0.61\alpha(1-\beta_{SF}) - 3\beta_{SF}}{3.2 \cdot (w/s + 0.14\beta_{SF}) + 1}, \qquad (6.46)$$

and

$$\varphi_p = 1 - \varphi_{C_3S} - \varphi_{CSH} - \varphi_{CH} = 1 - \frac{(1+1.31\alpha)(1-\beta_{SF}) + 3.67\beta_{SF}}{3.2 \cdot (w/s + 0.14\beta_{SF}) + 1} \qquad (6.47)$$

In the presence of silica fume the amounts of C-S-H and CH are no longer related by Eq. (6.12). Therefore the simplified Eq. (6.13) for the ANC is not valid anymore and Eq. (6.2) should be used instead, in which φ_{C-S-H} and φ_{CH} are computed separately to obtain the ANC. Using the f() function from Eq. (6.9) and Eqs. (6.45)-(6.47) for all volume fractions, $f(\beta_{SF})$ can be computed for samples with silica fume. In Fig. 6.6 the function $f(\beta_{SF})$ is plotted for various w/s, namely 0.35, 0.40, 0.5. α was taken as 0.7, which means that, according to Eq. (6.44), when $\beta_{SF} > 0.12$, $\varphi_{CH} = 0$ and silica remains in the sample.

The amount of silica fume is optimal when f() is as low as possible, but it should be noted that also silica fume should be as low as possible, considering its high price. From Fig. 6.6 it can be seen that such optima exist. Silica replaces CH with C-S-H in a sample. Because calcium is more strongly bound in C-S-H compared to CH this calcium contributes less to the ANC (see also Eq. 6.2). In other words, the replacement of CH for C-S-H makes the calcium less available for buffering. As from the point where all CH is consumed, the addition of more silica still has a negative effect on the ANC because then it replaces cement and less C-S-H is formed during hydration. Low amounts of silica have a negative effect on total porosity during the leaching process, because less CH is leached out. However at the point where silica remains, higher amounts of silica only acts as inert filler, replacing the initial amount of cement and increasing the final water porosity. These effects explain the shapes of the plots in Fig. 6.6.

The minimum values in these plots correspond to the point where all CH is consumed because at that point both water- and total porosities are minimal. This optimum can therefore be determined straightforward using Eq. (6.44). In this case, when $\alpha = 0.7$, the silica fume mass fraction where $f(\beta_{SF})$ is minimal is $\beta_{SF} = 0.12$. From Fig. 6.6 one can also see that for w/s < 0.5 adding more than 8 % (m/m) silica fume is not effective anymore.
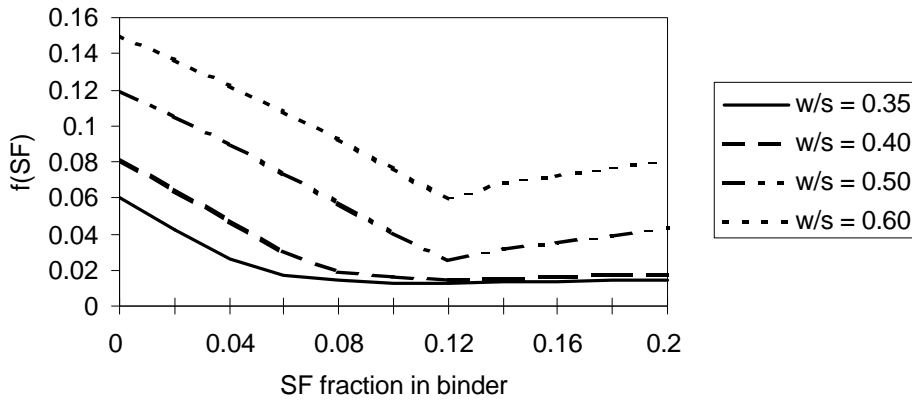
Figure 6.6. Leaching resistance function f(β_{SF}) (f(SF)) plotted against silica fume mass fraction β_{SF} (SF fraction in binder) for various w/s ($\alpha = 0.7$).

In Fig. 6.7 f(β_{SF}) is plotted for various α. The w/s was taken as 0.4. As can be seen from Fig. 6.7 low f(β_{SF}) values are only possible at high hydration rates and the minimum values are different for all considered α. The line $\alpha = 0.9$ ends at 8 % (m/m) silica fume because this degree of hydration is not achievable anymore for samples that contain more silica fume.
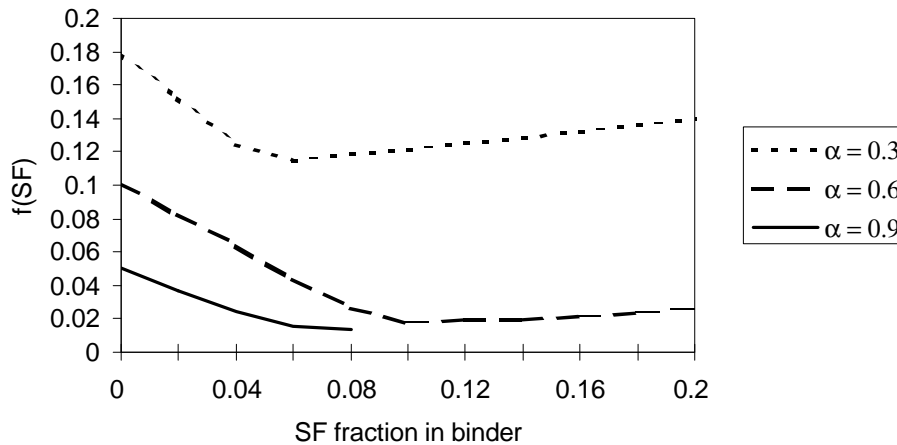
Figure 6.7. Leaching resistance function f(β_{SF}) (f(SF)) plotted against silica fume mass fraction β_{SF} (SF fraction in binder) for various α (w/s = 0.4).

From both figures it can be concluded that in general, for all w/s and α values used here, optimal silica fume contents in the binder vary between 8 and 10 % (m/m) when α ranges from 0.3 to 0.6, respectively. For low w/s or high degrees of hydration the addition of 8 % (m/m) silica fume would be the most appropriate in theory.

144

Fly ash is commonly used as an addition in waste stabilisation because of its pozzolanic properties and low price. The composition of fly ash varies greatly but the amount of SiO_2 is typically 50 %. Compared to the fine silica fume, fly ash has a higher particle size and was found to hydrate for only 50 % (Hooton, 1986). Considering these typical values this would result in a pozzolanic reactivity and corresponding CH reduction of about 25 % compared to silica fume. This CH reduction was observed in OPC containing 25 % (V/V) of fly ash (Hooton, 1986). Therefore a pozzolanic reactivity factor of 0.5 can be used for fly ash to account for both its lower amount of SiO_2 and its lower hydration rate compared to silica fume. Using a typical fly ash density of 2.2 kg/dm^3, the corresponding equations for fly ash can be derived in the same way as for silica fume, taking into account that one volume element of fly ash now consumes 0.5 CH instead of the 2.08 volume elements of CH that were consumed by pure S. The mass fraction fly ash based on mass of binder is defined as follows:

$$\beta_{FA} = \frac{m_{FA}^0}{m_b^0} \tag{6.48}$$

In case of remaining fly ash and $\varphi_{CH} = 0$, Eq. (6.40) can be used to calculate φ_{CSH} replacing β_{SF} by β_{FA}. Eqs. (6.49) and (6.50) should be used for φ_{FA} (unreacted pozzolanic fly ash) and φ_p.

1. All CH consumed by fly ash ($\varphi_{CH} = 0$)

$$\varphi_{FA} = \frac{1.45 \cdot \beta_{FA} - 1.22 \cdot \alpha \cdot (1 - \beta_{FA})}{3.2 \cdot (w/s + 0.14 \cdot \beta_{FA}) + 1} \tag{6.49}$$

$$\varphi_p = 1 - \frac{(1 + 0.828\alpha)(1 - \beta_{FA}) + 1.45\beta_{FA}}{3.2 \cdot (w/s + 0.14\beta_{FA}) + 1} \tag{6.50}$$

2. All fly ash has reacted with CH ($\varphi_{FA} = 0$).

In the case where all fly ash has reacted, Eqs. (6.51)-(6.53) should be used for φ_{CSH}, φ_{CH} and φ_p, respectively.

$$\varphi_{CSH} = \frac{1.52\alpha(1 - \beta_{FA}) + 1.67\beta_{FA}}{3.2 \cdot (w/s + 0.14\beta_{FA}) + 1} \tag{6.51}$$

$$\varphi_{CH} = \frac{0.61\alpha(1 - \beta_{FA}) - 0.725\beta_{FA}}{3.2 \cdot (w/s + 0.14\beta_{FA}) + 1}, \tag{6.52}$$

$$\varphi_p = 1 - \frac{(1 + 1.31\alpha)(1 - \beta_{FA}) + 0.945\beta_{FA}}{3.2 \cdot (w/s + 0.14\beta_{FA}) + 1} \tag{6.53}$$

Performing the same analysis as was performed in the case of silica fume, one can conclude that fly ash should be added in such an amount that all CH is consumed. Replacing the value of 2.08 for 0.5 in Eq. (6.43) results in Eq. (6.54), which is fulfilled when all CH is consumed by a certain amount of fly ash and can be used straightforward for the determination of the optimal amount of fly ash needed:

$$\beta_{FA}^{opt.} = \frac{\alpha}{\alpha + 1.24}$$
(6.54)

$\beta_{FA}^{opt.}$ = optimal fly ash mass fraction in binder

This means that for a typical degree of hydration $\alpha = 0.7$ the optimal amount of fly ash would be 36 mass % based on total mass of solids.

Note that for both the values of silica fume and fly ash as theoretically determined here, are indeed used and found effective in the field of waste immobilisation (Glasser, 1996).

6.6 Conclusions

Leaching of metals in a solidified cement sample as a result of an acid attack can be described by a shrinking core leaching model. Both the effective diffusion coefficient and the acid neutralisation capacity can be described in terms of hydrated cement paste volume fractions. Using the leaching model and a cement hydration model, it is possible to describe leaching rates as a function of cement paste composition with the help of a "leaching resistance" function f(). When the water porosity fraction is known a CH fraction can be computed at which leaching rates are minimal.

Because the water porosity only has a negative effect, it should always be as low as possible. Cement composition should therefore be optimised for the amount of CH. Best results are obtained when water porosity is 0 % and CH fraction is 13 %.

Leaching rates can also be determined as function of the w/c ratio and α, using a simplified cement hydration model that describes all phase fractions as a function of w/c and α. From this it follows that minimal leaching rates can only be obtained at very low w/c ratio. Furthermore, the results from the theoretical model presented here are in good agreement with the experimental data of Zamorani and Serrini (1992) (see Table 6.1).

To use all cement, additions such as silica fume or fly ash are needed. The optimal replacement fractions for these pozzolanic additions particularly depend on the expected degree of hydration α and less on the w/c ratio used. Optimal values of around 8 % (m/m) (silica fume) and 35 % (m/m) (fly ash) based on total mass of cement plus additions were computed. This is in close agreement with the additions that are used in (S/S) technology.

The theoretical concepts introduced here will contribute to the understanding of the relation between hcp composition and leaching resistance and its effects on durability of the solidified product. Moreover, in case of the application of non-standard OPC as solidifying agent, a similar analysis as executed here can be recommended and will help to find theoretical optima. The equations developed can be useful when designing a waste/cement mixture showing minimal leaching and a hence a good containment and immobilisation of contaminants.

Chapter 7

Constraints and possibilities in practice: institutional and commercial aspects

7.1 Introduction

Waste can be treated and converted into less harmful material using solidification/stabilisation (S/S) techniques. The producer of waste or an immobilisation facility has several options of treating a waste, e.g. washing, separating, S/S with cement or other binders, or thermal treatment (sintering). The purpose of this treatment is obtaining a solid product, the immobilisate that can be introduced as a secondary building material on the construction market.

A commonly applied method is mixing the waste with binders such as cement, fly ash or clay and thus creating a hardened product. In order to obtain a solidified product (the immobilisate) having the best possible technical and environmental properties it is necessary to take into account the properties of the waste stream and of the cementitious binders. In the previous chapters it was shown that this technical knowledge can be used to design optimal waste/cement recipes. When S/S is successful and optimal in a technical sense (strength and leachability) it can in theory be used as a construction material. The new secondary material can be used in road constructions, dykes, sound barriers or it can be used to raise soil level or to acclaim land along coasts or harbours. In that way it can replace primary raw materials.

When S/S treatment has resulted in a building material, this material has to be introduced on the construction market. For most waste producers this is a new market to be considered and to deal with. The construction market is known for its traditions and is strongly regulated by the use of mutual contracts, habits and by different levels of legislation (Haan and Adriaansens, 1996). In many cases waste supplying industries will not be familiar with this market. A supplier of secondary materials has to cope with traditional suppliers (e.g. of primary materials) that have more experience and are already familiar with the other construction parties, e.g. principals and builders. Another party that dominates the market is formed by the public administration. Public administration has set up legislation for the application and disposal of materials, which may strongly limit the freedom of action on the construction market for the waste supplier. Authorities may also play the role of a private party in the market when they act as principal of a work.

Whether the introduction of secondary materials is successful depends on the freedom of action in the market of its producer or supplier. When trying to introduce this product on the market, their freedom of action is limited. In other words they have to cope with limitations, because the market is strongly regulated by other parties and on the rules all parties of interest have to comply with. In the worst case, the limitation in freedom of action of the waste supplier means that he cannot introduce his material, even when the secondary material satisfies all primary product demands (e.g. strength) and environmental demands (leaching). In fact, this has been the case in the past (CUR, 1997).

When implementation of a secondary material as a building material is not successful, this means a major problem for the producer of secondary materials, because he has taken a lot of effort in designing and executing S/S techniques.

It is therefore clear that in order to increase acceptance and use by the construction market, taking into account technical aspects only is not sufficient. When designing a cement/waste recipe and making choices on technical aspects, application aspects, i.e. market aspects need to be taken into account. The producer of secondary material must cope with limitations of a strongly regulated market in which his product will be applied. The producer or supplier of secondary materials has to use all his powers in order to obtain a position in the market that gives it enough space to act as a serious trading partner and to reach his goals in the market.

For the producer of secondary materials it is important to have knowledge about the market, how the market is regulated by rules and other parties and how these parties will deal with his product. It is also important to know how his role in the market can be increased with respect to all other parties. He can take this knowledge into consideration when he is designing S/S techniques and making choices about which type(s) of treatment are necessary and for which type(s) of applications the final product should be suitable. Taking this into account, better choices for treatment can be made at forehand and better strategies can be developed in order to obtain a successful introduction of the obtained product in the construction market.

In order to describe these problems and to find solutions, a framework has to be developed in which the parties, their roles and power and the rules are described. The main parties are authorities, which can act in a public way (set up legislation) or in a private way (act as principal of a public work) and the construction industry. The space of the supplier of secondary materials is determined the size of the roles of all other parties. Purpose of this chapter is finding the instruments that can be used to influence freedom of action of the supplier of secondary materials and finding the ways how to use this power properly in order to penetrate into the market.

This chapter deals with how the supplier of secondary materials can use his powers when it introduces these materials as building materials in the construction market. In section 7.2 the theoretical framework will be developed based on a power game in which parties use power sources in order to increase their role and position in the market. In section 7.3 the players in the market will de described. These are the suppliers of secondary materials (the central party in this chapter), the construction industry, authorities in their public administrative role (their general policy) and authorities in their private role (authorities acting as principal of a work). In section 7.4 the effects of regulations on the freedom of action of the supplier of secondary materials is described. This space is determined by legislation and regulations set up by other parties. The theoretical framework will be used to explain the problems that can occur when introducing secondary materials. In section 7.5 solutions to these problems will be presented by showing how the instruments presented in chapter 7.2 can be used by supplier of secondary materials. This results in possibilities on the market. The beneficial role of certification in the introduction of secondary materials will be shown. And it will be shown how producers of secondary materials can increase freedom of space by collaborating. Two examples of successful collaborations will be given. In section 7.6 conclusions will be given by showing how instruments should be used by the supplier of secondary materials in order to deal with all other parties on the market, making a successful introduction of the materials more likely.

7.2 The power game and power sources

When different parties with different goals and interests are acting and trying to execute policy in the same field, this can be described as a power game. In this power game all players use their power in order to increase their own action of freedom and limit the freedom of action of other parties in order to reach their own goals and execute their own policy. Limitations follow from rules and policies that regulate the field of interest and all parties have to comply with. These rules can be set by an independent party, by the parties itself, or by mutual engagements.

The principle of a power game has been used in the past to describe the role of the Dutch government and the execution of its environmental policy (Bressers et al. 1993). However, these descriptions are one-directional, i.e. it describes how government can influence behaviour of citizens. This will be described in section 7.3.3, where the role of the government is described. In this chapter the waste supplying industry will be the central party in the power game, because this party can also use its powers to influence policies of other parties, including authorities.

In order to play the game, all parties can make use of power sources. These are instruments that can be used to execute policy and increase freedom of action or freedom of policy at the expense of the freedom of other parties. Such a use of power sources has been described in Van der Laan (1998) in order to describe the freedom of policy that municipalities obtain from the national government in order to execute municipal policy. In Van der Laan (1998) two types of power sources are mentioned: formal power sources and material power sources (see Table 7.1).

Table 7.1. Power sources.

Formal	Material
Competences	Knowledge
	Capacity
	Relations

The formal power source is the institutional competence to set up legislation, e.g. taking financial measures, in order to execute policy. This power source is the privilege of public administration. For the waste industry, the use of formal power sources by public administration can work in two ways: (1) it creates limitations because of prohibitions or restrictions in legislation or (2) it creates possibilities when industry is involved in setting up norm values, tests and regulations. This is called *self-regulation*. Also, the restrictions that follow from legislation can be reduced in practice when rules are applied.

Material sources are sources required to bring policy and legislation into practice. Three material sources will be considered here: (1) knowledge, (2) capacity and (3) relations.

Knowledge can be used in many ways. It can be used to understand interests and way of working of other parties and it can be used to persuade other parties to act in your own advantage. Knowledge can also be used strategically, i.e. selectively. Specifically juridical knowledge can be used for ones own advantage.

Capacity is formed by human power (number and skills). Available funding can also be considered as a type of capacity.

Relations with other types of parties make it possible to influence decisions of such other parties. When the relation is based on mutual dependence, the rules of one party limit the freedom of the dependent party. When the relations are based on mutual goals, they can enforce each other's powers. In both cases the existence of relations will help in obtaining more capacity and more knowledge.

While formal sources are the privilege of public administration, material resources are available to all parties of interest, including the supplier of secondary materials. The authorities play a double role. In their public administrative role, their interest is the protection of the environment and regulation of the market. In a private role they are the principal or owner of construction works. In that case their actions have to be of general interest and setting a good example is important. Fig. 7.1 presents an overview of all parties and their interests with respect to the market for building materials.
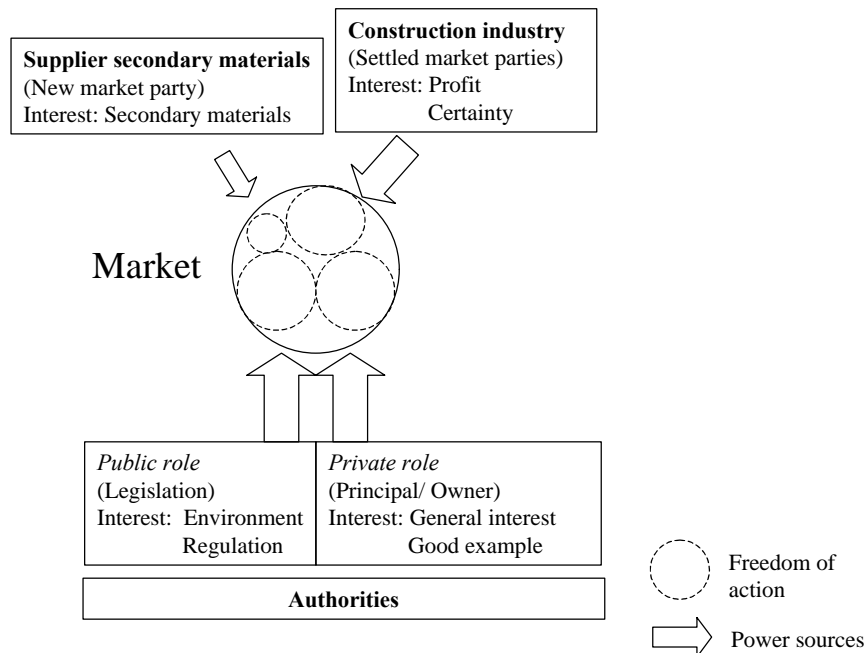
Figure 7.1. The power game. Parties, interests, freedom of action and power sources.

This chapter will be based on proper and optimal use of power sources by the waste supplying industry in order to maximise freedom of action with respect to all other parties. More available power sources and better use of them will result in a more significant role in the market and increase the freedom of action.

7.3 Involved parties

7.3.1 Waste producers and suppliers

Secondary materials are produced by different types of industries. Examples are the chemical industry (producer of slags or burning ashes), the power industry (producer of fly ash), waste incineration facilities (producers of incineration and bottom ashes), demolition industry (construction waste) and soil cleaning or dredging industry (contaminated soil and sludge). Moreover there are also treatment facilities that buy waste in order to convert it into

150

immobilisates that can be sold with profit. When these industries act as supplier to the construction industry they play the role of a new trading partner in the construction market.

7.3.2 The construction industry

The construction industry includes all parties involved in the building of a work. Two sectors are distinguished in the construction industry, each with their own characteristics: Housing (buildings) and Infrastructure (earth works, road building works or hydraulic engineering works).

In short a work is constructed as follows. The principal or owner gives orders to a designer (architect) to design a work. This results in the specifications, which contain the design and all demands of the principal. Next, the principal hires builders (in most cases contractors) to construct the work according to these specifications.

In the construction industry the following parties collaborate when a work is constructed: (1) traditional producers and suppliers, (2) owner or principal, (3) designer and (4) builders:

Traditional producer and supplier. Traditionally, the parties concerned with the production and supply of building materials included manufacturers of cement, concrete or concrete products, bricks, roof tiles, asphalt etc. They also included suppliers of natural aggregates, e.g. sand and gravel. Sometimes, these traditional suppliers supply secondary materials as an alternative, partial replacement or additive to their raw materials. An example is the supply of fly ash and slag cements by cement companies. The producer of secondary materials has to compete against these traditional parties.

Owner or principal. The owner or principal is the party that orders and instructs the construction of a work. It is generally also the party that after construction holds title in the work and is the user of the work. Property developers, estate agents, authorities, foundations, private individuals and companies can all be principal or owner of a work. In the Infrastructure, authorities are the principal in most cases, because these types of work are of general use. In Housing, authorities are the owner of public buildings. The role of the authorities as principal or owner will be described in section 7.3.4.

Designer. The designer (architect) writes the specifications for the construction. He advises the principal on the choice for building materials and is aware of the corresponding financial, technical and environmental consequences of this choice. In case of Housing the role of the designer is more important and more specialised because the types and sizes of construction vary from one project to the other. In case of Infrastructure, the role of the designer is more fixed.

Builders. Builders actually handle and apply the building materials when they construct a work, generally by order of owners or principals. Builders include construction companies, contractors and subcontractors.

Because the principal gives the orders and because he finances and holds title in the work, he will be the party with most participation, responsibilities and interests during the construction process (VROM, 2000). He will make the final decision on whether to use secondary materials or not and thus has the power to stimulate this use or constrain it. Designers can advise about the use of secondary materials and its consequences. This advising role of the

designer will have most impact when the principal does not have much experience and knowledge on constructing.

In some cases it is decided that the builders will play a more significant role during the construction process. This means that they will play an advising role during the designing process and communicate more directly with principal and designer. In that role they will have more participation in the choice for secondary materials. This can be advantageous when he has good experiences working with secondary materials.

Traditionally the specifications of a work contain the amounts and types of materials that will be used and the builders are not allowed to deviate from it. As an alternative the principal may choose to use specifications based on performance. This means that the specifications contain more general demands and the builder has more freedom in making choices in order to comply with the requested demands and performances. With this way of working the principal can set environmental demands, e.g. the use of a minimum amount of secondary materials. The Dutch government ordered the building of many road constructions and promised additional payments to the builders if they used secondary materials.

The builders will have to deal with proper application of building materials. For example they must obey the rules relating to isolation, control and monitoring when using category 2 building materials. Also, they must observe the rule governing removal, in other words they must use the material in a manner that allows it to be removed.

The principals is responsible for the quality and environmental impact of the work they order to build and must take all necessary measures in order to fulfil these demands (ministry of VROM, 2000). The principals must record or have recorded all information on the chemical composition and leaching behaviour of building materials, which are covered by the BMD. He must keep this information available and is sometimes required to furnish the information beforehand to the empowered authority. He is also required to ensure that any rules governing use (e.g. isolation measures) are complied with. Therefore he will demand that suppliers, builders and sometimes even designers will show him this information. In order to prevent misunderstandings during the construction process, it may be necessary that the principal makes clear to the builders what rules are to be complied with and exactly what types of information they require for his duty of information (e.g. a recognised approval or a batch inspection). The best way to achieve this is by writing it down explicitly in the specifications (Reijerkerk en de Sain, 2000). Thus, although the principal must provide the authorities with information, actually the suppliers or builders will supply the requisite information. This information will proof that batches of stony material or earth that will be delivered satisfy the quality requirements of the BMD.

When the producer of waste wants to supply secondary building materials he may be required to use S/S techniques first before the material can be used safely as a construction material. The price of the secondary material will in that case be determined by these treatment costs and the costs that would otherwise be needed when the material had to be transported and dumped. Taking this avoided costs into account the price of the material is often still higher than the price of its alternative on the construction market. In that case its properties should be worth this extra price. Otherwise the builder or designer will not consider it as a serious alternative. The extra environmental value is often only considered as a real extra value by principals and not by designers or builders working in a commercial market like the construction industry. For them, only physical material properties that differentiate it from the traditional material will be considered as real extra values. Such properties include a specific shape, colour or density. A secondary material is also a low-cost alternative when its application saves time, when its raw material is more easily available or when its processing is more straightforward compared to the traditional material. For a continuous long-term use

of secondary material instead of a primary material, builders want to have the certainty that its supply is insured for the long-term and that the quality and properties of the different batches will not deviate too much.

One can conclude that the goal of the construction industry is making profit and constructing a reliable work for their costumers. This conclusion is important for the waste industry. This industry should take this into account and note that a building material must have a commercial interesting price and both industry itself and the material to be introduced must be trustworthy for all parties.

7.3.3 Authorities in public role

The main goal with respect to waste and secondary materials of public administration is protection of the environment. This environment also includes humans, which means that aspects like safety and health are also important issues for public administration. In the Netherlands, four different types of authorities, each with their own role and competences in the field of waste and building materials are found:

1. National government.
   Develops new policy and legislation and sets rules on how it should be implemented, and enforced, making use of inspection.
2. Provinces.
   Interpret and translate national policy into terms relevant for their own area.
3. Municipalities.
   Play an important rule in granting and enforcing permits
4. Water authorities.
   They are responsible for maintenance of surface water.

Van der Doelen (1989) has presented three general types of policy instruments that can be used to change behaviour of other parties. Klok (1991) has used this typology for the development of an instrument theory that can be used to study effectiveness of measures, especially in environmental policy. The types of instruments are shown in Table 7.2.

Table 7.2. Policy instruments

Control type	Action	Example
Juridical	Prescribing	convenant, prohibition, order
Economical	financial measures	grants, levy, investments
Communication	give information	education

The national government develops environmental policy and accordingly sets up legislation on the handling of waste and materials in general. The Dutch environmental policy in general has been described in the introduction (Section 1.3). In order to reach the set goals on decreasing the amount of waste to be disposed and on stimulating the use of secondary materials, authorities can use the tools given above. Clear regulations can be set up including decrees on waste disposal and on the use of building materials (see section 7.3). Parties of interest can be informed about these rules in order to minimise uncertainties for the parties involved. Public administration can introduce landfill bans or increase disposal costs or put levies on the use of primary materials. It can also subsidise the use of secondary materials or the development of treatment technologies, e.g. solidification/stabilization technologies.

Authorities can be empowered for the enforcement of legislation. Generally, when building materials are applied onto or into soil, municipalities are the empowered authorities. When building materials are applied in surface water, water authorities are the empowered authority. Only in exceptional cases will provinces or the national government be the empowered authority. For a proper enforcement, human capacity is required.

In practice, many of these regulations and restrictions are reduced for the parties of interest, for example in case of self-regulation by waste industry, i.e. when this industry is involved in regulation making by public administration or when it creates its own regulation system, e.g. contracts, standards and certificates. Furthermore, when human capacity is insufficient, compliance of rules can not be verified sufficiently and this will decrease the actual power of the authorities.

7.3.4 Authority as principal or owner of a work.

Authorities can order the construction of works that are for governmental use (e.g. city hall) or public use (e.g. roads). Because most infrastructure is of general use, authorities are the main principal in that sector. In this private role authorities still have to comply with their own rules and regulations. They also have to comply with the governmental policy (e.g. environment). With that respect they can set an example by using secondary materials.

Because of their relation with higher authorities in a public role, authorities in a private role have the power to adjust rules and influence policy making. Authorities can deal flexible with the legislation in practice. For example they can make exceptions by giving temporarily permits or (temporarily) allow practices that were common in the past but would be illegal according to new rules.

The funding is obtained by higher authorities and authorities in a private role have less interest in making profit than commercial principals. Therefore they are more likely to spend more money on environment-friendly solutions for their construction works.

7.4 Regulations and constraints

7.4.1 Waste decrees

For the waste industry, two waste decrees are relevant regarding the disposal of waste: The landfill decree and the landfill ban decree.

Landfill decree

The landfill decree gives rules for isolation, control and monitoring of disposal sites (CUR, 1995). Disposal is only allowed for waste containing more than 90% of inorganic material, otherwise it should be incinerated. Three waste categories and corresponding disposal categories are defined as follows:

C2-category: Strong leaching. Leaching into the soil must be prevented.
C3-category: Medium leaching. Leaching into the soil must be inhibited.
C4-category: Low leaching.

The leachability of waste is measured according to a quick column test (NEN 7343, 1995) that requires the material to be crushed to a certain maximum particle size. For each

154

inorganic element in the waste two leaching levels are set: the U0 higher level and the U1 lower level. When leaching of one element of a waste exceeds the U1 norm, it is designated as a C2 waste. When the leaching of none of the elements exceed the U1 norm, but some exceed the U0 norm, the waste is of the C3 category. When leaching of all elements is below the U0 norm it is of the C4 category.

Landfill ban decree

The landfill ban decree (CUR, 1995) defines a number of waste categories that are not allowed to be disposed. These categories include: construction waste, batteries, paper, vegetable, food and garden waste, plastics, sieve sand and steel grit. In 2000 waste from all categories defined in this decree were not allowed to be disposed. The decree also states that organic waste should only be disposed if the national incineration capacity is insufficient.

The steps to be taken by the waste industry, taking into account the decrees on waste, can be shown in a decision scheme for the producer of waste (see Fig. 7.2).
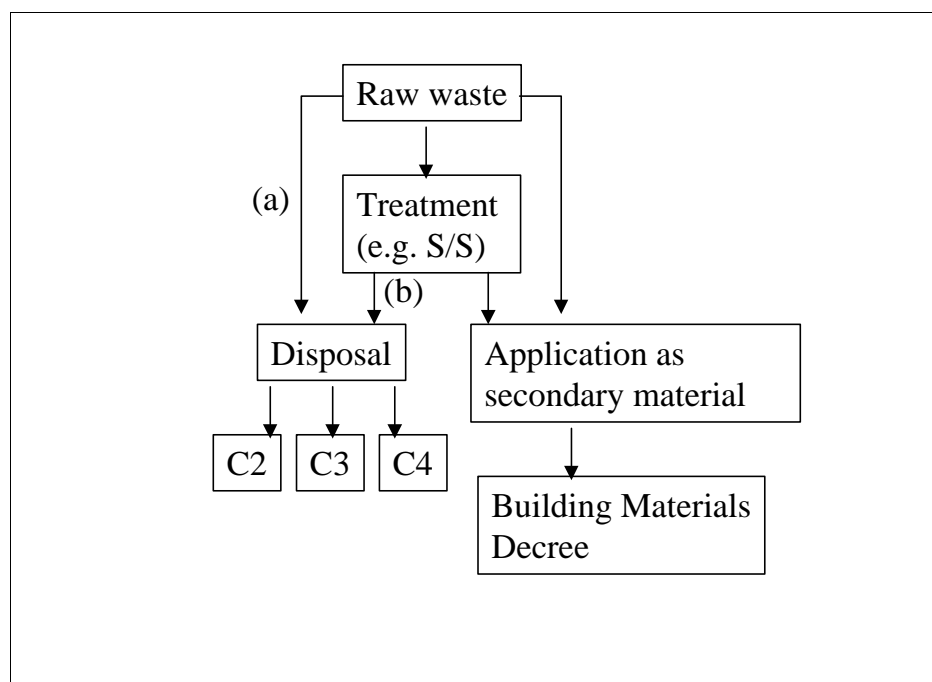
Figure 7.2. Decision scheme for producer of waste taking into account waste legislation. a) Prohibited in case of a landfill ban. b) Prohibited when increase in volume is more than 25% compared to untreated waste.

S/S techniques can be applied in order to convert a waste into a category of which the disposal requires less isolation measures and is cheaper. However, the waste industry has to take into account that disposal of treated wastes is only allowed when its volume has not increased by more than 25% compared to the volume of the untreated waste. This duty was implemented in order to prevent that waste streams are highly diluted as a result of the addition of binders.

155

7.4.2 The Building Materials Decree (BMD)

Aims

Recently in the Netherlands the Building Materials Decree (BMD) was introduced, in which application of construction materials is regulated (Ministry of VROM, 1995, 1998, 2000 and CUR, 1999). It provides norms and conditions that should be obeyed when building materials are applied in the outside environment. This also accounts for waste industry introducing solidified waste products as building material.

The decree is based on the laws for protection of soil and surface water. Thus, the quality criteria given in this decree are all set from a point of view of soil and water protection. Target values of clean soil are values based on concentrations of contaminants in the soil that are assumed to have a negligible risk for humans and ecology. These target values should be obtained and maintained as much as possible. Leaching of a contaminant is accepted when it does not exceed a level that would increase the target value by 1% in 1 meter of soil over 100 years (or within 1 year for chlorides and sulfates).

The BMD gives rules on allowed concentrations or leaching from construction materials, independent of their origin, in other words no distinction is made between primary, secondary, or waste materials. They are all required to meet the same conditions. It also prescribes how products should be certified and how their application should be controlled.

From the BMD, Ministerial Decisions are laid down that describe detailed instructions on how tests and enforcement should be carried out. Composition and immission values are also described in Ministerial Decisions. Adjusting or setting up a Ministerial Decision requires fewer procedures than adjusting the BMD itself.

Definitions

The building materials covered by the BMD must be stony, used in a work and used outside. Stony is defined as consisting a minimum content of 10% silicon, calcium or aluminium. Concrete, asphalt, clay, earth and sand are examples of stony materials. Wood, plastics and metals are not stony. A work is a construction work, an earthwork, a road building work or a hydraulic engineering work. The BMD does not cover storage or transport of materials. Outside use means that the building materials may come into contact with rainwater, groundwater or surface water. This definition excludes materials used inside. Handling of materials which is not regulated by the BMD will be considered as beyond the scope of this thesis.

Leaching and immission

Leaching is the release of contaminants from a building material after exposure to rain or groundwater (see Fig. 7.3). Leaching values are measured in a laboratory according to leaching tests, which are described in standard protocols. A shaped building material consists of solid, durable elements of at least 50 cm^3 each. The leaching from shaped building materials is measured according to the diffusion test described in NEN 7345 (NNI, 1995). In this test one element is placed in a bath containing acidified water. At different points in time, the water is replaced by fresh acidified water and analysed for leached contaminants. The leaching from granular materials is measured according to the column test described in NEN 7343 (NNI, 1995). In this test a column is filled with the material and flushed continuously with acidified water. After passing through the material the water is analysed for leached contaminants.

156

Immission is the dispersion of contaminants into soil or surface water as a result of leaching (see Fig. 7.3). It depends on the leaching of the building material and on the external circumstances under which it will be applied, e.g. the degree of contact with water, isolation measures taken and the application height (thickness of the layer). The expected immission values are calculated from the leaching results using a formula in which these external circumstances can be taken into account.
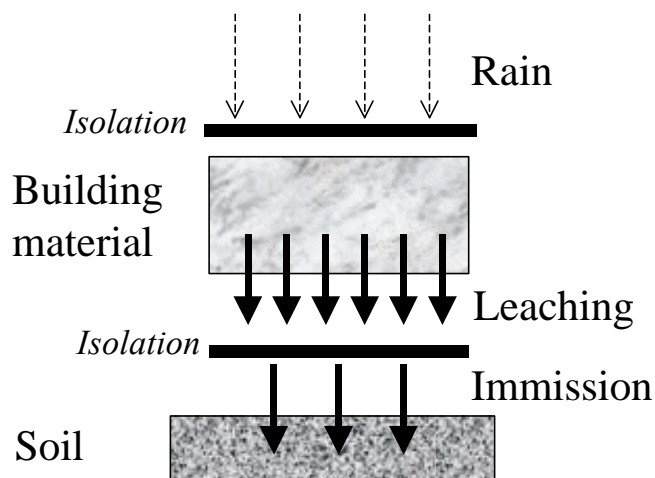
Figure 7.3. Leaching and immission.

Maximum immission values are prescribed for the following inorganic compounds: Antimony, arsenic, barium, cadmium, chromium, cobalt, copper, mercury, lead, molybdenum, nickel, selenium, tin, vanadium, zinc, bromides, chlorides, sulfates, cyanides and fluorides. For organic compounds the norm values are based on composition and not on leaching, because for many organic compounds no suitable leaching tests are available yet or they are still in development (RIVM, 1999a, 1999b). Maximum composition values are prescribed for polycyclical aromatic hydrocarbons (PAHs), mineral oils, pesticides, polychloro-biphenyls (PCBs) and many other organics.

Categories

Usually, building materials, e.g. clean earth or soil, will contain so little of harmful substances or these substances will be so well enclosed that pollution of the environment during the application stage is very unlikely. In some cases additional protective measures will be required to prevent excessive pollution. In that case, use of the building material will only be permitted if these measures are taken. When concentration or leaching of contaminants are so high that they exceed the prescribed values, even when protective measures are taken into account, this will result in a total ban on the use of this building material and its application is prohibited.

According to the above principles, the BMD defines different categories of building materials. A distinction is made on the basis of their composition values (for organic substances) and immission values, which are calculated from the leaching behaviour (for inorganic substances). The values for each separate compound are all-decisive.

Category 1 building materials do not exceed any compositional values and would also not exceed any immission value when used in a work without any isolation measures.

Category 2 building materials do not exceed any compositional values and would not exceed any immission value when used in a work only when additional isolation measures are taken.

A special category is defined in the BMD for bottom ash from waste incineration facilities and tarry asphalt aggregate in order to maintain its already common reuse. These materials do not satisfy compositional demands for some organic substances, but may still be applied when special isolation measures are taken.

The use of materials that do not fall into one of the above categories is prohibited.

Fig. 7.4 shows a decision scheme in which the application of secondary materials as building material is explained.
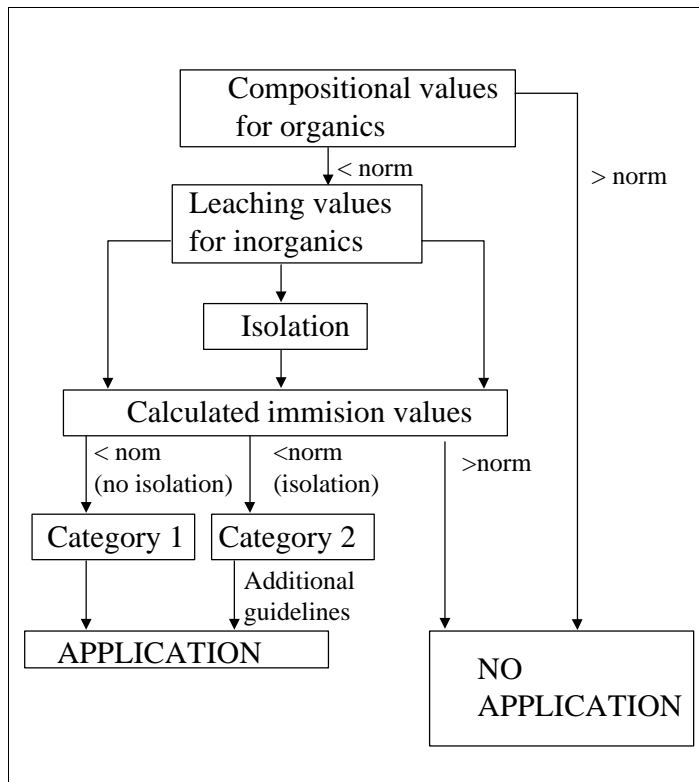
Figure 7.4. Decision scheme for the application of secondary materials.

Certification

During the set-up of the BMD the Dutch government has paid a lot of attention to the enforcement of the rules by the local authorities (Eikelboom, 1999). Therefore the possibility of certification for building materials was introduced in the BMD to improve effectiveness and efficiency of the enforcement. Certification is a means of ensuring products are in compliance with legal standards. All test methods have to be performed by accredited laboratories in order to get uniform results and to ensure proper interpretation of the test methods and a proper way of taking samples. The application and enforcement of a

certification system requires a lot of capacity. This was obtained by sharing this task with institutes and accredited laboratories.

The best way to prove that a building material meets the requirements is to have it certified. These certificates can only be given by certification institutes that are accredited by the Dutch Council for Accreditation. When this certificate is recognised by the Minister of Housing, Spatial Planning and the Environment and by the Minister of Transport, Public Works and Water Management, the manufacturer obtains a recognised approval, which will be published on a list. These recognised approvals must be accepted as sufficient proof by all empowered authorities.

A less expensive and less time consuming way of obtaining proof is by means of a batch inspection by a testing agency that is designated by the Minister of Housing, Spatial Planning and the Environment and by the Minister of Transport, Public Works and Water Management. This procedure results in an examination report for one specific stock of materials.

During the implementation of the BMD many problems occurred because implementation of this same certification system laid behind when BMD came into force and not enough laboratories were accredited in time. As a result many construction companies, especially small companies decided to use primary materials instead of the alternative secondary materials in order to minimise risks. (Cobouw 1999a, 1999b). This proves how much a successful implementation of secondary materials relies on a good certification system. A certification system in which also technical and durability aspects are considered is in development (CUR, 1997).

General duties

All building materials except clean earth have to be used in minimum quantities in one work in order to avoid small quantities of contaminated materials being used at too many different locations in the country. This would make the situation difficult to control.

All building materials, except clean earth, are subject to the duty of removal. As soon as a work is no longer in use or being maintained, the owner must remove the building materials. This duty was imposed to ensure that during the life of a work, or when it becomes redundant, the building materials do not mix with the soil.

7.4.3 Private law

Legal responsibility is regulated by private law, which regulates the relations among civilians. For example private law gives rules on how to deal with contracts made up by civilians. Legal responsibilities among parties in the construction industry are regulated by mutual contracts that are set-up for each new construction but also by habits and expectations common in this industry (Haan and Adriaansens, 1996). When contracts are made between parties in the construction industry, this implies that parties have to comply with it. Not complying with such a contract is an *unlawful act* and such action can be prosecuted. A party that does not comply with a contract Traditionally, the designer makes choices for building materials to be used and is responsible for his choice. When specifications based on performance are used, the builder must make these choices himself. In that way, responsibilities are shifted to the builder. Every builder has the duty to check the specifications before and during the building process. If he foresees that building according to the specifications will result in a work that will not comply with all requirements, he has the duty to report this to the principal. The

reporting duty is especially expected from the builder when it is likely that the principal is no professional, i.e. has not much experience in instructing works.

In the case of soil, the legal responsibility lies with its owner. Every owner has to look after that the soil is clean before building operations take place and is maintained clean afterwards. It is not allowed to build on contaminated soil. When soil is contaminated, the cleaning costs have to be paid by the party that caused it (i.e. the party that did the unlawful act) or otherwise by the owner itself (Haan and Adriaansens, 1996).

7.4.4 Institutional constraints

From Fig. 7.2 one can see that when application of the treated or untreated waste as building material is not possible, disposal is the other option. In that case the only purpose of the treatment is converting a waste into a waste of a less strict category. This waste can then be disposed at a disposal for which less regulations apply and which is thus cheaper.

When a landfill ban applies to the raw material but treatment, e.g. S/S, is not successful because it leads to a significant volume increase or its costs are higher than the benefit of the lower disposal costs, application is the only possible option. However, in the case of for example S/S treatment using cementitious binders, hardening may not occur properly or it may not be possible to bind all elements properly. This may lead to unreasonable high treatment and research costs because alternative treatment techniques have to be used or even still designed, e.g. thermal treatment. This is especially unwanted when the traditional treatment produced an immobilisate for which only one specific contaminant does not fulfil the composition or leaching norm values in the BMD. This is a typical example where the use of formal competences by authorities limits the freedom of action of supplier of secondary materials.

To deal with this problem the producer of waste requires influence on authorities to find ways to force application. The waste industry should approach authorities to obtain help with financing the required research, or to ask for adjustment of one of the specific norm values or to ask for allowance for the application of a specific type of material or to convince that an exception for a landfill ban should be made.

In all cases the industry has to convince authorities that their interference in advantage of the waste supplier is really required and will finally lead to environmental benefits. They will only change legislation or make exceptions when a significant benefit is expected or when the problems of more than one specific company are solved.

7.4.5 Commercial constraints

The producer is a new party on the construction market and has to convince all possible users in the construction industry that the secondary material is an environmentally and technically safe product. Therefore it is the task of the producer of secondary materials to supply information in order to proof this. He will have to do research on the product and on how it will perform under the circumstances of its expected application compared with the alternative in the same application. The required research and tests will clarify the possibilities and restrictions of application of the product and may finally lead to product certification.

Another way of convincing possible users of the secondary material is the set-up of trial projects in which they will be used. Collaboration with authorities is often required for financing or ordering such projects or for giving temporary permits.

When the supplier is a small company, its limited knowledge, experience and financial possibilities make it difficult to do research, to set-up trial projects and to obtain certification. A small supplier will also have difficulties to be acknowledged by builders as a serious new trading partner or a serious alternative for traditional and larger suppliers. Such a supplier on its own does not have sufficient power sources required to reach its goal.

7.5 Possibilities: using the power sources

7.5.1 Knowledge

Introduction of secondary materials requires that all parties of interest are convinced about its quality and safety. The government wants to minimise environmental effects when these materials are applied. Principals, designers and builders will consider the secondary materials as a good alternative only when both quality and safety are assured. It is of great interest to the supplier of secondary materials that he has this and additional information about his product available and that he shows this to the users. Therefore he requires the power source knowledge.

Technical knowledge requested by other parties can be shown in the form of a certificate. When the construction material is certified, the user will also be less worried about liability aspects during the service time of the material. This will greatly enhance the freedom of action of the supplier of secondary materials.

To obtain certification, the producer of waste must invest in research to obtain required technical knowledge about the environmental impacts of the product. Such information can also be used in order to convince parties about the advantages of the product, even before certification is obtained.

Thus, certification gives both users and authorities certainty about the quality and safety of the material and therefore is considered to be an important step towards successful introduction of secondary materials.

Finally, knowledge about the construction industry, its parties, strategies, roles and interests may help in understanding how these parties should be taken into account. When supplier of secondary materials knows the interests and demands of other parties, it can emphasise specific properties of his product that are important for the other party. This is an example of selective use of available knowledge.

7.5.2 Relations

For most suppliers of secondary materials the construction market is new. Therefore it is important to set up relations with parties already settled in this market. The most accessible party is the authority in a private role as principal, which is especially important in Infrastructure. Also, in practice the rules for infrastructural works are less strict than for housing projects. For example the special category created for Tarry Asphalt Granulate (TAG) has made reuse in road works easier. Furthermore, the types of constructions in infrastructural works makes it possible to apply isolation layers before secondary materials are applied (e.g. a road is always built up out of layers). This layer functions as isolation layer and secondary material applied on top of it only has to fulfil the conditions including isolation measures.

Because these authorities have a relation with higher (legislative) authorities, which policy stimulates reuse of materials, it is expected that they want to set a good example and

that they are willing to set up trial projects or order public works in which secondary materials are applied. Furthermore, they can create legislative possibilities in advance of suppliers of secondary materials when they are convinced that this has advantages for the environment.

Relations with traditional suppliers in the construction market can be advantageous, because they already have a settled position on the market and are known by other parties, e.g. principals, designers and builders. Relations with cement or concrete industry can be useful, because they can introduce new products on the market they are already familiar with. Such a new product may contain or consist of secondary materials.

7.5.3 Capacity

To be able to do joint investments, and to be treated as a serious discussion partner for the authorities and as a serious new trading partner for the construction industry the supplier of a secondary material needs capacity. Such capacity can be obtained by collaborating with other producers of the same specific type of waste. When parties with equal goals and interests collaborate, this increases their capacity and their roles and influence in the market. Thus, the availability of human and financial capacity helps in obtaining knowledge and setting up and maintaining relations.

7.5.4 Centre for Immobilisation

In the Netherlands producers of waste and immobilisates, research and knowledge institutes, governmental institutes and the cement industry founded a Centre for Immobilisation in 1998. The main task of this centre was performing an active and substantial contribution in cancelling observed obstructions for application of secondary materials (CUR, 1997). The centre combines knowledge and experience from industry and authorities and acts as discussion partner for all parties of interest. It gives information about technical and legislative possibilities and restrictions for applying secondary materials. It is also involved in research and setting up and improving legislation, unambiguous certification procedures and tests.

When an organisation that represents several producers of one type of waste communicates with the CIM, it can provide better information about their waste and products and about their practical problems and benefit more from the activities, knowledge and experience of the members of the centre.

7.5.6 The introduction of fly ash

A good example of the benefits of increasing capacity and making use of relations by collaboration between industrial parties is the power industry. Powder coal fly ash is the remaining product from the burning of powder coal in power plants. Both industry and government agreed that dumping of this material should be prevented. The Dutch coal power plants founded the Fly Ash Union, an institute that was given the task of implementing and sustaining sales of fly ash to the construction industry (Fly Ash Union, 1997, Cornelissen and Jenners, 1998). The collaboration between the suppliers (coal power plants) increased the overall capacity and the setting up of relations with customers (cement manufacturers and concrete companies) and government, led to a national research project that was partly financed by the government and helped to obtain product knowledge and certification. A

certification procedure was set up that fulfilled the demands of all participating parties. As a result of this collaboration Dutch powder coal fly ash is now reused for 100 % and applied successfully in the cement and concrete industry both as raw material and as Lytag (thermally treated fly ash). Table 7.3 shows the reuse percentages in the Netherlands (CUR, 1996b).

Table 7.3. Reuse percentages of powder coal fly ash in the Netherlands

Application in	Percentage
Cement	60
Lytag	22
Asphalt	9
Concrete	6
Other	3

7.6 Conclusions

For the supplier of a secondary material it is difficult to introduce his material as a building material on the construction market. The reason for this is that it has to deal with a market in which other parties with other interests play a role and use their possibilities to control the market in order to reach its own goals and interests.

The Dutch authorities play an important role by regulating the market of building materials and by acting as principal of public works. The strict environmentally policy of the Dutch authority is the main source of institutional constraints for the supplier of secondary materials.

Many commercial constraints arise from the fact that the producer of waste is a new trading partners with new products in the construction industry. The secondary material will be considered as an alternative to traditional primary materials. Principals, designers and builders have to be persuaded to use the secondary material.

The supplier of secondary materials can increase its freedom of policy in the market in the same way as authorities and other parties increase it: namely by using the power sources knowledge, capacity and relations.

Knowledge

Knowledge of the construction industry makes it possible to take into account the application aspects and the properties of the traditional (primary) building materials, all benefits and constraints of the use of the secondary material.

Communication with parties in the construction industry is necessary to find out their interests and demands and to inform them about possibilities and constraints of the application of their product. When supplier of secondary materials knows the interests and demands of other parties, it can emphasise specific properties of his product that are important for the other party. Such knowledge can be used strategically, i.e. for advantage of the supplier of secondary materials.

Obtaining a recognised approval on the secondary product convinces both authorities and users in the construction industry that the product is safe and durable. When the supplier of secondary materials has his product certified, this will greatly enhance his freedom of action in the market.

Relations

Relations with authorities are especially required when legislation inhibits a secondary material to be applied after reasonable efforts in finding the proper treatment. Consulting with legislative authorities is the last possibility in order to make application still possible. Authorities can also help in financing trial projects or ordering public works in which secondary materials are to be used.

The introduction of fly ash on the Dutch market is a good example of how relations enhanced freedom of action of a supplier of secondary materials. Collaborating with authorities and other parties of interest in the construction industry gives the supplier of secondary materials more power to execute its policy.

Capacity

Investments and trading with other involved parties will have more impact when the producer of a specific waste decides to collaborate with other producers of the same waste. This can be achieved for example by setting up an institute that represents one type of waste producers and can take care of the market implementation. This institute makes it possible to do joint investments and will be considered as a serious discussion partner by the authorities and a serious and reliable trading partner in the construction industry. When the implementation of a secondary material is successful the same institute can take care of a continuous delivery and quality of the product. The successful reuse of powder coal fly ash in the Netherlands gives a good example of where collaboration with parties having same interests can lead to.

Chapter 8

Conclusions and recommendations

8.1 Cement chemistry

In order to study the solidification/stabilisation (S/S) process, which starts as soon as cement, water, waste and additives are mixed, it is important to realise that the solidification process mainly corresponds with cement hydration. To understand and improve this process, cement hydration has to be studied in detail and thus, the chemical and physical properties of cement and additives have to be taken into account when designing a S/S recipe based on cement.

When cement is used to solidify waste products, fundamental knowledge about cement hydration, can be used to understand and improve the solidification process.

A 3D cement hydration model, the CEMHYD3D model from NIST, was chosen for simulation of cement hydration and for implementation of new theories and mechanism. CEMHYD3D was chosen because it was the most advanced and flexible cement hydration model available and because it already contained all required fundamental knowledge of cement chemistry. The model has been used successfully to describe solidification and microstructure development of Ordinary Portland Cement (OPC) mixtures based on ENCI cements.

To simulate the solidification process and the final structure of the resulting immobilisate, a cement hydration model such as CEMHYD3D can be used.

Important additives in concrete and S/S technology are silica fume and fly ash. Much is known about the pozzolanic reaction between silica (S) and CH and therefore reaction of silica fume, which is pure silica, can be considered well. However, for the reaction of fly ash, a major waste product as well as a common additive in concrete industry and S/S technology, no sufficient mechanism was available. Fly ash partially contains silica and its reactivity depends on the pH of pore water. Solubility and precipitation of contaminants also depend on pore water composition. Therefore, reaction mechanisms and pore water chemistry models have been developed to consider the presence of such compounds during cement hydration.

Pore water chemistry, especially $[Na^+]$, $[K^+]$, $[OH^-]$, $[Ca^{2+}]$ and $[SO_4^{2-}]$ concentrations determine reactivity of waste compounds and pozzolanic additives in a hydrating cement mixture.

Routines have been developed to calculate $[Na^+]$, $[K^+]$, $[OH^-]$, $[Ca^{2+}]$ and $[SO_4^{2-}]$, which were found to be the most important ions in cement pore water. To calculate $[Na^+]$ and $[K^+]$ an alkali release and sorption model was used and when alkali concentration was known, all other concentrations were computed using reduced set of relevant solid equilibria. Computed

pore water concentrations agreed well with experimental results reported in literature. In hydrating OPC and mixtures containing silica fume, concentrations during the first day of hydration as well as concentrations in mature hydrated pastes were predicted well.

The pore water routines are an important tool when designing cement/waste recipes. First, the effect of cement parameters, e.g. alkali contents, SO_3 content of the clinker and type of calcium sulphate (gypsum, anhydrite or hemihydrate) and particle size distribution (PSD) on pore water concentrations could now be studied. Secondly, the [OH^-] development could be used for the simulation of the hydration of fly ash and slags, because their reactions start at a threshold pore water pH, which can now be predicted by CEMHYD3D for different types of cement. Thirdly, because the equilibria mainly determining [Ca^{2+}] and [SO_4^{2-}] have been determined, the solubility of calcium and sulphate containing solids can now be treated. Such compounds are often formed as a result of the presence of contaminants in the pore water of cement/waste mixtures.

Pore water concentrations can be calculated from the alkali content of the used cement, the degree of hydration at some point in time and a set of solid equilibria relevant at that point in time.

Because fly ash is a major waste product and also an important additive in both concrete industry and in S/S technology, the reaction of fly ash particles is studied in detail. Based on dissolution experiments found in literature, it was concluded that the available amount of reactive fly ash is proportional to the glass (non-crystalline) part of the fly ash. Moreover, as the crystalline part forms an impermeable network, dissolution rates are also proportional to the glass content, especially while the effective diffusion coefficient is proportional to the square of the glass content. The derivation of an extended shrinking core model yields analytical equations that reckon with a hollow core, as well as the possibility of two regions with different composition and reactivity. Calculations revealed that the inner region is more reactive, and that about 7% and 9% of the silica is found in the outer region of fly ash solid spheres, respectively. From the fitting it also follows that the outer region of solid spheres and cenospheres have nearly the same thickness (about 2 μm). After dissolution of this layer, which needs less time in case of higher pH and/or temperature, the dissolution of the inner region at a higher rate starts.

The reaction of fly ash can be described by a shrinking core model, in which a particle can be considered as being made up of different shells having different compositions.

Furthermore, a reaction mechanism for fly ash glass is put forward that accounts for its silica, aluminium oxide, iron oxide, titanium oxide, alkali and earth alkali content (and which also be useful for slags). The resulting reaction product and the experimental application indicate a dissolution rate proportional to [OH^-]$^{0.9-1}$ for the outer region, and to [OH^-]$^{1.4}$ in inner region, at least for the fly ash studied here. This result suggests that the outer layer of fly ash particles is richer in earth alkalis (i.e. poorer in silica), which is in line with findings in other publications.

The pore water [OH^-] dependence of the reaction of a fly ash particle is related to the elemental composition of its shells.

166

Consideration of pore water composition and additional reaction mechanisms (e.g. for fly ash) make it possible to study the hydration of cement mixtures containing waste products, e.g. fly ashes and slags, and contaminants.

The results from these pore water and reactivity studies make it possible to use CEMHYD3D to describe the hydration of cement/fly ash mixtures as a function of the elemental composition of fly ash and pore water pH development of the paste. Furthermore, pore water calculations can be used to predict the effects of contaminants in a hydrating cement mixture. Combining CEMHYD3D with pore water calculations, hydration of different types of fly ash and different types of cement mixtures containing contaminants can be modelled, using different mass fractions of both materials used in practice.

Combining CEMHYD3D, pore water calculations and additional reactions makes it possible to simulate hydration of cement mixtures containing waste products, e.g. fly ashes and slags, and contaminants.

8.2 Chemistry of contaminants

When considering reactivity and solubility of waste components in a cement system, the most important parameter was the chemical environment of cement paste, especially the pH in the pore water, but also the redox potential. This environment can be adjusted and tailored using additives such as blast furnace slag (change potential) and alkali content (change pH) or specific additions such as waterglas and sulphides.

Knowledge about pore water chemistry in the presence of contaminants is essential to predict problems in solidification.

The most significant contaminants found in waste streams and bound by cement are metals, borates, chlorides and sulphates. The corresponding hydroxides and calcium compounds are slightly soluble in the high pH pore water of cement paste. This results in precipitation of such compounds on cement particles, resulting in disturbance of hydration and poor strength development. This coating effect was studied and modelled using the case of calcium borates. Besides the solubility of the contaminant in the mixing water, the PSD appears especially important, because a higher initial PSD implies a higher surface available for coating, thus a less dense coating layer and a higher chance of continuation of hydration. For each metal, using equations developed in this thesis, an estimate of which fraction of the cement surface is coated, can be made, and based on this, predictions about whether hydration and solidification will take place can be made. Also [OH⁻] and alkali concentrations are important, because it can result in redissolving of precipitated compounds. This implies that binding of contaminants can be regulated and improved by varying PSD of cement or by varying the pore water pH (e.g. by varying alkali content of the binder compounds, i.e. cement and fly ash).

Coating of cement particles is the most relevant mechanism responsible for poor strength development.

Coating effects and related retardation effects are significant when the amount of precipitated compound is sufficient to cover a significant fraction of the surface of unhydrated cement particles.

Negative effects of coating can be overcome by using cement of high PSD or by varying pore water pH.

The reactions in CEMHYD3D and the pore water extension are very useful in predicting reactions and chemical changes taking place when contaminants are present in hydrating cement paste.

CEMHYD3D can be used to study solidification of cement/waste mixtures containing most common contaminants; The model is able to predict when contaminants will result in poor strength development.

8.3 Structure of solidified product

The durability and quality of the solidified product, also referred to as the immobilisate, is characterised by the leaching rate of contaminants present in its structure. The leaching rate is tested using leaching tests and depends on the structure of the immobilisate.

The durability of the immobilisate depends on its strength and properties of its microstructure.

A shrinking core leaching model can describe acid induced leaching of metals in a solidified product. Both the effective diffusion coefficient and the acid neutralisation capacity can be described in terms of hydrated cement paste volume fractions. Using the leaching model and a cement hydration model, it is possible to describe leaching rates as a function of cement paste composition. When the water porosity fraction is known a CH fraction can be computed at which leaching rates are minimal.

Because the water porosity only has a negative effect, it should always be as low as possible. The composition of the solidified product should therefore be optimised for the amount of CH. Best results are obtained when water porosity is 0 % and CH fraction is 13 %.

Leaching from a solidified product depends on the expected degree of hydration, and porosity and Ca(OH)$_2$ content of the final product.

To have all cement reacted and to use it optimally, additions such as silica fume or fly ash are required. The optimal replacement fractions for these pozzolanic additions particularly depend on the expected degree of hydration and less on the w/c ratio used. Optimal values of around 8 % (m/m) silica fume and 35 % (m/m) fly ash based on total mass of cement plus additions were computed.

168

Using CEMHYD3D to predict the microstructure of a solidified product and applying a leaching model, gives a fundamental relation between the used cement/waste mixture and leaching properties of the solidified product.

Finally, taking into account all fundamental knowledge presented in this thesis, and results from numerical simulations, the following conclusion can be drawn:

When fundamental knowledge about pore water chemistry, coating mechanisms and structure related leaching are combined with a cement hydration model such as CEMHYD3D, an excellent tool is created that can be used to predict and improve the functional properties of an immobilisate.

8.4 Market for building materials

Both Dutch government and waste industry want to execute a policy of sustainable development. When the waste industry follows a strategy of sustainable development, one of its tasks is to treat and solidify waste products and, when possible, introduce the final solidified product as building material to close a material cycle. For the supplier of such solidified products, it is difficult to introduce these products as a building material on the construction market. These difficulties follow directly from this market in which other parties with other interests play a role and use their power to control the market by rules to reach their goals and interests.

The Dutch authorities play an important role by regulating the market of building materials and by acting as principal of public works. The strict environmental policy of the Dutch authorities is the main source of institutional constraints for the supplier of secondary materials.

Many commercial constraints arise from the fact that the producer of waste is a new trading partner presenting new and alternative products to the construction industry. The secondary material will be considered as an alternative to traditional primary materials. Principals, designers and builders have to be persuaded to use the secondary material.

To increase chances of acceptance of an immobilisate as a building material the waste industry has to obtain trust by commercial and administrative parties in the construction market.

A market in which different parties having different interests and powers play a role, can be described in terms of power sources knowledge, capacity and relations. The availability and application of such power sources gives the parties ways of increasing their freedom of space in the market. The waste industry should use and extend his power sources to deal with other parties, i.e. to obtain trust.

The waste industry can obtain trust from all parties of interest in the construction market by using its power sources, knowledge, capacity and relations.

Already during the design of a cement/waste mixture, the waste industry should consider knowledge about the product to be developed and about all other market parties to deal with. Only then, their interests and demands can be dealt with.

To bring a policy of sustainable development into practice and making the introduction of solidified waste product successful commercially, certification of the product is essential. Only certification will be accepted by other parties as a proof of reliability of the product itself as well as trustworthiness of the supplier. Thus, for the supplier it is the best way to present (product) knowledge about an immobilisate to other parties.

Collaboration with authorities can help in setting up legislation and tests that satisfy all parties demands and to set up trial-projects. Investments and trading with other involved parties will have more impact when the producer of a specific waste decides to collaborate with other producers of the same waste. This can be achieved for example by setting up an institute that represents one type of waste producers and can take care of the market implementation. This institute makes it possible to do joint investments and will be considered as a serious discussion partner by the authorities and a serious and reliable trading partner in the construction industry. When the implementation of a secondary material is successful the same institute can take care of a continuous delivery and quality of the product.

Collaboration with authorities (relations) and with other suppliers of solidified waste products (capacity) is the best way for the waste industry to make it a more serious negotiating partner for all other parties. This collaboration policy improves the chances of obtaining funds, permissions and reliability from other parties.

170

Symbols

Roman

a	power ([OH$^-$]^a in fly ash reaction)	
b	apparent/glass density ratio	
bf	binding factor	[m^3/kg]
b$_{RR}$	Rosin-Rammler parameter	
d	diameter	[m]
$\bar{d}$	geometric mean diameter	[m]
f	fraction	
m	mass	[g]
$\dot{m}_S$	molar flux	[mole/m^{2}s]
n	number of	
n$_{RR}$	Rosin-Rammler parameter	
p	probability	
r	radius	[m]
r*	dimensionless radius	
t	time	[s]
t$_0$	induction period	[s]
w/c	water/cement ratio	
w/s	water/solid ratio	
x	mole fraction	
z	charge (of ion)	[C]
A	surface area (of particle)	[m^2]
ANC	acid neutralisation capacity	[mole/m^3]
B	cycle to time parameter	
C	concentration	[mole/m^3]
CAL(t)	cumulative amount leached	[mole/m^2]
CFR(t)	cumulative fraction leached	
D	diffusion coefficient	[m^2/s]
D$_0$	molecular diffusion coefficient	[m^2/s]
D$_e$	effective diffusion coefficient	[m^2/s]
F	strength	[Pa]
G(d)	cumulative mass fraction of particles having diameter < d	
H()	Heaviside function	
I	ionic strength	[mole/m^3]
K	concentration or reaction product	[mole/m^3]^n
K^0	activity product	[mole/m^3]^n
M	molar mass	[kg/mole]
Q	Heat	[J]
S	solubility	[mole/m^3]
SA	surface area (internal)	[m^2]
Sh	shape factor	

M	molar concentration	[mole/m^3]
V	volume	[m^3]
T	temperature	[K]

Greek

α	degree of hydration or degree of dissolution	
β	binder mass fraction	
γ	activity coefficient	
ζ	molar ratio $\bar{x}_A / \bar{x}_S$	
η	molar ratio $(\bar{x}_C + \bar{x}_M)/\bar{x}_S$	
κ	molar ratio $(\bar{x}_N + \bar{x}_K)/\bar{x}_S$	
λ	molar ratio $\bar{x}_F / \bar{x}_S$	
θ	molar ratio $\bar{x}_T / \bar{x}_S$	
ϑ	porosity to diffusivity function	
ρ	density	[kg/m^3]
τ	reaction time	[s]
φ	volume fraction in microstructure or (hydrated) paste	
ϕ	porosity (in particle)	
Φ	gel/space ratio	

Subscript

+/-	cation/anion
ap	apparent
b	binder (cement + silica fume + fly ash etc.)
c	cement
com	compressive
CH	Ca(OH)$_2$
CSH	C-S-H
FA	fly ash
g	glass
h	hollow
hp	hydration product
in	inner region
int	intrinsic
max	maximum
min	minimum
mob	mobile
out	outer region
ox	oxide
p	porosity (pore water)
pal	porosity after leaching
ph	phase

172

prp	precipitate
r	reacting (core)
SF	silica fume
T	Total
Tprp	total precipitate
sides	pixel surface planes
w	water

Superscript

0	initial (t = 0) or standard
exp	exposed to water
opt	optimal
layer	in coating layer
r	reacted
sol	in solution

Abbreviations

AES	Auger Electron Spectroscopy
ANC	Acid Neutralisation Capacity
BFS	blastfurnace slag
BSE	backscattered electrons microscopy
CAL	cumulative amount leached
CFR	cumulative fraction leached
C/S	CaO/SiO_2 molar ratio
EDS	Energy Dispersive Spectroscopy
ENCI	Eerste Nederlandse Cement Industrie
FA	fly ash
FTIR	Fourier Transform Infra Red spectroscopy
hcp	hardened cement paste
H/S	H_2O/SiO_2 molar ratio
ITZ	interfacial transition zone
LOI	loss on ignition
L/S	liquid to solid ratio
NIST	National Institute of Standards and Technology
NMR	Nuclear Magnetic Resonance
OPC	ordinary Portland cement
ppm	part per million
PSD	particle size distribution
RH	relative humidity
SA	surface area
SEM	scanning electron microscopy
SF	silica fume
S/S	solidification/stabilisation
SSA	specific surface area
TEM	Transmission Electron Microscopy
w/c	water/cement mass ratio
w/s	water/solids mass ratio
XPS	x-ray Photoelectron Spectroscopy
XRD	x-ray diffraction

References

Adaska, W.S., Tresouthick, S.W. and West, P.B. (1991), Solidification and stabilization of wastes using Portland cement, Portland Cement Association.

Akhter, H., Cartledge, F.K., Roy, A. and Tittlebaum, M.E. (1993), A study of the effects of nickel chloride and calcium chloride on hydration of portland cement, Cem. Concr. Res. Vol. 23, p. 833-842.

Akhter, H., Cartledge, F.K., Roy, A. and Tittlebaum, M.E. (1997), Solidification/stabilization of arsenic salts: Effects of long cure times, J. Hazard. Mat. Vol. 52, p. 247-264.

Allison, J.D., Brown, D.S. Novo-Gradac, K.J. (1991), "Minteqa2/Prodefa2, A Geochemical Assessment Model for Environmental Systems: Version 3.0 User's Manual", EPA/600/3-91/021, U.S. Environmental Protection Agency, Office of Research and Development, Environmental Research Laboratory, Athens, Georgia.

ANSI/ANS 16.1 (1986), Measurement of the leachability of solidified low-level radioactive wastes by a short term test procedure, American Nuclear Society, La Grange Park.

Babushkin, V.I., Matveyev, G.M. and Mchedlov-Petrossyan, O.P. (1985), Thermodynamics of Silicates, Springer, Berlin.

Baker, P.G. and Bishop, P.L. (1997), Prediction of metal leaching rates from solidified/stabilized wastes using the shrinking unreacted core leaching procedure, J. Hazard. Mat. Vol. 52, p. 311-333.

Banfill, P.F.G.(1986), Precipitation of calcium hydroxide in the presence of organic compounds, J. Mat. Sci. Lett. Vol. 5, p. 33-34.

Banfill, P.F.G. and Saunders, D.C. (1986), The relationship between the sorption of organic compounds on cement and the retardation of hydration, Cem. Concr. Res. Vol. 16, p. 399-410.

Barret, P., Bertrandie, D., Casabonne-Masonnave, J.M. and Damidot, D. (1992), Short term processes of radionuclide immobilization in cement: a chemical approach, Appl. Geochem. Suppl. Issue No. 1, p. 109-124.

Batchelor, B. and Wu, K. (1993), "Effects of Equilibrium Chemistry on Leaching of Contaminants from Stabilized/Solidified Wastes", in Chemistry and Microstructure of Solidified Waste Forms, R.D. Spence (Ed.), Lewis Publishers, Boca Raton, Florida.

Bentz, D.P. (1997), Three-Dimensional computer simulation of portland cement hydration and microstructure development, J. Am. Ceram. Soc. 80(1), p. 3-21.

Bentz, D.P. and Garboczi, E.J. (1991), A digitized simulation model for microstructural Development, Ceramic Transactions 16, p. 211-226.

Bentz, D.P. and Garboczi, E.J. (1992), Modelling the leaching of calcium hydroxide from cement paste: effects on pore space percolation and diffusivity, Materials and structures 25, p. 523-533.

Bentz, D.P. and Haecker, C.J. (1999), An argument for using coarse cements in high-performance concretes, Cem. Concr. Res. Vol. 29, p. 615-618.

Bentz, D.P., Garboczi, E.J., Haecker, C.J. and Jensen, O.M. (1999), Effects of cement particle size distribution on performance properties of Portland cement-based materials, Cem. Concr. Res. Vol. 29, pp 1663-1671.

175

Bentz, D.P. and Stutzman, P.E. (1994), SEM analysis and computer modelling of hydration of portland cement particles, Petrography of cementitious materials, ASTM STP 1215, S.M. DeHayes and D. Stark (Eds.), ASTM, Philadelphia.

Bentz, D.P., Waller, V. and Larrard, F. de (1998), Prediction of adiabatic temperature rise in conventional and high-performance concrete using a 3-D microstructural model, Cem. Concr. Res. Vol. 28 No.2, 285-297.

Blaakmeer, J. and De Loo, M. (1999), Private Communications, ENCI, The Netherlands.

Bobrowski, A., Gawlicki, M. and Malolepszy, J. (1997), Analytical evaluation of immobilization of heavy metals in cement matrices, Environ. Sci. Technol. 31, p. 745-749.

Bressers, J.TH.A., Jong, Klok, P. de, Korsten, A.F.A. (1993), Beleidsinstrumenten bestuurskundig beschouwd (in Dutch), Van Gorcum, Assen, Netherlands.

Breugel, K. van (1995), Numerical simulation of hydration and microstructural development in hardening cement-based materials (I) Theory, Cem. Concr. Res. Vol. 25, No.2, p. 319-331.

Breugel, K. van (1995), Numerical simulation of hydration and microstructural development in hardening cement-based materials (II) Applications, Cem. Concr. Res. Vol. 25, No.3, p. 522-530.

Brouwers, H.J.H. (1997), Leaching models for multiply immersed materials and for granular materials flushed in a column, J. Hazard. Mat. 53, p. 1-17.

Buil, M. Revertegat, E. and Oliver, J.A. (1992), A model of the attack of pure water or undersaturated lime solutions on cement, Stab. Solid. Hazard. Radioact. wastes, 2nd Vol. STP 1123, Gilliam, T.M. and Wiles, C.C (Eds.), ASTM 1992, p. 217-226.

Butler, J.N. (1998), Ionic equilibrium. Solubility and pH calculations, John Wiley & Sons, N.Y.

Capelle, A. and de Vooys, F. (1983), Activated carbon... a fascinating material, Norit, Amersfoort, The Netherlands.

Carde, C. Francois, R. and Torrentini, J-M (1996), Leaching of both calcium hydroxide and CSH from cement paste: Modeling the mechanical behavior, Cem. Concr. Res. Vol. 26 No. 8, p. 1257-1268.

Cartledge, F.K. et al. (1990), Immobilization mechanisms in Solidification/Stabilization of Cd and Pb salts using Portland cement fixing agents, Env. Sci. Technol. 24(6), p. 867-873.

Casabonne Masonnave, J.M. (1987), Fixation of radioelements coming from nuclear wastes in form of insoluble compounds or by exchange reactions in concrete (in French), PhD. Thesis, University of Dijon, France.

Casabonne Masonnave, J.M. (1993) Immobilization of borates and phosphate anion with saturated lime solutions, Solid state ionics, Vol. 59, p. 133-139.

Cheng, K.Y. (1991), Controlling mechanisms of metal release from cement-based waste forms in acetic acid solution, PhD Thesis University of Cincinatti.

Cheng, K.Y. and Bishop, P. (1992), Metals distribution in solidified/stabilized waste forms after leaching, Hazard. Waste Hazard. Mat. Vol. 9 No. 2, p. 163-171.

Cheng, K.Y., Bishop, P. and Isenburg, J. (1992), Leaching boundary in cement-based waste forms, J. Hazard. Mat. 30, p. 285-295.

176

Cheng, K.Y., Bishop, P. and Isenburg, J. (1991), Cement stabilization/solidification techniques: pH profile within acid-attacked waste form, Waste Materials in Construction, Goumans, J.J.J.R, van der Sloot, H.A. and Aalbers, Th. G. (Eds.), Elsevier Science Publishers.

Christensen, B.J., Mason, T.O., Jenning, H.M., Bentz, D.P. and Garboczi, E.J. (1992), Experimental and computer simulation results for the electrical conductivity of portland cement paste, Mat. res. Soc. Symp. Proc. Vol. 245, p. 259-264.

Cocke, D.L. and Mollah, M.Y.A. (1993), The chemistry and leaching mechanisms of hazardous substances in cementitious solidification/stabilization systems, Chemistry and Microstructure of solidified waste forms, Spence, R.D. (Ed.), Lewis Publishers, Boca Raton, Florida.

Cocke, D.L., Mollah, M.Y.A., Vempati, R.K. and Hess, T.R. (1995), Multitechnique approach to understanding the microstructure of cement-based systems, Mat. Res. Soc. Symp. Proc. Vol. 370, p. 279-284.

Cocke, D., Ortego, J.D., McWhinney, H., Lee, K. and Shukla, S. (1989), A model for lead retardation of cement setting, Cem. Concr. Res. Vol. 19 No. 1, p. 156-159.

Conner, J.R. (1990), Chemical fixation and solidification of hazardous wastes, Van Nostrand Reinhold, N.Y.

Cornelissen, H.A.W. and Jenner, H.A. (1998), Fly ash; from waste to resource, Paper for the international conference "Fly ash disposal & utilization" New Delhi, India.

Csetenyi, L.J. and Glasser, F.P. (1993), Borate substituted ettringites, Mat. Res. Soc. Symp. Proc. Vol. 294, MRS Publ, Pittsburgh, PA, USA, p. 273-278.

Csetenyi, L.J. and Glasser, F.P. (1995), Borate retardation of cement set and phase relations in the system Na2O-CaO-B2O3-H2O, Adv. Cem. Res. Vol. 7 No. 25, p. 13-19.

CUR (1999), Aan het werk met het bouwstoffenbesluit (in Dutch), CUR report 99-4, ISBN 90-12-08779-1, stichting CUR, Gouda, Netherlands.

CUR (1995), Handleiding voor het beoordelen van immobilisaten (in Dutch), CUR report 183, ISBN 90-376-0048-4, stichting CUR, Gouda, Netherlands.

CUR (1996), Vliegas in cement, toeslag en beton (in Dutch).

CUR (1997), Immobilisatie: een haalbaar alternatief (in Dutch), CUR report 97-7, ISBN 90-376-0210, stichting CUR, Gouda, Netherlands.

Damidot, D. and Glasser, F.P. (1995), Thermodynamic investigation of the CaO-Al2O3-CaSO4-CaCO3-H2O closed system at 25 oC and the influence of Na2O, Adv. Cem. Concr. Res. Vol.7, No.27, p. 129-134.

Diamond, S. (1975), Long-term status of calcium hydroxide saturation of pore solutions in hardened cements, Cem. Concr. Res. Vol. 5, p. 607-616.

Diez, J.M., Madrid, J. and Macias, A. (1997), Characterization of cement-stabilized Cd wastes, Cem. Concr. Res. Vol. 27, p. 337-343.

Duchesne, J. and Reardon, E.J. (1995), Measurement and prediction of portlandite solubility in alkali solutions, Cem. Concr. Res. Vol. 25 No. 5, p. 1043-1053.

Dullien, F.A.L. (1979), Porous media: fluid transport and pore structure, Academic Press, New York.

Eijk, R.J. van and Brouwers, H.J.H. (1997), Simulation of cement hardening in the presence of carbon using Hydra2D, Proceedings of the 10th International Congress on the Chemistry of Cement, Göteborg, Paper 2ii052.

Eikelboom, R.T. (1999), The Building Materials Decree: an example of a Dutch regulation based on the potential impact of materials on the environment, Proceedings of Waste Stabilization & Environment, Lyon, April 13-16, 1999, Eds. J. M. Hu, G. Keck, A. Navarro and T. Soci, Alpine de Publications, Grenoble (1999).

EPA (1985), TCLP, Solid waste procedure manual, SW-924, Cincinnati, U.S.

Fair, G.M. and Hatch, L.P. (1933), Fundamental factors governing the streamline flow of water through sand, J. Amer. Water Works Assoc. Vol. 25.

Fattuhi, N.I. and B.P. Hudges (1988), The performance of cement paste and concrete subjected to sulfuric acid, Cem. Concr. Res. Vol. 18, p. 545-553.

Faucon, P. et al. (1996), Leaching of cement: Study of the surface layer, Cem. Concr. Res. Vol. 26 No. 11, p. 1707-1715.

Feller, W. (1950), An introduction to probability theory and its applications, Wiley, N.Y.

Fly ash Union (1997), Year report 1997 (in Dutch), NV GKE, Vliegasunie BV, De Bilt, Netherlands.

Fraay, A.L.A., Bijen, J.M. and De Haan, Y.M. (1989), The reaction of fly ash in concrete, a critical examination, Cement and Concrete Res., Vol. 19, p. 235-246.

Garboczi, E.J. and Bentz, D.P. (1992), Computer simulation of the diffusivity of cement-based materials, J. Mater. Sci 27, p. 2083-2092.

Gawlicki, M. and Czamarska, D. (1992), Effect of ZnO on the hydration of Portland cement, J. Therm. Anal. Vol. 38, p. 2157-2161.

Glasser, F.P. (1993), Chemistry of cement-solidified waste forms, Chemistry and microstructure of solidified waste forms, Spence, R.D. (Ed.), Lewis Publishers, Boca Raton, Florida.

Glasser, F.P. (1997), Fundamental aspects of cement solidification and stabilisation, J. Hazard. Mat. Vol. 52, p. 151-170.

Glasser, F.P. (1996), Properties of cement waste composites, Waste management Vol.16 No. 1-3, p. 159-168.

Godbee, H.W. and Joy, D.S. (1974), Assessment of the Loss of Radioactive Isotopes from Waste solids to the Environment, Part 1, Background and theory, Oak Ridge National Laboratory ORNL/TM-4333, Oak Ridge, TN.

Gougar, M.L.D., Scheetz, B.E. and Roy, D.M. (1996), Ettringite and CSH Portland cement phases for waste ion immobilization: A review, Waste Manag. Vol.16 No. 4, p. 295-303.

Gutowitz, J. (1991), Cellular Automata. Theory and Experiment, MIT press, Cambridge, MA.

Haan, P. de and Adriaansens, C.A. (1996), Bouwrecht in kort bestek (in Dutch), Kluwer, Deventer, The Netherlands.

Heiman, R.B. et al. (1992), Leaching of simulated heavy metal waste stabilized/solidified in different cement matrices, J. Hazard. Mat. 31, p. 39-57.

Helfferich, F.G. (1995), Ion exchange, Dover, New York.

Hemmings, R.T. and Berry, E.E. (1988), On the glass in coal fly ashes: recent advances, Mat. Res. Soc. Symp. Proc. Vol. 113, p. 3- 28.

178

Hewlett, P.C. (1998), Lea's chemistry of cement and concrete 4th Ed., Arnold, London, U.K.

Hills, C.D., Sollars, C.J. and Perry, R. (1994), A calorimetric and microstructural study of solidified toxic wastes-Part 1: A classification of OPC/waste interference effects, Waste Management Vol. 14 No. 7, p. 589-599.

Hills, C.D., Sollars, C.J. and Perry, R. (1994), A calorimetric and microstructural study of solidified toxic wastes-Part 2: A model for poisoning of OPC hydration, Waste Management Vol. 14 No. 7, p. 601-612.

Hills, C.D., Sollars, C.J., Koe, L.C. and Perry, R. (1995), A calorimetric study of the effect of organic compounds on the initial behaviour of cement-based solidified wastes, Waste management & Research Vol. 13, p. 21-36.

Hinsenveld, M. and Bishop, P. (1994), Use of the shrinking core/exposure model to describe the leachability from cement stabilized wastes Stabilization and solidification of hazardous, radioactive and mixed wastes, ASTM STP 1240, Gilliam, M. and Wiles, C.C. Eds., Am. Soc. of testing and Mat., Philadelphia.

Hong, S-Y and Glasser, F.P. (1999), Alkali binding in cement pastes Part I. The C-S-H phase, Cem. Concr. Res. Vol. 29, pp 1893-1903.

Hooton, R.D. (1986), Permeability and pore structure of cement pastes containing fly ash, slag and silica fume Blended cements, ASTM STP 897, G. Frohnsdorff, Ed., ASTM, Philadelphia, p. 128-143.

Hulett, L.D. and Weinberger A.J. (1980), Some etching studies of the microstructure and composition of large aluminosilicate particles in fly ash from coal-burning power plants, Env. Sci and Technology Vol. 14, p. 965-970.

Ivey, D.G., Neuwirth, M., Conrad, D., Mikula, R.J., Lam, W.W. and Heimann, R.B. (1993), Electron microscopy characterization techniques for cement solidified/stabilized metal wastes, Chemistry and Microstructure of solidified waste forms, Spence, R.D. (Ed.), Lewis Publishers, Boca Raton, Florida.

Jeffrey, J., Garner, L. and House, W. (1991), Cement as a stabilization media, Waste Management Vol. 2, pp 359-63.

Jennings, H.M. and Johnson, S.K. (1986), Simulation of microstructure development during the hydration of a cement compound, J. Am. Ceram. Soc. Vol. 69, p. 790-795.

Jennings, H.M. et al. (1996), Modelling and materials science of cement-based materials. Part I: An overview. The modelling of microstructure and its potential for studying transport properties and durability, Jennings, H.M. et al. (Eds.), Kluwer academic publishers, Netherlands.

Kindness, A., Macias, A. and Glasser, F.P. (1994), Immobilization of chromium in cement matrices, Waste Management Vol. 14 No. 1, p. 3-11.

Klok, P-J (1991), Een instrumententheorie voor milieubeleid (in Dutch), PhD. Thesis, University of Twente, Netherlands.

Koenders, E.A.B. (1997), Simulation of volume changes in hardening cement-based materials, PhD. Thesis, Delft, Netherlands.

Kyi, A.A. and Batchelor, B. (1994), An electrical conductivity method for measuring the effects of additives on effective diffusivities in Portland cement pastes, Cem. Concr. Res. Vol. 24 No. 4, p. 752-764.

Laan, F. van der (1998), Binnenland Bestuur en Verandering Deel 5: Wondermiddelen zijn niet voorhanden (in Dutch), Uitgeverij Eburon, Delft, Netherlands.

Larbi, J.A., Fraay, A.L.A. and Bijen, J.M.J.M. (1990), The chemistry of the pore fluid of silica fume-blended cement systems, Cem. Concr. Res. Vol. 20, No. 4, p. 506-516.

Levenspiel, O. (1999), Chemical Reaction Engineering (3rd ed.), John Wiley, New York.

Lide, D.R.L. (ed.) (1995), CRC Handbook of chemistry and physics, (76th ed.), CRC Press, Boca Raton.

Lieber, W. and Richartz, W. (1972), Einfluβ von Triäthanolamin, Zucker und Börsäure auf das Erstarren von Zementen (in German), Zement-Kalk-Gips, 61 (9), p.403-409.

Lin, T-T and Lin, C-F (1994), Mechanisms of metal stabilization in cementitious matrix: interaction of dicalcium silicate (C2S) paste and copper oxide, Toxic. Environ. Chem. 43, p. 51-62.

Lin, T-T, Lin, C-F and Wei, W-C.J. (1994), Mechanisms of metal stabilization in cementitious matrix: Transmission electron microscopic study of C3A/CuO fixation system, J. Hazard. Mat. 36, p. 55-68.

Longuet, P. Burglen, L. and Zelwer, A. (1973), The liquid phase of hydrated cement, Rev. Mat. Constr. (France) 676, p. 35-41.

Macphee, D.E. and Glasser, F.P. (1993), Immobilization science of cement systems, MRS Bull., Vol. 18, No. 3, p. 66-71.

McWhinney, H.G. and Cocke, D.L. (1993), A surface study of the chemistry of zinc, cadmium, and mercury in Portland cement, Waste Management Vol. 13, p. 117-123.

McWhinney, H.G.A. et al. (1990), Surface characterization of priority metal pollutants in cement, Proc. Natl. Conf. Hazard. Wastes Hazard. Mater., 7th, p. 107-113.

Matsuo, T., Nishi, T. and Matsuda, M. (1995), LiNO3 addition to prevent hydrogen gas generation from cement-solidified aluminium wastes, J. Nucl. Sci. Technol. 32(9), p. 912-920.

Matsuo, T., Nishi, T. and Matsuda, M. (1995), Prevention of hydrogen gas generation from cement-solidified aluminium wastes, Transactions of the American Nuclear Society Vol. 72, p. 76-77.

Mattus, C.H. and Mattus, A.J. (1996), Literature review of the interaction of select inorganic species on the set and properties of cement and methods of abatement through waste pretreatment, ASTM-STP, 1240, Williamsburg.

Ministry VROM (1995), Building Materials Decree soil and surface water protection, Bulletin of acts, orders and decrees, No. 567.

Ministry VROM (1998), Ministerial decision based on the Building Materials Decree, Netherlands Government Gazette, 30, SDU.

Ministry VROM (2000), Building Materials Decree Brochure. The Building Materials Decree affects the entire industry, distribution number: 23021, Ministry VROM, Netherlands.

Mollah, M.Y.A., Tsai, Y-N and Cocke, D.L. (1992), J. Environm. Health, A27, p. 1213

Moragues, A., Macias, A. and Andrade, C. (1987), Equilibria of the chemical composition of the concrete pore solution. Part I: comparative study of synthetic and extracted solutions, Cem. Concr. Res. Vol. 17, p. 173-182.

Mulder, E. (1996), Pre-treatment of MSW fly ash for useful application, Waste management Vol.16 No. 1-3, p. 181-184.

NEN 7343 (1995), Leaching characteristics of solid earthy and stony building and waste materials, Determination of the leaching of inorganic components from granular materials with the column test, Nederlands Normalisatie Instituut, Delft (in Dutch).

NEN 7345 (1995), Leaching characteristics of solid earthy and stony building and waste materials, Determination of the leaching of inorganic components from buildings and monolithic waste materials with the diffusion test, Nederlands Normalisatie Instituut, Delft (in Dutch).

NEN-EN 196-1 (1995), Nederlands Normalisatie Instituut, Delft (in Dutch).

Nocun-Wczelik, W. and Malolepszy, J. (1997), Studies on immobilization of heavy metals in cement paste-C-S-H leaching behaviour, Proc. 10th ICCC, Vol. IV, 4iv043, Gothenburg 1997.

Omotoso, O.E., Ivey, D.G. and Mikula, R. (1996), Quantitative x-ray diffraction analysis of chromium(III) doped tricalcium silicate pastes, Cem. Concr. Res. Vol. 26 No. 9, p. 903-914.

Omotoso, O.E., Ivey, D.G. and Mikula, R. (1998), Containment mechanism of trivalent chromium in tricalcium silicate, J. hazard. Mat. 60, p. 1-28.

Ortego, J.D., Jackson, S., Yu, G.S.,McWhinney, H. and Cocke, D.L. (1989), Solidification of hazardous substances. A TGA and FTIR study of Portland cement containing metal nitrates, J. Environ. Sci. Health, Vol. A24(6), p. 589-602.

Park, J-Y. and Batchelor, B. (1999), Prediction of chemical speciation in stabilized/solidified wastes using a general chemical equilibrium model Part I. Chemical representation of cementitious binders, Cem. Concr. Res. Vol. 29, p. 361-368.

Park, J-Y. and Batchelor, B. (1999), Prediction of chemical speciation in stabilized/solidified wastes using a general chemical equilibrium model II: Doped waste contaminants in cement porewaters, Cem. Concr. Res. Vol. 29, p. 99-105.

Paul, A. (1977), Chemical durability of glasses; a thermodynamic approach, J. of Mat. Sci. Vol. 12, p. 2246-2268.

Paul, A. (1990), Chemistry of Glass (2nd ed.), Chapman, London.

Pietersen, H.S. (1990), Reactivity of fly ash at high pH, Mat. Res. Soc. Symp. Proc. Vol. 178, p. 139-157, Materials Research Society.

Pietersen, H.S. (1993), Reactivity of fly ash and slag in cement, Ph.D. Thesis, Delft University of Technology, The Netherlands.

Pietersen, H.S. (2000), private communications.

Pitzer, K.S. (1991), Activity coefficients in electrolyte solutions, CRC press, Boca Raton, FL

Pollit, H.W.W. and A.W. Brown (1969), in 5th ISCC, Vol. 1 (1969), p. 322.

Poon, C.S., Clark, A.I., Perry, R., Barker, A.P. and Barnes, P. (1986), Permeability study on the cement based solidification process for the disposal of hazardous wastes, Cem. Concr. Res. Vol. 16, p. 161-172.

Pourbaix, M.(1966), Atlas of electrochemical equilibria in aqueous solutions, Pergamon, Oxford.

Powers, T.C. and Brownyard, T.L. (1948), Studies of the physical properties of hardened portland cement paste, Bull. 22, PCA, Chicago, IL, U.S.

Powers, T.C. (1962), 4th ISCC, Vol.2 , p. 577.

Ramachandran, V.S. (1984), Concrete admixtures handbook, Noyes Publications, New Jersey, U.S.

Reardon, E.J. (1990), An ion interaction model for the determination of chemical equilibria in cement/water systems, Cem. Concr. Res. Vol. 20, pp 175-192.

Reardon, E.J. (1992), Problems and approaches to the prediction of the chemical composition in cement/water systems, Waste management, Vol.12, p. 221-239.

Reijerkerk, L. and Sain, M. de (2000), Het bestek als drager van het bouwstoffenbesluit (in Dutch), Wegen 2, p. 33-35.

Revertegate, E. Richet, C. and Gegout, P. (1992), Effect of pH on the durability of cement pastes, Cem. Concr. Res. Vol. 22, p. 259-272.

RIVM (1999), Ontwikkeling van een diffusieproef voor PAK (in Dutch), RIVM report 771402024.

RIVM (1999), Ontwikkeling van diffusieproeven voor PCB, OCB en EOX (in Dutch), RIVM report 771402025.

Rossetti, V.A. and Medici, F.(1995), Inertization of toxic metals in cement matrices: effects on hydration, setting and hardening, Cem. Concr. Res. Vol. 25, p. 1147-1152.

Smith, R.D. (1980), The trace element chemistry of coal during combustion and the emissions from coal-fired plants, Prog. Energy Combust. Sci., Vol. 6, p. 53-119.

Snyder, K.A. and J.R. Clifton (1995), 4sight manual: A computer program for modelling degradation of underground low level waste concrete vaults, NISTIR 5612, U.S. Dept. of Commerce.

Song, S. and Jennings, H.M. (1999), Pore solution chemistry of alkali-activated ground granulated blast-furnace slag, Cement and Concrete Res., Vol. 29, p. 159-170.

Song, S., Sohn, D., Jennings, H.M. and Mason, T.O. (2000), Hydration of alkali-activated ground granulated blast furnace slag, J. of Mat. Sci., Vol. 35, p. 249-257.

Spence, R.D. (1993), Chemistry and Microstructure of solidified waste forms, Lewis Publishers, Boca Raton, Florida.

Tazawa, E., Miyazawa, S. and Kasai, T. (1995), Chemical shrinkage and autogeneous shrinkage of hydrating cement paste, Cem. Concr. Res. 25(2), p. 288-292.

Taylor, H.F.W. (1987), A method for predicting alkali ion concentrations in cement pore solutions, Adv. Cem. Res. Vol.1, p. 5-16.

Taylor, H.F.W. (1997), Cement chemistry (2nd Edition), Thomas Telford publishing, London.

Thomas, N.L., Jameson, D.A. and Double, D.D. (1981), The effect of lead nitrate on the early hydration of Portland cement, Cem. Concr. Res. Vol. 11, p. 143-153.

Trussell, S. and Batchelor, B.(1996), Chemical characterization of pore water of a solidified hazardous waste, Stab. Solid. Hazard. Radioact. Mixed Wastes, 3rd Vol. STP 1240, Gilliam, T.M. and Wiles, C.C (Eds.), ASTM 1996, p. 94-115.

Trussel, S. and Spence, R.D. (1994) A review of solidification/stabilization interferences, Waste management Vol.14 No. 6, p. 507-519.

Uchikawa, H., Hanehara, S. and Hirao, H. (1997), Behavior of heavy metal elements in the hardening of cement paste, Proc. 10th ICCC, Vol. IV, 2ii014, Gothenburg 1997.

Wakao, N. and Smith, J.M. (1962), Diffusion in catalyst pellets, Chem. Eng. Sci. Vol. 17, p. 825-834.

Wang, S.Y. and Vipulanandan, C.   (1996), Leachability of lead from solidified cement-fly ash binders, Cem. Concr. Res. 26(6), p. 895-905.

Warren, C.J. and Reardon, E.J. (1994), The solubility of ettringite at 25 oC, Cem. Concr. Res. Vol. 24 No. 8, p. 1515-1524.

Xu, A. and Sarkar, S.L. (1994), Microstructural development in high-volume fly-ash cement system, J. of Mat. in Civil Eng., Vol. 6, p. 117-136.

Yagi, S. and Kunii, D. (1955), Studies on combustion of carbon particles in flames and fluidized beds, Proc. 5th Int. Symp. on Combustion.

Young, J.F. and Hansen, W. (1987), Volume relationships for CSH formation based on hydration stoichiometries, Mat. Res. Soc. Symp. Proc. Vol. 85, p. 313-322.

Yousouf, M., Mollah, A., Vempati, R.,K., Lin, T.-C and Cocke, D.L. (1995), The interfacial chemistry of solidification/stabilization of metals in cement and pozzolanic material systems, Waste Management Vol. 14 No. 2, p. 137-148.

Zamorani, E., Seikh, I. and Serrini, G. (1989), A study of the influence of nickel chloride on the physical characteristics and leachability of Portland cement, Cem. Concr. Res. Vol. 19, p. 259-266.

Zamorani, E. and G. Serrini (1992), Effect of hydrating water on the physical characteristics and the diffusion release of cesium nitrate immoblized, Cement Stab. Solid. Hazard. Radioact. wastes, 2nd Vol. STP 1123, Gilliam, T.M. and Wiles, C.C (Eds.), ASTM, p. 217-226.

Zhou, H. and Colombo, P. (1984), Solidification of radioactive waste in a cement/lime mixture, Waste management 1984, p. 164-168.

Appendix 1: Oxides in cement chemistry

Oxide	Symbol	Molar mass
Al_2O_3	A	102.0
B_2O_3	B	69.6
CaO	C	56.1
CO_2	$\overline{C}$	44.0
H_2O	H	18.0
Fe_2O_3	F	159.6
K_2O	K	94.2
MgO	M	40.3
Na_2O	N	62.0
P_2O_5	P	142.0
SiO_2	S	60.1
SO_3	$\overline{S}$	80.1
TiO_2	T	79.9

Appendix 2: Compounds in cement chemistry

C_3S	alite
C_2S	belite
C_3A	aluminate
C_4AF	ferrite
$C\bar{S}H_2$	gypsum
$C\bar{S}$	anhydrite
$C\bar{S}H_{0.5}$	hemihydrate
C-S-H	calcium silicate hydrate
CH	portlandite
$C_6A\bar{S}_3H_{32}$	ettringite
$C_4A\bar{S}H_{12}$	monosulphate
C_3AH_6	hydrogarnet
FH_3	iron hydroxide
MH	brucite
$K_2\bar{S}$	arcanite
$N_2\bar{S}$	thenardite
$KC_2\bar{S}_3$	Ca-langbeinite
$K_2C\bar{S}_2$	syngenite
$Mg_3Al(OH)_8(CO_3)_{0.5}.2H_2O$	hydrotalcite
$C_3A(CaCl_2).10H_2O$	Friedel's salt
A_3S_2	mullite
C_2ASH_8	stratlingite

Appendix 3: Particle sizes in CEMHYD3D

Diameter (mm)	Number of pixels	CEM 32,5R	CEM 42,5R	CEM 52,5R	Gypsum
		Mass	**fractions**		
1	1	0.048	0.083	0.128	0.1
3	19	0.053	0.084	0.116	0.2
5	81	0.053	0.079	0.102	0.2
7	179	0.051	0.073	0.089	0.2
9	389	0.05	0.067	0.077	0.2
11	739	0.047	0.062	0.067	0.1
13	1189	0.045	0.056	0.058	0
15	1791	0.043	0.051	0.05	0
17	2553	0.041	0.046	0.044	0
19	3695	0.038	0.042	0.038	0
21	4945	0.036	0.038	0.032	0
23	6403	0.034	0.034	0.028	0
25	8217	0.032	0.03	0.024	0
27	10395	0.03	0.027	0.021	0
29	12893	0.028	0.025	0.018	0
31	15515	0.026	0.022	0.015	0
33	18853	0.025	0.02	0.013	0
35	22575	0.023	0.018	0.011	0
37	26745	0.021	0.016	0.01	0
39	31103	0.275	0.128	0.058	0
		-----	-----	-----	-----
	Total:	1.000	1.000	1.000	1.000

Appendix 4: Calculation of activity coefficients

Davies equation

Activity coefficients are determined by the total composition of the solution. The ionic strength of a solution according to the Debye-Hückel theory is based on a summation of the concentrations off all types of ions present in solution and computed as follows (Butler, 1998):

$$I = \frac{1}{2} \sum_i [i] \cdot z_i^2 \tag{1}$$

I = ionic strength
[i] = concentration of ion i
z_i = charge of ion i

The fact that z_i is squared implies that all terms, for positive or negative ions, are positive. Furthermore, ions of high charge count more heavily than ions of lower charge.

Table 1. Activity coefficients as a function of ionic strength and charge, according to Davies equation.

I	γ_z (z = 1)	γ_z (z = 2)
0.00	1.00	1.00
0.01	0.90	0.66
0.02	0.87	0.58
0.03	0.85	0.52
0.04	0.83	0.48
0.05	0.82	0.45
0.10	0.78	0.36
0.20	0.73	0.29
0.30	0.71	0.26
0.40	0.70	0.24
0.50	0.70	0.24
1.00	0.71	0.25

An equation that is commonly used for computing activity coefficient for single ions is the Davies equation (Butler, 1998):

$$-\log \gamma_z = A z^2 \left(\frac{\sqrt{I}}{1 + \sqrt{I}} - 0.2I \right) \tag{2}$$

γ_z = activity coefficient of ion with charge z

$$A = 1.825 \cdot 10^6 \cdot (\varepsilon T)^{-3/2} \ (= 0.51 \text{ at } 25 \ ^{\circ}C \text{ in water}) \tag{3}$$

ε = di-electric constant of solvent (78.54 in water at 298 K)
T = temperature [K]

Eq. (2) can be used to compute an activity coefficient and only requires the ionic strength of the solution and the charge of the ion of interest. Example values are given in Table 1.

Pitzer ion interaction approach

In the Pitzer ion interaction approach the activity coefficient of a specific ion is based on its interaction with all other ions in solution. This interaction can be calculated using empirical equations that were fitted to many experimental data. From these fits interaction parameters were produced for each ion pair. The equations and parameters are derived from Pitzer (1979) and Harvie and Weare (1980). In this study, only the interaction between two ions of opposite charge are taken into account. Thus, interactions between two ions of equal charge, between more than two different ions and between neutral ions are neglected, which is allowed for most cases according to Pitzer (1979). Taken that into account, each cation-anion interaction can be described by four parameters, denoted P^0, P^1, P^2 and Q^0. In Table 2, these interaction parameters are given for some relevant ion pairs.

Table 2. Ion interaction parameters P^0, P^1, P^2 and Q^0.

		Ca^{2+}	Na^+	K^+
OH^-	P^0	-0.1747	0.0864	0.1298
	P^1	-0.2303	0.2530	0.3200
	P^2	-5.72	0	0
	Q^0	0	0.0044	0.0041
SO_4^{2-}	P^0	0.2000	0.0196	0.0499
	P^1	3.1973	1.1130	0.7793
	P^2	-54.24	0	0
	Q^0	0	0.0050	0
$Al(OH)_4^-$	P^0	0.2145	0.0454	-0.0003
	P^1	2.5300	0.3960	0.1735
	P^2	0	0	0
	Q^0	0	0	0

The constants required for further calculations are presented in Table 3. and the required g functions are presented in Eqs. (4-5).

Table 3. Constants.

Constant	Value
A_φ	0.3915
A	2
B	1.2
a1	1.4
a2	12

$$g(x) = 2 \cdot [1-(1 + x) \cdot e^{-x}]/x^2 \tag{4}$$

$$g'(x) = -2 \cdot [1-(1 + x + \tfrac{1}{2} x^2) \cdot e^{-x}]/x^2 \tag{5}$$

188

For each ion pair C-A, a P term is calculated using Eqs. (6–7):

$$P_{CA} = P_{CA}^0 + P_{CA}^1 g(a\sqrt{I})$$ (6)

$$P_{CA}^{'} = P_{CA}^1 g'(a\sqrt{I})/I$$ (7)

or Eqs. (8–9) for pairs having a P^2 parameter (Ca-OH pair and Ca-SO$_4$ pair):

$$P_{CA} = P_{CA}^0 + P_{CA}^1 g(a1\sqrt{I}) + P_{CA}^2 g(a2\sqrt{I})$$ (8)

$$P_{CA}^{'} = P_{CA}^1 g'(a1\sqrt{I})/I + P_{CA}^2 g'(a2\sqrt{I})/I$$ (9)

For each ion pair C-A, a Q term is calculated using Eq. (10)

$$Q_{CA} = \frac{Q_{CA}^0}{2\sqrt{|z_C z_A|}}$$ (10)

When the P, P' and Q terms are calculated for all C-A ion-pairs, the activity coefficients for a specific cation X and the specific anion Y can be calculated using the following equations:

$$Z = \sum_i [i] \cdot |z_i|$$ (11)

$$F = -A_\varphi \cdot \left(\sqrt{I}/(1+b\sqrt{I}) + (2/b)\ln(1+b\sqrt{I})\right) + \sum_C \sum_A [C][A]P_{CA}^{'}$$ (12)

$$\ln \gamma_X = z_X^2 F + \sum_A [A](2P_{XA} + ZQ_{XA}) + |z_X|\sum_C \sum_A [C][A]Q_{CA}$$ (13)

$$\ln \gamma_Y = z_Y^2 F + \sum_C [C](2P_{CY} + ZQ_{CY}) + |z_Y|\sum_C \sum_A [C][A]Q_{CA}$$ (14)

where A_φ and b are constants (see Table 3) and the P, P' and Q interaction terms follow from the ion interaction parameters of the ion pair C-A. C and A are cations and anions respectively, X and Y are the cation or anion for which the activity coefficient is calculated and z is the ion charge.

Example

To illustrate the ion interaction calculations, an example will be given based on a solution containing 0.5 M Na$^+$, 0.502 M OH$^-$ and 0.01 M Ca^{2+}. The relevant cation-anion interactions are those between Ca^{2+} and OH$^-$ and between Na$^+$ and OH$^-$. From Eq. (1) and Eq. (11) it follows that I = 0.521 and Z = 1.022 respectively. From Eqs. (4–10) the relevant interaction terms can be calculated (see Table 4).

189

Table 4. Cation-anion interaction terms.

	Ca-OH	Na-OH
P	-0.448	0.189
P'	0.361	-0.083
Q	0	0.0022

From Eq. (12) follows $F = A_\varphi$ term + P' term = -0.559 – 0.019 = -0.577.

Activity coefficients for Ca^{2+}, Na^+ and OH^- can now be calculated by filling in Eqs. (13–14):

$$Ln\,(\gamma_{Ca2+}) = z^2_{Ca}\cdot F + [OH^-]\cdot(2P_{Ca-OH} + ZQ_{Ca-OH}) +$$

$$|z_{Ca}|\cdot([Ca^{2+}][OH^-]Q_{Ca-OH} + [Na^+][OH^-]Q_{NaOH}) = -2.758$$

$\gamma_{Ca2+} = 0.063$.

$$Ln\,(\gamma_{Na+}) = z^2_{Na}\cdot F + [OH^-]\cdot(2P_{Na-OH} + ZQ_{Na-OH}) +$$

$$|z_{Na}|\cdot([Ca^{2+}][OH^-]Q_{Ca-OH} + [Na^+][OH^-]Q_{NaOH}) = -0.386$$

$\gamma_{Na+} = 0.680$.

$$\ln\,(\gamma_{OH-}) = z^2_{OH}\cdot F + [Ca^{2+}]\cdot(2P_{Ca-OH} + ZQ_{Ca-OH}) +$$

$$[Na^+]\cdot(2P_{Na-OH} + ZQ_{Na-OH}) +$$

$$|z_{Na}|\cdot([Ca^{2+}][OH^-]Q_{Ca-OH} + [Na^+][OH^-]Q_{NaOH}) = -0.396$$

$\gamma_{OH-} = 0.673$

Note that the activity coefficients calculated using Pitzer's method are different than the values that would follow from the Davies equation (see Table 1 at I = 0.5: $\gamma = 0.70$ and $\gamma = 0.24$ for monovalent and divalent ions respectively). According to Pitzer's method, the values of activity coefficients for OH^- and Na^+ are not the same and differ a few percent compared with Davies Equation. For the divalent Ca^{2+} ion the value calculated with Pitzer's method (0.063) differs with the value from Davies Equation (0.24) almost by a factor of 4. This difference is of major importance in cement chemistry and solubility calculations in which calcium compounds play an important role..

Summary

Limited use of natural resources, proper handling of waste materials and proper use of building materials result in a sustainable development. Treatment of waste materials results in a product that can be handled or applied more safely than the untreated waste. When treatment results in a product that can be used as a secondary building material, its application can save natural materials like sand and gravel. Thus, such an application contributes to a sustainable development.

Many waste streams can be treated by mixing it with cement and additives. The mixture will solidify and convert into a solid product in which contaminants, present in the waste material, are bound. Solidification is a result of the complex hydration process taking place in the mixture, i.e. the reaction between cement and water. Contaminants can interfere with this hydration process, thus disturbing or even preventing solidification. For a better understanding of the solidification process and the reason of failure, cement hydration must be considered in detail. The availability of analysing techniques and computer power has made it possible to model this process using the principle of a cellular automaton. This is a system of discrete elements of which the phase (e.g. a cement clinker mineral or water) or the location changes according to a set of rules (e.g. diffusion rules or chemical reactions). Such a system is very useful for the simulation of the complex hydration process.

When a solid product is obtained and has all required functional properties, it can be introduced as building material. Such a market introduction is not always successful and the secondary material is often rejected as alternative for primary building materials. Therefore, the waste industry and supplier of secondary materials should have a better understanding of the market with respect to building materials.

In this thesis the solidification process and the introduction of the solidified product as building material are described. This information can be used for better understanding of hydration of cement mixtures (possibly containing contaminants) and a for better understanding of the construction market in which the final product must be introduced. From this knowledge, technical and practical recommendations have been formulated that can be used by the cement and waste industry for the design and application of solidified products.

In chapter 2, CEMHYD3D is introduced, a 3D cement hydration model, originally developed at the National Institute of Standards and Technology (NIST). This model has been used successfully to describe microstructure development of cement mixtures based on ENCI cements with different particle size distributions. CEMHYD3D proved to be a tool that can be used to describe the solidification process and predict the microstructure of the solid product and relevant properties such as porosity and strength.

In chapter 3 pore water chemistry in hydrating cement mixtures is considered and it was concluded that $[Na^+]$, $[K^+]$, $[OH^-]$, $[Ca^{2+}]$ and $[SO_4^{2-}]$ concentrations determine reactivity and solubility of waste compounds and pozzolanic additives in a hydrating cement mixture. Pore water concentrations can be calculated from the alkali content of the used cement, the degree of hydration at some point in time and a set of solid equilibria relevant at that point in time, taking into account that the portlandite $(Ca(OH)_2)$ equilibrium is relevant at all times during

hydration. Using (1) a method to describe release and sorption of alkalis, (2) a limited set of solid equilibria, (3) Pitzer's ion interaction approach to calculate activity coefficients and (4) the degree of hydration as predicted by CEMHYD3D, pore water concentrations were calculated as a function of hydration time and agreed well with experimental pore water measurements reported in literature.

Chapter 4 deals with hydration of cement/fly ash mixtures. Fly ash is a major waste material and one of the main additives used in cement, and used as binder in solidification/stabilisation as well. A theoretical study is presented on the dissolution (reaction) of pulverised powder coal fly ash. A shrinking core model is derived for hollow spheres that contain two regions (outer hull and inner region). The resulting analytical equations are applied to the dissolution experiments by Pietersen (1990, 1993), yielding reaction rates at various temperatures and pH for two class F fly ashes. It is revealed that the available amount of reactive fly ash is proportional to the glass content of the fly ash, and that the reaction rate is proportional to this glass content as well. Moreover, it is concluded that the outer region is less reactive than the inner region, and that these reactivities are proportional to a power of the hydroxyl concentration. This power was found to be related to the composition of the fly ash particle. Subsequently, experimental data and model are used to assess the magnitude of inner and outer region. It seems that the outer hull of solid spheres and cenospheres are having the same thickness, about 2 μm. Based on the observed trends a reaction mechanism is proposed which accounts for the glass content and composition of the fly ash.

Chapter 5 deals with the contaminants present in most waste streams treated with cement, e.g. heave metals, borates and salts. The effects of these contaminants on cement hydration are described as well as the binding mechanisms. The main interference mechanism was found to be precipitation, resulting in coating of unhydrated cement grains, and disturbed hydration. A coating model has been developed, based on coating packages to be distributed over cement particles before hydration starts. This coating model has been implemented in CEMHYD3D and the decrease in degree of hydration was simulated this way and compared with strength measurements of hydrating cement mixtures containing borates. Good agreement was found between experiments reported in literature and numerical simulations.

Chapter 6 describes the link between material properties of the solidified product and it's leaching properties. The shrinking core leaching model and information on the microstructure of hydrated cement paste (e.g. porosity and $Ca(OH)_2$ fraction) are combined, yielding a "leaching resistance" function. Comparing this theoretical concept with leaching experiments taken from literature yield good agreement. Furthermore, using the "leaching resistance" function, optimal structures of hydrated cement pastes were defined, corresponding with mixtures containing 8 % (m/m) and 35 % (m/m) of pozzolanic additives silica fume and fly ash respectively. These computed amounts correspond well with amounts used in practice.

Chapter 7 describes the problems that arise when the immobilisate is introduced as construction material. Difficulties follow directly from this market in which other parties with other interests play a role and which will use their power to control the market by rules in order to reach their goals and interests. It is the main task of the waste industry to obtain the from these parties. An important party in the market for building materials is public

administration. This party sets up regulations for the use of materials, e.g. the Building Materials Decree and all other parties have to comply with this. This may result in limitations for the waste industry, when introducing secondary building materials. However, many limitations can be overcome in practice when industry decides to collaborate and communicate with both public administration and authorities in a private role as principal of a work. This can result in a joint set-up of legislation, adjustments in regulations or exceptions or joint trial projects. Already during the design of a cement/waste mixture, the waste industry should consider knowledge about the product to be developed and about all other market parties to deal with. Only then, their interests and demands can be dealt with. Introduction of a solidified waste product will only be successful commercially when it is certified, because certification only will be accepted by other parties as a proof of reliability of the product itself as well as trustworthiness of the supplier. Thus, for the supplier it is the best way to present (product) knowledge about an immobilisate to other parties. Furthermore, collaboration with authorities and with other suppliers of solidified waste products is the best way for the waste industry to make it a more serious negotiating partner for all other parties. This collaboration policy improves the chances of obtaining funds, permissions and reliability from other parties.

Chapter 8 presents the main conclusions and recommendations:

When cement is used to solidify waste products, fundamental knowledge about cement hydration, can be used to understand and improve the solidification process.

To simulate the solidification process and the final structure of the resulting immobilisate, a cement hydration model such as CEMHYD3D can be used.

Pore water chemistry, especially $[Na^+]$, $[K^+]$, $[OH^-]$, $[Ca^{2+}]$ and $[SO_4^{2-}]$ concentrations determine reactivity of waste compounds and pozzolanic additives in a hydrating cement mixture.

Pore water concentrations can be calculated from the alkali content of the used cement, the degree of hydration at some point in time and a set of solid equilibria relevant at that point in time.

The reaction of fly ash can be described by a shrinking core model, in which a particle can be considered as being made up of different shells having different compositions.

The pore water $[OH^-]$ dependence of the reaction of a fly ash particle is related to the elemental composition of its shells.

Coating of cement particles is the most relevant mechanism responsible for poor strength development.

Coating effects and related retardation effects are significant when the amount of precipitated compound is sufficient to cover a significant fraction of the surface of unhydrated cement particles.

Negative effects of coating can be overcome by using cement of high PSD or by varying pore water pH.

CEMHYD3D can be used to study solidification of cement/waste mixtures containing most common contaminants; The model is able to predict when contaminants will result in poor strength development.

Leaching from a solidified product depends on the expected degree of hydration, and porosity and $Ca(OH)_2$ content of the final product.

When fundamental knowledge about pore water chemistry, coating mechanisms and structure related leaching are combined with a cement hydration model such as CEMHYD3D, an excellent tool is created that can be used to predict and improve the functional properties of an immobilisate.

From chapter 7 the following main conclusions were drawn:

To increase chances of acceptance of an immobilisate as a building material the waste industry has to obtain trust by commercial and administrative parties in the construction market.

Collaboration with authorities and with other suppliers of solidified waste products is the best way for the waste industry to make it a more serious negotiating partner for all other parties. This collaboration policy improves the chances of obtaining funds (for research or trial projects), permissions and certification.

For the industry, a policy of collaboration is the best strategy to obtain the trust by parties in the market, required when introducing alternative construction materials.

194

Samenvatting

Beperking in het gebruik van natuurlijke bronnen, zorgvuldige omgang met afvalstoffen en zorgvuldige toepassing van bouwmaterialen dragen bij aan een duurzame ontwikkeling. Cement wordt vaak gebruikt voor immobilisatie, de bewerking van afvalstoffen, die een product moet opleveren dat veiliger bewerkt en toegepast kan worden dan het onbewerkte afval. Als deze bewerking een product oplevert dat kan worden gebruikt als secundaire grondstof, het zogenaamde immobilisaat, dan zal de toepassing ervan natuurlijke grondstoffen, zoals zand en grind, besparen. Op die manier draagt een dergelijke toepassing bij aan een duurzame ontwikkeling.

Veel afvalstromen kunnen worden bewerkt door het te mengen met cement en toevoegingen. Dit mengsel zal verharden en wordt omgezet in een vast product waarin verontreinigingen, die eventueel in de afvalstof aanwezig waren, gebonden zijn. De verharding van dit product is een gevolg van het ingewikkelde hydratatieproces dat in het mengsel plaatsvindt en voornamelijk bestaat uit de reacties tussen cement en water. Verontreinigingen kunnen dit hydratatieproces negatief beïnvloeden en op die manier de verharding belemmeren of zelfs volledig verhinderen. Om het verhardingsproces en de oorzaak van onvoldoende verharding te begrijpen moet de hydratatie van cement in detail worden beschouwd. Dankzij geavanceerde analyse technieken en de computerkracht die tegenwoordig beschikbaar zijn is het mogelijk geworden dit ingewikkelde hydratieproces te beschrijven en te modelleren volgens het principe van een cellulaire automaat. Dit is een systeem van discrete cellen waarvan de fase (bijvoorbeeld een cementmineraal of water) of de locatie kan veranderen als gevolg van een set regels (bijvoorbeeld verplaatsingsregels of chemische reacties). Een dergelijk systeem is zeer geschikt om het ingewikkelde hydratatieproces te simuleren.

Wanneer het verharde product voldoet aan de functionele eisen van een bouwmateriaal (bv. sterkte) kan het worden geïntroduceerd op de bouwmarkt. Een dergelijke introductie heeft echter vaak geen succes, omdat de secundaire grondstof niet wordt geaccepteerd als alternatief voor primaire, natuurlijke grondstoffen. Daarom moeten de afvalverwerkende industrie en leveranciers van secundaire grondstoffen een beter begrip krijgen van de bouwmarkt met betrekking tot bouwmaterialen.

In dit proefschrift worden zowel het verhardingsproces als de introductie van het verharde product als bouwmateriaal behandeld. Dit moet leiden tot een beter inzicht in het verhardingsproces, al dan niet in aanwezigheid van verontreinigingen, en een beter begrip van de bouwmarkt. Uit die kennis volgen technische en praktische aanbevelingen die de industrie (afval-, cement-, immobilisatie-) kan gebruiken bij het ontwikkelen van cement en cement/afvalstof recepturen en het toepassen van de verharde producten..

Hoofdstuk 2 behandelt de theorie van de hydratatie van cement en de modellen die hiervoor worden gebruikt. Een belangrijke parameter die in alle modellen voorkomt is de hydratatiegraad van het cement, gedefinieerd als de fractie van alle cement die op een bepaald moment heeft gereageerd. Het meest geavanceerde hydratatiemodel dat beschikbaar is, is CEMHYD3D, dat werd ontwikkeld op het National Institute of Standards and Technology (NIST) in de Verenigde Staten. Dit 3D computermodel is gebaseerd op het principe van een cellulaire automaat en kan worden gebruikt voor het beschrijven van de verharding en het

ontstaan van de microstructuur van het verharde product. CEMHYD3D werd gekalibreerd voor ENCI Portland cementen met verschillende korrelgrootteverdelingen. Alle ontwikkelde theorieën en modellen zijn gekoppeld aan CEMHYD3D, waardoor dit model kan worden gebruikt om, uitgaande van verschillende mengsels die onder verschillende omstandigheden verharden, de eigenschappen van het verharde product te voorspellen, zoals sterkte, porositeit en doorlaatbaarheid.

Hoofdstuk 3 behandelt de poriewaterchemie van hydraterende cementmengsels. Ongereageerd water blijft achter in smalle, capillaire poriën in het verhardende product en de samenstelling van dit zogenaamde poriewater heeft veel invloed op de reacties en de eigenschappen van het eindproduct. Uit de literatuur blijkt dat met name de pH en de concentraties alkaliën ($[Na^+]$ en $[K^+]$), calcium ($[Ca^{2+}]$) en sulfaten ($[SO_4^{2-}]$) een belangrijke rol spelen. Deze bepalen de reactiviteit en oplosbaarheid van verontreinigingen en bijvoorbeeld van vliegas en hoogovenslakken, twee veel gebruikte toevoegingen in cement. Concentraties in poriewater kunnen worden berekend uit het alkali gehalte van het cement, de hydratatiegraad op een bepaald moment en een set vaste stof evenwichten die op dat moment gelden. Het belangrijkste evenwicht is dat van $Ca(OH)_2$, dat altijd geldt. Poriewater concentraties werden als functie van de hydratatietijd berekend met behulp van een methode om oplossing en binding van alkaliën te beschrijven, een overwogen selectie evenwichten, Pitzers methode om activiteitscoëfficiënten te berekenen en de hydratatiegraad die werd gegeven door CEMHYD3D. De berekende concentraties kwamen goed overeen met metingen uit de literatuur.

Hoofdstuk 4 behandelt de hydratatie van cement/vliegas mengsels. Poederkoolvliegas is een belangrijk afvalproduct uit de energie industrie en wordt gebruikt als cement toevoeging en als bindmiddel voor immobilisatie. Een model werd ontwikkeld om de oplossing (reactie) van vliegaskorrels te beschrijven. Een "shrinking core" model werd ontwikkeld voor holle bollen die uit twee schillen bestaan (binnen en buitenschil). Hieruit volgden analytische vergelijkingen die werden toegepast op oplossingsexperimenten van Pietersen (1990, 1993). Dit leverde voor twee F klasse vliegassen reactiesnelheden op als functie van temperatuur en pH. Het bleek dat zowel de hoeveelheid vliegas beschikbaar voor reactie als de reactiesnelheid evenredig waren met het glasgehalte van de vliegas. Ook kon worden geconcludeerd dat de buitenschil minder reactief was dan de binnenschil en dat de reactiviteit evenredig is met de OH$^-$ concentratie tot een bepaalde macht. Deze macht is een functie van de samenstelling van de vliegaskorrel. Vervolgens werden de experimentele data uit de literatuur en het model gebruikt om de grootte van binnen- en buitenschil te bepalen en hieruit bleek dat de buitenschil van zowel dichte als holle vliegaskorrels ongeveer een dikte van 2 micrometer hadden. Uit al deze resultaten werd een reactiemechanisme voor een vliegaskorrel opgesteld, die rekening houdt met glasgehalte en samenstelling van de korrel.

Hoofdstuk 5 behandelt de verontreinigingen die aanwezig zijn in veel van de afvalstromen die worden behandeld met cement. Deze verontreinigingen zijn bijvoorbeeld zware metalen, boraten, sulfaten en chloriden. Zowel de manier waarop deze verontreinigingen worden gebonden in de eindstructuur als de effecten die ze hebben op het hydratatieproces zijn hier beschreven. De belangrijkste verstoring die kan optreden is neerslag, wat kan leiden tot coating van cementkorrels. De korrels worden op die manier afgesloten van water, waardoor

196

de reactiviteit van de cement sterk afneemt. Dit leidt tot beperkte of geen verharding en producten met hoge porositeit en lage sterkte. Uit simulaties met CEMHYD3D bleek dat pas wanneer meer dan 90 % van het oppervlak van alle cementkorrels was bedekt, de hydratatiegraad significant verminderde. Om dit effect in meer detail te simuleren werd een coating model ontwikkeld, gebaseerd op coating pakketjes die over het oppervlak van cementkorrels worden geplaatst voordat deze beginnen te reageren. Deze pakketjes konden het oppervlak ook weer verlaten (heroplossen) wanneer de pH in het poriewater toeneemt. Dit coating model werd in CEMHYD3D ingebouwd. Het volume aan coating pakketjes werd gekoppeld aan concentraties verontreinigingen in het poriewater en resultaten van simulaties werden vergeleken met sterktemetingen uit de literatuur, die betrekking hadden op mengsels met boraten. De berekende en gemeten afname in sterkteontwikkeling werd vergeleken en bleek goed overeen te komen.

Hoofdstuk 6 behandelt de relatie tussen de microstructuur van het verharde product en de uitloging van verontreinigingen uit het product. Het "shrinking core" uitlogingsmodel en informatie over de microstructuur van het verharde cementproduct (bv. de fracties $Ca(OH)_2$ en porositeit) werden gecombineerd en dit leverde een functie op die de uitlogingsweerstand van een verhard product beschrijft. Met deze functie waren uitlogingsexperimenten uit de literatuur goed te verklaren. Vervolgens werd dezelfde functie gebruikt om microstructuren met een zo hoog mogelijke uitlogingsweerstand te definiëren. Deze konden bijvoorbeeld worden gevormd door in het uitgangsmengsel respectievelijk 8 en 25 % (m/m) van cement te vervangen door respectievelijk silica fume of vliegas. Deze waarden corresponderen uitstekend met waarden die in de praktijk worden gekozen en succes hebben.

Hoofdstuk 7 beschrijft de problemen die ontstaan wanneer een immobilisaat wordt geïntroduceerd als bouwmateriaal. Deze problemen volgen direct uit de markt waarin andere actoren (betrokken en belanghebbende partijen), elk met hun eigen belangen en wensen, een rol spelen en hun macht zullen gebruiken om hun eigen doelen in de markt te bereiken. Voor de afval- en immobilisatie industrie is het belangrijk om het vertrouwen van deze actoren te winnen alvorens secundaire grondstoffen te introduceren.

Een belangrijke actor is de publieke overheid. Deze zet regelgeving op met betrekking tot het gebruik van bouwmaterialen. Een van die regelingen is het Bouwstoffenbesluit, waar alle betrokken partijen rekening mee moeten houden. Voor de introductie van secundaire grondstoffen kan dergelijke strenge regelgeving beperkingen opleveren. In de praktijk echter kunnen veel beperkingen overwonnen worden wanneer de industrie samenwerkt en communiceert met publieke overheid en met de overheid als private partij (bv. als opdrachtgever van een civiel werk). Deze samenwerking kan resulteren in het gezamenlijk opstellen van regelgeving, standaarden en uitvoeringsregelingen en eventuele aanpassingen of uitzonderingen in de regels of er kunnen gezamenlijke proefprojecten worden opgezet waarin secundaire grondstoffen worden gebruikt.

Al tijdens het ontwerp van een immobilisaat moet de industrie investeren in kennis over het product en kennis over de markt waarin het toegepast gaat worden. Alleen dan kan rekening worden gehouden met de eisen die de markt aan het product stelt. De introductie van een immobilisaat is alleen succesvol als het gecertificeerd is, omdat dat de enige manier is waarop andere partijen kunnen worden overtuigd van de betrouwbaarheid van zowel het product als de leverancier zelf. Samenwerking tussen industrie en overheid en tussen

industriële partijen onderling levert meer financiële en beleidsmatige mogelijkheden, hetgeen kan helpen bij het verkrijgen van kennis over het product en uiteindelijk certificering oplevert. Een strategie van samenwerking geeft een leverancier van immobilisaten ook een betere onderhandelingspositie. Met dit alles kan sneller het vertrouwen worden gewonnen van de partijen in de bouw.

Hoofdstuk 8 bevat een overzicht van de belangrijkste conclusies van dit proefschrift:

Wanneer cement wordt gebruikt voor immobilisatie van afvalstoffen kan fundamentele kennis over de cementhydratatie worden gebruikt om het verhardingsproces te begrijpen en te verbeteren.

Een cementhydratatiemodel zoals CEMHYD3D kan uitstekend worden gebruikt om het verhardingsproces en de structuur van het verharde product te simuleren.

De samenstelling van poriewater en voornamelijk de pH en concentraties alkaliën ($[Na^+]$ en $[K^+]$), calcium ($[Ca^{2+}]$) en sulfaten ($[SO_4^{2-}]$) bepalen in sterke mate de reactiviteit en oplosbaarheid van verontreinigingen en vliegassen.

Alle relevante poriewater concentraties zijn te berekenen uit het alkaligehalte van het cement, de hydratatiegraad en een kleine set vaste stof evenwichten.

De reactie van vliegas in een cement systeem kan worden beschreven met een "shrinking core" model, waarin een vliegaskorrel bestaat uit verschillende schillen met verschillende samenstellingen.

De afhankelijkheid tussen de reactiviteit van een vliegaskorrel en $[OH^-]$ is direct gerelateerd aan de samenstelling van de schillen in de korrel.

De meeste problemen met verharding zijn het gevolg van neerslag op cementkorrels, resulterend in coating. Problemen ontstaan pas als een significante fractie van het oorspronkelijke cement oppervlak is bedekt.

Problemen als gevolg van coating kunnen worden beperkt door toepassing van cement met een fijne korrelgrootteverdeling (groot specifiek oppervlak) of door variëren van poriewater pH (bv. door variëren van alkaligehalte in cement mengsel).

CEMHYD3D kan worden gebruikt om de verharding van cementmengsels met de meest voorkomende verontreinigingen te simuleren en te voorspellen wanneer sterkteontwikkeling zal achterblijven.

De mate van uitloging van verontreinigingen uit een immobilisaat wordt bepaald door de verwachte uiteindelijke hydratatiegraad, de porositeit en de $Ca(OH)_2$ fractie in het verharde eindproduct.

198

Bovenstaande deelconclusies leiden tot de volgende eindconclusie:

Als fundamentele kennis over poriewaterchemie, coating mechanismen en structuurafhankelijke uitloging worden gecombineerd met een cementhydratatiemodel als CEMHYD3D ontstaat een hulpmiddel, dat kan worden gebruikt om de functionele eigenschappen van een immobilisaat te voorspellen en te verbeteren.

De belangrijkste conclusies die volgen uit hoofdstuk 7 zijn:

Om de kansen op acceptatie van een immobilisaat als bouwmateriaal te verhogen moet de industrie vertrouwen kweken bij commerciële partijen in de bouw en bij de overheid.

Samenwerking tussen leveranciers/producenten van immobilisaten onderling en met de overheid, levert de industrie een betere onderhandelingspositie op. Dit samenwerkingsbeleid leidt tot meer financiële en beleidsmatige speelruimte, resulterend in proefprojecten, technische kennis over het product en certificering.

Samenwerking is de beste uitgangsstrategie om het vertrouwen van partijen in de bouw te krijgen, dat nodig is om immobilisaten op de markt te introduceren.

About the author
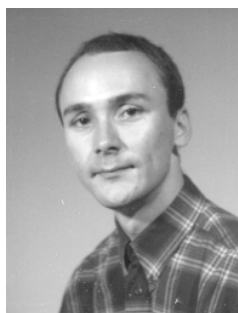
Ronald Jozef van Eijk was born in The Hague, The Netherlands, on May 7th, 1973. In 1991 he received his Gymnasium diploma at the Emmauscollege in Rotterdam. In the same year he started his study in Chemistry at the University of Utrecht, where he followed courses in inorganic chemistry, solid state chemistry, chemical informatics, food product technology and biochemistry. In 1996 he graduated at the Centre for Biomembranes and Lipid Enzymology (CBLE) on lipid transport from inner to outer membrane of E. Coli cells. In august 1996 he started his PhD. research at the University of Twente, Department of Civil Engineering. Subject of this study was the solidification/ stabilisation of waste materials using cement. Cement hydration was modelled using CEMHYD3D, a 3D cement hydration computer model based on a cellular automaton. This model was originally developed at the National Institute of Standards and Technology (NIST) in Gaithersburg in the U.S. The results of his PhD. study include computation models and practical recommendations, which can both be used by the cement and waste industry for the design, production and commercialisation of cement-based solidified products. The research was supported by Dutch cement industry (ENCI) and the KEMA research institute. In 1998 he followed the 9th ACBM/NIST Computer modelling workshop at NIST and in 2000 he followed a PhD. summer course on Microstructure, Transport Phenomena and Degradation of Concrete at the Denmark Technical University. He presented his work at several conferences, including the 10th ICCC (International Congress on the Chemistry of Cement) in Gothenburg, Sweden (in 1997) and WASCON 2000 in Harrogate, England. Furthermore, results from his work have been published in the journals "Cement and Concrete Research" and "Waste Management".